

Nitric Oxide, Salivary Hypofunction and Sjögren's syndrome

Thesis submitted in accordance with the requirements of The University
of Liverpool for the degree of Doctor of Philosophy

By

Vicky Louise Caulfield

December 2008

**The Faculty of Medicine
(School of Dental Sciences)**



UNIVERSITY OF
LIVERPOOL

“ Copyright © and Moral Rights for this thesis and any accompanying data (where applicable) are retained by the author and/or other copyright owners. A copy can be downloaded for personal non-commercial research or study, without prior permission or charge. This thesis and the accompanying data cannot be reproduced or quoted extensively from without first obtaining permission in writing from the copyright holder/s. The content of the thesis and accompanying research data (where applicable) must not be changed in any way or sold commercially in any format or medium without the formal permission of the copyright holder/s. When referring to this thesis and any accompanying data, full bibliographic details must be given, e.g. Thesis: Author (Year of Submission) "Full thesis title", University of Liverpool, name of the University Faculty or School or Department, PhD Thesis, pagination.”

ABSTRACT

Nitric Oxide, Salivary Hypofunction and Sjögren's Syndrome

Vicky Louise Caulfield

Sjögren's syndrome is a systemic autoimmune disorder which specifically targets the exocrine glands, primarily the salivary and lacrimal glands and leads to an impairment of secretory function and is characterised by lymphocytic infiltration of the salivary and lacrimal glands. Until relatively recently it was believed that the glandular hypofunction was a direct consequence of immune mediated destruction of the acinar tissue but most recent data suggests that the glandular hypofunction is more likely to be the result of immune mediated inhibition of acinar function, which if prolonged could lead to acinar atrophy.

Many factors may induce this observed glandular hypofunction in Sjögren's syndrome but, based on the presence of elevated levels of nitric oxide (NO) in the saliva and expired air of Sjögren's syndrome patients, NO was suggested as a possible cause of this induced hypofunction. The findings presented here demonstrate that NO has the ability to both amplify and inhibit the acinar cells response to ACh, which suggested that NO may have a role in acinar cell desensitisation. This response pattern was observed in both submandibular and lacrimal cells from both humans and mice. The use of four NO donors (SNAP, NOC-12, SNP and NOC-5) makes it unlikely that the responses were an artefact of the NO donor and the use of multiple cell types suggests the process might be a universal mechanism. The initial amplification induced by NO was significant with all four NO donors in the mouse submandibular acinar cells (SNAP $P < 0.01$, NOC-12 $P < 0.001$, SNP $P < 0.05$ and NOC-5 $P < 0.05$). The induced inhibition following prolonged NO exposure was also significant with SNAP ($P < 0.001$) and SNP ($P < 0.01$) and total inhibition of response to ACh following prolonged exposure to SNAP occurred within 36 minutes.

Following the use of four NO donors, the downstream activity of NO was determined. The amplification was shown to act through the cGMP pathway through use of two inhibitors of this pathway, ODQ and Ryanodine. However, the chronic NO effect resulting in desensitisation to ACh appeared to be independent of cGMP pathway as desensitisation to ACh still occurred in the presence of both inhibitors. These data may suggest a role for NO in the development of glandular hypofunction in Sjögren's syndrome.

Following the determination that NO was able to induce desensitisation of the acinar response in individual acinar cells the possible effect at the acinus level was investigated. It initially had to be determined if cell to cell communication did occur in salivary acinar cells. The data indicate that there was some degree of cell to cell communication occurring between salivary acinar cells and that this may result in the production of a synchronous oscillatory response pattern which was clearly observed in some instances. However, NO was shown to have no effect on the oscillatory response pattern which suggested that NO did not appear to desensitise at the acinus level and in fact NO may function under normal conditions to sensitise the cells to ACh by enhancing the level of cell to cell coupling.

Overall the work has demonstrated, for the first time that NO induced desensitisation may have an important role in the development of glandular hypofunction in Sjögren's syndrome.

CONTENTS

ABSTRACT.....ii

CONTENTS.....iii

LIST OF FIGURES.....v

LIST OF TABLES.....xiii

ACKNOWLEDGEMENTS.....xiv

ABBREVIATIONS.....xv

CHAPTER 1:

INTRODUCTION

1.1 Salivary Secretion.....2

1.2 Nitric Oxide25

1.3 Adenosine Tri-Phosphate.....38

1.4 Cell - Cell Coupling in Salivary Acinar Cells.....46

1.5 Sjögrens Syndrome.....55

1.6 Aims of the Study.....67

CHAPTER 2:

MATERIALS AND METHODS:

2.1 Solutions.....69

2.2 Nitric Oxide Donors.....72

2.3 Nitric Oxide Inhibitors.....73

2.4 Preparation of Mouse Acinar Cells.....74

2.5 Preparation of Human Acinar Cells.....75

2.6 Primary Cell Culture.....76

2.7 Suitability of Cells Selected.....77

2.8 Experimental Procedures and Nitric Oxide Protocol.....78

2.9 Measurement of $[Ca^{2+}]_i$82

2.10 Microfluorimetry.....83

2.11 Perfusion Procedure.....85

2.12 Statistics and Data Presentation.....86

CHAPTER 3:

RESULTS:

Nitric Oxide

Mouse Submandibular Acinar Cells.....87

CHAPTER 4:

RESULTS:

Nitric Oxide

Human Submandibular Acinar Cells.....131

CHAPTER 5:

RESULTS:

Nitric Oxide

Mouse Lacrimal Acinar Cells.....164

CHAPTER 6:

RESULTS:

Adenosine Tri-Phosphate as a Stress signal Inducer.....190

CHAPTER 7:

RESULTS:

Cell – Cell Coupling and the Effects of Nitric Oxide.....206

CHAPTER 8:

DISCUSSION:

8.1 Introduction.....236

8.2 A Possible role for nitric oxide in acinar hypofunction.....238

8.3 A Possible role for adenosine tri-phosphate in acinar hypofunction.....
.....244

8.4 A Possible role for cell - cell coupling in acinar hypofunction.....246

8.5 A mechanism to account for acinar hypofunction in Sjögren's
Syndrome..... 251

CONCLUSION.....253

FURTHER WORK.....254

BIBLIOGRAPHY.....255

LIST OF FIGURES

Number	Page
Figure 1.1.1: Diagram of the Afferent and Efferent pathways in the control of salivary secretion.	3
Figure 1.1.2: (A) Epilemmal and (B) Hypoepilemmal relationship of neurones to acinar cells.	5
Figure 1.1.3: Diagrammatic representation of the orientation of the components of muscarinic receptors in the cell membrane. I-VII represent transmembrane domains. i1-i4 intracellular loops.	9
Figure 1.1.4: Detailed diagrammatic representation of the series of steps from interaction of neurotransmitter to production of IP_3 which diffuse into the cytoplasm.	11
Figure 1.1.5: Detailed diagrammatic representation of the activation of IP_3R by IP_3 and release of Ca^{2+} .	13
Figure 1.1.6: Diagrammatic representation of the ER arrangement to allow for Ca^{2+} - tunnelling. The diagram also introduces the concept of Ca^{2+} -induced Ca^{2+} release and the coordination of receptors by the level of Ca^{2+} .	17
Figure 1.1.7: Series of cell images clearly showing that the $[Ca^{2+}]_i$ increases and decreases very rapidly at only the apical pole.	19
Figure 1.1.8: Shows a highly simplified diagram of an acinar cell including movement of Ca^{2+} from the basolateral to the apical pole of the cell via calcium tunnelling for calcium release at the apical pole of the cell.	20
Figure 1.1.9: Simple Flow Diagram representing the simple steps of secretion.	23
Figure 1.1.10: Diagrammatic overview of the formation of primary saliva by salivary acinar cells in response to stimulation by ACh.	24
Figure 1.2.1: Diagrammatic representation of the likely NO pathway in salivary acinar cells.	26
Figure 1.2.2: Diagram depicting the pathway of NO activity and control.	33

Figure 1.5.1: H&E stained histological section of a labial gland from a patient with Sjögren's syndrome.	56
Figure 2.8.1: Change in $[Ca^{2+}]_i$ in response to 50nM ACh and the $[Ca^{2+}]_i$ variation in response to 50, 500 and 5000nM ACh.	79
Figure 2.8.2: Experimental Protocol.	81
Figure 2.9.1: Figure illustrating the chemical structure of Fura-2.	82
Figure 2.10.1: Schematic diagram of the microfluorimetry rig used to visualize and record acinar cell responses induced by agonists.	83
Figure 2.11.1: Illustration of the primary perfusion system.	85
Figure 3.1.1: Change in $[Ca^{2+}]_i$ in response to 200 μ M SNAP, illustrating how NO alone induced a $[Ca^{2+}]_i$ signal response.	90
Figure 3.1.2 parts A and B: Change in $[Ca^{2+}]_i$ in response to 50nM ACh, illustrating how 100 μ M SNAP induced amplification of the $[Ca^{2+}]_i$ signal.	92
Figure 3.1.2 parts C and D: Change in $[Ca^{2+}]_i$ in response to 50nM ACh, illustrating how 200 μ M NOC-12 induced amplification of the $[Ca^{2+}]_i$ signal.	93
Figure 3.1.3 parts A and B: Change in $[Ca^{2+}]_i$ in response to 50nM ACh, illustrating how 75 μ M SNP and 200 μ M NOC-5 respectively induced amplification of the $[Ca^{2+}]_i$ signal.	96
Figure 3.1.4 parts A and B: Change in $[Ca^{2+}]_i$ in response to 50nM ACh, illustrating how 100 μ M SNAP induced amplification and inhibition of the $[Ca^{2+}]_i$ signal.	98
Figure 3.1.4 parts C and D: Change in $[Ca^{2+}]_i$ in response to 50nM ACh, illustrating how 200 μ M NOC-12 induced amplification and inhibition of the $[Ca^{2+}]_i$ signal.	99
Figure 3.1.5 parts A and B: Change in $[Ca^{2+}]_i$ in response to 50nM ACh, illustrating how 75 μ M SNP and 200 μ M NOC-5 respectively induced amplification and inhibition of the $[Ca^{2+}]_i$ signal.	100
Figure 3.1.6: Change in $[Ca^{2+}]_i$ in response to 50nM ACh did not diminish with repeated application over the experimental time period.	103

Figure 3.1.7: Change in $[Ca^{2+}]_i$ in response to 50nM ACh in the presence of 100 μ M SNAP initially increases but then gradually decreases with repeated application over the experimental time period.

104

Figure 3.1.8: Change in $[Ca^{2+}]_i$ in response to 50nM ACh in the presence of 200 μ M NOC-12 initially increases but then gradually decreases with repeated application over the experimental time period.

105

Figure 3.1.9: Change in $[Ca^{2+}]_i$ in response to 50nM ACh in the presence of 75 μ M SNP initially increases but then gradually decreases with repeated application over the experimental time period.

106

Figure 3.1.10: Change in $[Ca^{2+}]_i$ in response to 50nM ACh in the presence of 200 μ M NOC-5 initially increases but then gradually decreases with repeated application over the experimental time period.

107

Figure 3.1.11 Trace A: Change in $[Ca^{2+}]_i$ in response to 50nM ACh in the presence of 100 μ M SNAP, 200 μ M NOC-12, 75 μ M SNP and 200 μ M NOC-5 respectively over the experimental period.

108

Figure 3.1.11 Trace B: Change in $[Ca^{2+}]_i$ in response to 50nM ACh in the presence of 100 μ M SNAP, 200 μ M NOC-12, 75 μ M SNP and 200 μ M NOC-5 respectively over the experimental period.

108

Figure 3.1.12: Change in $[Ca^{2+}]_i$ in response to 50nM ACh, illustrating how 200 μ M NOC-12 induced amplification and inhibition of the $[Ca^{2+}]_i$ signal but how cells were still able to respond to Thapsigargin.

110

Figure 3.1.13 parts A and B: Change in $[Ca^{2+}]_i$ in response to 50nM ACh in the presence of 100 μ M SNAP and 200 μ M NOC-12 respectively in the presence 10 μ M ODQ acutely.

112

Figure 3.1.13 parts C and D: Change in $[Ca^{2+}]_i$ in response to 50nM ACh in the presence of 100 μ M SNAP and 200 μ M NOC-12 respectively in the presence 10 μ M ODQ chronically.

114

Figure 3.1.14: Change in $[Ca^{2+}]_i$ in response to 50nM ACh in the presence of 100 μ M SNAP and 10 μ M ODQ showing gradual decrease in response over the experimental time period.

116

Figure 3.1.15: Change in $[Ca^{2+}]_i$ in response to 50nM ACh in the presence of 200 μ M NOC-12 and 10 μ M ODQ showing gradual decrease in response over the experimental time period.

117

Figure 3.1.16: Change in $[Ca^{2+}]_i$ in response to 50nM ACh and 50nM ACh in the presence of 100 μ M SNAP with 10 μ M ODC and 200 μ M NOC-12 with 10 μ M ODC respectively over the experimental time period.

118

Figure 3.1.17 parts A and B: Change in $[Ca^{2+}]_i$ in response to 50nM ACh in the presence of 10 μ M Ryanodine and 200 μ M NOC-12 in the presence 10 μ M Ryanodine acutely.

120

Figure 3.1.17 parts C and D: Change in $[Ca^{2+}]_i$ in response to 50nM ACh in the presence of 10 μ M Ryanodine and 200 μ M NOC-12 in the presence 10 μ M Ryanodine chronically.

121

Figure 3.1.18: Change in $[Ca^{2+}]_i$ in response to 50nM ACh in the presence or absence of 10 μ M Ryanodine showing decrease with repeated application.

123

Figure 3.1.19: Change in $[Ca^{2+}]_i$ in response to 50nM ACh in the presence or absence of both 10 μ M Ryanodine and 200 μ M NOC-12 showing gradual decrease in response.

124

Figure 3.1.20: Change in $[Ca^{2+}]_i$ in response to 50nM ACh and 50nM ACh in the presence of 200 μ M NOC-12 with 10 μ M Ryanodine and 10 μ M Ryanodine respectively over the experimental time period.

125

Figure 3.1.21: Average responses for all experimental groups for 3rd response to ACh compared to control

126

Figure 4.1.1 parts A and B: Change in $[Ca^{2+}]_i$ in response to 50nM ACh, illustrating how 75 μ M SNP induced amplification of the $[Ca^{2+}]_i$ signal.

135

Figure 4.1.1 parts C and D: Change in $[Ca^{2+}]_i$ in response to 50nM ACh, illustrating how 200 μ M NOC-12 induced amplification of the $[Ca^{2+}]_i$ signal.

136

Figure 4.1.2 parts A and B: Change in $[Ca^{2+}]_i$ in response to 50nM ACh, illustrating how 75 μ M SNP induced amplification and inhibition of the $[Ca^{2+}]_i$ signal.

138

Figure 4.1.2 parts C and D: Change in $[Ca^{2+}]_i$ in response to 50nM ACh, illustrating how 200 μ M NOC-12 induced amplification and inhibition of the $[Ca^{2+}]_i$ signal.

139

Figure 4.1.3: Change in $[Ca^{2+}]_i$ in response to 50nM ACh did not totally diminish with repeated application over the experimental time period.

141

Figure 4.1.4: Change in $[Ca^{2+}]_i$ in response to 50nM ACh in the presence of 75 μ M SNP initially increases but then gradually decreases with repeated application over the experimental time period.

142

Figure 4.1.5: Change in $[Ca^{2+}]_i$ in response to 50nM ACh in the presence of 200 μ M NOC-12 initially marginally increases but then gradually decreases with repeated application over the experimental time period.

143

Figure 4.1.6: Change in $[Ca^{2+}]_i$ in response to 50nM ACh only and 50nM ACh in the presence of 75 μ M SNP and 200 μ M NOC-12 respectively over the experimental time period.

144

Figure 4.1.7 parts A and B: Change in $[Ca^{2+}]_i$ in response to 50nM ACh in the presence of 200 μ M NOC-12 and 200 μ M NOC-12 with 10 μ M ODQ respectively acutely.

146

Figure 4.1.7 parts C and D: Change in $[Ca^{2+}]_i$ in response to 50nM ACh in the presence of 200 μ M NOC-12 and 200 μ M NOC-12 with 10 μ M ODQ respectively chronically.

147

Figure 4.1.8: Change in $[Ca^{2+}]_i$ in response to 50nM ACh in the presence of 200 μ M NOC-12 and 10 μ M ODQ gradually decreases with repeated application over the experimental time period.

149

Figure 4.1.9: Change in $[Ca^{2+}]_i$ in response to 50nM ACh and 50nM ACh in the presence of 200 μ M NOC-12 and 10 μ M ODQ respectively over the experimental time period.

150

Figure 4.1.10 parts A and B: Change in $[Ca^{2+}]_i$ in response to 50nM ACh in the presence of 10 μ M Ryanodine and 200 μ M NOC-12 with 10 μ M Ryanodine respectively acutely.

152

Figure 4.1.10 parts C and D: Change in $[Ca^{2+}]_i$ in response to 50nM ACh in the presence of 10 μ M Ryanodine and 200 μ M NOC-12 with 10 μ M Ryanodine respectively chronically.

154

Figure 4.1.11: Change in $[Ca^{2+}]_i$ in response to 50nM ACh in the presence of 10 μ M Ryanodine decreases with repeated application over the experimental time period.

155

Figure 4.1.12: Change in $[Ca^{2+}]_i$ in response to 50nM ACh in the presence of both 10 μ M Ryanodine and 200 μ M NOC-12 over the experimental time period.

156

Figure 4.1.13: Change in $[Ca^{2+}]_i$ in response to 50nM ACh only and 50nM ACh in the presence of 10 μ M Ryanodine only and 10 μ M Ryanodine and 200 μ M NOC-12 together respectively over the experimental time period.

158

Figure 5.1.1 parts A and B: Change in $[Ca^{2+}]_i$ in response to 50nM ACh, illustrating how 200 μ M NOC-12 induced amplification of the $[Ca^{2+}]_i$ signal.

167

Figure 5.1.1 parts C and D: Change in $[Ca^{2+}]_i$ in response to 50nM ACh, illustrating how 200 μ M NOC-12 induced amplification and inhibition of the $[Ca^{2+}]_i$ signal.

169

Figure 5.1.2: Change in $[Ca^{2+}]_i$ in response to 50nM ACh did not diminish with repeated application over the experimental time period.

171

Figure 5.1.3: Change in $[Ca^{2+}]_i$ in response to 50nM ACh in the presence of 200 μ M NOC-12 initially increases but then gradually decreases with repeated application over the experimental time period.

172

Figure 5.1.4: Change in $[Ca^{2+}]_i$ in response to 50nM ACh and 50nM ACh in the presence of 200 μ M NOC-12 respectively over the experimental time period.

173

Figure 5.1.5 parts A and B: Change in $[Ca^{2+}]_i$ in response to 50nM ACh and 50nM ACh in the presence of 200 μ M NOC-12 in the presence of 10 μ M ODQ acutely.

175

Figure 5.1.5 parts C and D: Change in $[Ca^{2+}]_i$ in response to 50nM ACh and 50nM ACh in the presence of 200 μ M NOC-12 in the presence of 10 μ M ODQ chronically.

176

Figure 5.1.6: Change in $[Ca^{2+}]_i$ in response to 50nM ACh in the presence of 200 μ M NOC-12 and 10 μ M ODQ gradually decreases with repeated application over the experimental time period.

178

Figure 5.1.7: Change in $[Ca^{2+}]_i$ signal in response to 50nM ACh and 50nM ACh in the presence of 200 μ M NOC-12 and 200 μ M NOC-12 with 10 μ M ODQ respectively over the experimental time period.

179

Figure 5.1.8 parts A and B: Change in $[Ca^{2+}]_i$ in response to 50nM ACh and 50nM ACh in the presence of 200 μ M NOC-12 in the presence of 10 μ M Ryanodine acutely.

181

Figure 5.1.8 parts C and D: Change in $[Ca^{2+}]_i$ in response to 50nM ACh in the presence of 200 μ M NOC-12 in the presence of 10 μ M ODQ and 10 μ M Ryanodine respectively over the experimental time period.

182

Figure 5.1.9: Change in $[Ca^{2+}]_i$ signal in response to 50nM ACh in the presence of 10 μ M Ryanodine and 200 μ M NOC-12 initially maintained then rapidly decreases with repeated application over the experimental time period.	184
Figure 5.1.10: Change in $[Ca^{2+}]_i$ signal in response to 50nM ACh and 50nM ACh in the presence of 200 μ M NOC-12 only and 200 μ M NOC-12 with either 10 μ M ODQ and 10 μ M Ryanodine respectively over the experimental time period.	186
Figure 6.1.1: 3 separate traces showing the change in $[Ca^{2+}]_i$ signal in response to 50nM ACh and 100 μ M ATP stimulation respectively.	193
Figure 6.1.1 Trace D and Trace E: Average responses to ATP at 100, 250 and 500 μ M concentrations and ACh at 500nM in human and mouse submandibular cells.	194
Figure 6.1.2: Change in $[Ca^{2+}]_i$ in response to 50nM ACh.	196
Figure 6.1.3: Change in $[Ca^{2+}]_i$ signal in response to 100 μ M ATP.	198
Figure 7.1.1: Change in $[Ca^{2+}]_i$ signal in response to 50nM ACh in the absence and presence of 200 μ M NOC-12 demonstrating no degree of synchronisation.	209
Figure 7.1.2: Change in $[Ca^{2+}]_i$ signal in response to 50nM ACh demonstrating no degree of synchronisation.	211
Figure 7.1.3: Change in $[Ca^{2+}]_i$ signal in response to 50nM ACh demonstrating lack of synchronisation.	213
Figure 7.1.4: Change in $[Ca^{2+}]_i$ signal in response to 50nM ACh demonstrating lack of synchronisation at 5 th stimulation point.	215
Figure 7.1.5: Change in $[Ca^{2+}]_i$ signal in response to 50nM ACh demonstrating lack of synchronisation at 13 th stimulation point.	217
Figure 7.1.6: Change in $[Ca^{2+}]_i$ signal in response to 50nM ACh demonstrating cell – cell communication.	219
Figure 7.1.7: Change in $[Ca^{2+}]_i$ signal in response to 50nM ACh in the absence and presence of 200 μ M NOC-12 demonstrating synchronisation.	221

Figure 7.1.8: Change in $[Ca^{2+}]_i$ signal in response to 50nM ACh demonstrating synchronisation at the 1st stimulation point.

223

Figure 7.1.9: Change in $[Ca^{2+}]_i$ signal in response to 50nM ACh in the presence of 200 μ M NOC-12 demonstrating synchronisation at the 7th stimulation point.

225

LIST OF TABLES

Number	Page
Table 1.1.1: Basic data for M3R for rat, mouse and human.	9
Table 1.5.1: Sjögren's syndrome classification criteria part 1.	60
Table 1.5.2: Sjögren's syndrome classification criteria part 2.	62
Table 2.1.1: Table of all chemical details.	70
Table 3.1.1: Table of results for mouse submandibular acinar cells.	89
Table 4.1.1: Table of results for human submandibular acinar cells.	133
Table 5.1.1: Table of results for mouse lacrimal acinar cells.	166

ACKNOWLEDGEMENTS

I wish to thank my supervisors, Dr Pete Smith and Dr Luke Dawson for all their encouragement, support and guidance throughout my PhD, without whom this thesis would not have come to fruition.

I would like to thank Dr John Stanbury for all his help with technical aspects of the practical work for this thesis, and for his relentless support and friendship.

A personal thank you is extended to Lee Cooper for his humour, friendship and support during some of the most difficult times in the last few years.

A big thank you to all the people who have helped me during my time at The Edwards Building: Professor Sue Higham, Jan Chesters, Emma Felton, Lynne Saunders, Ghada Mahmoud, Dr Janet Risk, Martin Ralph, Dr Richard Shaw, Shelley Nolan, Dr Norah Flannigan, Tom Coxon, Liza Finney, Brenda Smith, Jim Hibbard, Andrew Birss, Irene Wardle and Gill Lloyd.

A huge thank you to my mum and dad for all their encouragement, their unwavering support and the unconditional love they have given me throughout the duration of this PhD, without them I would be lost.

And finally my horses for all the pleasure, company and release from stress they have brought me throughout my PhD, they allowed me to maintain what sanity remains.

ABBREVIATIONS

$[Ca^{2+}]_i$ =	Intracellular calcium ion concentration
aa =	Amino acid
ACh =	Acetylcholine
AEC =	Auto-immune exocrinopathy
CCh =	Carbacol
BSA =	Bovine serum albumin
cADPr =	Cyclic adenosine diphosphate ribose
CGRP =	Calcitonin gene-related peptide
CHO cells =	Chinese Hamster Ovary cells
CICR =	Calcium induced calcium release
CIF =	Calcium influx factor
CNS =	Central nervous system
DAG =	Diacylglycerol
EDRF =	Endothelial derived relaxing factor
ER =	Endoplasmic reticulum
GAL =	Galanin
GAP =	GTP activating protein
GDP[S] =	Guanosine 5'-[β -thio]disphosphate
cGMP =	Cyclic guanosine 3',5'-monophosphate
GTP =	Guanosine 5'-triphosphate
HAP =	Hydroxyapatite
I_{CRAC} =	Calcium release activated current
Ig =	Immunoglobulin
INF =	Interferon
IP_3 =	Inositol 1,4,5 trisphosphate
IP_3R =	Inositol 1,4,5 trisphosphate receptor
L-NAME =	N ^G -nitro-L-arginine methyl ester
M3R =	Muscarinic type m3 receptor
mAChR =	Muscarinic receptors
NA =	Noradrenaline
NAADP =	Nicotinic acid-adenine dinucleotide phosphate
NANC =	Non-adrenergic, non-cholinergic
ODQ =	1H-[1,2,4]Oxadiazolo[4,3- α]quinoxalin-1-one
NO =	Nitric Oxide
NOC-5 =	3-[2-hydroxy-1-(1-methylethyl)-2-nitrosohydrazino]-1-propanamine

NOC-12 =	N-ethyl-2-(1-ethyl-2-hydroxy-2-nitrosohydrazino)ethanamine
NOS =	Nitric oxide synthase
NPY =	Neuropeptide Y
P2 =	Purinergic receptor
PACAP =	Pituitary activating peptide
PIP2 =	Phosphatidylinositol 4,5-bisphosphate
PI-PLD =	Phosphatidylinositol specific phospholipase-D
PKG =	Protein kinase-G
PNS =	Peripheral nervous system
RGS =	Regulators of G-protein signalling proteins
RNS =	Reactive nitrogen species
RyR =	Ryanodine receptor
SERCA =	Sarco-endoplasmic reticulum Ca^{2+} pumps
SFR =	Stimulated whole salivary flow rate
sGC =	Soluble guanylate cyclase
SGH =	Salivary gland hypofunction
SjS =	Sjögren's syndrome
SNAP =	S-nitroso-N-acetyl-penicillamine
SNP =	Sodium nitroprusside
SOC =	Store-operated channels
SP =	Substance P
TM =	Transmembrane domain
TNF =	Tumour necrosis factor
VIP =	Vasoactive intestinal polypeptide
β PLC =	β -class of phosphoinositide-specific-phospholipase C enzymes

Chapter One

Introduction



UNIVERSITY OF
LIVERPOOL

1.1 Salivary Secretion

Nervous Control of Fluid Secretion

Salivary secretion as a result of nervous stimulation was demonstrated over a hundred years ago, using electrical stimulation of the lingual nerve and the submandibular glands from a dog (Ludwig, 1850). More recent studies have shown that salivary secretion is dependent on nerve-mediated mechanisms (Smith, 1996). The neural control of salivation is outlined in figure 1.1.1. Taste is the primary stimulation for salivation (Hector MP, *et al*, 1999) and the afferent pathway for input from taste is carried to the solitary nucleus within the medulla via the facial (VII) and the glossopharyngeal (IX) nerves. The solitary nucleus may also integrate input from mastication and responses in higher centres to senses such as smell or sight or even thought but mastication and taste are by far the most important stimulators of salivary secretion. The parasympathetic efferent pathways for the submandibular and sublingual glands are produced from the facial nerve via the submandibular ganglion.

The efferent (secreto-motor nerves) are controlled by both the sympathetic and parasympathetic divisions of the autonomic nervous system. Experimental animal models have demonstrated that stimulation of each nerve type independently leads to a variation in release and subsequently a variation in response. The parasympathetic nerves, which release acetylcholine (ACh), stimulate fluid secretion whilst the sympathetic nerves, which release noradrenalin (NA), stimulate protein secretion (Starling, 1927).

Many factors have the ability to affect salivary secretion. The classic examples for demonstration of this point are the 'conditioned-reflex' experiments performed by Pavlov, who induced salivation in dogs in response to the sound of a bell (Pavlov, 1927). For the parotid glands the parasympathetic efferent supply is from the

glossopharyngeal nerve via the otic ganglion. The sympathetic postganglionic pathways are from the cervical ganglion of the sympathetic chain (Smith, 1996). In addition there are several additional reflexes that are responsible for salivation; these include vomiting and stimulation of mechanoreceptors in the periodontal ligaments of the teeth (Hector and Linden, 1987; Scott et al., 1999) and oral mucosa (Scott et al., 1998). The stomach or upper intestines may also stimulate salivation in order to dilute or neutralize irritating substances such as when an individual feels nauseated (Dawes, 2004). In addition resting salivary flow is also subject to the natural circadian rhythms, which peak late afternoon and fall to almost zero during sleep (Dawes, 2004).

As a result of all these findings it was determined that fluid secretion by salivary acinar cells is ultimately controlled by the afferent and efferent nerve pathways.

Figure 1.1.1. Outlines the neural control of secretion.

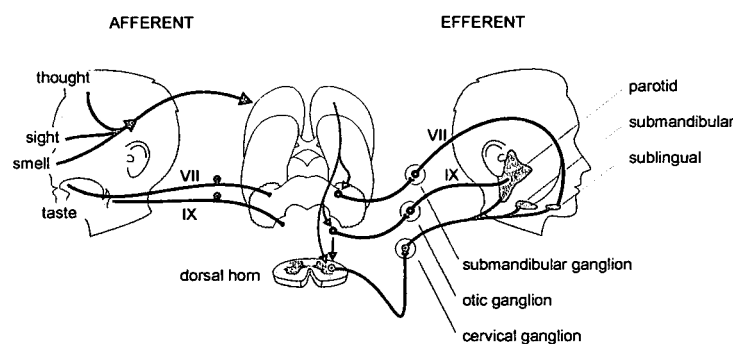


Figure 1.1.1: Diagram of the Afferent and Efferent pathways in the control of salivary secretion. Reproduced by the kind permission of Dr. P.M.Smith

So in summary the afferent pathways allow the response induced by taste to travel along the facial and glossopharyngeal nerves to the solitary nucleus in the medulla, which also integrates signals from other response centres such as smell or sight. The efferent pathways include both the parasympathetic and sympathetic nervous systems. Parasympathetic stimulation, by the facial nerve via the submandibular ganglion, results in secretion by the sublingual and submandibular glands.

Parasympathetic stimulation of the parotid gland is by the glossopharyngeal nerve via the otic ganglion. The sympathetic pathway is primarily responsible for protein secretion and involves the post ganglionic fibres from the cervical ganglion of the sympathetic chain.

The two nerve types, sympathetic and parasympathetic, travel by separate routes outside of the salivary glands but once within the glands they intermingle to form Schwann axon bundles (Garrett and Kidd 1993). The general distribution and number of cholinesterase positive parasympathetic nerves is similar in both the submandibular and parotid gland in man. The main nerve trunks run in the connective tissue adjacent to the main ducts and blood vessels. Nerve fibres are seen distributed to the blood vessels, acini and ducts. Adrenergic sympathetic nerves follow a similar pattern of distribution to the cholinergic nerves but are fewer in number (Garrett 1967).

Work conducted by Garrett and Kidd in 1993 focused on the neuro-effector relationships with the acinar cells at the terminal branches of the axons. Their data demonstrated that there were two possible relationships between the acinar cells and the nerves innervating the glands. These relationships were termed *Epilemmal* and *Hypolemmal* (Garrett and Kidd 1993). The key difference was how open the arrangement was between the axon and the acinar cell. The *Epilemmal* arrangement consisted of an axon which maintained its association with its Schwann cell and was positioned approximately 100nm beneath the basement membrane of the acinar cells but had a free surface exposed to the acinar cells. This particular arrangement is also observed between the axons and the smooth muscle of blood vessels occurring within the salivary glands.

The alternative, hypolemmal, situation occurs much less frequently. In this arrangement the axon is bare and dissociated from its Schwann cell laying between two acinar cells. Therefore, in this situation the axon is contained within the basement membrane and is in almost direct contact with the acinar cells as there is only a gap of 25nm or less (Garrett and Kidd 1993) (Figure 1.1.2).

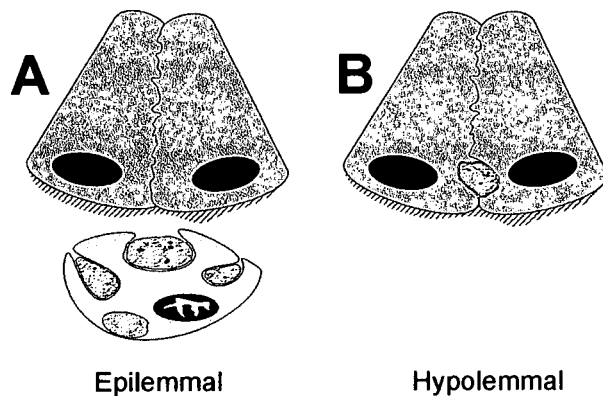


Figure 1.1.2: (A) Epilemmal and (B) Hypolemmal relationship of neurones to acinar cells. Used with the permission of Dr.L.J. Dawson

Within the submandibular and minor glands of humans both neuro-effector relationships have been demonstrated to occur (Garrett and Kidd 1993) but the situation in mice is as yet unknown. The hypolemmal arrangement is far more suited to situations which require more rapid responses to stimulation as the diffusion distance is greatly reduced allowing more rapid transit of the transmitter molecule to its designated receptor.

The more common, epilemmal arrangement, is consistent with the 1959 autonomic nervous system *ground plexus* concept described by Hilarp. This particular arrangement involves the neurons from both the sympathetic and parasympathetic nervous systems running side by side with maintained association with a Schwann cell. The axon then innervates a group of cells and the transmitter molecule moves by simple transmitter diffusion (Hilarp 1959). In situations when tissue is more sparsely innervated fewer cells will be directly contactable by axons. In such situations it is plausible that only one cell within a group is maintained in an effector

relationship with an axon. So as a direct result of this the whole group of cells are reliant on the transmission of signal from the axon contacted cell to the rest of the group and this would require some form of intercellular communication.

Intercellular communications have been demonstrated in many cell types and often involve the diffusion of second messengers and calcium through gap junctions (Rottingen and Iversen 2000) however with relation to acinar cells no such processes have, to date been, identified. This particular area of research will be considered further in the cell-cell introduction section.

Dual innervation is also observed in blood vessels as parasympathetic stimulation induces vasodilation and sympathetic stimulation induces vasoconstriction. However, vasoconstriction is independent of the salivary reflex (Garrett, Kerr et al. 1999).

Salivary glands also contain other types of transmitters as well as the main neurotransmitters acetylcholine (ACh) and adrenaline, and so do not rely solely on cholinergic and adrenergic stimulation (Ekstrom 1999). These alternative non-adrenergic, non-cholinergic (NANC) transmitters consist of neuropeptides and have also been described in the major and minor salivary glands. Gland fibres isolated from human submandibular tissue have been shown to be positive for neuropeptide Y (NPY), Vasoactive intestinal polypeptide (VIP), galanin (GAL), substance P (SP) and calcitonin gene-related peptide (CGRP) (Kusakabe, Matsuda et al. 1997). Further data suggest that the NPY, VIP, SP, CGRP and GAL fibres are densely distributed around the acini, ducts and blood vessels. In addition, when mucous and serous acini are compared (Kusakabe, Matsuda et al. 1997) fibres containing VIP, NPY and GAL are at a higher density around mucous acini and nerves containing VIP are more numerous in human submandibular glands (Kusakabe, Matsuda et al. 1998). However expression of particular nerves and transmitter may vary over time

with changes in salivary glands during development (Virta, Tornwall et al. 1992) and in the case of some conditions such as Sjögren's syndrome where there is focal infiltration of inflammatory mediators the nerve expression of neuropeptides may be downregulated (Pedersen, Dissing et al. 2000).

Signal transduction in salivary acinar cells

The neurotransmitter of the parasympathetic pathways is ACh which regulates fluid secretion.

ACh was the first neurotransmitter to be recognised. It was initially identified by Henry Hallett Dale in 1914 (Dale 1914) for its actions on heart tissue and subsequently confirmed as a neurotransmitter by Otto Loewi (Loewi 1921). ACh is a chemical transmitter involved in both the peripheral nervous system (PNS) and the central nervous system (CNS) of many organisms and is the neurotransmitter in all autonomic ganglia. ACh may be viewed as the classical neurotransmitter of the parasympathetic nervous system. In the salivary gland, once ACh is released from the nerve terminus it must diffuse a short distance before binding and stimulating cell surface muscarinic receptors (mAChR).

Muscarinic Receptors

The mAChR belong to a 7-membrane spanning domain receptor family but also belong to a class of metabotropic receptors which use heterotrimeric guanine nucleotide-binding proteins (G-proteins) as their signalling mechanism (Wess, Blin et al. 1995) and are separated into five subtypes. The five subtypes of mAChR are designated M1-M5 based on data from cDNA cloning, their intracellular coupling through different G-proteins and observable interactions with agonists and

antagonists of these receptors (Caulfield and Birdsall 1998). The use of the competitive mAChR antagonist atropine demonstrated that the release of ACh from parasympathetic nerves acts as the main inducer of fluid secretion.

Based on data from rat parotid gland (Baum and Wellner 1999), until relatively recently, there was widespread acceptance that an increase in salivary secretion in response to muscarinic agonists was mediated entirely through the mAChR type 3 receptor (M3R) (Caulfield 1993). M3R is known to predominate in rat, mice and human salivary glands (Perez Leiros, Sterin-Borda et al. 1999), but more recent data from rat and rabbit submandibular and rat sublingual glands have suggested that M1 receptors and other non-M3 receptors may also partially mediate fluid secretion (Culp, Luo et al. 1996); (Tobin 1995); (Tobin, Giglio et al. 2002). Tobin and co-workers also noted that cholinergic effects via M1 receptors involving nitric oxide may occur in the submandibular gland (Tobin 2002). More recent studies using knockout mice have enabled a much greater insight into the various mAChR subtypes involvement in salivary secretion (Gautam, Heard et al. 2004); (Nakamura, Matsui et al. 2004). These more recent data suggest that both M1 and M3 receptors may make contributions towards salivary secretion, but also that compared with M3 receptors, M1 receptors are not ubiquitously expressed on submandibular acinar cells (Nakamura, Matsui et al. 2004).

With respect to M3R there do not seem to be significant differences between species with regard to receptor homologs based on their pharmacological profiles (Caulfield and Birdsall 1998). Their amino acid sequences (aa) are highly conserved between species and they vary very little with regard to molecular mass as shown (table 1.1.1.). Mouse and rat aa M3R sequences only differ by 16h aa and the rat subsequently only varies from humans by 49 aa. So if you allow for conservative aa

changes this equates to a 94.4% homology between the M3R seen in the rat and that in the human.

Species	GenPet accession	Amino acid	Molecular mass
	Code	Number	
Rat	P08483	589	64.79kd
Mouse	AAG14344	589	64.79kd
Human	P20309	590	64.90kd

Table 1.1.1: Basic data for M3R for rat, mouse and human.

M1-M5, share a very similar three-dimensional arrangement. This structure comprises seven membrane-spanning domains which are referred to as transmembrane domains (TM) I –VII and these spanning domains are inter-linked by three extracellular and three intracellular loops referred to as i1-i3 (Wess, Blin et al. 1995) as demonstrated in figure 1.1.3.

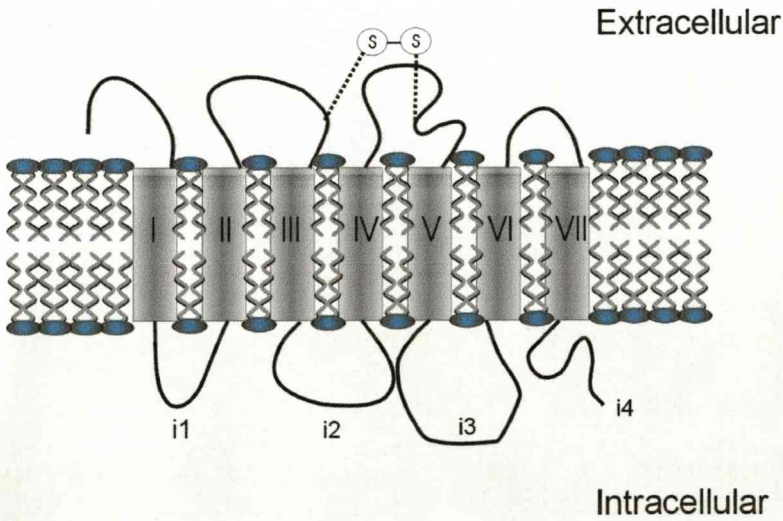


Figure 1.1.3: Diagrammatic representation of the orientation of the components of muscarinic receptors in the cell membrane. I-VII represent transmembrane domains. i1-i4 intracellular loops. Used with the permission of Dr.L.J. Dawson

Data suggest that ACh binds within a narrow cleft which is enclosed by a ring like arrangement of the seven TM domains and is believed to be about 1 to 1.5 nm away from the surface of the membrane. Site directed mutagenesis studies conducted using rat M3 receptors suggested that the ACh binding domain is formed from a series of hydrophilic aa that are located within the upper half of the TM domains between regions III, V, VI and VII and most likely consisted of Aspartate (Asp) and Tyrosine (Tyr). The most likely site of the interaction is the negatively charged TM III Aspartate residue, which is highly conserved between all biogenic amine receptors, as ACh is positively charged (Wess, Blin et al. 1995).

Signal Cascade

When the whole process of fluid secretion is broken down into individual parts of the signal cascade the point of initiation occurs when ACh binds to M3R and termination occurs with the secretion of electrolytes and fluid (Berridge 1993). The key point of this signal transduction process is that it has in-built amplification because the target enzyme is stimulated to generate multiple molecules of 2nd messenger for as long as the α -subunit of the G-protein is bound by guanosine 5'-triphosphate (GTP). Amplification is extremely significant to 2nd messenger signalling because it allows a very small extra-cellular stimulus to produce a very large intracellular event (Rodbell 1995).

G-Proteins

Once ACh binds to the M3R it activates the associated G-protein (figure 1.1.4: Part 1) which stimulates a cascade of responses involving subsequent 2nd messengers.

ACh acts as a ligand and binds with high specificity to M3R. How the M3R then interact with their G-protein is not completely understood (Wess, Blin et al. 1995; Kostenis, Zeng et al. 1999). The most likely scenario is that binding of ACh within the proposed cleft induces a conformational change which in turn allows a distinct intracellular domain to then interact with specific G-proteins. The most likely points of interaction are areas within the i2 and i3 loops as well as a long portion of the i4 tail as these are all thought to have the ability to form a three dimensional surface which would allow G-proteins to interact but only upon binding of ACh to the receptor (Wess, Blin et al. 1995).

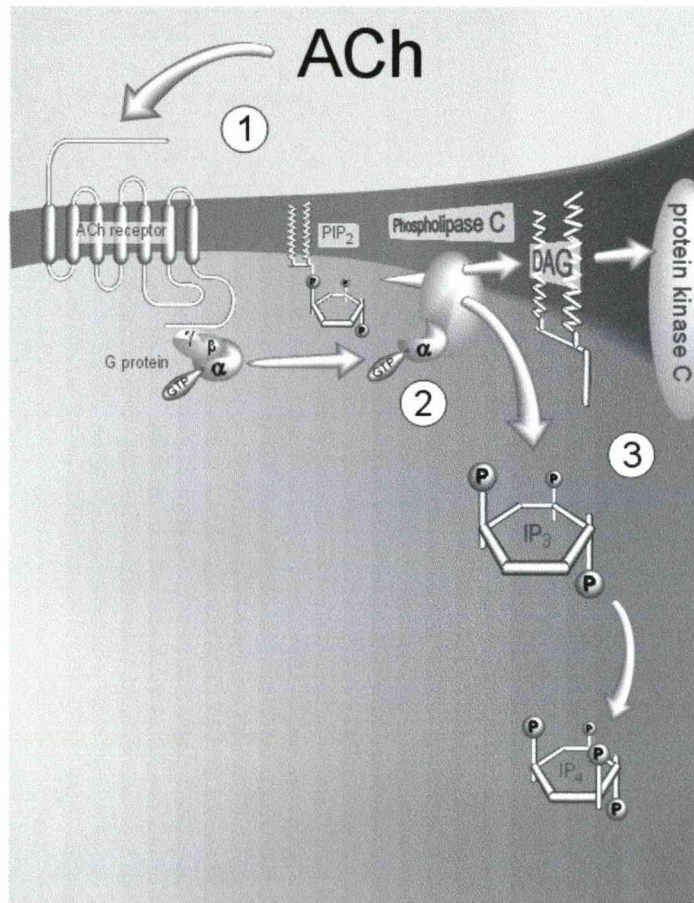


Figure 1.1.4: 1 = the binding of ACh to M3R activates Gα_q which binds GTP. 2 = the α subunit activates βPLC. 3 = PLC splits PIP₂ into DAG which activates protein kinase C and Ins(1,4,5)P₃ which diffuse into the cytoplasm. This picture was reproduced by the kind permission of Dr. P.M. Smith.

dimensional surface which would allow G-proteins to interact but only upon binding of ACh to the receptor (Wess, Blin et al. 1995).

The G-proteins themselves have a unique heterotrimeric structure, which is comprised of α, β and γ subunits and may be divided into four families based on their

α -subunits, termed s, i, q and 12/13 (Morris and Malbon 1999). With regard to fluid secretion the G-protein of interest are the $G\alpha_q$ (Wess, Blin et al. 1995) as these are linked to the M3R within the salivary glands. Upon activation of the G-protein the α -subunit dissociates leaving a $\beta\gamma$ -dimer and subsequently activates its target enzyme (Hancock 1997) (Figure 1.1.4: Part 2).

Dissociation of the heterotrimer into the α -subunit and $\beta\gamma$ -dimer occurs because the normally bound GDP is released from its guanine nucleotide-binding site and is rapidly replaced by GTP. The α -subunit also has an intrinsic GTP-ase which determines the duration of activation time. The heterotrimer is rapidly re-formed following hydrolysis of the GTP to GDP which allows for subsequent activations (Morris and Malbon 1999). The dissociation of the G-protein into its subunits provides the next link in the signal cascade.

The target of the newly dissociated α -subunits is β PLC with which they interact and regulate the activity of (Morris and Malbon 1999). Data also demonstrated that the $\beta\gamma$ -dimer is also active within this process (Boyer, Waldo et al. 1992) and that the β PLC enzyme is also able to function as a GTP activating protein (Berstein, Blank et al. 1992). β PLC is known to have 4 isoforms produced from soluble multidomain proteins (Rebecchi and Pentiyala 2000). The larger region is responsible for the interaction with G-proteins and the different isoforms have been shown to have different sensitivities to the α -subunit and $\beta\gamma$ -dimer which may also bind at different regions and have the ability to act additively (Rhee and Bae 1997); (Katan 1998).

When activated by the α -subunit of the G-protein β PLC function by cleaving the polar head group from inositol phospholipids and hydrolyse the membrane bound phospholipid phosphatidylinositol 4, 5-bisphosphate (PIP₂). Within the salivary glands hydrolysis of PIP₂ generates two intracellular 2nd messengers: Inositol 1,4,5,

triphosphate (IP_3) and diacylglycerol (DAG) (Berridge 1993) (Figure 1.1.4: Part 3). The purpose of IP_3 generation is to activate the release of intracellular Ca^{2+} and DAG is produced to activate protein kinase C (Rebecchi and Pentyla 2000). For the purpose of this discussion IP_3 will only be considered in relation to fluid secretion in salivary acinar cells.

Inositol 1,4,5, triphosphate (IP_3)

IP_3 is the intracellular 2nd messenger that is responsible for fluid secretion in salivary acinar cells (Ambudkar 2000). Upon its formation IP_3 diffuses rapidly into the cytosol where it binds to the IP_3 receptors (IP_3R). The IP_3R are predominately located at the apical

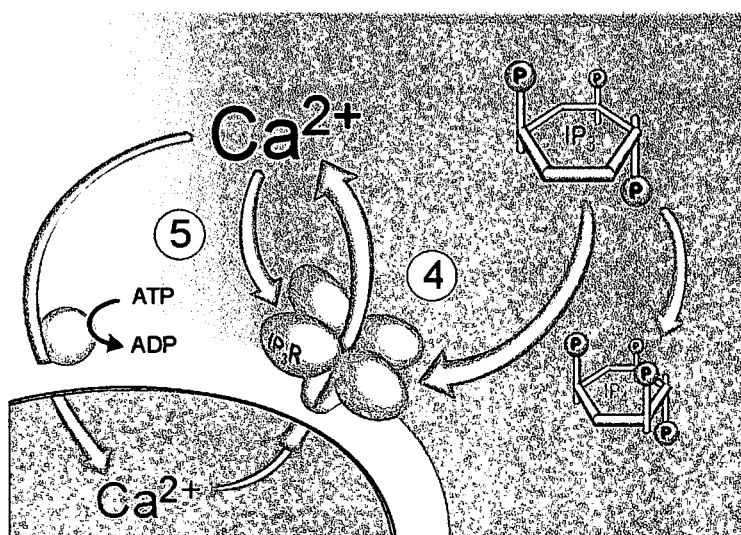


FIGURE 1.1.5. 4 = $\text{Ins}(1,4,5)\text{P}_3$ binds to a tetrameric IP_3R on the intracellular Ca^{2+} stores and causes Ca^{2+} release into the cytoplasm. There are at least 3 isoforms of IP_3R (I, II & III), the complete receptor may be a homo- or heterotetramer. 5 = Ca^{2+} released from the stores feeds back onto the IP_3R to stimulate Ca^{2+} -induced Ca^{2+} release. This picture was reproduced by the kind permission of Dr. P.M. Smith.

pole of acinar cells (Lee, Xu et al. 1997; Zhang, Wen et al. 1999).

The IP_3R are located on the endoplasmic reticulum (ER) which is generally accepted as the intracellular Ca^{2+} - store. IP_3R function as a receptor with an integral calcium channel. Their purpose is to facilitate Ca^{2+} release from intracellular stores (Berridge 1997; Gallacher and Smith 1999; Ambudkar 2000) as demonstrated by Figure 1.1.5: Part 4.

IP₃R is a homo- or heterotetrameric intracellular Ca²⁺-release channel that has a monomeric molecular mass of approximately 313kDa. The IP₃R's are tetramers and have three distinct domains, the ligand-binding domain, a regulatory domain and the Ca²⁺ - channel domain (Gallacher and Smith 1999). Three isoforms of IP₃R designated IP₃R1-3 have been identified in mammalian tissue and all three isoforms are structurally and functionally related (Gallacher and Smith 1999; Ambudkar 2000). All three isoforms have also been identified in salivary acinar cells and more importantly identified at the apical pole (Lee, Xu et al. 1997). It has also been determined that the different isoforms have different sensitivities to Ca²⁺ and IP₃ (Gallacher and Smith 1999). Of the three isoforms IP₃R1 is the most widely expressed and is found in all tissue types at all stages of development. Along with the 3 receptor isoforms four IP₃R genes have also been identified (Berridge 1997).

Based on the location of the binding site for IP₃ the major part of the protein resides in the cytosol (reviewed in (Bezprozvanny 2005)). Ca²⁺ acts as a complex regulator of IP₃Rs as high concentrations of intracellular Calcium (Ca²⁺) ion concentrations ([Ca²⁺]_i) inhibit IP₃R while inversely low [Ca²⁺]_i stimulate IP₃R activity (Finch, Turner et al. 1991); (Bezprozvanny, Watras et al. 1991). The regulation of IP₃R by Ca²⁺, IP₃ itself, sites of phosphorylation and calmodulin (Berridge 1997; Gallacher and Smith 1999; Ambudkar 2000) offers considerable scope for the dynamic regulation of IP₃R sensitivity. Its most likely that this positive regulation of the IP₃R by calcium is largely due to a direct binding of Ca²⁺ to the receptor ((Miyakawa, Mizushima et al. 2001); (Mak, McBride et al. 2003)) (figure 1.1.6. Part 5) but the mechanism by which calcium deactivates the receptor is much less clear but Calmodulin (CaM) has been suggested as being important to this process (Nadif Kasri, Bultynck et al. 2002).

The response of IP₃R to cytosolic Ca²⁺ levels is biphasic and upon activation IP₃R remain open longer when local [Ca²⁺]_i is low but rapidly close when a threshold level

of cytosolic Ca^{2+} is exceeded. This ability of IP_3R to regulate Ca^{2+} provides a dramatic enhancement of the Ca^{2+} mobilising properties of IP_3 and this phenomena is known as Ca^{2+} -induced Ca^{2+} release (CICR) (Berridge 1997). This process is believed to be a fundamental feature and determines the spatial extent and also the magnitude to which IP_3 induces $[\text{Ca}^{2+}]_i$ signals (Berridge 1997); (Marchant and Parker 2000).

Ryanodine Receptors (RyR)

In addition to IP_3R (Berridge 2005) there are also a second set of receptors, the Ryanodine receptors (RyR), which also facilitate Ca^{2+} release from the ER. Some cells contain both receptor types and may have more than one isoform of each (Morton-Jones et al., 2006; Yang et al., 2005). Like the IP_3R , RyR also undergo CICR. However, the sensitivity of RyR to Ca^{2+} is controlled by the cytosolic concentration of an alternative 2nd messenger to IP_3 , known as cyclic adenosine diphosphate-ribose (cADPr). cADPr is a product of βNAD which is in turn a product of ribosyl cyclase which is regulated by cyclic GMP and Nitric Oxide (NO) levels (see Introduction section 1.2 Nitric Oxide).

RyR are named after the plant alkaloid ryanodine to which they have a high affinity. RyR are also known to exist in 3 isoforms in mammals and each is encoded by a different gene (Conti, Gorza et al. 1996; Marziali, Rossi et al. 1996). Although found in small amounts in many types of tissues the RyR are also named after sources where they are found at high concentrations. RyR1 is expressed in skeletal muscle and was first isolated in rabbit fast twitch skeletal muscle and so may also be termed skeletal. RyR2 is expressed in the myocardium (muscle of the heart) and was first isolated in tissue from a canine heart and so is also termed cardiac. RyR3 is expressed widely, but at highest concentrations in the brain and so is also termed

brain but was first isolated in bovine diaphragm muscle (Vites and Pappano 1994); (Jeyakumar, Copello et al. 1998); (reviewed (Fleischer 2008)).

The functional RyR was initially thought to be a homotetramer which has a quarter foil shape and a size of approximately 22-27nm on each side and forms a cation-selective channel for the release of Ca^{2+} from the ER (Zucchi and Ronca-Testoni 1997). RyR were determined to be the largest channel structures with dimensions of approximately 29nm x 29nm x 12nm and a smaller trans-membrane assembly which protrudes 7nm. The isoforms are very similar but the variations between them are very important. Natural mutations in the human receptors are associated with a number of muscle diseases. The receptor has a mass of 2.3 ± 0.3 megadaltons (Saito, Tnui et al. 1989), the size of the polypeptide was subsequently estimated using northern blot analysis and was found to be about 550kDa (Marks, Tempst et al. 1989). The full aa sequence of RyR1 was found to be approximately 565 kDa. From all this data it was determined that the RyR must be comprised of 4 identical subunits or receptor protomers and is therefore a homotetramer (reviewed (Fleischer 2008)).

Within excitable tissues RyR's are considered to be the principal mediator of Ca^{2+} -induced- Ca^{2+} release in (CICR) (Gallacher and Smith 1999), the primary reason for this is that other ligands are unable to activate the channel when Ca^{2+} is absent (Zucchi and Ronca-Testoni 1997). The two receptor types are found at opposing poles in acinar cells because as previously stated the IP_3R are predominantly located at the apical pole where as the RyR's are primarily located in the basolateral pole In the rat parotid gland (Lee, Xu et al. 1997; Zhang, Wen et al. 1999). Therefore, the Ca^{2+} signal is triggered by the activity of IP_3 but then actively propagated across the acinar cell by CICR following the activity of both IP_3R and RyR.

Calcium Signals

In salivary acinar cells the brief burst of Ca^{2+} needed for the initiation of cellular signalling events is usually derived from the stores of Ca^{2+} present within the ER, as a result of the coordinated opening of the IP_3R and/or the RyR (Berridge 1997). Both the IP_3R and the RyR are sensitive to Ca^{2+} i.e. they display the phenomenon of CICR. As is found in the IP_3R Ca^{2+} also has a biphasic effect upon RyR , as the $[\text{Ca}^{2+}]_i$ increases there is a positive feedback resulting in more Ca^{2+} release, but as soon as the $[\text{Ca}^{2+}]_i$ reaches a certain level the feedback switches from positive to negative inhibiting further channel activity (Berridge 1997). Due to the regenerative nature of the Ca^{2+} signal the activity of the IP_3R and RyR can be coordinated directly via the level of Ca^{2+} (Figure 1.1.6.).

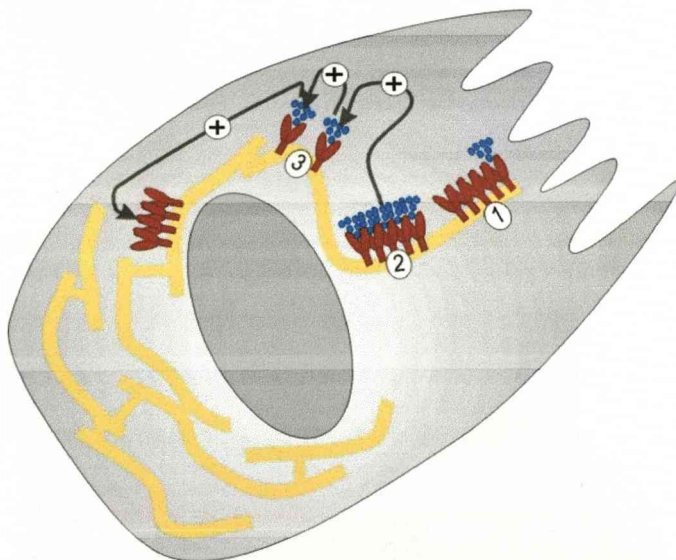


Figure 1.1.6: Diagrammatic representation of the ER arrangement to allow for Ca^{2+} - tunnelling. The diagram also introduces the concept of Ca^{2+} - induced Ca^{2+} release and the coordination of receptors by the level of Ca^{2+} . 1 = Ca^{2+} blip/quark. 2 = Ca^{2+} puff/spark. 3 = propagation of intracellular Ca^{2+} wave. Yellow lines = endoplasmic reticulum, Blue circles = Ca^{2+} and Red 'Y' shapes IP_3R and RyR . The level of Ca^{2+} released determines the over all outcome and extent of the cellular response hence the smaller Ca^{2+} releases stated here. Used with the permission of Dr.L.J. Dawson

The main function of ACh-evoked Ca^{2+} -signalling in salivary acinar cells is to drive movement of water from the basolateral pole of the acinar cell to the apical pole situated along the glandular lumen. This whole process is made possible by the activation of Ca^{2+} -dependent Cl^- and K^+ channels which are situated in the apical and basolateral parts of the acinar cell plasma membrane respectively (Smith 1996)

which in turn leads to mobilisation of electrolytes and fluid secretion (Melvin, Yule et al. 2005).

The secretory process also utilises extra-cellular Ca^{2+} as well as mobilising stored Ca^{2+} . Movement of Ca^{2+} from the extra-cellular environment to the intracellular Ca^{2+} stores across the plasma membrane is stimulated by depletion of intra cellular Ca^{2+} and is known as capacitance Ca^{2+} entry (CCE) ((Putney 1990); (Berridge 1995) but is still poorly understood but most likely depends on the conformational coupling between IP_3 receptors and the plasma membrane Ca^{2+} influx channels, this whole process is termed calcium influx.

Calcium signals are highly expensive in metabolic terms because the cell has to actively pump Ca^{2+} out of the cytoplasm as sustained elevated Ca^{2+} levels are cytotoxic. The ability of acinar cells to spatially restrict Ca^{2+} signals offers a solution to the problem. The polarisation of the acinar cell and arrangement of all the secretory processes in the apical pole of the cell also makes discrete Ca^{2+} signals possible.

The images in figure 1.1.7 are of a mouse submandibular acinar cell, loaded with a Ca^{2+} sensitive fluorescent dye and stimulated with a low concentration of ACh. They demonstrate the ability of salivary acinar cells to generate local Ca^{2+} signals. The fluorescence intensity is colour coded to produce a clear visualisation of variations in Ca^{2+} concentration. The apical pole is at the bottom right of the images which were captured at 500ms intervals (see sections 2.8 measurement of $[\text{Ca}^{2+}]_i$ and 2.9 microfluorimetry).

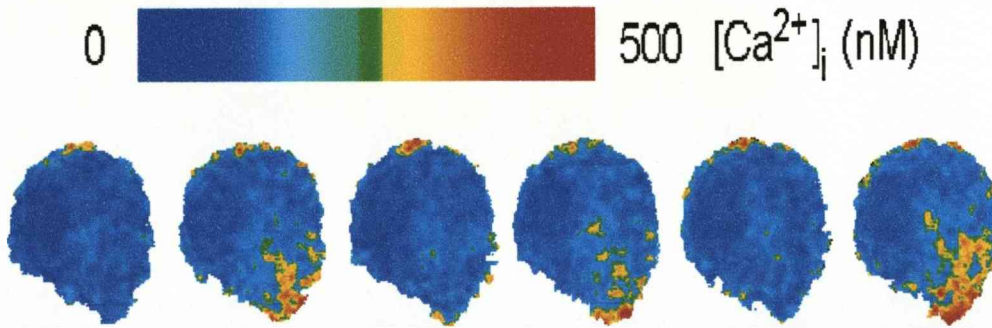


Figure 1.1.7: Series of cell images clearly showing that the $[Ca^{2+}]_i$ increases and decreases very rapidly at only the apical pole. Data suggest that it is possible to stimulate fluid secretion with a signal as small as the one demonstrated here (Harmer, Smith et al. 2005). The most simplistic explanation as to why these small local Ca^{2+} signals do not develop into global Ca^{2+} signals is that they are so brief that they do not have time to do generate sufficient Ca^{2+} levels around the IP_3R or RyR to induce CICR. Images used with kind permission of Dr P.M.Smith.

Salivary acinar cells have a wide repertoire of Ca^{2+} signals they are capable of that include very brief localised signals through to cell-wide sustained elevations in $[Ca^{2+}]_i$ that may persist for minutes at a time. It is unclear which of these responses is the most "physiological". However, spatially restricted, low level, signals in many ways make the most biological sense because they will be least cytotoxic and the most energy efficient.

As stated earlier, in salivary acinar cells Ca^{2+} signals initiate at the apical pole of the cell. This observation has caused some controversy as the main Ca^{2+} store is the ER that is primarily situated at the basolateral pole of the cell. Available data support the model of *Calcium tunnelling* (Mogami, Nakano et al. 1997). In this model there are tiny strands of ER at the apical pole of the cell from which Ca^{2+} is released. Localised on these strands of ER are high concentrations of IP_3R (Nathanson, Fallon et al. 1994) and would therefore be more sensitive to IP_3 (Thorn, Lawrie et al. 1993). Furthermore, the ER is a continuous element throughout the cell so Ca^{2+} stored in the ER at the basolateral pole of the cell could in theory "tunnel" through the cell to be released at the apical pole as shown in figure 1.1.8.

blood

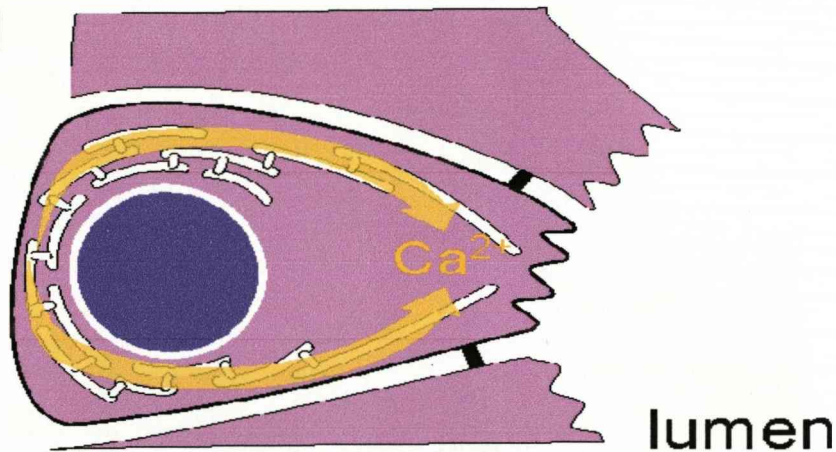


Figure 1.1.8: Shows a highly simplified diagram of an acinar cell including movement of Ca^{2+} from the basolateral to the apical pole of the cell via calcium tunnelling for calcium release at the apical pole of the cell. Diagram by kind permission Of Dr P.M.Smith.

Cyclic adenosine diphosphate-ribose (cADPr)

Cyclic adenosine diphosphate-ribose (cADPr) is a relatively recently described second messenger. It was originally identified in 1989 by Lee and colleagues (Lee et al., 1989), whilst studying calcium release by microsomes derived from the endoplasmic reticulum of sea urchin eggs, and was subsequently demonstrated to have a role in Ca^{2+} mobilisation in both sea urchin eggs (Galione, McDougall et al. 1993; Galione, White et al. 1993) and pancreatic acinar cells (Thorn, Gerasimenko et al. 1994). cADPr was found to be a low molecular weight metabolite of the pyridine nucleotide; nicotinamide adenine dinucleotide (NAD^+). Lee and co-workers also provided direct evidence that both cADPr and IP_3 were involved in mediating the increase in during fertilisation in sea urchin eggs (Lee, Aarhus et al. 1993).

These data suggested that cADPr, was likely to be an important addition to the family of cyclic nucleotides acting as second messengers.

Following the experimental determination that cADPr was as functionally active as IP₃ in terms of its ability to mobilise intracellular calcium in sea urchin eggs, the production of the enzyme responsible for cADPr had to be determined. The enzyme was originally purified in *Aplysia californica* as an aqueous soluble enzyme from the ovotestis (Hellmich and Strumwasser 1991) and was immediately suggested to be some type of NADase. Work done by Lee and Aarhus (1991) (Lee and Aarhus 1991) demonstrated that the *Aplysia* enzyme catalysed the conversion of NAD⁺ to cADPr and nicotinamide. In order to distinguish this enzyme from other conventional NADases that also produce ADP-ribose, the name ADP-ribosyl cyclase was suggested.

Data indicated that either cADPr was functioning along a totally alternative receptor system pathway or it had a much higher affinity for IP₃ receptors than IP₃ itself (Worley, Baraban et al. 1987). The idea of a higher affinity for IP₃ receptors was rapidly dismissed because high concentrations of cADPr had little effect on IP₃ response and functioned only to desensitise the microsomes to it. The receptor responsible for binding cADPr was determined to be different to IP₃ receptor as the use of heparin, a competitive inhibitor of IP₃ binding, still allowed cADPr to function (Worley, Baraban et al. 1987); (Dargie, Agre et al. 1990).

It was also determined that IP₃ and cADPr had an inverse relationship with one another in terms of the amount of calcium available for release. When the release of calcium by one activator (IP₃ or cADPr) was small the response induced by the other activator, at maximal dose, would be great although there was no change in total amount of releasable calcium (Dargie, Agre et al. 1990). These data strongly suggested that IP₃ and cADPr released calcium from overlapping stores. There was also no obvious evidence of synergy between the activators as the use of both only

increased the amount of calcium released by 20-30% compared to each individually. Experimental results for cADPr suggested: (a) that the effectiveness of cADPr *in vivo* was comparable to IP₃; and (b) the mechanism for calcium release was independent to IP₃ (Dargie, Agre et al. 1990).

Although there was obviously a specific binding site for cADPr on sea urchin egg microsomes, its exact nature was at this point undetermined (Lee 1991). Upon identification of the second class of intracellular calcium release channels, the RyR, in sea urchin eggs (Galione, Lee et al. 1991), the idea that cADPr was an endogenous regulator of the RyR formed.

Recent data suggest cADPr may have a role in Ca²⁺ mobilisation in salivary gland cells isolated from the rat (Yamaki, Morita et al. 1998), dog (Masuda and Noguchi 2000) and mouse (Harmer, Smith et al. 2001). Data demonstrate that when mouse submandibular acinar cells were exposed to a RyR agonists such as caffeine it evoked localised Ca²⁺ 'spikes' (Smith and Gallacher 1992). These data provide support for c-ADP-ribose/RyR interactions having an important role in Ca²⁺-signalling in salivary tissue.

The original research conducted in sea urchin eggs suggested that the RyR/cADPr pathway was 'redundant' (Galione, McDougall et al. 1993) as the traditional IP₃ mediated Ca²⁺-release pathway seemed to fulfil all the requirements for a signal transduction pathway. However, it has more recently been demonstrated that the level of cADPr within the acinar cell has the ability to determine the magnitude of the response to stimulation with ACh (Harmer, Smith et al. 2001). These subsequent findings suggest that acinar cells may have an alternative mechanism to adjust their sensitivity to agonist stimulation.

Fluid Secretion

The main function of ACh-evoked Ca^{2+} -signalling in salivary acinar cells is to drive the movement of water from the basolateral pole of the acinar cell to the apical pole situated along the glandular lumen. This whole process is made possible by the activation of Ca^{2+} -dependent Cl^- and K^+ channels which are situated in the luminal and basolateral parts of the acinar cell plasma membrane respectively (Smith, 1996). This step is pivotal for fluid secretion and is regulated by $[\text{Ca}^{2+}]_i$ and determines whether or not the cell secretes. It would be impossible to study fluid secretion in individual acinar cells so the study of Ca^{2+} is the most appropriate research method for fluid secretion as it is a direct representation but only became possible with the development of calcium sensitive dyes such as Fura-2AM (Tsien 1980). The vital point to note is that mobilisation of Ca^{2+} drives fluid secretion as demonstrated by the simple flow diagram below (Figure 1.1.9).

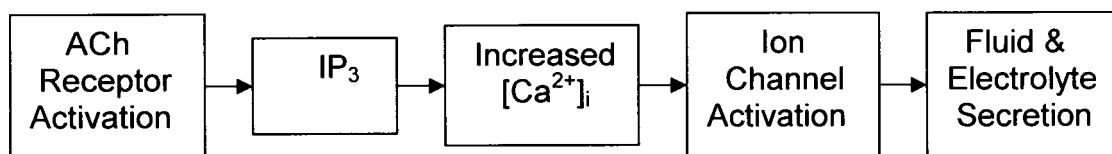


Figure 1.1.9: simple flow diagram representing simple steps of secretion

Once Ca^{2+} mobilisation has been stimulated by ACh receptor activation and production of IP_3 , as explained in full in previous sections, the subsequent processes involved in fluid secretion may be broken down into three steps as shown in figure 1.1.10:

- (1). Although not shown in the diagram there is a Na^+/K^+ ATPase present in the basolateral membrane of the cell which uses energy produced from the break down of ATP to pump Na^+ out of the acinar cell. So the acinar cells use active transport to increase cytoplasmic Cl^- concentrations. This creates an inwardly directed Na^+ gradient which energises a $\text{Na}^+/\text{K}^+ / 2\text{Cl}^-$ co-transporter

which is also situated at the basolateral membrane of the cell. The $\text{Na}^+/\text{K}^+/\text{2Cl}^-$ co-transporter ensures a continuous flow of Cl^- .

(2). As the concentration of Cl^- increases above its electrochemical potential it moves along its gradient and once Ca^{2+} has induced opening of the Ca^{2+} - dependent K^+ and Cl^- channels Cl^- will cross the apical membrane into the lumen of the acinus. So activation of the luminal Cl^- channel allows Cl^- to enter the glandular lumen along its electrochemical gradient. The purpose of the Ca^{2+} -dependent K^+ channel is to balance the loss of Cl^- as if left unchecked the movement of Cl^- would result in a change in membrane potential.

(3). As Cl^- accumulates in the glandular lumen Na^+ crosses the acinar cell to maintain *Electro-neutrality*. As the levels of NaCl increase the resultant osmotic gradient moves water (Smith, 1996). So ultimately the movement of Na^+ and Cl^- drives the movement of water resulting in fluid secretion.

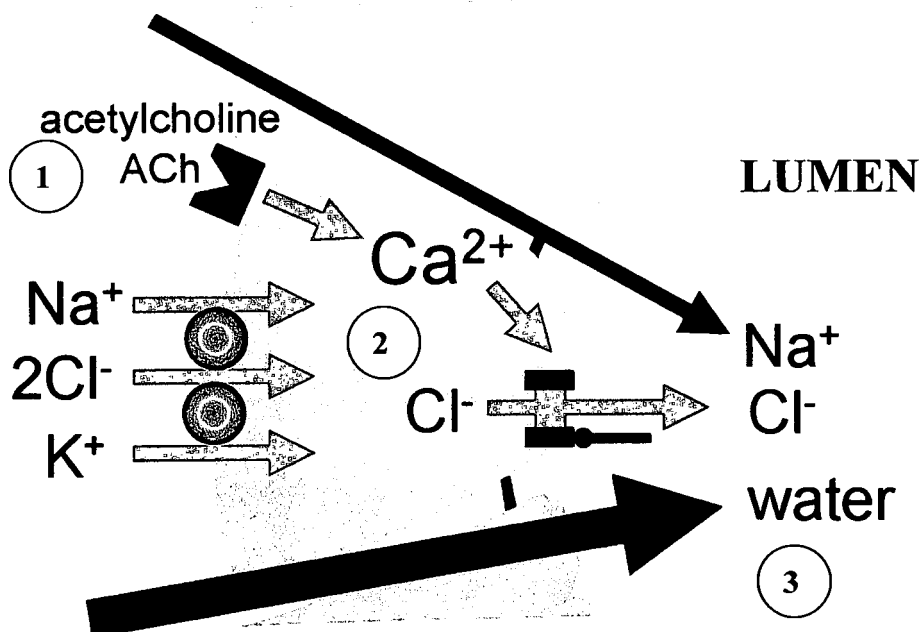


FIGURE 1.1.10: Diagrammatic overview of the formation of primary saliva by salivary acinar cells in response to stimulation by ACh. This picture was reproduced by kind permission of Dr. P.M. Smith.

1.2 Nitric Oxide (NO)

Background

In recent years NO has been viewed as a *double edged sword* capable of inducing both positive and negative effects on biological systems. NO has been found to be produced in virtually every type of cell in the body and to play important roles in controlling the normal functions of the cells. NO may also be involved in the regulation of much larger scale processes such as the immune and nervous systems.

NO was first identified in 1772 by Joseph Priestly as a simple gaseous molecule which consisted of just one atom of nitrogen and one atom of oxygen and was simply viewed as an atmospheric pollutant. However, in the 1980 Robert Furchgott, and co-workers, (Furchgott and Zawadzki 1980) were investigating the mechanism of vasodilatation and noted that ACh could only induce blood vessel relaxation if endothelial cells were present. They demonstrated that endothelial cells release a vasodilator when stimulated with agonists. These data suggested that the endothelial cells released something required by the smooth muscle cells for relaxation of the blood vessels. As a result of this finding this potent vasodilator was termed Endothelial Derived Relaxing Factor (EDRF) and was initially assumed to be a protein like most other signalling molecules and so stimulated intense research to identify what EDRF actually was. During a similar period of time Ferid Murad was independently investigating how nitroglycerin functioned. His data demonstrated that nitroglycerin released NO which is able to cause relaxation of the smooth muscle cells (Murad 1978). However, in 1986 Louis Ignarro (Ignarro, Buga et al. 1987) finally put these two pieces of the puzzle together, and identified that EDRF was in fact NO. The discovery that EDRF was actually NO, a highly reactive gas, led to an explosion of interest in this field and has resulted in the publication of over 60,000 papers. In

1998, in recognition of the impact of this discovery Furchgott, Murad and Ignarro were awarded the Nobel Prize in medicine or physiology.

Biological diversity of NO

NO is a major signalling molecule and has important roles as a bio-regulator within the nervous, immune and cardiovascular systems (Moncada, Radomski et al. 1988); (Moncada, Palmer et al. 1991); (Stefano, Liu et al. 1996); (Cooke and Dzau 1997); (Cooke and Dzau 1997); (Kinoshita, Tsutsui et al. 1997); (Faraci, Sigmund et al. 1998); (Blaise, Gauvin et al. 2005). NO participates in normal cellular function but may also initiate cytotoxic events either directly by the formation of free radicals, or indirectly by inducing apoptosis. Data suggest that NO acts primarily along the cyclic guanosine 3',5'-monophosphate (cGMP) pathway (Blaise, Gauvin et al. 2005), which is hypothesised to be the main physiological pathway of NO (Chung, Pae et al. 2001) as shown in figure 1.2.1.

However, NO is also able to act independently of this pathway (Chung, Pae et al. 2001). NO is unique, by being: (i) a gas neurotransmitter; (ii) a small hydrophobic molecule able to diffuse up to several hundred microns removing the need for a specialised transport system; and (iii) being able to affect sites distant from its point of origin. Though it is only able to persist

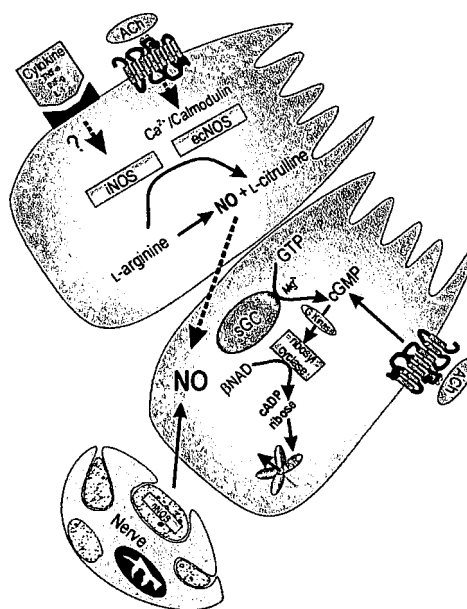


Figure 1.2.1: The likely NO pathway in salivary acinar cells. Abbreviations: NO, diatomic radical nitric oxide; iNOS, inducible nitric oxide synthase; eNOS endothelial nitric oxide synthase; nNOS nerve nitric oxide synthase; sGC, soluble guanylate cyclase; cADPr, cyclic adenosine diphosphate-ribose; RyR, ryanodine receptor.

and diffuse a limited distance, only several cell diameters, from its point of synthesis (Taha, Kiechle et al. 1992); (Malinski, Taha et al. 1993); (Lancaster, Werner-Felmayer et al. 1994); (Huang, von Rad et al. 2002) because it is readily oxidised to NO_2^- and NO_3^- under normal physiological conditions and therefore needs no separate mechanism for its removal.

The biological effects of NO are mediated through its reaction with a number of targets such as heme groups, cysteine residues and iron and zinc clusters, as it has a high affinity for metal ions.

In the absence of metals and proteins which contribute to NO destruction, and at low concentrations of NO, the decomposition of NO is much slower (Denninger and Marletta 1999), in these circumstances NO could have the ability to accumulate and reach higher concentration levels. When NO is at higher concentration levels it is known to react with O_2 producing N_2O_3 which is recognised as a powerful nitrosilating agent and is capable of reacting with any sulphur or cysteine aa residues (Denninger and Marletta 1999).

In the immune system, NO plays a vital role and is produced at high concentrations by specialised immune cells such as macrophages and lymphocytes (Forstermann, Gath et al. 1995); (Lomniczi, Suburo et al. 1998). The production of NO by immune cells helps to protect the body against infection including bacterial, viral and parasitic infections. However, just as too much NO is toxic to invading cells, the host cells may also be damaged by high NO levels and as a result NO has been implicated in conditions involving auto-immunity such as rheumatoid arthritis and Sjögren's syndrome (Konttinen, Platts et al. 1997); (Wanchu, Khullar et al. 2000). NO has also been shown to be involved with both the central and peripheral nervous system and

appears to play a role in promoting the transfer of nerve signals from one neuron to another, as a result of this NO has been implicated in nervous system diseases such as Parkinson's, Huntington's and Alzheimer's disease (Tabuchi, Oh et al. 1996); (Fitzsimonds and Poo 1998); (Hawkins, Son et al. 1998); (Tao and Poo 2001). NO has also been implicated in numerous physiological and pathophysiological neurodegenerative diseases due to its role as a key modulator in physiological processes such as memory, long term potentiation and also long term depression (Blaise, Gauvin et al. 2005).

Production of NO

NO is a short-lived, highly reactive molecule with a half life of only a few seconds. It is produced by a group of enzymes known as nitric oxide synthases or NOS (Moncada, Rees et al. 1991); (Moncada and Higgs 1993). These enzymes cause conversion of L-arginine into citrulline, NADP and NO through their enzymatic oxidation activity on the aa guanidine group of L-arginine (Marletta, Hurshman et al. 1998). The process occurs in two sequential monooxygenase reactions and requires NADPH and molecular Oxygen (Blaise, Gauvin et al. 2005). There are three known isoforms of NOS and they were named according to their mode of activity or the type of tissue they were originally described in. The three forms are referred to as: Type 1 neuronal NOS or n-NOS; Type 2 inducible NOS or i-NOS; and Type 3 endothelial NOS or e-NOS (Forstermann, Gath et al. 1995). Mitochondria also contain a unique NO-producing enzyme known as mt-NOS (Haynes, Elfering et al. 2004).

Data from experimental immunohistochemistry has subsequently demonstrated that nNOS is expressed in sympathetic ganglia, adrenal glands, peripheral nerves and in the endothelial cells of the lung, uterus and stomach (Forstermann, Gath et al. 1995). In addition nNOS has also been identified in the neurones which stimulate the

salivary acini. NO has also been found, but to a much lesser extent, within the ductal cells of rat submandibular and sublingual glands (Takai, Uchihashi et al. 1999); and human labial glands (Feher, Zelles et al. 1999; Pedersen, Dissing et al. 2000). However, the distribution of iNOS was much more variable particularly dependent on the origin of the detection antibody (Konttinen, Platts et al. 1997) so the definitive location of iNOS within acinar cells remains open to conjecture.

As the name implies eNOS was first identified in blood vessel endothelial cells (Forstermann, Gath et al. 1995). eNOS has been demonstrated in the cytosolic fractions of mouse and rat parotid and submandibular glands (Mitsui, Yasuda et al. 1997). However, in human salivary glands it has only been observed at very low levels (Konttinen, Platts et al. 1997; Brennan, Umar et al. 2000). Unlike nNOS and iNOS, eNOS is over 90% particulate, but in common with nNOS its activity is modulated by physiological levels of Ca^{2+} /calmodulin (Forstermann, Gath et al. 1995). nNOS and eNOS are constitutively expressed and Ca^{2+} dependent whereas iNOS is inducible and Ca^{2+} independent. The genes encoding for the three forms of NOS are distinct and located on three separate chromosomes, 7, 12 and 17 respectively (Cooke and Dzau 1997); (Kinoshita, Tsutsui et al. 1997); (Moncada 1997); (Faraci, Sigmund et al. 1998). The existence and presence of both constitutive and inducible forms of NOS suggests that they may have distinct functions (Cotton, Herrick et al. 1999).

The three types of NOS differ in their: (a) amino acid sequence; (b) post-translational modifications; (c) function; and (d) cellular location. There is also a variation in their capacity to be regulated by levels of Ca^{2+} / Calmodulin (Forstermann, Gath et al. 1995). The three main NOS types share a 49-56% homology, which makes identifying them via western blot difficult due to the limited antibodies commercially available of which most of these antibodies are directed against the C-terminal half of

the enzyme (the reductase domain) where most of the homology among the NOSs is present and this region also shows pronounced sequence similarities to cytochrome P450 reductase (Bredt, Hwang et al. 1991); (Haynes, Elfering et al. 2004). nNOS and eNOS are constitutively expressed and are involved in signal cascades whereas levels of iNOS increase in response to cytokines. The constitutive forms, nNOS and eNOS, are thought to account for the rapid, transient, calcium-dependent production of NO (Bredt and Snyder, 1990; Mayer et al., 1989, 1990) as they produce NO at low levels for short periods of time. iNOS is only expressed once activated by a signal transduction cascade in response to immunological or pathophysiological conditions (MacMicking, Xie et al. 1997).

iNOS produces high levels of NO and is independent of Ca^{2+} / Calmodulin levels but may be induced by many cell types (including lymphocytes, macrophages and endothelial cells) in response to contact with both cytokines and bacterial lipopolysaccharides (Forstermann, Gath et al. 1995). No other control mechanisms have so far been identified for iNOS. Therefore iNOS functions as both a regulator and an effector of the immune response. Within the salivary glands iNOS has been suggested to be present within macrophages and ducts (Lomniczi, Suburo et al. 1998) as well as with the acinar cells themselves (Kontinen, Platts et al. 1997).

The functional NOS protein is a dimer formed from two identical sub-units. Within each sub-unit there are three distinct domains: (1). a reductase domain; (2). a calmodulin-binding domain; and (3). an oxygenase domain. The Reductase domain contains Flavin Adenine Dinucleotide (FAD) and Flavin Mononucleotide (FMN) moieties which functions to transfer electrons from NADPH to the oxygenase domain of the opposite sub-unit of the dimer. The calmodulin binding domain is extremely important as calmodulin is necessary for the activity of the constitutive NOS isoforms eNOS and nNOS and is able to detect changes in $[\text{Ca}^{2+}]_i$ although exact

function does vary between these NOS isoforms. The oxygenase domain contains the binding site for tetrahydrobiopterin, heme and arginine and acts to catalyse the conversion of L-arginine into citrulline and NO (Marletta 1994).

The direct effect that NO exerts for most of its physiological actions is through binding to a specialised heme moiety on the enzyme soluble guanylyl cyclase (sGC). This interaction results in a conformational change, which in turn activates sGC. The activation of sGC induces the production of cGMP from GTP and this molecule is able to engage numerous targets downstream. In salivary acinar cells the activation sGC by NO results in the accumulation of cGMP which is produced from GTP (Michikawa, Mitsui et al. 1998; Denninger and Marletta 1999; Tritsarlis, Looms et al. 2000; Looms, Tritsarlis et al. 2001). The RyR are known to be the primary target of the cGMP mediated NO signal cascade and interaction with RyR induces release of Ca^{2+} from intracellular stores (Chapter 1 Introduction 1.1 salivary secretion section).

Increasing $[\text{cGMP}]_i$ is believed to lead to formation of cADPr through the action of PGK and sGC (Galione, White et al. 1993; Looms, Tritsarlis et al. 2001) on βNAD^+ . Subsequent data demonstrated that once formed, cADPr has the capacity to activate RyR's which leads to a rise in $[\text{Ca}^{2+}]_i$ (Smith and Gallacher 1992; Yamaki, Morita et al. 1998; Harmer, Gallacher et al. 2001; Looms, Tritsarlis et al. 2001).

Overall, these findings may have important implications in Sjögren's syndrome, as the data strongly suggest that NO may have the ability to modulate the magnitude of the $[\text{Ca}^{2+}]_i$ subsequent to salivary acinar cell stimulation by agonist. In Sjögren's syndrome sources of NO include not only that produced by invading immune cells but also NO may be produced by the salivary and lacrimal acinar cells themselves as NOS activity and cGMP production were significantly increased following activation of muscarinic receptors by antimuscarinic antibodies or carbachol (Bacman, Berra et al.

1998; Perez Leiros, Sterin-Borda et al. 1999; Bacman, Berra et al. 2001) in a Ca^{2+} -dependent manner.

Control of NO production

One of the main factors which control NO production is the actual location of the NO production or, more precisely, where the NOS are found. Data indicate that: (a) NOS isoforms can be targeted to different regions of the cell, so NO will be produced in close proximity to its target proteins (Harris, McCormick et al. 2008) as it is rapidly broken down; and (b) that there is very little region cross-over between NOS isoforms, so the variations in regions may determine that the NO produced has different functions and interacts with different targets. The NOS isoforms may also be regulated by the phosphorylation and de-phosphorylation of specific residues. eNOS shows increased activity following phosphorylation of specific residues (Looms, Tritsarlis et al. 2002) but data suggests that phosphorylation of nNOS may only induce inhibition (Looms, Tritsarlis et al. 2002).

NO synthesis may be inhibited by methylated analogues or arginine, asymmetric dimethylarginine (ADMA) and mono methylarginine (L-NMMA). These are competitive inhibitors of NOS which are produced endogenously by post-translational methylation of arginine residues in proteins but may be liberated by hydrolysis (MacAllister, Parry et al. 1996); (Fickling, Holden et al. 1999); (Dayoub, Achan et al. 2003); (Ayling, Whitley et al. 2006).

1H-[1,2,4]Oxadiazolo[4,3-a]quinoxalin-1-one (ODQ) may be used as a pharmacological control of NO. It is cell permeable and a potent and selective inhibitor of NO-sensitive guanylyl cyclase. ODQ doesn't chemically inactivate NO itself but does however inhibit cGMP generation in response to donors of NO. ODQ does

not inhibit NO-mediated macrophage toxicity, which is unrelated to cGMP and it also doesn't affect the activity of particulate guanylyl cyclase or adenylyl cyclase (Wang, Rechenmacher et al. 1998); (Southam, Charles et al. 1996); (Brunner, Stessel et al. 1995).

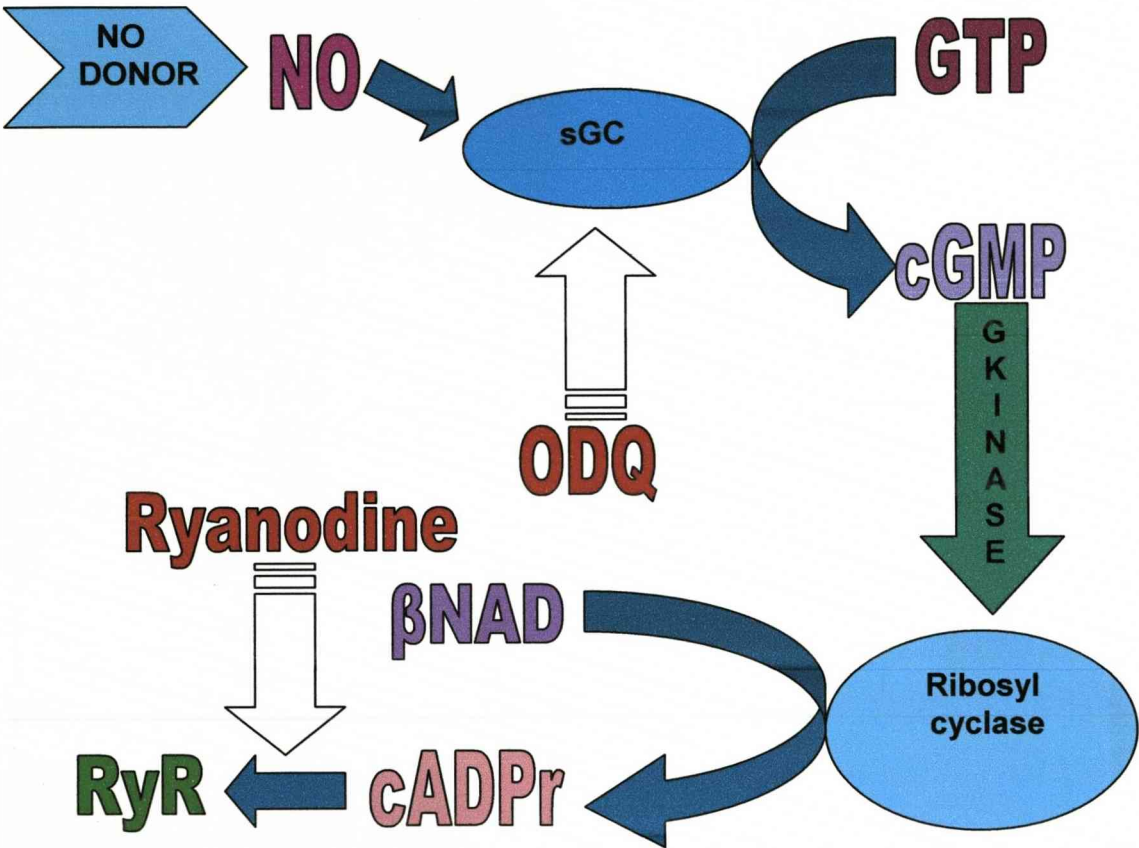


Figure 1.2.2: Diagram depicting the pathway of NO activity and control. White arrows signify points of inhibition and blue arrows refer to downstream reactions. **NO** – Nitric Oxide, **sGC** – soluble guanylate cyclase, **GTP** – Guanosine 5'-triphosphate, **cGMP** – cyclic guanosine 3',5'-monophosphate, **βNAD** – beta nicotinamide adenine dinucleotide, **cADPr** – cyclic adenosine diphosphate ribose, **RyR** – Ryanodine receptor and **ODQ** - 1H-[1,2,4]Oxadiazolo[4,3-a]quinoxalin-1-one

ODQ has been shown to specifically inhibit the NO-sensitive sGC (Garthwaite, Southam et al. 1995); (Olesen, Drejer et al. 1998) as indicated in figure 1.2.2. This inhibitory effect has been demonstrated in a number of tissue types (Garthwaite, Southam et al. 1995); (Brunner, Stessel et al. 1995); (Moro, Russel et al. 1996); (Abi-Gerges, Hove-Madsen et al. 1997). The binding of ODQ is in a non NO-competitive manner but inhibits NO-stimulated activity but leaves basal enzymatic activity

unchanged. Subsequent research identified oxidation of the heme iron as the underlying mechanism (Schrammel, Behrends et al. 1996); (Zhao, Brandish et al. 2000).

In vivo, the cellular levels of ADMA and L-NMMA are regulated by the enzyme dimethylarginine dimethylaminohydrolase (DDAH). When cells were observed in culture, if the level of DDAH was inhibited then the level of ADMA increased. The subsequent increase in ADMA then inhibited endothelium-dependent relaxation (Ayling, Whitley et al. 2006). These data demonstrate that DDAH is active at the basal level and if DDAH is inhibited for long enough, the level ADMA increases and accumulates within the cell until it reaches a concentration where it can actively inhibit NOS. NO has also been described to inhibit sGC expression and sGC activity in a cGMP-dependent manner (Filippov, Bloch et al. 1997). It is believed that this inhibition of sGC expression acts as a negative feed-back loop which may be a way of controlling the efficacy of the NO-cGMP pathway (Francois and Kojda 2004).

Biological activity of NO

There are several ways in which NO is thought to be able to mediate its biological effect(s) (reviewed (Blaise, Gauvin et al. 2005)):

1. Directly through the NO/cGMP/cADPr pathway
2. Indirectly by reactive nitrogen species (RNS) due to NO reacting with O₂ to form nitrates, nitrites and peroxynitrite which are highly destructive and unstable.

3. React with cysteine residues in proteins, a process known more commonly as s-nitrosylation and this mechanism is emerging as the most important mechanism of NO mediated effect and as an important signalling mechanism in cells (Marshall and Stamler 2001; Stamler, Lamas et al. 2001; Sun, Xin et al. 2001).

S-nitrosylation is an important post-translational protein modification which affects a large number of proteins that are involved in a number of cellular processes. S-nitrosylation is the modification of cysteine groups of proteins by NO. The role and importance of nitrosylation has only recently been recognised, mainly because the simple structure of NO was thought to lack the specificity and control observed in other post-translational modification systems such as phosphorylation. However, current data suggests that nitrosylation does share many properties with phosphorylation (Hess, Matsumoto et al. 2005); (Greco, Hodara et al. 2006) and may be equally important for post-translational modification of proteins (Mannick and Schonhoff 2004). Both nitrosylation and phosphorylation exhibit: (i) substrate specificity; (ii) strict spatial and temporal regulation; and (iii) are reversible. With nitrosylation the consequences to function are highly dependent on the particular protein which is affected and may result in inhibition, in the case of caspases, or enhancement, in the case of cGMP-dependent protein kinases (Dash, Cartwright et al. 2003). Protein s-nitrosylation exhibits strict spatial and temporal regulations and is reversible (Mannick, Hausladen et al. 1999). Proteins identified as being nitrosylated are over a hundred in number (Stamler, Lamas et al. 2001). Despite its potential importance to biological systems a detailed understanding of s-nitrosylation is currently lacking.

There is a general agreement that NO exerts many of its physiological effects through cGMP. NO binds to a specific region of the enzyme sGC within a specialised

heme moiety forming a nitrosyl-heme adduct of sGC and this is also considered to be the most important way to activate this enzyme (Wolin, Wood et al. 1982); (Ignarro, Wood et al. 1982). As a consequence of this interaction a conformational change results in the heme iron being shifted out of the plane of the porphyrine ring which initiates the production of cGMP from GTP as it binds at the now available site (Ignarro, Cirino et al. 1999). Once formed cGMP is able to engage numerous targets downstream.

In salivary acinar cells the accumulation of cGMP produced from GTP follows the activation of sGC by NO (Michikawa, Mitsui et al. 1998; Denninger and Marletta 1999; Tritsaris, Looms et al. 2000; Looms, Tritsaris et al. 2001). cGMP activates ribosyl cyclase causing the formation of cADPr from β NAD. Once formed, cADPr has been shown to be capable of activating RyR's leading to a rise in $[Ca^{2+}]_i$ following release of Ca^{2+} from intracellular stores (Smith and Gallacher 1992; Yamaki, Morita et al. 1998; Harmer, Smith et al. 2001; Looms, Tritsaris et al. 2001). The Use of ODQ as an inhibitor of NO demonstrates that NO acts through the cGMP pathway as in the presence of ODQ NO has no obvious effect upon intracellular calcium levels (Looms, Tritsaris et al. 2002).

NO used in experiments is derived from NO donors due to the inconvenience of using NO in its natural gas form. NO donors are compounds that are capable of releasing NO in situ and can be divided into different groups (Soff, Cornwell et al. 1997). A commonly used NO donor is sodium nitroprusside or SNP which is an example of an inorganic nitroso-compound. S-nitroso-N-acetyl-penicillamine or SNAP is an example of an S-nitrosothiols and these compounds vary in their modes of action for the release of NO (Al-Sa'doni and Ferro 2000); (Al-Sa'doni, Khan et al. 2000). More recently the NOC's and NONATES have been developed. These are zwitterions formed from polyamines. These more recent NO donors release fewer

biologically reactive bi-products than SNP and SNAP and so reduce the possibility that any bi-products are having an effect upon experimental results. They release more predictable amounts of NO and their structures have a striking resemblance to amino acids which may render them more amenable to participation in biological processes (Hrabie 1993; Maragos, Wang et al. 1993). NO acts as a first messenger but it differs significantly from all other first messengers in that it is also capable of acting as an intracellular messenger. sGC has been proven to be a receptor of NO (Denninger and Marletta 1999).

As NO has potent vasodilator ability it would also be reasonable to suggest NO could influence salivary secretion by modulation of blood flow within the salivary glands. Initial *in vivo* whole animal experiments demonstrated that there appeared to be no direct connection between total glandular blood flow and salivary fluid secretion (Larsson and Olgart 1989; Damas 1994). However, A. V. Edwards and colleagues conducted experiments in 1999 using cats which demonstrated that when blood pressure was reduced (approximately 50%) there was a significant reduction in submandibular blood flow and subsequently a reduction in the salivary secretion (Edwards et al. 1999). This work demonstrated that submandibular secretion may be reduced under conditions which effect blood flow to the gland. Subsequent work conducted by Edwards and colleagues in 2002 and 2003 but utilising sheep as the model animal again demonstrated that reduction of blood flow reduces salivary output and also demonstrated that these findings were not species specific (Edwards et al. 2002; Edwards et al. 2003).

Summary of NO and Salivary Acinar Cells

In salivary glands (Looms, Tritsarlis et al. 2001) and other cell types (Galione, McDougall et al. 1993; Galione, White et al. 1993) the formation of cADPr has been directly linked to the formation of cGMP, which is itself formed in response to cell stimulation with NO (Denninger and Marletta 1999). The ability of cGMP to increase the $[Ca^{2+}]_i$ in response to ACh stimulation is also consistent with findings using cADPr (Harmer, Smith et al. 2001) and therefore suggests further evidence of a link between cGMP and cADPr in mouse submandibular acinar cells (Looms, Tritsarlis et al. 2001). Previous data has also demonstrated that NO donors can stimulate Ca^{2+} mobilisation in salivary acinar cells (Looms, Tritsarlis et al. 2001). Furthermore, the use of ODQ, which is an inhibitor of sGC, demonstrates that NO acts through the cGMP pathway as in the presence of ODQ NO has no obvious effect upon $[Ca^{2+}]_i$ (Looms, Tritsarlis et al. 2002). The use of the RyR inhibitor Ryanodine also strengthened this argument over the effect of NO on the cGMP pathway, as the use of Ryanodine also removed the effect of NO on $[Ca^{2+}]_i$. (Data in this thesis also confirms these observations).

Increased levels of NO have been demonstrated in both the saliva (Konttinen, Platts et al. 1997) and expired air from patients with SjS (Ludviksdottir, Janson et al. 1999). In addition data have demonstrated increased levels of NOS are present in the labial glands of SjS patients (Konttinen, Platts et al. 1997). Taken together these findings may indicate that NO could have a possible role in the glandular hypofunction observed in SjS. Additional evidence for a role for NO in SjS is that SjS IgG has the ability to increase the levels of both NOS and cGMP in both salivary and lacrimal acinar cells (Bacman, Berra et al. 1998; Perez Leiros, Sterin-Borda et al. 1999; Bacman, Berra et al. 2001).

1.3 Adenosine Tri-Phosphate (ATP)

ATP is stored and co-secreted with many neurotransmitters and may have the ability to act as a neurotransmitter or a neuromodulator like its metabolite adenosine (Fredholm and Hedqvist 1980); (Burnstock 1981); (Stone 1981); (White 1984); (Gordon 1986); (Richardson and Brown 1987). Studies using a variety of cells have demonstrated that extracellular ATP can cause various changes which include: alteration of ion fluxes; cell growth; contraction and relaxation of smooth muscle; modulation of vascular tone, platelet aggregation and trans-epithelial chloride secretion (Stone 1981); (Chahwala and Cantley 1984); (Gordon 1986); (Reilly, Saville et al. 1987); (Harden, Lazarowski et al. 1997); (Boarder and Hourani 1998); (King, Townsend-Nicholson et al. 1998); (Kunapuli and Daniel 1998).

Purinergic receptor types

ATP receptors are now known to be widely expressed in mammalian tissues. Data from pharmacological studies utilising analogues of ATP have demonstrated the existence of two main types of purinergic (P2) receptor. These P2 receptors have been classified into two distinct families designated P2X and P2Y. The P2X receptors are associated with ligand-gated non-selective cation activity, whereas the P2Y receptors are associated with G-protein activation (Abbracchio and Burnstock 1994). The ATP-gated P2 purinergic receptors which are designated P2X₁ - P2X₆ (cation only channels) and P2X₇ (a dual function cation channel/pore) all display extensive sequence identity (North 1996) but data show considerable variation with relation to tissue distribution, bio-physical properties, agonist profiles and pharmacology (P2X₁, (Valera, Hussy et al. 1994); P2X₂ - P2X₆, (Collo, North et al. 1996); P2X₇, (Surprenant, Rassendren et al. 1996). The P2X receptors functionally resemble ACh-gated channels with respect to gating and ionic permeability but are structurally unique (Ross, Ehring et al. 1997). Four P2 receptor sub-types: P2X₄, P2X₇, P2Y₁ and

P2Y₂ have been identified in mammalian salivary glands and were expressed by acini and ducts in both parotid and submandibular glands (Turner, Landon et al. 1999). P2Y₂ have been identified in a variety of permanent submandibular and parotid gland cell lines of salivary gland origin (Quissell, Barzen et al. 1997; Quissell, Barzen et al. 1998); (Yu and Turner 1991). Salivary glands are now known to express mostly P2X₇ (Pochet, Gomez-Munoz et al. 2003) which are some what unique among the P2X.

The P2Y have seven transmembrane domains which are coupled to a regulatory GTP-binding protein. The P2X on the other hand have only two transmembrane domains which are separated by approximately 300 amino acids which form a large extracellular loop (North 2002). It is highly likely that both the –NH₂ and the –COOH termini are cytoplasmic and the extracellular loop was determined to contain several conserved N-glycosylation sites and ten cysteine residues which in turn form five disulfide bridges (Ennion and Evans 2002). Unlike the P2Y, P2X are not coupled and do not have a regulatory protein, so upon activation by an agonist they form a cationic channel and it has been speculated that at least three subunits must assemble to form the channel, regardless of whether the units are identical or not (North 2002).

There is some variation between P2X₁ - P2X₆ and P2X₇. P2X₇ has 595 aa whereas the other six P2X have only 450 aa (Surprenant, Rassendren et al. 1996). This variation in aa number is accounted for by a variation in C-terminus which is 120 aa longer in P2X₇ (North 2002). P2X₇ requires this much longer C-terminus (240 aa) to allow it to form pores, however, if this extended C-terminus is removed the receptors ability to form pores is abolished but this does not affect its ability to form a channel, this data also confirmed the role of the extended C-terminus in pore formation (Smart, Gu et al. 2003). The formation of this pore can lead to cell death (Virginio,

MacKenzie et al. 1999) and as a result this receptor also has the capacity to trigger apoptosis (Chow, Kass et al. 1997) in two ways: 1) as a consequence of massive uptake of chloride (Tsukimoto, Harada et al. 2005); and 2) leakage of intracellular potassium (Kahlenberg and Dubyak 2004).

Purinergic receptors and Calcium

Data suggest that ATP shares similarities with other Ca^{2+} mobilising agents such as vasopressin and phenylephrine inasmuch as it was able to activate Phosphoinositide-specific-phospholipase C enzymes (PLC) and stimulate the breakdown of phosphatidylinositol 4,5-bisphosphate (PIP_2) and produce IP_3 (Charest, Blackmore et al. 1985); (Okajima, Tokumitsu et al. 1987); (Dubyak, Cowen et al. 1988). Other evidence also suggested that hepatic P2 type receptors were coupled through guanine-nucleotide-binding proteins to other 2nd messenger pathways, but the contributions to the effect of ATP were as yet unclear (Irving and Exton 1987); (Okajima, Tokumitsu et al. 1987). The elevation of $[\text{Ca}^{2+}]_i$ appears to be a common effect induced by ATP in many tissue types and rat parotid acinar cells are a useful system for studying the effects of extracellular ATP since the mechanisms of other Ca^{2+} mobilising agonists, such as the muscarinic agonist carbachol (CCh), are well characterised in this tissue (McMillian, Soltoff et al. 1988).

It was originally reported by Gallacher that the electrophysiological response of parotid glands to ATP was indistinguishable from that induced by other Ca^{2+} mobilising agonists. However, this work was conducted in mice parotid acinar cells (Gallacher 1982) and not rat. Alternative experiments were then conducted in rat parotid acinar cells. The effect of extracellular ATP on $[\text{Ca}^{2+}]_i$ were characterised in quin2-loaded rat parotid acinar cells and ATP was shown to specifically increase the $[\text{Ca}^{2+}]_i$ six-fold above a basal level of 180nM (McMillian, Soltoff et al. 1987). McMillian

found that ATP elevates $[Ca^{2+}]_i$ in these cells in a highly specific) but reversible manner which was considered consistent with the activation of a P2 type purinergic receptor (McMillian, Soltoff et al. 1987). These experiments also illustrated that the increased $[Ca^{2+}]_i$ induced by ATP was similar to that induced by CCh through its activation of muscarinic receptors, because like CCh the extracellular ATP stimulated the release of K^+ and the $[Ca^{2+}]_i$ response could be induced by both agonists in the absence of extracellular Ca^{2+} (McMillian, Soltoff et al. 1987). These data suggests that ATP may be an important neurotransmitter for the parotid gland.

Subsequent work done by McMillian and co-workers determined that there were marked contrasts between ATP and the receptor agonists linked to PLC (McMillian, Soltoff et al. 1988). Their theories were based on data which illustrated four distinct variations: (i). A combination of maximum concentrations of CCh, substance P and phenylephrine had no greater effect on $[Ca^{2+}]_i$ than did CCh alone but there was some observable synergism between CCh and a maximum concentration of ATP; (ii). The use of guanosine 5'-[β -thio]disphosphate (GDP[S]) by intracellular dialysis blocked the muscarinic receptors activated by CCh but did not block activation of ion channels by ATP; (iii). In spite of the effects on $[Ca^{2+}]_i$ observed, ATP had little effect on cellular turnover of phosphatidylinositol which was in complete contrast to CCh and other Ca^{2+} mobilising agents; and (iv). ATP was able to stimulate the release of amylase from parotid acinar cells but only at a reduced level ($33 \pm 9\%$) when compared to PLC-linked receptor agonists (McMillian, Soltoff et al. 1988). The sum of these findings suggested that ATP increased $[Ca^{2+}]_i$ through activation of a pathway which is distinct from that which is shared by PLC-linked receptor agonists such as CCh (McMillian, Soltoff et al. 1988).

P2X₄ and P2X₇ function as non-selective cation channels activated by ATP with high and low affinity, respectively. Once activated these receptors stimulate an increase in

the $[Ca^{2+}]_i$ level as a result of calcium influx (McMillian, Soltoff et al. 1987); (Soltoff, McMillian et al. 1990).

Purinergic receptors and salivary secretion

The ability to secrete in response to stimulation by exogenous ATP has been demonstrated in both the rat submandibular (Dehaye, Moran et al. 1999) and mouse parotid gland (Gallacher 1982) and data suggests that this may be mediated by the activation of both P2X and P2Y. P2X and P2Y have also been demonstrated in human submandibular salivary gland cell lines (Liu, Singh et al. 1999) and more recent data have demonstrated the ability of isolated human labial glands to respond to ATP (Pedersen, Dissing et al. 2000). Data obtained in other studies also demonstrated that when rat submandibular gland acinar cells are placed in culture the expression and activity of the P2Y₂ increased as a function of time in culture, from marginally detectable, when freshly isolated, to a dramatic increase post short term culture (Turner, Weisman et al. 1997). As a result of this P2Y₂ are up-regulated in response to stress or injury and are activated by extracellular ATP and have been identified in a variety of tissues including submandibular glands (Koshiba, Apasov et al. 1997); (Kishore, Wang et al. 1997); (McMillian, Soltoff et al. 1987); (Turner, Landon et al. 1999); (Ahn, Camden et al. 2000); (Seye, Gadeau et al. 1997; Seye, Kong et al. 2002). These results suggest a role for P2Y₂ in the response to damage and disruption of normal salivary gland structure and function. In addition P2Y₁ are known to be expressed in rat submandibular glands and have subsequently been suggested to have a role in salivary gland development (Park, Garrad et al. 1997). More recent research has determined that P2Y₁ are most active in submandibular glands from immature animals (Schrader, Camden et al. 2005), but as the animal develops the Ca^{2+} response to agonists of P2Y₁ diminished (Park, Garrad et al. 1997). P2Y₂ receptor expression was barely detectable in salivary glands under

normal conditions but was up-regulated when tissue homeostasis was disrupted using various methods (Turner, Weisman et al. 1997);(Ahn, Camden et al. 2000).

Purinergic receptors and disease

Under pathological conditions nucleotides are released from the cytoplasm of cells in a number of ways following activation of cellular responses which include cell adhesion, neurotransmission, apoptosis and cell growth (Wilden, Agazie et al. 1998); (Bodin and Burnstock 2001); (Chaulet, Desgranges et al. 2001); (Ciccarelli, Ballerini et al. 2001); (Coutinho-Silva, Parsons et al. 2003); (Weisman, Wang et al. 2005). These responses occur when cells become injured or stressed during periods of oxidative stress, ischemia, hypoxia or mechanical stretch (Bergfeld and Forrester 1992); (Ciccarelli, Di Iorio et al. 1999); (Pedersen, Pedersen et al. 1999); (Bodin and Burnstock 2001); (Ostrom, Gregorian et al. 2001). In salivary glands it is believed that P2 nucleotide receptors are actually activated by ATP that has been co-packaged with various neurotransmitters and released from neurons (Brown, Bruce et al. 2004).

P2Y₂ up-regulation occurs in the submandibular glands of NOD.B10 mice and also demonstrated disease progression as P2Y₂ activity in the submandibular gland acinar cells increased with age (Schrader, Camden et al. 2005). The NOD.B10 mouse, which develops an auto-immune exocrinopathy (AEC) similar to Sjögren's syndrome at approximately 8 weeks of age, is an acceptable animal model for primary Sjögren's syndrome (Hu, Nakagawa et al. 1992); (Humphreys-Beher, Hu et al. 1994); (Robinson, Brayer et al. 1998; Robinson, Cornelius et al. 1998); (Humphreys-Beher and Peck 1999). This up-regulation could suggest an important role for P2Y₂ in Sjögren's syndrome as P2Y₂ and their signalling pathways could contribute to the autoimmune exocrinopathy observed in Sjögren's syndrome

(Schrader, Camden et al. 2005). However, the P2Y₂ may also be up-regulated to act in a more positive role, as alternatively P2Y₂ up-regulation may play an important role in tissue repair by stimulating mitogenesis (Turner, Landon et al. 1999) or may provide an alternative pathway for fluid secretion in the NOD.B10 mouse (Schrader, Camden et al. 2005). However, the physiological consequences of P2Y₂ up-regulation in salivary glands are as yet unknown (Baker, Camden et al. 2008).

1.4 Cell - Cell Coupling in Salivary Acinar Cells

No cell lives in isolation, and the survival of all multi-cellular organisms requires an elaborate network of communication at the intra and intercellular level. Organisms need to co-ordinate and regulate their growth and metabolism with strict control over the multitude of cells which make up the many diverse tissue types and organs. Intercellular communication is mediated through soluble factors including hormones, contact with extracellular matrix and even through direct cell to cell interaction. Direct cell to cell interactions occur either by cell membrane proteins or through channels between the cells which are termed gap junctions.

The use of gap junctions in intercellular signalling may function to co-ordinate and synchronise cells that are connected in this manner. Gap junctions allow the movement of molecules smaller than 1.5kDa which would allow the involvement of the most common second messengers such as cADPr and IP₃. Furthermore, a Ca²⁺ signal can also propagate from cell to cell and may induce co-ordinated behaviour in adjacent cells (Rottingen and Iversen 2000). It has long been known that myocytes in the heart function as a unit through cell to cell Ca²⁺ signals. Such cell to cell communication has also been observed in other excitable cells including glial and nerve cells (Giaume and Venance 1998). Importantly, cell to cell communication has now been observed in non-excitable cells such as hepatocytes which also seem to co-ordinate their function through gap junctions utilising Ca²⁺ (Eugenin, Gonzalez et al. 1998).

Ca²⁺ oscillations are frequently observed in single cells but are normally asynchronous with one another and have variable frequencies and would generally be observed as a constant elevated Ca²⁺ level when the sum responses of many

cells are summarised. This fact also explains why only biphasic responses are observed in populations of cells which are grown in suspension or upon coverslips (Rottingen and Iversen 2000). It was not until 1988 that sinusoidal synchronous Ca^{2+} oscillatory signals were observed and reported in both endothelial monolayers (Sage, Adams et al. 1989) and pancreatic acini (Pralong, Wollheim et al. 1988).

Using endothelial cell monolayers to demonstrate synchronised Ca^{2+} oscillations, it was observed that synchrony only occurred in cells which were seeded at low density and grown to confluence as this favoured the formation of gap junctions (Sage, Adams et al. 1989). Work conducted in 1991 by two separate groups, Pedersen and Pickles and co-workers, demonstrated similar sinusoidal Ca^{2+} oscillations in monolayers of sweat gland/ duct cells (Pedersen 1991); (Pickles, Brayden et al. 1991). Synchronised Ca^{2+} oscillations have also been observed in recordings from a whole pancreatic acinus (approximately 10 cells) (Pralong, Wollheim et al. 1988).

Data derived from electrophysiological recordings demonstrated that a Ca^{2+} dependent current is increased when cells are coupled in pairs or triplets (Petersen and Petersen 1991). When pairs of pancreatic acinar cells were stimulated with cholecystokinin they oscillated in synchrony and by clamping the two cells membrane potentials to a common value, electrical coupling was ruled out as a possible synchroniser (Ngezahayo and Kolb 1993). However, it was also noted that different agonists differed in their modulating roles upon gap junctions as cholecystokinin seemed to inhibit gap junctional transport following a brief period of exposure (Ngezahayo and Kolb 1993); (Stauffer, Zhao et al. 1993); (Yule, Stuenkel et al. 1996) and similar results were observed with ATP (Ritter and Lang 1991); (Rottingen, Camerer et al. 1997).

The best studied cells are hepatocytes which are coupled by gap junctions allowing the transport of both Ca^{2+} and IP_3 (Saez, Connor et al. 1989). This was observed for up to four coupled cells which responded by oscillations which were synchronised though sequential activation of the cells. The most interesting point of such data was the fact that the sequence of activation was the same for each transient which suggested that the first cell to respond was the most sensitive to that particular agonist and controlled the other cells within the multiplet but when other agonists were used to stimulate the cells the controlling cell was different which suggested heterogeneous agonist sensitivity (Rottingen and Iversen 2000).

Based on work conducted on individual hepatocytes, Ca^{2+} signals have also been studied in the whole perfused liver (Robb-Gaspers and Thomas 1995). Perfusion of the whole liver demonstrated that when agonist was infused all hepatocytes within a lobule oscillated in synchrony and this synchronisation was produced by a wave of Ca^{2+} moving from cells at the periphery to more central cells upon each transient. The signal always originated at the same point and within the same cell which suggested a pace-maker role for this leading cell. The wave of Ca^{2+} was determined to travel intracellularly at a constant velocity and appeared independent of agonist concentration (Tordjmann, Berthon et al. 1997).

Experiments conducted with relation to synchronisation in situ are highly relevant as the structure and architecture of the cell are preserved and any physiologically important variations in sensitivity to agonist which may be organised in a gradient fashion would be maintained which would be highly advantageous to the researcher (Rottingen and Iversen 2000). It was observed that in the salivary glands of blow flies, agonist-induced Ca^{2+} oscillations were synchronised through regenerative intercellular Ca^{2+} waves (Zimmermann and Walz 1997). It was noted that these oscillations were independent of Ca^{2+} influx but relied on the release and refilling of

internal Ca^{2+} stores. There were no observable delays between cells but blocking of gap junctions by administration of octanol resulted in asynchronous oscillations suggesting the importance of gap junctions in this system (Zimmermann and Walz 1997).

The main mechanism proposed for intercellular Ca^{2+} waves which are dependent on gap junctions is diffusion of IP_3 through these intercellular connections (Sanderson 1995). This suggestion was based on the initial observation of the effect induced by heparin on oocytes and airway epithelia, as heparin blocked the intercellular Ca^{2+} wave from follicular cells to the oocytes (Sandberg, Ji et al. 1992) and Ca^{2+} waves in airway epithelia (Boitano, Dirksen et al. 1992). Toyofuku and co-workers produced a mouse model system through transfection (Toyofuku, Yabuki et al. 1998). The model was developed to present cells expressing both RyR and connexin 43 to be surrounded by cells only expressing connexin and upon administration of caffeine an intercellular Ca^{2+} wave was induced. Based on the absence of RyR in adjacent cells, the wave must be mediated through the IP_3R and Ca^{2+} release from IP_3 sensitive stores. It is highly likely that the initial Ca^{2+} increase which was mediated by caffeine led to the activation of PLC which resulted in production of IP_3 and this theory was substantiated by the fact that the use of U73122 was able to abolish the caffeine-induced Ca^{2+} wave (Toyofuku, Yabuki et al. 1998).

Following focal application of agonist or mechanical stress, PLC is activated and produces IP_3 which diffuses to neighbouring cells. IP_3 acts to sensitise the cells for the subsequent Ca^{2+} wave that propagates much more slowly though CICR (Rottingen and Iversen 2000). The Ca^{2+} wave also induces to production of more IP_3 as it activates PLC in the adjacent cells and this allows for further and more distant cells to be sensitised for the Ca^{2+} wave. This model comprises of two regenerative waves, the more rapid IP_3 wave and the much slower Ca^{2+} wave but the two waves

are inter-dependent for their regenerative properties (Rottingen and Iversen 2000). This theory was further substantiated by work done by Hirose and co-workers who demonstrated that a wave of IP_3 from the stimulated cell ran in parallel with a Ca^{2+} wave (Hirose, Kadowaki et al. 1999).

The use of a global agonist will stimulate PLC activation and production of IP_3 in all cells, but at the single cell level the amount of IP_3 produced is entirely dependent on the individual cells sensitivity to a particular agonist. When Ca^{2+} waves are generated the so called 'pacemaker' cell is the cell with the highest sensitivity to the agonist. The wave spreads from this cell to other adjacent cells where the primary IP_3 wave acts to sensitise the cells IP_3 Rs to Ca^{2+} allowing the intercellular Ca^{2+} wave originating from the 'pacemaker' cell to co-ordinate a synchronised oscillatory Ca^{2+} signal. However at low concentrations the wave would not perpetuate and several local waves would be initiated as opposed to a global wave induced by the pacemaker cell which would result in asynchronous temporal oscillations being observed. In contrast to this, high agonist concentration would stimulate IP_3 production above threshold level simultaneously in most cells and the pacemaker would be unable to control the phase of others in such a situation which would result in asynchronous oscillations or a sustained Ca^{2+} response. This model was proposed by Rottingen and Iversen in 2000 and may be viewed as analogous to the models of fundamental and global Ca^{2+} signals in single cells but at a much higher organisation level (Rottingen and Iversen 2000).

Although much is known about the intracellular signalling cascades of salivary acinar cells, very little is actually known about the intercellular signalling which has been suggested to occur. The mechanisms which drive fluid secretion in acinar cells are extremely important. Cytosolic Ca^{2+} is known to be involved in an extensive number of cellular functions and its physiological and pathophysiological roles have been

extensively studied (Berridge 1993; Berridge 1994); (Berridge 1998); (Mooren and Kinne 1998). The whole process must occur at the correct time, in the correct order, at the correct place, as spatial and temporal factors are extremely important and play a vital role in fluid secretion (Harmer, Smith et al. 2005). The process by which acinar cells allow fluid secretion to occur is well known, as discussed previously (chapter 1 Introduction 1.1 salivary secretion). Ca^{2+} is the most versatile intracellular messenger which has been discovered to date since it is known to be involved in the regulation of virtually all known cellular functions and reactions (Petersen, Michalak et al. 2005). However, it is also known to play a role in intercellular signalling in some cell types such as human neuroepithelioma cells (Palmer, Yule et al. 1996). Could Ca^{2+} function as an intercellular signalling molecule in salivary acinar cells to allow communication between acinar cells or is it some other molecule which is responsible for this function and what implications could such findings represent in relation to Sjögren's syndrome? Such questions about cell coupling in salivary acinar cells must be addressed.

Through use of a high-speed confocal microscope Ca^{2+} signalling patterns were observed in rat salivary ducts (Yamamoto-Hino, Miyawaki et al. 1998) and acini (Takemura, Yamashina et al. 1999). The data produced from millisecond analyses demonstrated that $[\text{Ca}^{2+}]_i$ responses in the ducts originated in some 'pioneer' cells and then moved to neighbouring cells which demonstrated asynchrony and heterogeneity (Yamamoto-Hino et al., 1998), but the $[\text{Ca}^{2+}]_i$ responses observed in the acini demonstrated synchronicity (Takemura, Yamashina et al. 1999). These data suggested that the Ca^{2+} signalling system in salivary glands may be constructed according to the architecture of the tissue (Segawa, Takemura et al. 2002).

The function of exocrine glands is primarily achieved by the compartmentalisation of epithelial domains, acini and ducts which are also known to demonstrate

characteristic morphological specialisation (Young and van Lennep 1978); (Pinkstaff 1979). Segawa and co-workers subsequently demonstrated in 2002 that the pattern of Ca^{2+} signalling is also distinct between acini and ducts in the rat parotid gland in response to ATP and CCh stimulation (Segawa, Takemura et al. 2002). Their data also demonstrated that acinar cells within an acinus respond synchronously and behave as a functional syncytium but the ductal cells respond heterogeneously which demonstrates diverse signalling kinetics. In addition their data also demonstrated that the molecular distribution of connexin 32 and $\text{IP}_3\text{R2}$ varied between the two domains and produced domain distinct patterns. Stimulation with CCh was also observed to induce a rise in $[\text{Ca}^{2+}]_i$ in the acini before the ducts. However, no observations were made regarding Ca^{2+} waves from acini to ducts and the propagation of such a signal was considered unlikely. The sum of this data suggests that the Ca^{2+} signalling system in the rat parotid gland is organised in parallel with the architecture of the tissue (Segawa, Takemura et al. 2002).

Segawa and co-workers also observed considerable variations in the pattern of Ca^{2+} response to CCh and ATP between the two domains in the presence or absence of extracellular Ca^{2+} . The acinar domains responded well to CCh but not to ATP. However, the responsiveness to CCh did not require extracellular Ca^{2+} which indicates that the acinar domain induces increased $[\text{Ca}^{2+}]_i$ through release of Ca^{2+} from intracellular stores following muscarinic receptor stimulation. Conversely, based on the lack of response to ATP, purinergic receptor stimulation appears to have little effect on both the intra- and extra-cellular Ca^{2+} signalling mechanisms on cells within the acinar domain. In contrast to this the ductal cells responded to both CCh and ATP and removal of extra-cellular Ca^{2+} abolished responsiveness to CCh (Segawa, Takemura et al. 2002). The variation in response of the cells from the ductal regions combined with their lack of synchronicity may be a direct result of the heterogeneous

cell populations present within the ductal regions of salivary glands (Sato and Miyoshi 1988; Sato and Miyoshi 1998).

The $[Ca^{2+}]_i$ response synchronicity observed in the acini may be a direct result of gap junctional communication as has previously been implicated in synchronised Ca^{2+} signalling (Stauffer, Zhao et al. 1993); (Guerineau, Bonnefont et al. 1998). The presence of gap junctions in mammalian salivary gland tissue has been demonstrated previously using electron microscopy (Dewey and Barr 1964); (Hand 1972); (Nagato and Tandler 1986) and connexin immunohistochemistry (Hirono et al., 1995; Lee et al., 1998; Shimono et al., 2000). Gap junctions appear to be primarily present in the acinar domains of salivary glands (Segawa, Takemura et al. 2002). Other data demonstrated abolishment of synchronisation of Ca^{2+} response in the acini by use of octanol which strongly suggested that the acinar domain acts as a functional syncytium through gap junctions (Segawa, Takemura et al. 2002). Similar to the data from the gap junction localisation experiments immunohistochemical distribution data for IP_3R2 also demonstrated that the IP_3R2 distribution was also primarily within the acini as they were homogeneous here and only heterogeneous with relation to ductal regions (Segawa, Takemura et al. 2002).

The epilemmal arrangement of the nerves and the limited innervation within the salivary glands (Garrett and Kidd 1993) would suggest that salivary acinar cells are reliant on cell coupling for the whole gland to function. Furthermore, this innervation arrangement would lend itself to the need for “pacemaker” cells responsible for coordination of the cellular activity in the salivary acinus.

The key diagnostic features of SjS are focal perivascular lymphocytic infiltrations within the salivary glands (Fox and Maruyama 1997) and severe glandular hypofunction. This key feature which is as yet unexplained in SjS may be explained

by the pacemaker hypothesis as it would explain why a limited number of infiltrating lymphocytes which appear at specific loci within the salivary glands could affect the whole gland. A demonstration of pacemaker cell activity within the salivary acinus and their subsequent inhibition through immune modulators would provide an attractive explanation to this problem.

1.5 Sjögren's syndrome

History of Sjögren's syndrome

The original description of Sjögren's syndrome was made by Johannes von Mikulicz in 1892. He described a 42 year old man exhibiting bilateral enlargement of the parotid and lacrimal glands which was associated with infiltration of a small round cell type (Mikulicz 1892). It was subsequently documented that this individual continued to suffer with recurrent episodes throughout his lifetime and following his death, a post-mortem examination revealed that his glands were found to contain "*extensive lymphocytic infiltrations, but with no evidence of malignancy or infection*". Prior to his identification of this particular condition the term Mikulicz's syndrome had been used to describe a wide variety of conditions including lymphoma, sarcoidosis, tuberculosis and other infections and so the term fell into disuse based on its inefficiency to provide adequate prognostic or therapeutic information (Daniels and Fox 1992). However the term may occasionally be used as a histological reference when focal lymphocytic infiltrates are observed on salivary-gland biopsy samples (Morgan and Castleman 1953).

The disorder was subsequently named after Danish ophthalmologist Henrik Sjögren (1899-1986), who first encountered it in 1930 when he was presented with a female patient suffering from dry and painful eyes. The case fascinated him and from this point he proceeded to identify similar cases and by 1933 he had described clinical and histological findings in a total of 19 patients all suffering from dry mouth and eyes and 13 of whom had probable rheumatoid arthritis. Through collection and observations made on conjunctival biopsies from each patient he was also able to characterise the histological nature of the disorder (Bell, Askari et al. 1999; Wollheim

1999). He presented the sum of this data as a doctoral thesis written in German in 1933 (Sjögren 1933) and so Sjögren's syndrome was born.

Sjögren also introduced the term *keratoconjunctivitis sicca* for use with this syndrome so that it was clearly distinguishable from dry eyes induced by a lack of vitamin A which is termed xerophthalmia. The data collected by Sjögren went largely unnoticed for two decades until American investigators William Morgan and John Castleman presented a case study in 1953 at a clinical pathological conference involving a patient with Sjögren's syndrome and re-ignited interest in the disorder originally known as Mikulicz's disease but re-named Sjögren's syndrome (Morgan and Castleman 1953). It was Morgan and Castleman who suggested that Sjögren's syndrome and the earlier reported Mikulicz disease were actually the same disorder. In 1956 Bloch and colleagues outlined the clinical features of the syndrome and are still relevant today (Bloch, Buchanan et al. 1956). Over five decades later the condition which still bears Sjögren's name remains as intriguing a subject and an area of intensive research for systemic auto-immune disorders.

Clinical aspects of Sjögren's Syndrome

Sjögren's syndrome (SjS) is an autoimmune disorder which specifically targets the exocrine glands, primarily the salivary and lacrimal glands. SjS leads to an impairment of secretory function and is characterised by lymphocytic infiltration of the salivary (Figure 1.5.1.) and lacrimal glands.

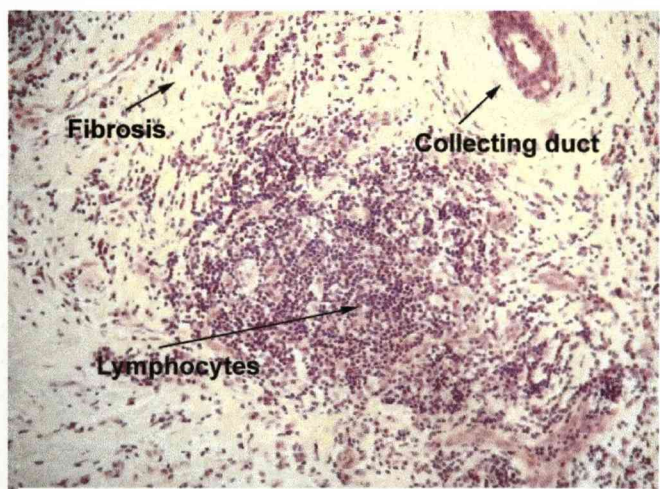


Figure 1.5.1: H&E stained histological section of a labial gland from a patient with Sjögren's syndrome. There is a distinct loss of glandular architecture with areas of fibrosis. A dense lymphocytic infiltration is also seen which is characteristic of the disease.

SjS is one of the three most common autoimmune disorders (Pillemer, Matteson et al. 2001) with population prevalence believed to be similar to that of rheumatoid arthritis (Hazes and Silman 1990) having an estimated overall incidence of 3% (Thomas, Hay et al. 1998; Jonsson, Haga et al. 2000). In keeping with the majority of autoimmune diseases there is a bias in the prevalence of the illness, with females being affected nine times more commonly than men (Scully 1986). There also appears to be two age peaks of sufferers: the first after menarche (approximately 20-30 years of age); the second after menopause (approximately 50-60 years of age) (Bowman, Ibrahim et al. 2004); (Fox 2005). Sjögren's syndrome is rare in children and when it does occur it is reported to be milder than in adults insofar as the most frequent primary symptoms are benign parotid swelling, whereas the sicca symptoms occur later and much less frequently (Cimaz, Casadei et al. 2003).

The term syndrome is used in connection with SjS because a “*Syndrome*” is defined as “*a combination of signs and/or symptoms that form a distinct clinical picture indicative of a particular disorder*”. In SjS these symptoms typically range from difficulty in speaking and eating, oral *candidiasis* and rampant caries to chronic sialadenitis, blindness and B-cell lymphoma (Scully 1986). The typical clinical picture is keratoconjunctivitis sicca (drying and inflammation of the conjunctiva as a result of insufficient lacrimal secretion (dry eyes)) and xerostomia (a dryness of the mouth from salivary gland hypofunction (dry mouth)) (Fox, Stern et al. 2000).

Patients suffering with SjS also produce a wide variety of serum auto-antibodies such as anti-Ro and anti-La which provides compelling evidence to support an autoimmune origin for the disease (St Clair 1992); (Jonsson, Moen et al. 2002). However, to date definitive anti-secretory antibodies have remained elusive but most recent

data further promotes the idea by demonstrating IgG antibodies from patients with SjS having the ability to inhibit secretion in salivary acinar cells (reviewed by, (Dawson, Fox et al. 2006)).

In spite of extensive molecular, histological and clinical studies, the underlying cause of Sjögren's syndrome and its pathogenesis remains unknown (Garcia-Carrasco, Fuentes-Alexandro et al. 2006).

Criteria for Diagnosis of Sjögren's syndrome

In Sjögren's syndrome there are prominent and consistent oral and dental findings which were directly related to the loss of salivary function (Daniels and Fox 1992). However, establishing the diagnosis of Sjögren's syndrome has proved difficult in light of the non-specific primary symptoms of dry mouth and eyes and the total lack of both sensitive and specific laboratory markers (Fox 2007). Another factor which makes diagnosis problematic is the lack of intermediary subjects as all studies to date have been done on subjects in whom the disease is already established so it remains debatable whether the changes identified are actually a cause or an effect of the disease (Fox 2007).

For a patient to be diagnosed with Sjögren's syndrome it must be established that they have subjective and objective symptoms of both lacrimal and salivary gland hypofunction in combination with evidence of immunological abnormalities, which may be indicated by the presence of autoantibodies and/or lymphocytic infiltration of the labial salivary glands (Fox, Robinson et al. 1986; Vitali, Bombardieri et al. 1993; Fox and Saito 1994; Vitali, Bombardieri et al. 1996). The current universally accepted diagnostic criteria are summarised in the two SjS tables (Tables 1.5.1. and 1.5.2.).

Primary Sjögren's syndrome is classified as an autoimmune disease but to date no truly specific auto-antigens or auto-antibodies have ever been identified (Fox and Speight 1996). Many auto-antibodies have been suggested and described including anti-salivary and anti-nuclear antibodies. Of these anti-nuclear antibodies the most well known are the anti-Ro/SSA and anti-La/SSB auto-antibodies which although not specific to Sjögren's syndrome are highly characteristic and occur in 60% and 40% of primary Sjögren's syndrome respectively (Scully 1986; Jonsson, Haga et al. 2000). Although extremely useful for establishing a diagnosis such auto-antibodies are not specific enough to Sjögren's syndrome to be used in isolation.

Sjögren's syndrome does however share many features in common with autoimmune diseases: (i) evidence suggests that it is mediated and antigen driven; (ii) patients share HLA types with other autoimmune disease; (iii) it shares systemic features with other autoimmune diseases such as production of rheumatoid factors; and (iv) the histopathology of the salivary gland implicates an autoimmune component (Fox and Speight 1996).

Table 1.5.1: Sjögren's syndrome classification criteria part 1

American-European Consensus Group classification criteria for Sjögren's syndrome (Vitali, Bombardieri et al. 2002))	
1. Ocular symptoms:	A positive response to at least 1 of the following 3 questions:
a)	Have you had daily, persistent, troublesome dry eyes for more than 3 months?
b)	Do you have a recurrent sensation of sand or gravel in the eyes?
c)	Do you use tear substitutes more than 3 times day?
2. Oral symptoms:	A positive response to at least 1 of the following 3 questions:
a)	Have you had a daily feeling of dry mouth for more than 3 months?
b)	Have you had recurrent or persistently swollen salivary glands as an adult?
c)	Do you frequently drink liquids to aid swallowing dry foods?
3. Ocular signs	Objective evidence of ocular involvement determined on the basis of a positive result on at least 1 of the following 2 tests:
a)	Schirmer-I test (< 5 mm in 5 minutes)*
b)	Rose bengal score (> 4, according to the van Bijsterveld's scoring system)
4. Histopathology:	In minor salivary glands (obtained through normal-appearing mucosa) focal lymphocytic sialoadenitis evaluated by an expert histopathologist, with a focus score >1, as defined as lymphocytic foci (which are adjacent to normal-appearing mucous acini and contain more than 50 lymphocytes) per 4 mm ² of glandular tissue.
5. Salivary gland involvement	Objective evidence of salivary gland involvement, determined on the basis of a positive result on at least 1 of the following 3 tests:
a)	Salivary scintigraphy showing delayed uptake, reduced concentration and/or delayed excretion of tracer
b)	Parotid sialography showing the presence of diffuse sialectasias (punctuate, cavitary or destructive pattern), without evidence of obstruction in the major ducts.
c)	Unstimulated salivary flow (<1.5 ml in 15 minutes)*
6. Autoantibodies:	Presence of at least 1 of the following serum autoantibodies:
a)	Antibodies to Ro/SS-A or LA SS-B antigens, or both.

Therefore to summarise the pathogenesis of the disease is multi-factorial and requires several steps to establish the disease. It has been suggested that environmental factors initiate inflammation in individuals who have a genetic pre-disposition but the processes which drive autoimmunity and lead to the differentiation of auto-reactive lymphocytes into autoantibody-producing plasma cells remains largely unknown. To date several epitope mapping studies have suggested autoimmunity in primary Sjögren's syndrome to be driven by autoantigens (Dorner and Lipsky 2002). Fox and co-workers have also proposed an excellent model for Sjögren's syndrome that incorporates all the current histopathological, genetic, serological and gene-profiling data available (Fox, Michelson et al. 2000); (Fox 2005).

This area of research considered the importance of studying the outcome measures in SjS patients which was also the focus of recent conferences (Bowman 2002). Assessment of the disease must be broken down into subdivisions: exocrine (inclusive of sicca symptoms and signs) and non-exocrine disease activity and systemic symptoms (objective evidence of extra-glandular activity and damage (present for over six months)); health-related and generic quality of life (inclusive of fatigue); standard approaches to adverse events and toxic effects; and health-economic elements (Fox 2005). There was also suggestion that the use of bio-markers similar to those in systemic lupus erythematosus (Illei, Tackey et al. 2004), inclusive of auto-antibodies, chemokines and cytokines would supplement clinical measurements.

Primary versus secondary

Clinically, Sjögren's syndrome is described as primary if dry mouth and dry eye's occur in isolation but secondary if it occurs in conjunction with another connective tissue disease (Scully 1986), such as rheumatoid arthritis, systemic lupus erythematosus and primary biliary cirrhosis (Jonsson, Haga et al. 2000).

Primary Sjögren's syndrome represents an idiopathic inflammatory exocrinopathy clearly characterised in two ways: (i) Organ-specific autoimmunity involving the salivary and/or lacrimal glands being preferentially chronically attacked by immune cells (Dorner and Lipsky 2002); (Li, Dai et al. 2004); (ii) numerous extra-glandular systemic features including fatigue, arthritis, pulmonary complications, interstitial nephritis, peripheral neuropathy and vasculitis (Garcia-Carrasco, Fuentes-Alexandro et al. 2006). Sjögren's syndrome may also be characterised by other severe complications such as lymphoma, congenital heart blocks, neonatal lupus and secondary infections as well as problems with caries (Fox, Howell et al. 1984);(Fox, Michelson et al. 2000);(Ramos-Casals, Anaya et al. 2004).

Table 1.5.2: Sjögren's syndrome classification criteria part 2.

<u>American-European rules for classification and exclusion criteria of Sjögren's syndrome (Vitali, Bombardieri et al. 2002)</u>
<p><i>For Primary Sjögren's syndrome</i> In patients without any potentially associated diseases, primary Sjögren's syndrome may be defined as follows:</p> <ol style="list-style-type: none"> 1. The presence of any 4 of the 6 items as indicative of primary Sjögren's syndrome, as long as either item 4 (Histopathology) and 6 (Serology) is positive. 2. The presence of any 3 of the 4 objective criteria items (that is items 3, 4, 5 and 6 from previous table). 3. The classification tree procedure represents a valid alternative method for classification, although it should be more properly used in clinical-epidemiological surveys. <p><i>For Primary Sjögren's syndrome</i> In patients with a potentially associated disease (for instance, another well defined connective tissue disease), the presence of item 1 or item 2 plus any 2 among items 3, 4 and 5 (from the previous table) may be considered as indicative of secondary Sjögren's syndrome.</p> <p><i>Exclusion criteria:</i></p> <p>Past head and neck radiation treatment Hepatitis C infection Acquired immunodeficiency disease (AIDS) Pre-existing lymphoma Sarcoidosis Graft versus host disease Use of anticholinergic drugs (since a time shorter than 4 – fold the half life of the drug)</p>

When groups of patients with primary Sjögren's syndrome were compared to those with secondary Sjögren's syndrome there were some striking differences in terms of HLA types (Moutsopoulos, Mann et al. 1979; Moutsopoulos, Chused et al. 1980) (HLA DR and DQ) and lymphocyte antigen expression (Kroneld, Halse et al. 1997). However, when comparing the degree of glandular hypofunction experienced by patients with primary Sjögren's syndrome to those with secondary Sjögren's syndrome, no obvious differences were found (Dawson, Holt et al. 2001). The available evidence suggests that primary and secondary Sjögren's syndrome probably do represent conditions with different aetiologies but the conditions do share similar features and common mechanisms related to the glandular hypofunction.

Causes of glandular hypofunction: Traditional view versus Current view of Sjögren's syndrome

Traditionally, the lack of glandular fluid secretion associated with Sjögren's syndrome was attributed to the immune mediated destruction of acinar cells within the salivary and lacrimal glands (Fox and Saito 1994). However, recently it has become clear that this traditional view is unable to explain more recent findings which included: (i) data which determined that in many patients experiencing glandular hypofunction there were large areas of apparently healthy tissue remaining (Fox and Maruyama 1997; Fox, Tornwall et al. 1999; Humphreys-Beher, Brayer et al. 1999); (ii) data from Immunohistochemical experiments demonstrated that Sjögren's syndrome glandular tissue, of both human and animal origin, presented overall neuronal innervation which remained intact subsequent to acinar cell loss (Konttinen, Platts et al. 1997; Zoukhri, Hodges et al. 1998); (iii) previous reports demonstrated that glandular hypofunction may be reduced in some SjS patients by the administration of immune-modulating drugs such as hydroxychloroquine (Tishler, Yaron et al. 1999) or interferon- α (Shiozawa, Tanaka et al. 1998; Ship, Fox et al. 1999) which would suggest that glandular hypofunction required components of the inflammatory process.

The sum of this data suggested that in many patients with Sjögren's syndrome the glandular hypofunction was not a direct result of loss of acinar tissue as was previously suggested (Kong, Ogawa et al. 1997; Nakamura, Koji et al. 1998) and subsequently led to the suggestion that glandular hypofunction was actually related to functional quiescence of the acinar cells (Humphreys-Beher and Peck 1999). The situation observed in SjS was very surprising as hypofunction was still occurring when physiologically normal tissue remained and the situation was complicated further by other data which demonstrated that acinar atrophy occurs in non-Sjögren's

elderly individuals but there is no accompanying reduction in salivary flow rate (Heft and Baum 1984; Ship and Baum 1990; Sreebny 1996) which would suggest that salivary glands have a functional reserve.

Although the late stages of the disease are characterised by the significant degree of fibrous-atrophy within the salivary glands and it would be sensible to assume that there would be a correlation between loss of acinar tissue and reduction in fluid secretion this is not the case when many patients are diagnosed with SjS. Data from numerous studies have also demonstrated a direct correlation between the degree of minor salivary gland infiltration and the resulting reduction in stimulated parotid salivary flow rates (Daniels 1984; Tsianos, Tzioufas et al. 1985; Hernandez and Daniels 1989; Saito, Fukuda et al. 1997). Glandular hypofunction has also been observed in other inflammatory conditions involving the salivary glands which include sialadenitis (Scully 1986) and SOX (Kassimos, Shirlaw et al. 1997).

The traditional model to explain glandular hypofunction in Sjögren's syndrome is loss of tissue as a direct result of immune attack mediated by a combination of apoptosis and cytotoxic cell death (Reviewed (Ramos-Casals and Font 2005)). This '*classical*' model stipulates that the process of glandular destruction is self-sustained by continued production of novel auto-antigens following formation of an apoptotic bleb or cell-death (Nagaraju, Cox et al. 2001) and organ failure was perceived to directly follow tissue loss. This was the research direction for Sjögren's syndrome for six decades with experiments conducted to determine the underlying mechanisms which resulted in destruction of the salivary and lacrimal acinar tissue. Such research considered the salivary glands to be only a 'reactor' for the infiltrating lymphocytes and not having a direct role in the pathological process of the disease (Dawson, Fox et al. 2006).

Most recent data suggests that the lack of secretory function in Sjögren's syndrome is due to hypofunction of the salivary acinar cells not actual destruction of the gland tissue, the destruction of the tissue is most likely subsequent to hypofunction and a direct result of this hypofunction as proposed in Dawson and co-workers non-apoptotic model of glandular hypofunction (Dawson, Fox et al. 2006). The remaining residual acinar tissue found present in many individuals should have the ability to maintain fluid secretion which would suggest a functional disruption of the any remaining acinar/neural tissue. Dawson and co-workers made a surprising discovery when they found that it was possible to stimulate Ca^{2+} mobilization in human labial cells, taken from labial gland biopsies of SjS patients, with ACh (Dawson, Field et al. 2001). This proved the cells were able to function in vitro but a clear right shift in ACh concentration was observable demonstrating a dose-dependence activity (Dawson, Field et al. 2001).

This relatively new idea of a 'non-apoptotic' model for glandular hypofunction observed in Sjögren's syndrome has been proposed and accommodates these previously stated findings (Fox and Maruyama 1997); (Humphreys-Beher, Brayer et al. 1999); (Dawson, Smith et al. 2000); (Gordon, Bolstad et al. 2001). This new model puts an alternative spin on the 'classical' model and suggests that glandular atrophy actually follows chronic immune-mediated inhibition of acinar secretory function but the many mechanisms of glandular hypofunction implicated in the 'classical' model apply equally well to this new 'non-apoptotic' model (Dawson, Fox et al. 2006). The key difference is that the atrophy is a consequence of salivary gland hypofunction and not the direct cause of it and this new theory therefore has significant implications from a clinical perspective as glandular destruction is irreversible whereas this immune-mediated glandular hypofunction may not be (Dawson, Fox et al. 2006). This new model offers hope to Sjögren's syndrome patients because identification of the underlying mechanisms may lead to the development of more

direct and sensitive diagnostic tools and hopefully to the development of disease modifying treatments.

So to summarise the numerous recent observations made challenge the 'classical' model and cast serious doubt upon the principles upon which it was based: (i) apoptosis of epithelial cells within the salivary glands has been determined to be a rare event (Ohlsson, Skarstein et al. 2001); (ii) as stated previously many patients with Sjögren's syndrome who have significantly reduced or totally absent glandular function (demonstrated by fluid secretion output) have large residual amounts of histologically normal acinar tissue within their salivary glands (Fox and Maruyama 1997); (iii) this residual tissue is able to function *in-vitro* (Pedersen, Dissing et al. 2000); (Dawson, Field et al. 2001), however, the acinar cells do demonstrate a reduced sensitivity to muscarinic stimulation (Dawson, Field et al. 2001). This final point is the most remarkable and a crucial observation as this outcome may also be observed *in-vivo* by the administration of systemic sialogogues to Sjögren's syndrome patients to stimulate secretion (Rhodus 1997). This observation is in total contrast to the 'classical' model as Sjögren's syndrome patients with no salivary flow should have no functional salivary tissue present but this is obviously not the case (Dawson, Fox et al. 2006).

1.6 Aims of the Study

The main aim of this project was to investigate the effect of NO on salivary acinar cells and determine if it had a role in fluid secretion. Previous work demonstrated that NO has the ability to mobilise calcium independently of ACh and also enhance the ability of ACh to mobilise calcium which could suggest a role for NO in secretion.

Sjögrens syndrome (SjS) is an auto-immune condition characterised by salivary and lacrimal gland hypofunction resulting from failure of acinar cells to secrete. NO is known to be elevated in SjS patients and the project focussed on determining if NO could have a role in glandular hypofunction. Previous work suggested NO could induce hyper-function but the work presented in this thesis may suggest that NO could have a role in hypo-function.

There were also two smaller sub-projects based on two separate hypotheses:

- (1). That a signal induced by a marker of stress such as ATP may induce a signal pattern other to that induced by mediators of salivary secretion such as ACh but our experimental techniques were unable to visualise any obvious variations but did observe an additive effect when ACh and ATP were used in combination.
- (2). That cells designated as so called 'pacemaker' cells, such as those found in the heart, may be present in the salivary glands and may account for the specific focal lymphocytic infiltration observed in SjS and the likelihood and importance of cell to cell signalling within the salivary glands.

Chapter Two

Materials and Methods



UNIVERSITY OF
LIVERPOOL

Materials and Methods

2.1 - Solutions

Standard Extra-cellular Bathing Solution

The extracellular bathing solution "Na HEPES" used for all experiments comprised the following (mM): NaCl (BDH 10241AP) 140, KCl (BDH 101985M) 4.7, MgCl₂ (BDH 101494V) 1.13, Glucose (Sigma G-7021) 10 and HEPES (Sigma H-3375) 10 ± CaCl₂ (Sigma C-4901) 1.

Na HEPES was constituted in deionised water, titrated to pH 7.4 using 1M NaOH (Sigma S-5881) and stored at 4°C. When required, Ca²⁺ was added immediately prior to the experiment.

Test Solutions

Stock solutions were generally 1000x working solution and stored at 4°C or -20°C.

When DMSO (Sigma D-5879) was used as a vehicle, final concentrations of DMSO were <0.1% to avoid effect on cells.

Table 2.1.1: Table of all chemical details.

Chemical	Supplier		Primary Vehicle	Secondary Vehicle	Stock Conc.	Working Conc.
Acetylcholine	Sigma 2661	A-	Water	Na HEPES	10mM - 1µM	5 - 5000nM
ATP	Sigma 2383	A-	Water	Na HEPES	100mM	50 - 1000µM
Atropine	Sigma 0132	A-	Water	Na HEPES	2mM	2µM
Carbachol	Sigma 4382	C-	Water	Na HEPES	10mM - 50µM	5 – 5000nM
EGTA	BDH E-4378		Water	Na HEPES	100mM	1 - 10µM
FURA-2	Sigma 0888	F-	DMSO	Na HEPES	1mM	2µM
Ionomycin	Sigma I-0634		DMSO	Na HEPES	10mM	1 - 10µM
NOC-5	Calbiochem 487950		NaOH	Na HEPES	100mM	100µM
NOC-12	Calbiochem 487955		NaOH	Na HEPES	100mM	100 - 1000µM
ODQ	Sigma 3636	O-	DMSO	Na HEPES	10mM	10µM
Ryanodine	Sigma 6017	R-	Water	Na HEPES	10mM	10µM
SNAP	Sigma 3398	N-	DMSO	Na HEPES	200mM	50 - 200µM
SNP	Sigma 228710		Water	Na HEPES	100mM	50 - 200µM
Thapsigargin	Sigma 9033	T-	DMSO	Na HEPES	10mM	1 - 10µM

Tissue Culture Medium

Primary Tissue Culture

When cells were in primary culture, Gibco D-MEM: F-12 (1:1) + L-Glutamine + 15mM HEPES (Ref: 31330-038) was used in conjunction with 1% antibiotics/ antimycotics (Sigma A-5955). Media was serum free, to limit proliferation, reducing the risk of any phenotypic changes.

Cell Line Culture

When cells were in continuous cell culture, such as the standard CHO cell line, then Gibco D-MEM: F-12 (1:1) + L-Glutamine + 15mM HEPES (Ref: 31330-038) was supplemented with 5% foetal calf serum (Sigma F-7524).

Cell Isolation Solution

Acinar cells were harvested from the isolated salivary glands using collagenase (200U/ml) in calcium containing "Na HEPES" (Worthington Biochemical Corporation, USA Ref: 5273). Following reconstitution the collagenase solution was stored at -20°C in 1ml aliquots. This type of collagenase based solution was used for both human and mouse tissue digestion.

2.2 - Nitric Oxide Donors

SNAP – S-nitroso-N-acetylpenicillamine

SNAP (Table 2.1.1) was stored at -20°C. Each day SNAP was dissolved in DMSO, forming a 100mM stock solution. The stock solution was then diluted in “Na HEPES” forming the 100 to 200µM working solution.

SNP – Sodium nitroprusside

SNP (Table 2.1.1) was stored at room temperature. Each day SNP was dissolved in water forming a 100mM stock solution. The stock solution was then diluted in “Na HEPES” forming the 100 to 200µM working solution.

NOC-5 - 3-[2-hydroxy-1-(1-methylethyl)-2-nitrosohydrazino]-1-propanamine

NOC-12 - N-ethyl-2-(1-ethyl-2-hydroxy-2-nitrosohydrazino)ethanamine

NOC-5 and NOC-12 (Table 2.1.1) were stored at -20°C. The solutions were initially dissolved in DMSO to form 100mM stock solutions. These stock solutions were then dispensed into 10µl and 20µl aliquots and maintained at -20°C for 3 months. At the start of an experiment the stock solution aliquots were diluted in “Na HEPES” to form the working solution of 200µM.

2.3 - Nitric Oxide Inhibitors

ODQ - 1H [1,2,4]oxadiazolo[4,3,α] quinoxaline-1-one

ODQ (Table 2.1.1) was stored at 4°C. The solution was initially dissolved in DMSO to form a 10mM stock solution. This stock solution was then dispensed into 100μl aliquots and maintained at -20°C for 3-4 weeks or 4 °C for 3-4 days. Prior to an experiment the stock solution aliquots were diluted in “Na HEPES” to form the working solution of 10μM.

RYANODINE

Ryanodine (Table 2.1.1) was stored at room temperature. The solution was initially dissolved in water to form a 10mM stock solution. This stock solution was then dispensed into 10μl aliquots and maintained at -20°C for 6 months. The stock solution aliquots were diluted in “Na HEPES” to form the working solution of 10μM.

Precautions

All working solutions were used on the day they were made up and any remaining solution discarded at the end of the day due to the instability of all working solutions once made up in calcium containing “Na HEPES”. All solutions were also light sensitive so were maintained in the dark and used under red light conditions only. All NO donors and inhibitors are more fully described and explained in detail within the introduction and result sections.

2.4 - Preparation of Mouse Acinar Cells

Submandibular salivary acinar cells were obtained from Male CD-1 mice (5-8 weeks of age). The CD-1 mice strain is a standard out-bred strain and was obtained from Charles River Laboratories (Charles River UK Ltd, Margate, UK) but maintained within the University animal house for up to 3 weeks.

Following sacrifice, by cervical dislocation, the submandibular and/or lacrimal glands were removed. Acinar cells were obtained from the glands following digestion with the cell isolation solution. Digestion was facilitated by injection of cell isolation solution directly into the gland lobules followed by microdissection and removal of the glandular capsule. To facilitate the disassociation of the acinar cells from the glandular connective tissue, the injected gland sample was then incubated in an additional 1ml of cell isolation solution at 34°C for 15 minutes in a shaking water bath with additional vigorous manual agitations at 5 minute intervals. After the 15 minute incubation period large undigested glandular fragments were removed and the smaller fragments were further dissociated using a pastette to agitate the solution. The free acinar cells were then concentrated via centrifugation at 370 RCF for 2 minutes at room temperature. The supernatant was decanted and the cell pellet was re-suspended in experimental medium ("Na HEPES" or Primary Tissue Culture medium), to extinguish any residual collagenase activity by dilution. This procedure for cell isolation yielded either individual acinar cells or small clumps of 2 to 10 acinar cells.

2.5 - Preparation of Human Acinar Cells

Following local ethical committee approval (Ref EC.75.98) and informed consent, small samples of submandibular gland were obtained from patients that were undergoing routine head and neck surgery. The samples obtained were so small that they had no impact on the subsequent diagnosis or treatment of the patients. Tissue was not obtained from patient'-s who had undergone radiation to the head and neck, had salivary gland malignancy or were taking known xerogenic medications.

Upon removal from the patient, the tissue samples were immediately placed into ice cold primary tissue culture medium and transported on ice to the laboratory within 1 hour. On arrival in the laboratory the human tissue samples required micro-dissection to facilitate dispersal of the acinar cells. To aid digestion all the connective tissue was removed and the tissue sample was opened up manually to allow better digestion and dispersal of cells from the connective tissues. Following dissection of the sample acinar cells were obtained using cell isolation media and the methods stated previously for mouse acinar cells.

2.6 - Primary Cell Culture

Matrigel coated coverslips:

The experimental protocols required the acinar cells to be immobilised on coverslips. To facilitate this we pre-coated coverslips with matrigel (Cat No. 354234) which acts as a synthetic basement membrane, allowing the cells to anchor to the glass coverslip.

The matrigel was allowed to set on the coverslips for 30 minutes at 37°C within a humidified 95%O₂/5%CO₂ incubator. The individual cover-slips were maintained within separate wells of a 6 well plate (Greiner Bio-one Cell star No. 657160). Once the cells were dispensed onto the cover-slips they were allowed to settle for approximately 30 minutes to allow for attachment. The coverslips were then covered with approximately 3ml of primary tissue culture medium. Identical procedures were used for both mouse and human cell types for primary cell culture. The cover-slips were used for their size and shape (22mm circular cover-slips thickness No.1 VWR International Cat-No. 631-0158) as these were able to act as the base of the perfusion chamber once incorporated into the custom built chamber.

2.7 – Suitability of Cells Selected

The acinar cell preparation procedure ensures the removal of the majority of non-acinar cells such ductal cells. The ductal cells would remain primarily within the connective tissue fraction following collagenase digestion and mechanical agitation. So due to the discarding of any undigested tissue prior to dispersal of cells onto coverslips the majority of the ductal cells would be discarded. It is however impossible to ensure that all ductal cells are removed from the test sample but ductal cells will not respond as acinar cells do so would not be selected for experimentation.

Each coverslip is only used for a single experiment which ensures continuity of results so cells are not pre-exposed to any agonists prior to experimental runs.

The number of experiments conducted was totally dependent on the experimental outcome i.e. if it was a clearly observable, large response then fewer experiments were conducted, however, in all cases enough experiments were conducted to give an acceptable number of runs with relation to statistical analyses.

There was no observable variation between time points, if cells were viable they were viable regardless of time spent in culture so viability was independent of time with relation to these experiments.

Cells were considered healthy if they had an irregular shape and a low resting calcium level.

2.8 - Experimental Procedures and Nitric Oxide Protocol

Ca^{2+} concentration is used as an indicator of secretion so by studying the effect of NO on Ca^{2+} secretion the effect which NO may or may not elicit on salivary secretion can be demonstrated.

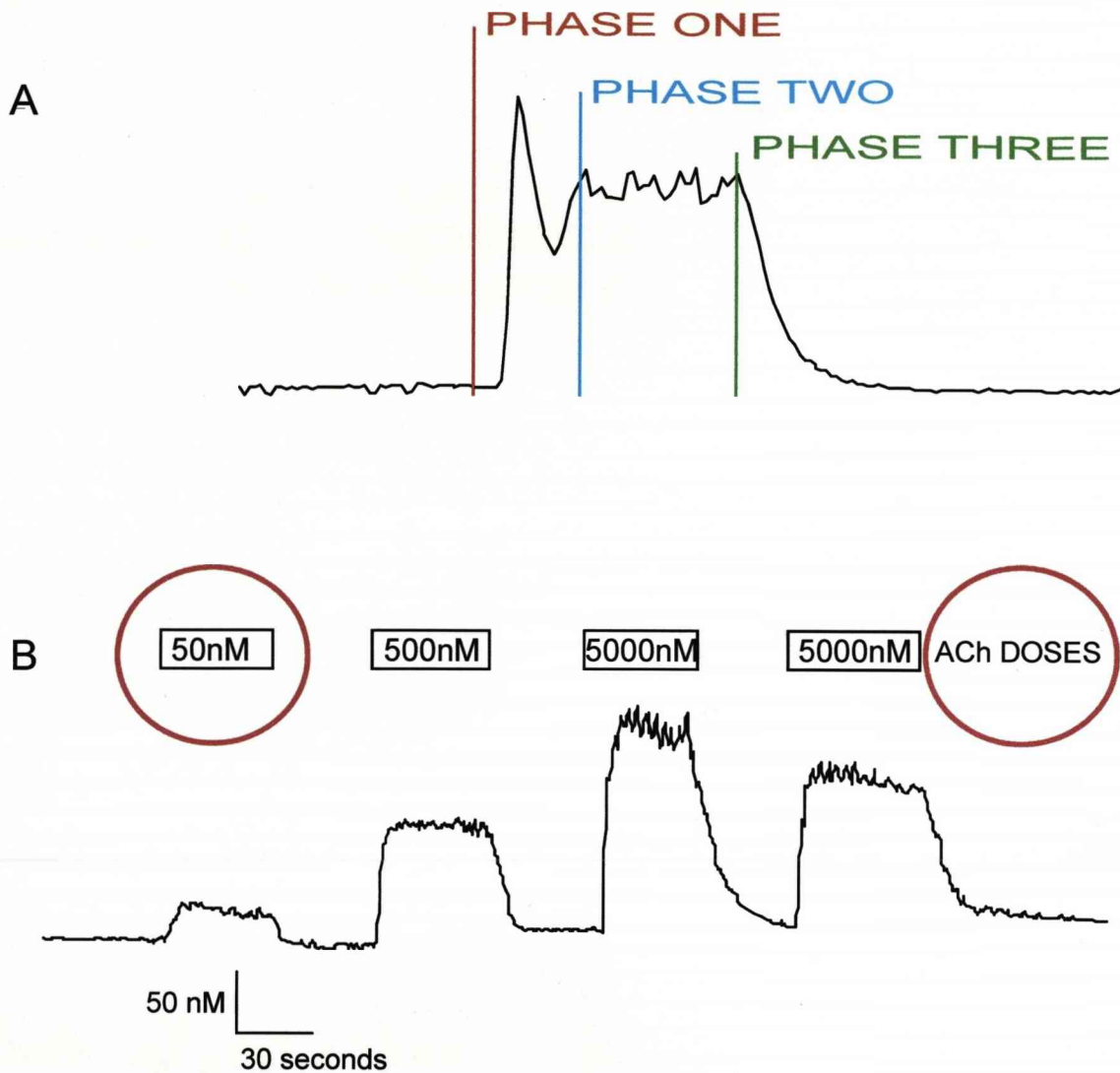
The response of mouse submandibular acinar cells to ACh follows a typical pattern, which may be divided into three phases (figure 2.8.1: trace A). Phase one was initiated immediately upon exposure to stimulus and is characterised by a rapid rise in $[\text{Ca}^{2+}]_i$, observed as an upward "spike" in the trace from resting $[\text{Ca}^{2+}]_i$ level. The presence, absence, or size of the spike is largely independent of the agonist concentration. In phase two the $[\text{Ca}^{2+}]_i$ level stabilises and is characterised by a sustained plateau in the $[\text{Ca}^{2+}]_i$, at a level below that of the "spike". The magnitude of the plateau phase of the response increased in proportion with agonist concentration. In phase three, once the stimulus was removed there was a return to the resting $[\text{Ca}^{2+}]_i$ level. A rapid rate of recovery was used as a further indicator of cell viability.

The data in figure 2.8.1: trace B show the time-course of the change in the $[\text{Ca}^{2+}]_i$ response following application of ACh in mouse submandibular acinar cells. Three concentrations of ACh were used; 50, 500 and 5000nM. Low resting $[\text{Ca}^{2+}]_i$ was used as an indicator of cell viability and cells with elevated resting $[\text{Ca}^{2+}]_i$ levels were discarded. Application of ACh induced a rapid rise in the $[\text{Ca}^{2+}]_i$ that persisted for the duration of the stimulus. Once ACh was removed the $[\text{Ca}^{2+}]_i$ rapidly returned to pre-stimulus resting levels.

On average, 50nM ACh caused an increase in $[\text{Ca}^{2+}]_i$ of $62.40 \pm 10.96\text{nm}$ (n=25), 500nM ACh caused an increase in $[\text{Ca}^{2+}]_i$ of $156.60 \pm 19.80\text{nm}$ (n=25) and 5000nM

Figure 2.8.1

Change in $[Ca^{2+}]_i$ in response to 50nM ACh and the $[Ca^{2+}]_i$ variation in response to 50, 500 and 5000nM ACh.



ACh (50, 500 and 5000nM) stimulated increased $[Ca^{2+}]_i$ measured in mouse submandibular acinar cells maintained in primary tissue culture fluid for 24hours.

Trace A shows single response to 50nM ACh and illustrates the phases of the response.

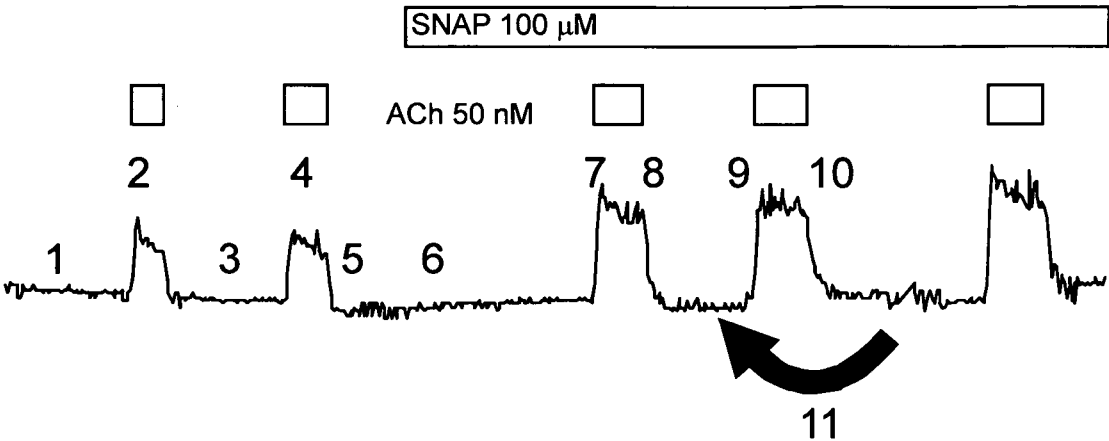
Trace B shows repeated responses to ACh at three concentrations, which increase in magnitude, the second response to 5000nM ACh illustrates how repeated exposure to higher concentrations of ACh cause a decrease in the level of response. The red circles highlight the rectangles, numbers and agonist, the rectangles demonstrate duration of exposure to agonist, the number defines the specific concentration of agonist and agonist stated.

ACh caused an increase in $[Ca^{2+}]_i$ of 202.40 ± 26.27 nm (n=22). Based on these data, a 50nM concentration of ACh was selected as being suitable for this particular set of experiments on the basis that this concentration of ACh would stimulate consistent responses in $[Ca^{2+}]_i$.

The experimental protocol used in this thesis was designed to allow direct evaluation of the effect of Ca^{2+} signal modulators, such as Nitric Oxide (NO), on the acinar cell $[Ca^{2+}]_i$ response (figure 2.8.2). The protocol allowed the experiments to be clearly divided into two group's, control and NO exposed, and then further sub-divided into pre and post NO exposure responses, with the response to ACh being determined prior to application of NO donor and then throughout the duration of exposure to the NO donor. Control experiments demonstrated that any changes, amplifications or reductions in the $[Ca^{2+}]_i$ response were attributable only to the effects of the NO donor.

The acinar cells were initially stimulated two or three times with 50nM ACh until a consistent response was achieved. Then, dependent on experiment protocol, the cells were either maintained under control conditions (NO free) or continuously subjected to the NO donor. Three minutes post exposure to the NO donor the cells were again exposed to 50nM ACh. Control cells were given an equivalent time gap. For the remainder of the experiment acinar cells were subjected to 50nM ACh approximately every four minutes.

Figure 2.8.2
Experimental Protocol



Time Point	Experimental Procedure Description	Average Duration (Seconds)
1	Experiment initiates and cells bathed in hepes only which sets base line	60
2	Cells exposed to ACh to determine response	30
3	Cells returned to hepes and recover to baseline	60
4	Cells exposed to ACh to ensure consistency of response , this step repeated if 2 and 4 vary	30
5	Cells returned to hepes and recover to baseline	60
6	Dependent on experimental type (i.e. If control or NO affected) cells are either maintained in hepes (control) or are continuously exposed to NO donor, NO inhibitor or combined NO donor/ inhibitor solution (NO effect)	180
7	Cells exposed to ACh to demonstrate response (If NO effect experiment expect variation)	30
8	Cells returned to control hepes or experimental hepes dependent on experiment type	150
9	Cells exposed to ACh to demonstrate response (If NO effect experiment expect variation)	30
10	Cells returned to control hepes or experimental hepes dependent on experiment type	150
11	Steps 9 and 10 repeated as many times as necessary either until cells no-longer responsive or a comparable time point for controls achieved	

2.9 - Measurement of $[Ca^{2+}]_i$

Cell Loading

Fura-2 was used to detect changes in the cytoplasm calcium concentration. This indicator could be loaded into individual cells, with minimal alteration in cellular homeostasis (Tsien 1980), allowing for the determination of changes in $[Ca^{2+}]_i$ occurring within the individual acinar cells. Fura-2 (Figure 2.9.1.) represents the latest generation of Ca^{2+} indicators (Grynkiewicz, Poenie et al. 1985). The cells were loaded at room temperature, which took approximately 30 minutes when the cells were in acute form or 15 minutes under primary culture conditions.

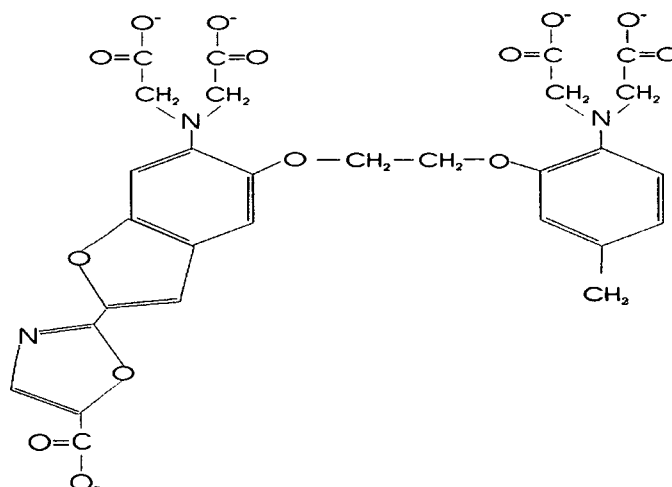


Figure 2.9.1: Figure illustrating the chemical structure of Fura-2.

The concentration of free calcium also alters the fluorescent properties of Fura-2 in that in its absence, the excitation maximum is approximately 380nm and when calcium is present the excitation maximum is 340nm. The variations in these two values are therefore functional in relation to $[Ca^{2+}]_i$ as the light emitted by fura is relative to the concentration of calcium present when excited at either wavelength. To remove any effect induced by the dye the light emitted at 340nm and 380nm is ratioed as the concentration of the dye also affects intensity of light emitted. When Fura-2 is excited at either 340 or 380nm it emits maximally at 510nm.

2.10 - Microfluorimetry

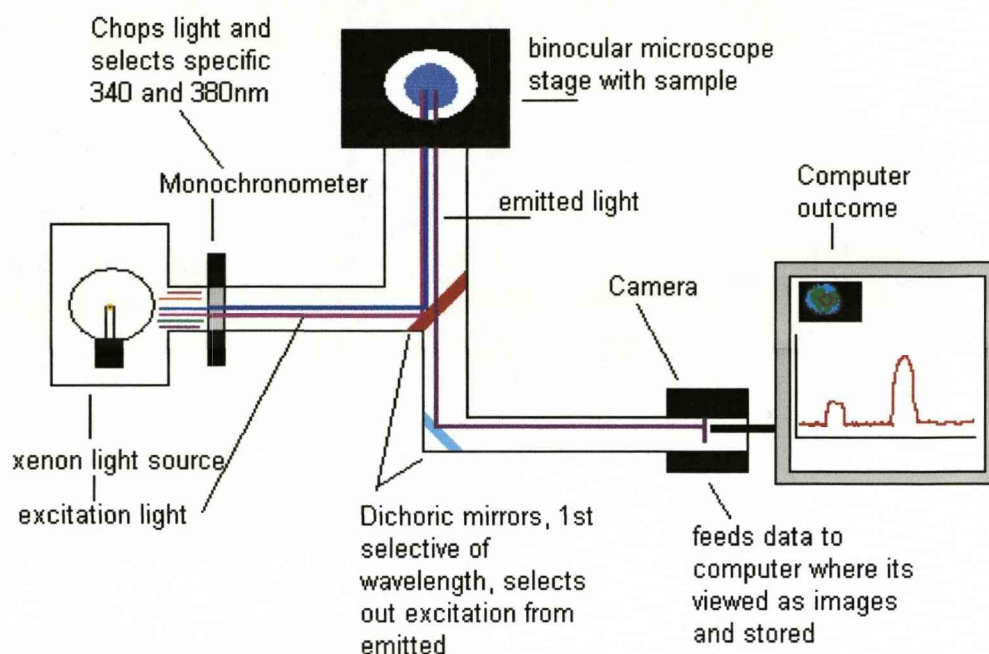


Figure 2.10.1: Schematic diagram of the microfluorimetry rig used to visualize and record acinar cell responses induced by agonists.

Measurement of $[Ca^{2+}]_i$ was determined in individual acinar cells or small clumps (with no more than 8 cells present) using a Cairn Spectrophotometer (Cairn Research, Cambridge). A Xenon arc lamp produces the excitation wavelengths and the output is controlled via a monochromator, which cuts the light into the selected 340/380nm wavelengths and thus selects for fura-2 wavelengths.

The alternating light is then passed along a quartz light guide, which guides it directly into the Nikon-diaphot inverted binocular microscope (TMD 100; Nikon, Kingston, UK). Upon entering the microscope the light is reflected using a dichroic mirror, which has a cut-off of approximately 400nm. The light is focussed upon the specimen within the experimental chamber upon the microscope stage via a CF Fluor oil quartz

objective. The light then emitted by the specimen is reflected through a 510nm long pass emission filter and images captured using a CCD camera. The camera feeds the paired images, captured every 120 to 500 milliseconds dependent on acquisition rate, directly to the computer, which visualises and stores data. Figure 2.10.1 shows a simple diagrammatic representation of the Microfluorimetry rig.

It is also possible to alter the orientation of the emitted light using a plane mirror so that the emitted light can either be detected through the microscope eyepiece or to the CCD camera. Two dichoric mirrors allow for light selection, the first selects excitation from emitted wavelength and the second bounces the appropriate wavelength to the CCD camera. The camera detects emerging light at 510nm and allows visualisation of the cells during data collection. This type of calcium imaging was developed and employed to reveal changes in $[Ca^{2+}]_i$ in various regions of the cell.

2.11 - Perfusion Procedure

The cover-slips formed the base of a custom built perfusion chamber. The chamber itself was placed onto the stage of an inverted binocular microscope (Nikon, Japan). The cells were perfused continuously by a gravity fed system consisting of 8 parallel pipettes (0.5mm internal diameter). The system allowed for application of multiple test solutions and rapid changing of the bathing solution, approximately every 3 seconds. The parallel pipettes were gathered at the terminal end and placed into a single perfusion tip which was in turn positioned 1mm from the cell under experimental investigation (figure 2.11.1).

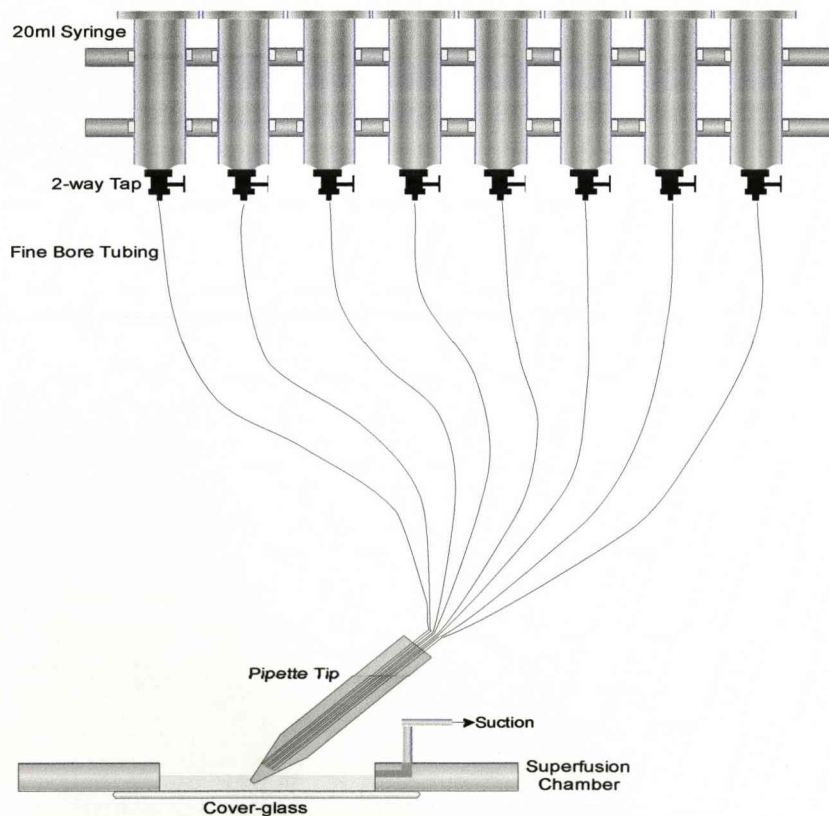


Figure 2.11.1: Illustration of the primary perfusion system. Diagram courtesy of Dr. Luke Dawson.

2.12 Statistics and Data Presentation

Data are presented as Mean \pm Standard Error of the mean (with number of observations i.e. n=).

The experimental data for the Nitric Oxide sections are presented as percentages compared to original response i.e. at the first experimental response (post addition of NO maintenance solution or control solution dependent on experiment) the cumulative control result is $101.5 \pm 3.39\%$ of the original which is taken to be 100%. This allowed all data to be directly comparable as all cells were being compared to themselves initially then their final values compared with all other results.

Statistical test used = unpaired two tail T-test.

Significance stated at the 0.1, 1 and 5% levels where appropriate.

Chapter Three

Results

Nitric Oxide

Mouse Submandibular Acinar Cells



UNIVERSITY OF
LIVERPOOL

Introduction

The starting point of these experiments was reproduction of previous work to ensure consistency of data. In the initial experiments NO induced Ca^{2+} mobilisation not inhibition and was thus causing hyperfunction and not hypofunction. These results support previous findings and confirm the expected effect of NO on Ca^{2+} as you would expect hyperfunction based on the ability of NO to stimulate the release of Ca^{2+} via its activity on the cGMP/cADPr pathway. The initial experiments and all work done previously were performed acutely and so only demonstrated the ability of NO to mobilise Ca^{2+} and not its ultimate effect. Subsequent experiments presented in this thesis were performed under more chronic conditions to show the effect of NO on acinar cells in the long term.

The experiments were performed using Mouse submandibular acinar cells. This cell type was chosen as it is readily available and from an acceptable model animal. All experiments were performed in accordance with the strict protocol described previously (Chapter 2 materials and methods section 2.8, figure 2.8.2), which was also prototyped using the mouse submandibular acinar cells. The response of mouse submandibular acinar cells to ACh follows a typical pattern as described previously (Chapter 2 materials and methods section 2.8, figure 2.8.1 trace A).

The experiments were conducted using four NO donors: S-nitroso-N-acetylpenicillamine (SNAP), Sodium nitroprusside (SNP), N-Ethyl-2-(1-ethyl-2-hydroxy-2-nitrosohydrazino)ethanamine (NOC-12), 3-[2-hydroxy-1-(1-methylethyl)-2-nitrosohydrazino]-1-propanamine (NOC-5) and two NO pathway inhibitors: 1H [1,2,4]oxadiazolo[4,3, α] quinoxaline-1-one (ODQ) and Ryanodine.

Results

The first set of experiments were performed using S-nitroso-N-acetylpenicillamine (SNAP) only to ensure consistency of results with previous work. Figure 3.1.1 shows a representative trace demonstrating the effect of the NO donor SNAP on mouse submandibular acinar cells. The NO released by SNAP induced mobilisation of $[Ca^{2+}]_i$ independently of ACh which is demonstrated by the gradual rise in level.

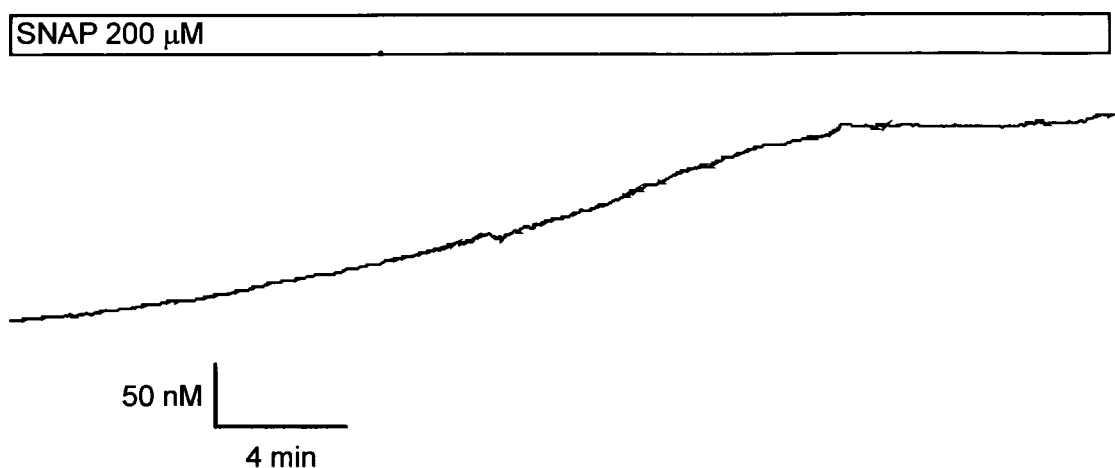
SNAP was selected based on the work carried out previously by Looms and colleagues (Looms, Tritsarlis et al. 2001). In the first instance the protocol outlined by Looms was followed using a 200 μ M concentration of SNAP. However, it was subsequently identified that 100 μ M SNAP produced reproducible $[Ca^{2+}]_i$ responses under the experimental conditions discussed here. This concentration of SNAP was the minimum dose which gave reproducible responses.

Table 3.1.1: Table of results for mouse submandibular acinar cells

Number of samples	Type of Response	Degree of Response (Mean \pm SE) as a Percentage	Time Taken to decrease to zero (where applicable)
n=12	Control	101.5 \pm 3.39%	N/A
n=15	SNAP	235.8 \pm 35.39%	32
n=22	NOC-12	162.5 \pm 10.4%	74
n=9	SNP	151.7 \pm 23.03%	40
n=5	NOC-5	200.2 \pm 48.5%	N/A
n=5	ODQ + SNAP	113.6 \pm 3.83%	28
n=5	ODQ + NOC-12	103.3 \pm 2.23%	36
n=7	Ryanodine	115.2 \pm 5.11%	N/A
n=8	Ryanodine + NOC-12	121.3 \pm 10.84%	N/A

Figure 3.1.1

Change in $[Ca^{2+}]_i$ in response to 200 μ M SNAP, illustrating how NO alone induced a $[Ca^{2+}]_i$ signal response.



SNAP (200 μ M) stimulated increased $[Ca^{2+}]_i$ measured in mouse submandibular acinar cells maintained in primary tissue culture fluid for 24 hours. Trace shows response to stimulation with NO donor SNAP only(see scale bar).

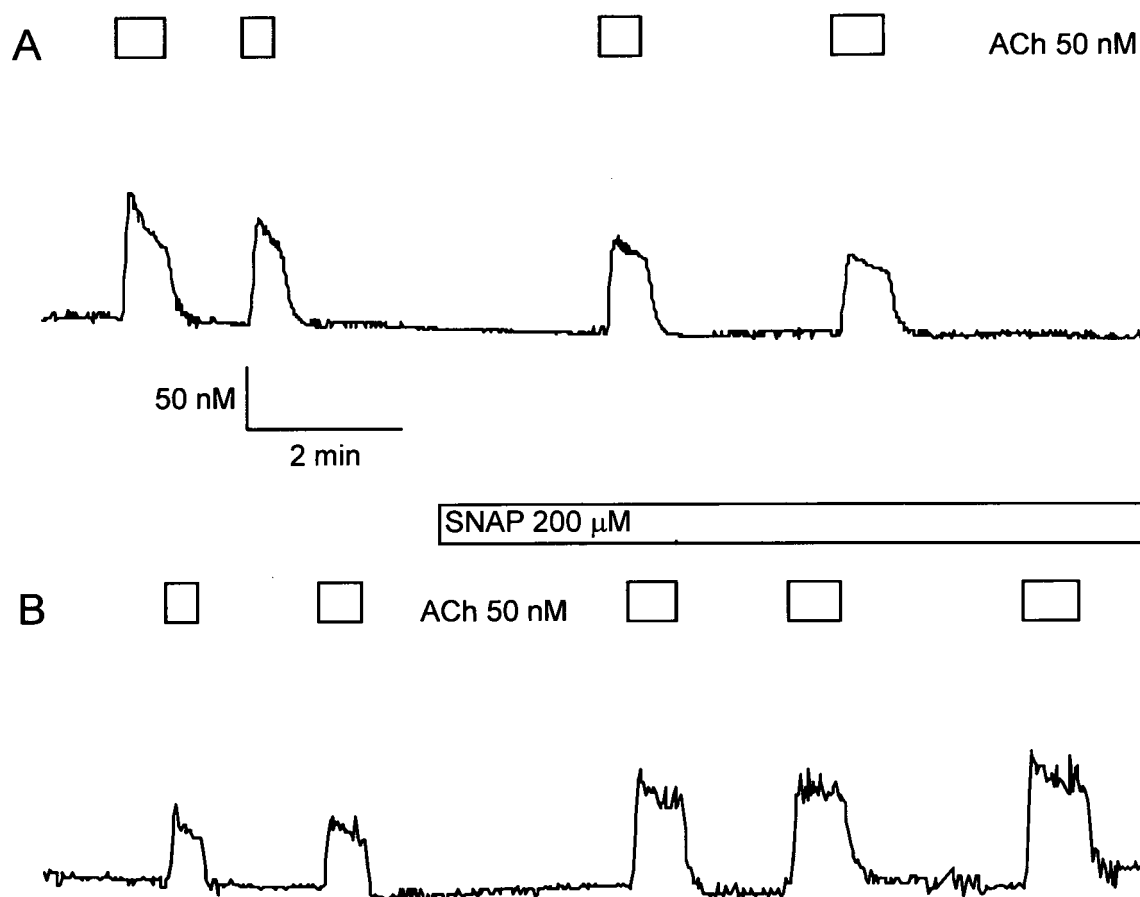
Acute Experiments

The second set of experiments were performed using all four NO donors acutely to show the effect of NO on ACh-evoked Ca^{2+} signal. Figure 3.1.2 parts A and B shows representative traces demonstrating the effect of the NO donor SNAP on the ACh-evoked increase in $[\text{Ca}^{2+}]_i$ in mouse submandibular acinar cells. Trace A shows a series of control responses to ACh (50nM) over the protocol defined time points. Trace B shows the responses to ACh (50nM) in the presence of SNAP (200 μM) over the same protocol defined time points. Comparison of the cell response to ACh (50nM) under control conditions (A) to that obtained following exposure to SNAP (B) at equivalent time points, shows that exposure of the mouse submandibular acinar cells to SNAP significantly ($P < 0.01$) increased the $[\text{Ca}^{2+}]_i$ plateau of response to ACh (50nM) from an average control response of $101.5 \pm 3.39\%$ ($n=12$) to $235.8 \pm 35.39\%$ ($n=15$). The data in figure 3.1.2 demonstrate NO induced amplification of the ACh-evoked increase in $[\text{Ca}^{2+}]_i$.

Following the use of SNAP other alternative NO donors were identified and selected. This group of alternative NO donors included the "NOC's" and N-Ethyl-2-(1-ethyl-2-hydroxy-2-nitrosohydrazino)ethanamine (NOC-12) was subsequently selected as a suitable alternative to SNAP because NOC-12 releases no biologically relevant degradation by-products. The by-products released by SNAP were considered to possibly have the ability, independently of NO, to induce a reduction in the $[\text{Ca}^{2+}]_i$ response through cellular inhibition, so NOC-12 was considered as a more suitable NO donor in order to eliminate any possibility of result bias being introduced by the SNAP by-products. The suitability of each NO donor is discussed further within the introduction.

Figure 3.1.2

Change in $[Ca^{2+}]_i$ in response to 50nM ACh, illustrating how 100 μ M SNAP induced amplification of the $[Ca^{2+}]_i$ signal.



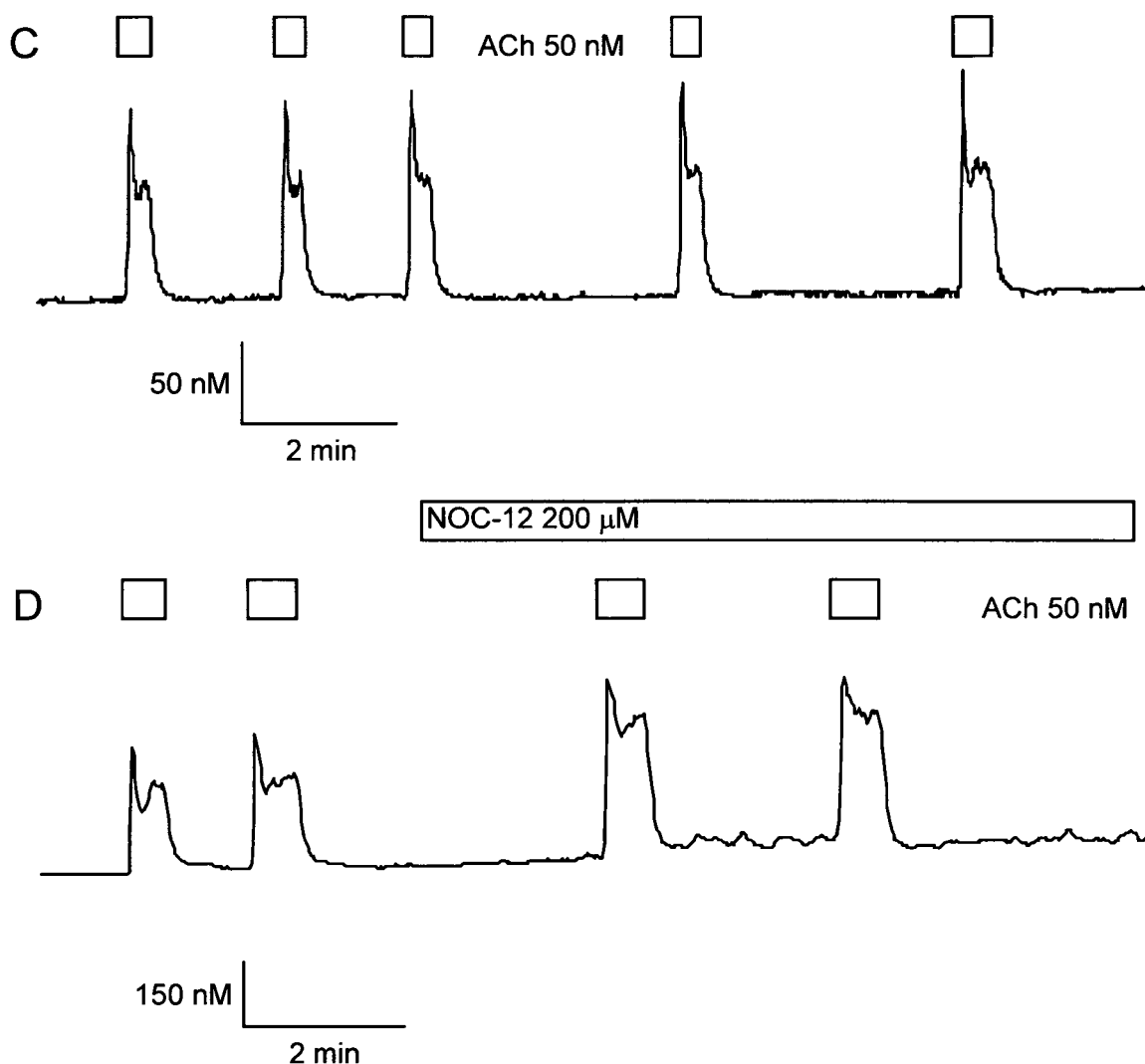
ACh (50 nM) stimulated increased $[Ca^{2+}]_i$ measured in mouse submandibular acinar cells maintained in primary tissue culture fluid for 2 (trace A) and 48 hours (trace B) respectively.

Trace A shows response to repeated stimulation with 50nM ACh only (see scale bar).

Trace B shows responses to repeated stimulation with 50nM ACh before and after application of the NO donor SNAP acutely (see scale bar).

Figure 3.1.2

Change in $[Ca^{2+}]_i$ in response to 50nM ACh, illustrating how 200 μ M NOC-12 induced amplification of the $[Ca^{2+}]_i$ signal.



ACh (50 nM) stimulated increased $[Ca^{2+}]_i$ measured in mouse submandibular acinar cells maintained in primary tissue culture fluid for 24 hours.

Trace C shows response to repeated stimulation with 50nM ACh only (see scale bar).

Trace D shows responses to repeated stimulation with 50nM ACh before and after application of the NO donor NOC-12 acutely (see scale bar).

Figure 3.1.2 parts C and D shows representative traces which demonstrate the effect of the NO donor NOC-12 on the ACh-evoked increase in $[Ca^{2+}]_i$ in mouse submandibular acinar cells. Trace C shows a series of control $[Ca^{2+}]_i$ responses to ACh (50nM) over the protocol defined time points. Trace D shows the $[Ca^{2+}]_i$ responses to ACh (50nM) in the presence of NOC-12 (200 μ M) over similar protocol defined time points. Comparison of the $[Ca^{2+}]_i$ response of cells to ACh under control conditions (C) to that obtained following exposure to NOC-12 (D) at equivalent time points, shows that exposure of the mouse submandibular acinar cells to NOC-12 significantly ($P < 0.001$) increased the plateau of response to ACh from an average control response of $101.5 \pm 3.39\%$ ($n=12$) to $162.5 \pm 10.4\%$ ($n=22$). So the amplification induced by either NO donor was statistically significant.

Following the use of SNAP and NOC-12 as donors of NO two other NO donors were selected to validate the results achieved. Sodium Nitroprusside (SNP) and 3-(2-Hydroxy-1-(1-methylethyl)-2-nitrohydrazino)-1-propanamine (NOC-5) were selected as alternative donors of NO. SNP allows direct comparison with SNAP as it is from the same group of NO donors, the s-nitrothiols, and it too releases biologically relevant degradation by-products (as discussed Chapter 1 Introduction 1.2 Nitric oxide section). NOC-5 belongs to the NOC family so allows direct comparison with NOC-12, however, NOC-5 releases NO much more rapidly, approximately 3 times faster than NOC-12, at a rate more equivalent to SNAP. SNP and NOC-5 were used under the same experimental protocol and the results compared to those achieved using SNAP and NOC-12. A concentration of 75 μ M was selected for SNP as this was the lowest dose which would induce reproducible responses. NOC-5 was used at 200 μ M to keep it directly comparable to NOC-12.

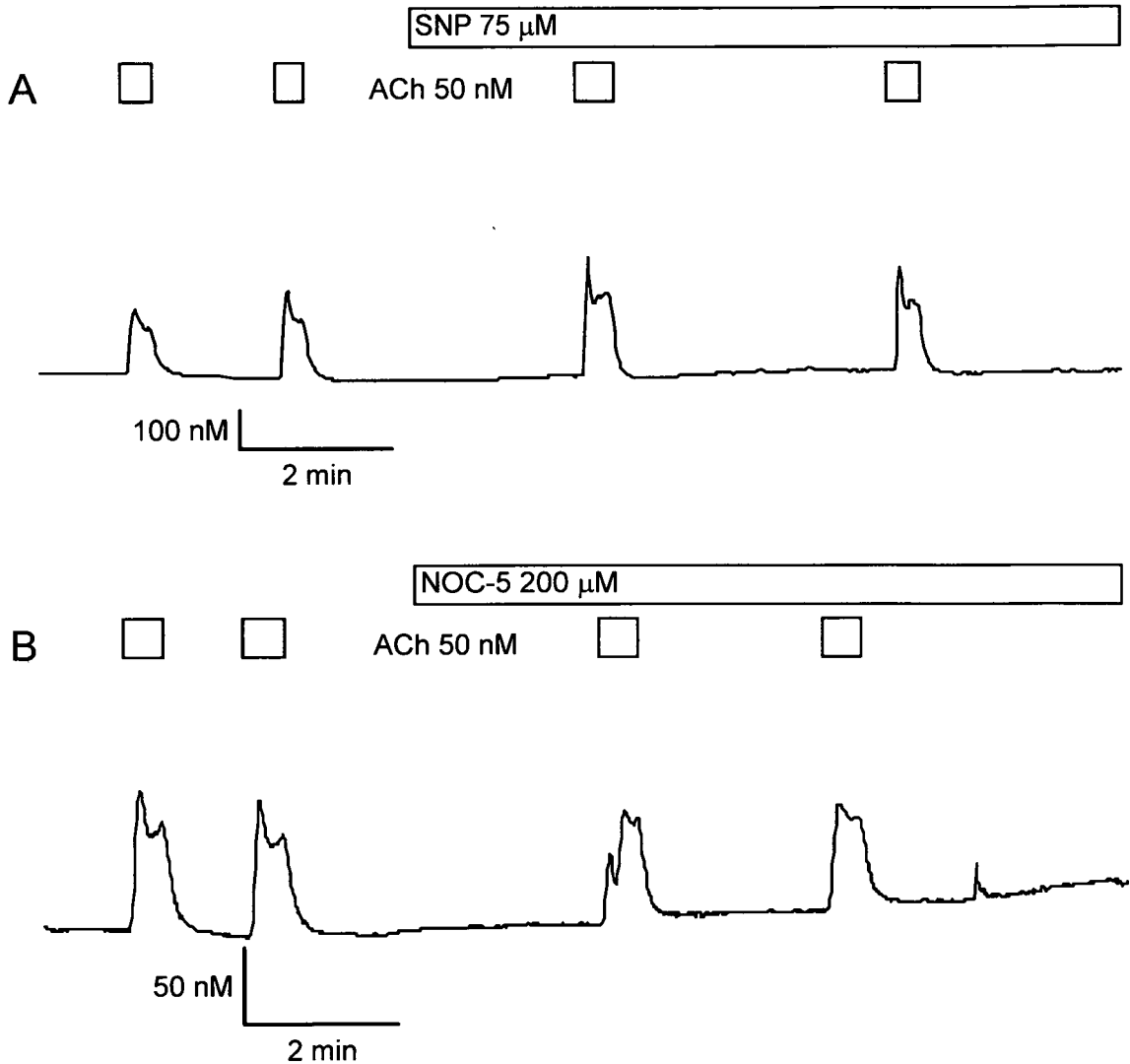
Figure 3.1.3 shows representative traces illustrating the acute affect of NO donor SNP (A) and NOC-5 (B) on the ACh-evoked increase in $[Ca^{2+}]_i$ in mouse submandibular acinar cells. Trace A shows the $[Ca^{2+}]_i$ responses to ACh (50nM) in the presence of SNP (75 μ M) over the protocol defined time points. Trace B shows the responses to ACh (50nM) in the presence of NOC-5 (200 μ M) over the protocol defined time points. Comparison of the $[Ca^{2+}]_i$ responses of cells to ACh under control conditions (Figure 3.1.2 trace A) shown previously to that which was obtained following exposure to SNP and NOC-5 respectively at equivalent time points, shows that exposure of the mouse submandibular acinar cells to SNP or NOC-5 initially significantly ($P<0.05$) and ($P<0.01$) respectively increased the response to ACh from an average control response of $101.5 \pm 3.39\%$ ($n=12$) to $151.7 \pm 23.03\%$ ($n=9$) for SNP and from $101.5 \pm 3.39\%$ ($n=12$) to $200.2 \pm 48.5\%$ ($n=5$) for NOC-5. Both sets of results demonstrated NO induced amplification of the ACh-evoked increase in $[Ca^{2+}]_i$.

The data in figures 3.1.2 parts A to D and figure 3.1.3 demonstrate that the use of any of the four NO donors SNAP, NOC-12, SNP or NOC-5 induced amplification of the ACh-evoked increase in $[Ca^{2+}]_i$.

NO has been implicated in the pathogenesis of salivary gland hypofunction in SjS (Konttinen, Platts et al. 1997); (Looms, Tritsarlis et al. 2001);(Looms, Tritsarlis et al. 2002), in contrast my data indicate NO would induce hyper, not hypo-function. However, these experiments only determined the acute effect of NO on acinar cells. The levels of NO are known to be elevated in SjS patients, so the acinar cells of SjS patients are likely to be exposed chronically to NO. Therefore, longer duration experiments were performed to determine the chronic effect of NO.

Figure 3.1.3

Change in $[Ca^{2+}]_i$ in response to 50nM ACh, illustrating how 75 μ M SNP and 200 μ M NOC-5 respectively induced amplification of the $[Ca^{2+}]_i$ signal.



ACh (50 nM) stimulated increased $[Ca^{2+}]_i$ measured in mouse submandibular acinar cells maintained in primary tissue culture fluid for 24 hours.

Trace A shows responses with repeated stimulation with 50nM ACh before and after application of the NO donor SNP acutely (see scale bar).

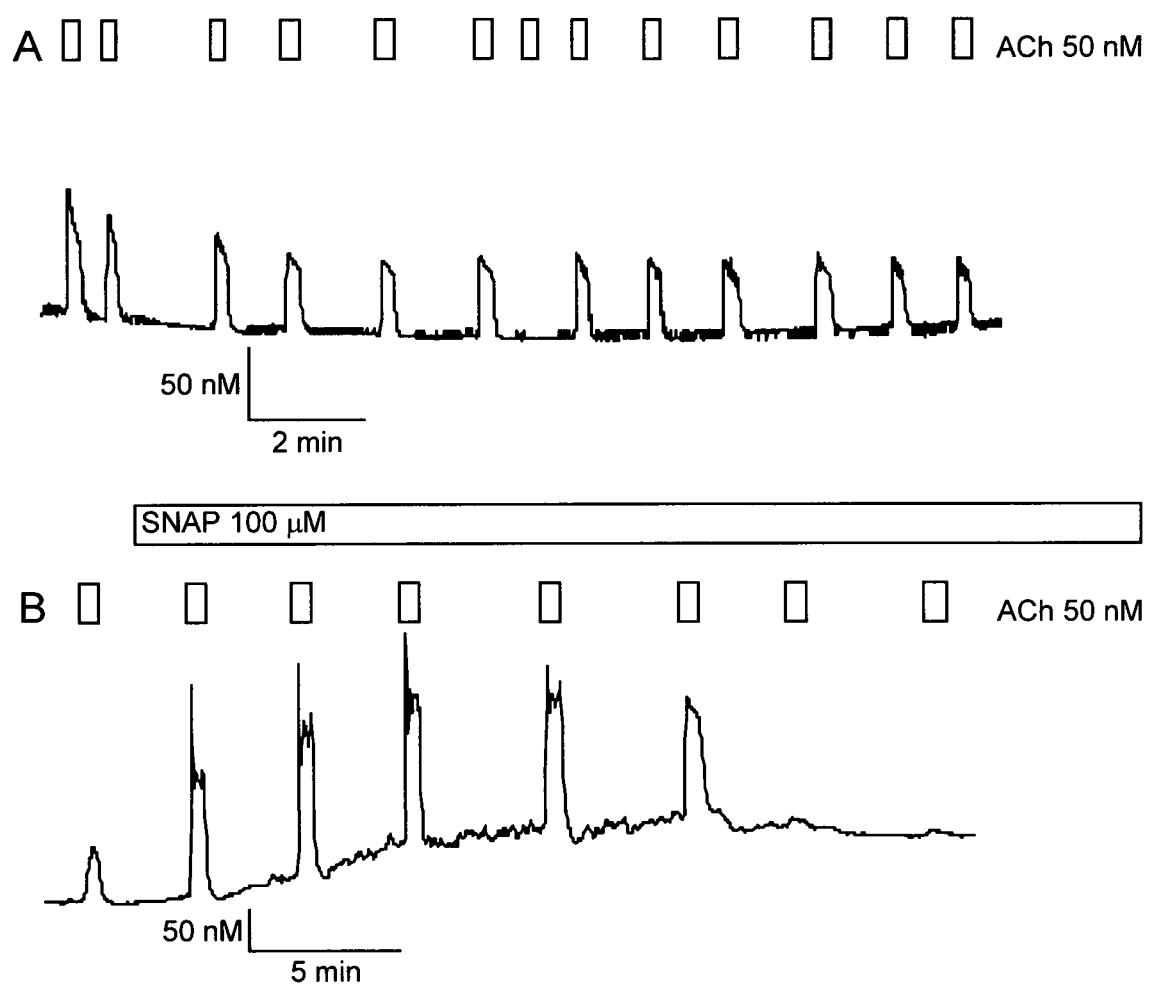
Trace B shows responses with repeated stimulation with 50nM ACh before and after application of the NO donor NOC-5 acutely (see scale bar).

Chronic Experiments

Figure 3.1.4 parts A and B shows representative traces demonstrating the chronic effect of the NO donor SNAP on the ACh-evoked increase in $[Ca^{2+}]_i$ in mouse submandibular acinar cells. Trace A shows a prolonged series of control $[Ca^{2+}]_i$ responses to ACh (50nM) over the protocol defined time period and shows how the cells maintained their ability to respond under control conditions over the expanded experimental protocol. Trace B shows the $[Ca^{2+}]_i$ responses to ACh (50nM) in the presence of SNAP (100 μ M) over the same protocol defined time points. As described previously comparison of the acinar cell $[Ca^{2+}]_i$ response to ACh under control conditions (A) to that obtained following exposure to SNAP (B), shows that exposure of the mouse submandibular acinar cells to NO alters the series of responses induced by ACh. At 32 minutes the ACh stimulated increase in $[Ca^{2+}]_i$ response in the presence of SNAP was not significantly different from zero.

Figure 3.1.4 parts C and D shows representative traces demonstrating the chronic effect of NO donor NOC-12 on the ACh-evoked increase in $[Ca^{2+}]_i$ in mouse submandibular acinar cells. Trace A shows a prolonged series of control $[Ca^{2+}]_i$ responses to ACh (50nM) over the protocol defined time points, with cells maintaining the level of response. Trace B shows the $[Ca^{2+}]_i$ responses to ACh (50nM) in the presence of NOC-12 (200 μ M) over the same protocol defined time points. Comparison of the $[Ca^{2+}]_i$ response of cells to ACh under control conditions (C) to those obtained following exposure to NOC-12 (D) at equivalent time points shows the variation in response pattern over the experimental time period. At 74 minutes the ACh stimulated increase in $[Ca^{2+}]_i$ response in the presence of NOC-12 was not significantly different from zero (figure 3.1.8).

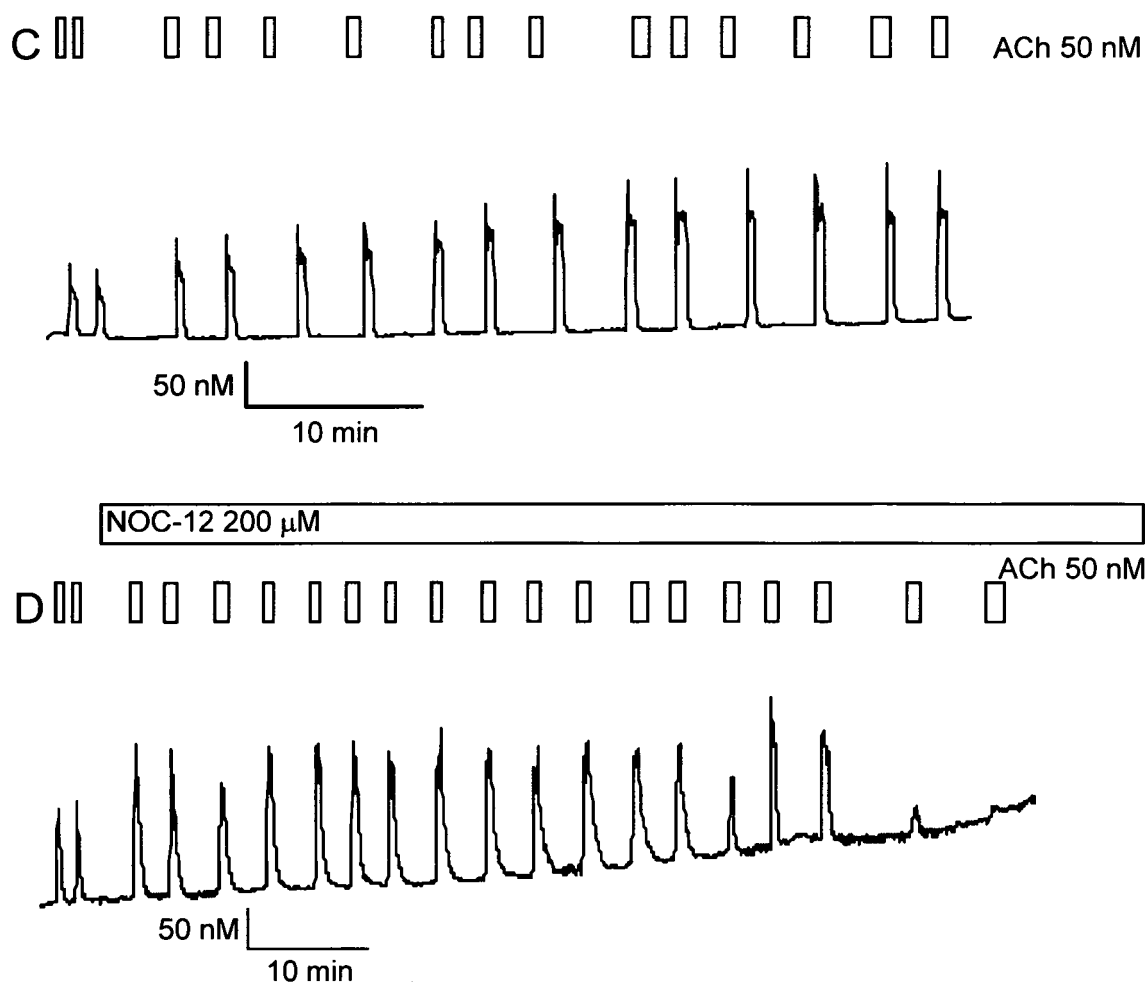
Figure 3.1.4
 Change in $[Ca^{2+}]_i$ in response to 50nM ACh, illustrating how 100 μ M SNAP induced amplification and inhibition of the $[Ca^{2+}]_i$ signal.



ACh (50 nM) stimulated increased $[Ca^{2+}]_i$ measured in mouse submandibular acinar cells maintained in primary tissue culture fluid for 24 hours. Trace A shows response to repeated stimulation with 50nM ACh only chronically (see scale bar). Trace B shows responses to repeated stimulation with 50nM ACh before and after application of the NO donor SNAP chronically (see scale bar).

Figure 3.1.4

Change in $[Ca^{2+}]_i$ in response to 50nM ACh, illustrating how 200 μ M NOC-12 induced amplification and inhibition of the $[Ca^{2+}]_i$ signal.



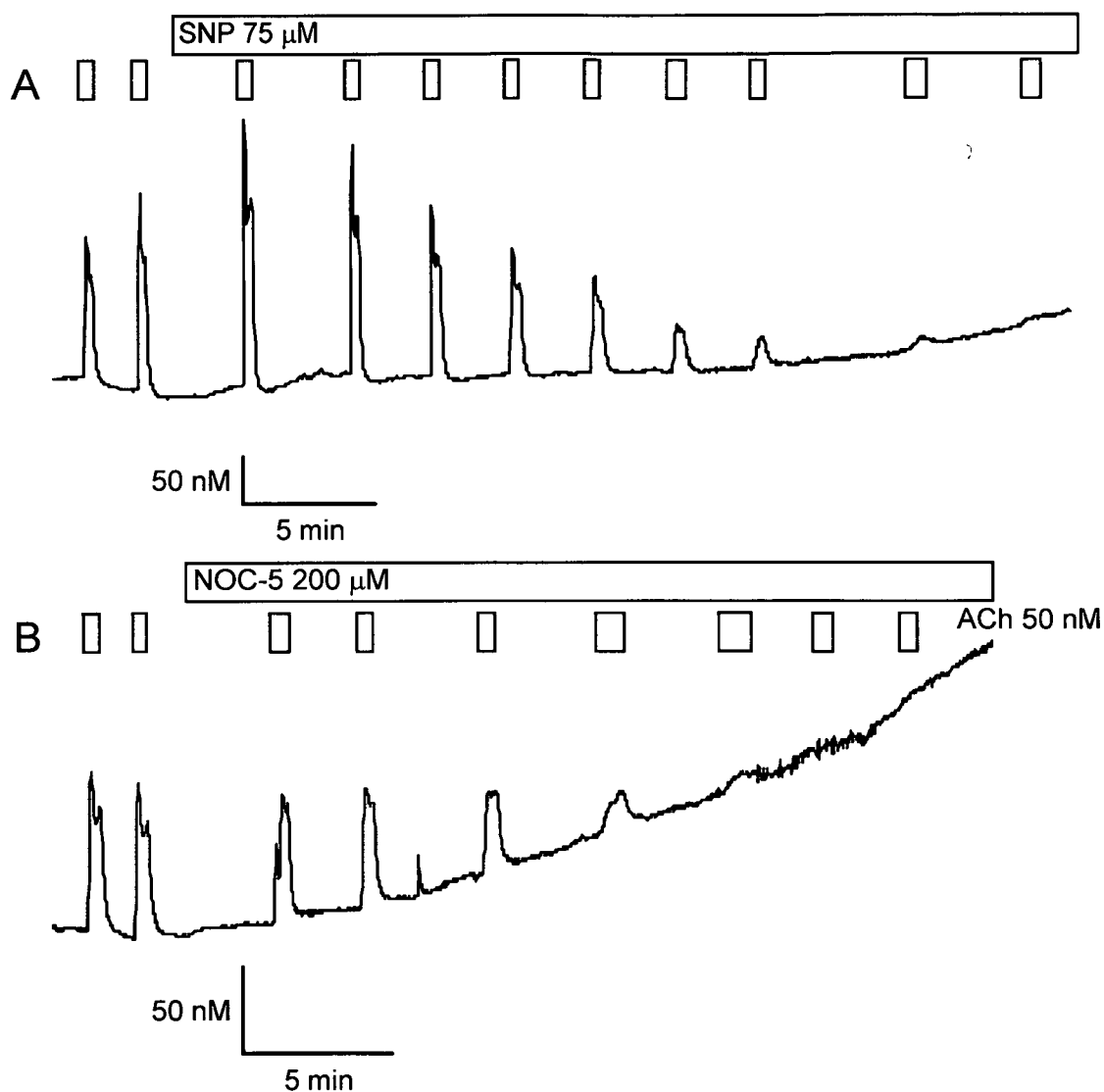
ACh (50 nM) stimulated increased $[Ca^{2+}]_i$ measured in mouse submandibular acinar cells maintained in primary tissue culture fluid for 24 hours.

Trace C shows response to repeated stimulation with 50nM ACh only chronically (see scale bar).

Trace D shows responses to repeated stimulation with 50nM ACh before and after application of the NO donor NOC-12 chronically (see scale bar).

Figure 3.1.5

Change in $[Ca^{2+}]_i$ in response to 50nM ACh, illustrating how 75 μ M SNP and 200 μ M NOC-5 respectively induced amplification and inhibition of $[Ca^{2+}]_i$ signal.



ACh (50 nM) stimulated increased $[Ca^{2+}]_i$ measured in mouse submandibular acinar cells maintained in primary tissue culture fluid for 24 hours.

Trace A shows responses with repeated stimulation with 50nM ACh before and after application of the NO donor SNP chronically (see scale bar).

Trace B shows responses with repeated stimulation with 50nM ACh before and after application of the NO donor NOC-5 chronically (see scale bar).

Figure 3.1.5 shows representative traces demonstrating the chronic affect of NO donors SNP and NOC-5 respectively on the ACh-evoked increase in $[Ca^{2+}]_i$ in mouse submandibular acinar cells. Trace A shows the $[Ca^{2+}]_i$ responses to ACh (50nM) in the presence of SNP (75 μ M) over the protocol defined time points. Trace B shows the $[Ca^{2+}]_i$ responses to ACh (50nM) in the presence of NOC-5 (200 μ M) over the same protocol defined time points. Comparison of the $[Ca^{2+}]_i$ responses of cells to ACh under control conditions shown previously to that which was obtained following exposure to SNP or NOC-5 respectively at equivalent time points, shows that exposure of the mouse submandibular acinar cells to SNP or NOC-5 initially induced amplification of the response but over time the response to ACh diminished. At 40 minutes the ACh stimulated increase in $[Ca^{2+}]_i$ response in the presence of SNP (cumulative data figure 3.1.9) was not significantly different from zero and NOC-5 (cumulative data figure 3.1.10) was also able to inhibit the response to ACh. The data for NOC-5 does however show that the level of response never decreased to zero but this may be explained by the short half life of this particular NO donor. The data in figure 3.1.5 show that SNP and NOC-5 induced amplification and inhibition of the ACh-evoked increase in $[Ca^{2+}]_i$ and that over a prolonged period of time the cells stop responding to stimulus.

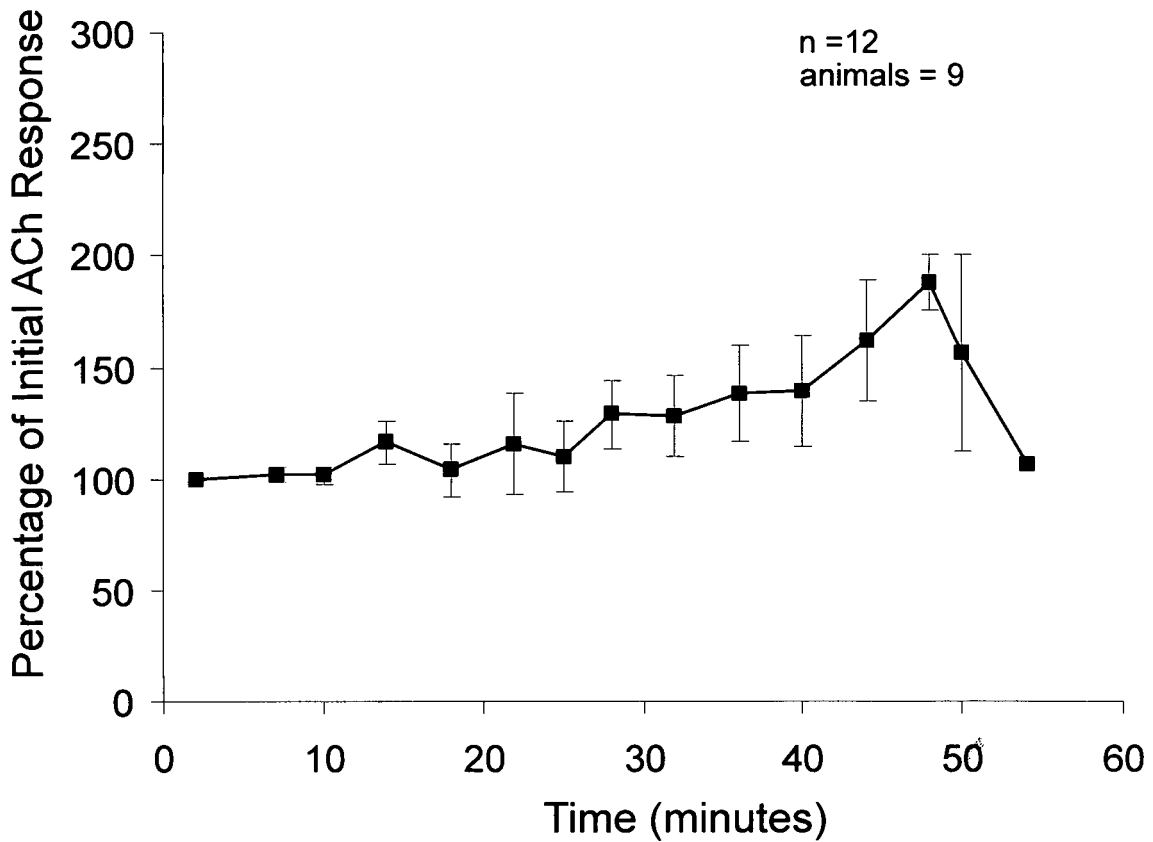
Comparison of data in figures 3.1.4 and 3.1.5 shows that following prolonged application of any of the four NO donors induced inhibition of the ACh-evoked increase in $[Ca^{2+}]_i$ when compared to control. The data presented in figure 3.1.6 shows the cumulative average responses achieved under control conditions and may be compared directly to those presented in figures 3.1.7 to 3.1.10 which represent the cumulative data for SNAP, NOC-12, SNP and NOC-5 respectively. When the average data in figures 3.1.7 to 3.1.10 is reviewed it suggests a chronic response pattern for all four NO donors. The average data for SNAP (figure 3.1.7) and SNP (figure 3.1.9) show that exposure of the mouse submandibular acinar cells to SNAP

or SNP significantly ($P < 0.001$) and ($P < 0.01$) inhibited the response to ACh respectively compared to control (figure 3.1.6). These four alternative NO donors all induced amplification of the ACh-evoked increase in $[Ca^{2+}]_i$ and also induced inhibition of the ACh-evoked increase in $[Ca^{2+}]_i$ upon prolonged chronic exposure. The cumulative data presented as bar charts in figures 3.1.11 parts A and B allows direct comparison between the four NO donors patterns of $[Ca^{2+}]_i$ response but also demonstrates their varying levels of activity.

Figure 3.1.12 shows a representative trace demonstrating the chronic affect of NO donors NOC-12 ACh-evoked increase in $[Ca^{2+}]_i$ in mouse submandibular acinar cells followed by SERCA pump inhibitor Thapsigargin once response was not significantly different from zero. The data presented in figure 3.1.12 shows that the induced inhibition of response is not simply the result of a lack of Ca^{2+} within intracellular stores as the use of the thapsigargin post NO inhibition still induces a considerable mobilisation of Ca^{2+} which goes some way to prove that the cells still contain considerable Ca^{2+} stores. These post NO exposures to thapsigargin ensure that a lack of $[Ca^{2+}]_i$ is not responsible for the inhibition of response observed following exposure of the acinar cells to NO. This observation was made in 6/7 similar experiments.

Figure 3.1.6

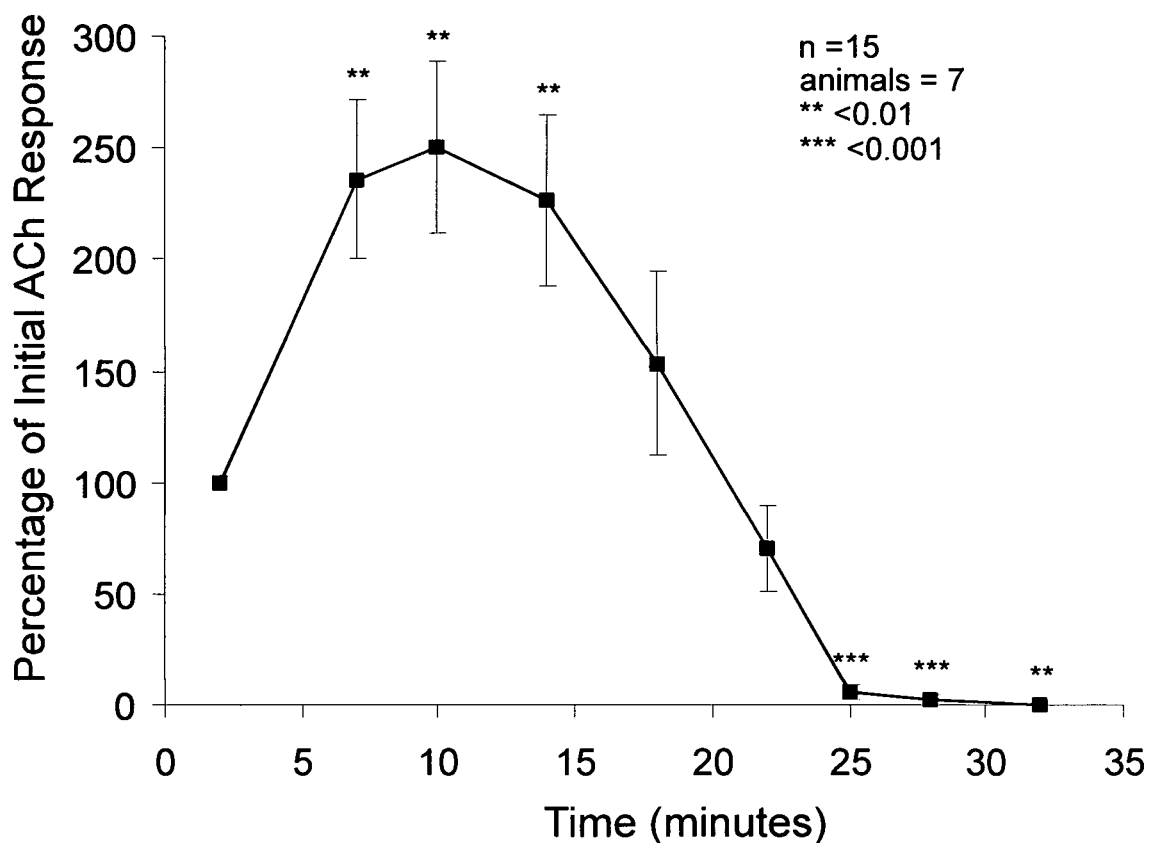
Change in $[Ca^{2+}]_i$ in response to 50nM ACh did not diminish with repeated application over the experimental time period.



Time course showing cumulative data for 50nM ACh in mouse submandibular acinar cells. The data show the series of experimental time points where responses to 50nM ACh occurred. These data show the standard response of mouse submandibular acinar cells to 50nM ACh under control conditions.

Figure 3.1.7

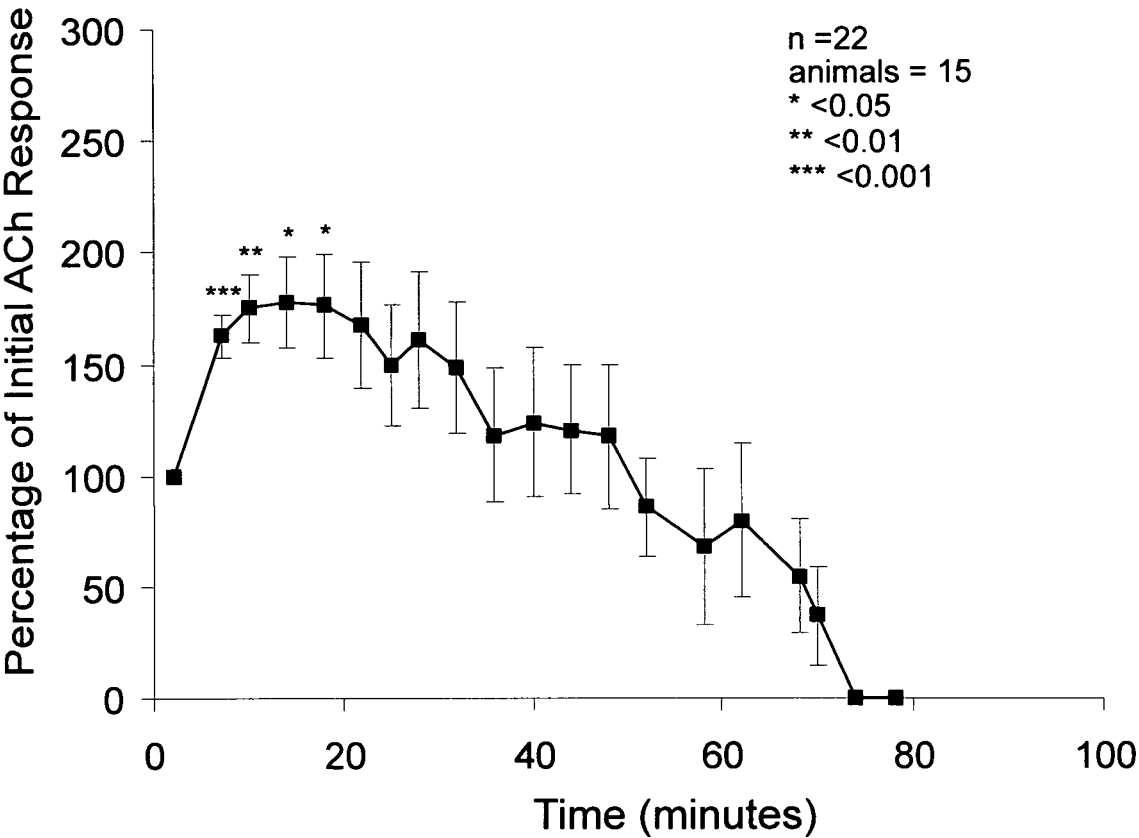
Change in $[Ca^{2+}]_i$ in response to 50nM ACh in the presence of 100 μ M SNAP initially increases but then gradually decreases with repeated application over the experimental time period.



Time course showing cumulative data for 50nM ACh in the presence of 100 μ M SNAP in mouse submandibular acinar cells. The data show the series of experimental time points where responses to 50nM ACh in the presence of 100 μ M SNAP occurred. Statistical significance compared to control and any error bars absent due to a lack of sample size.

Figure 3.1.8

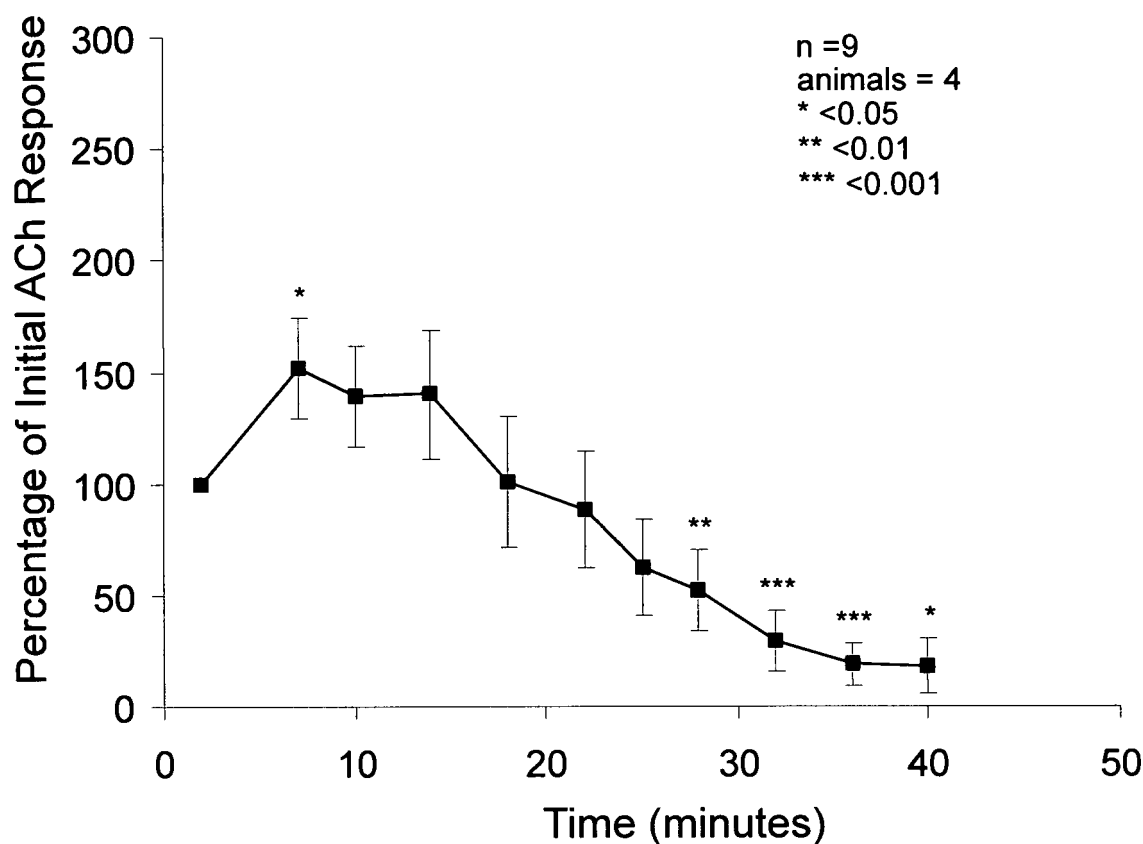
Change in $[Ca^{2+}]_i$ in response to 50nM ACh in the presence of 200 μ M NOC-12 initially increases but then gradually decreases with repeated application over the experimental time period.



Time course showing cumulative data for 50nM ACh in the presence of 200 μ M NOC-12 in mouse submandibular acinar cells. The data show the series of experimental time points where responses to 50nM ACh in the presence of 200 μ M NOC-12 occurred. The final two time points have error bars absent due to a lack of sample size and any statistical significance is compared to control

Figure 3.1.9

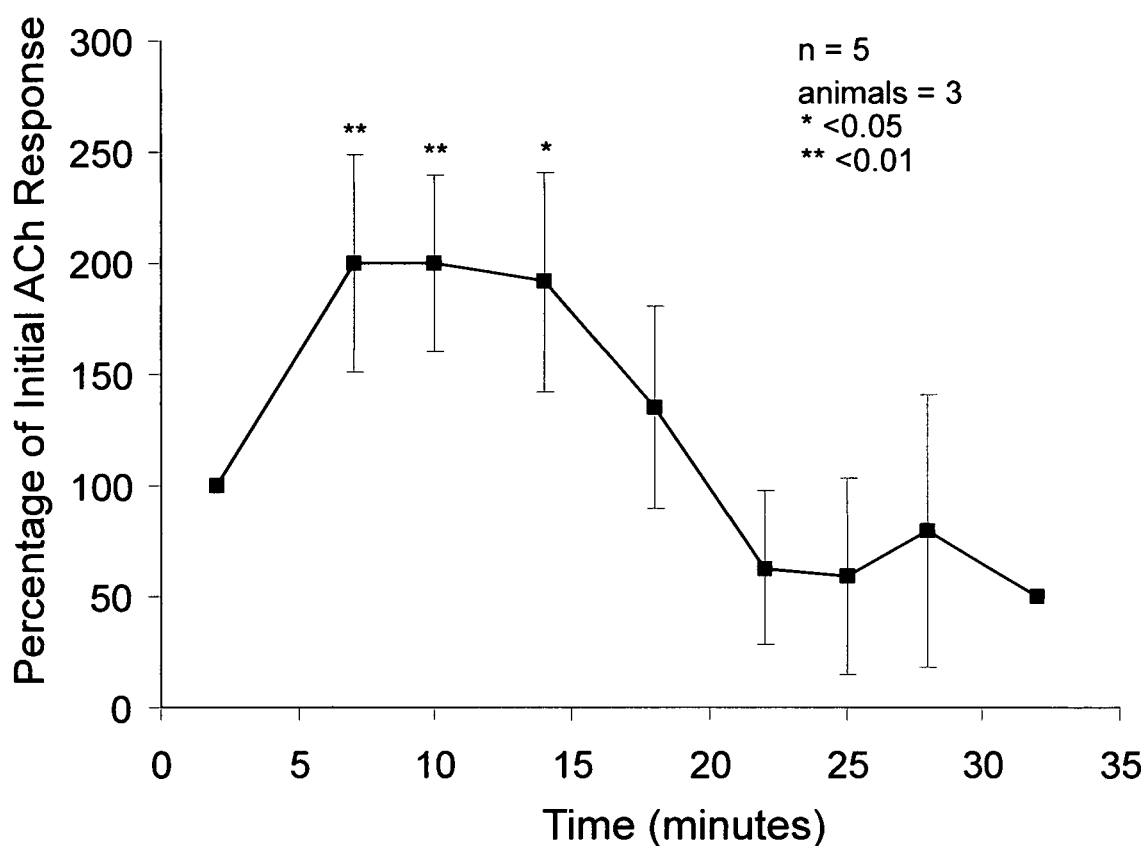
Change in $[Ca^{2+}]_i$ in response to 50nM ACh in the presence of 75 μ M SNP initially increases but then gradually decreases with repeated application over the experimental time period.



Time course showing cumulative data for 50nM ACh in the presence of 75 μ M SNP in mouse submandibular acinar cells. The data show the series of experimental time points where responses to 50nM ACh in the presence of 75 μ M SNP occurred. Statistical significance compared to control.

Figure 3.1.10

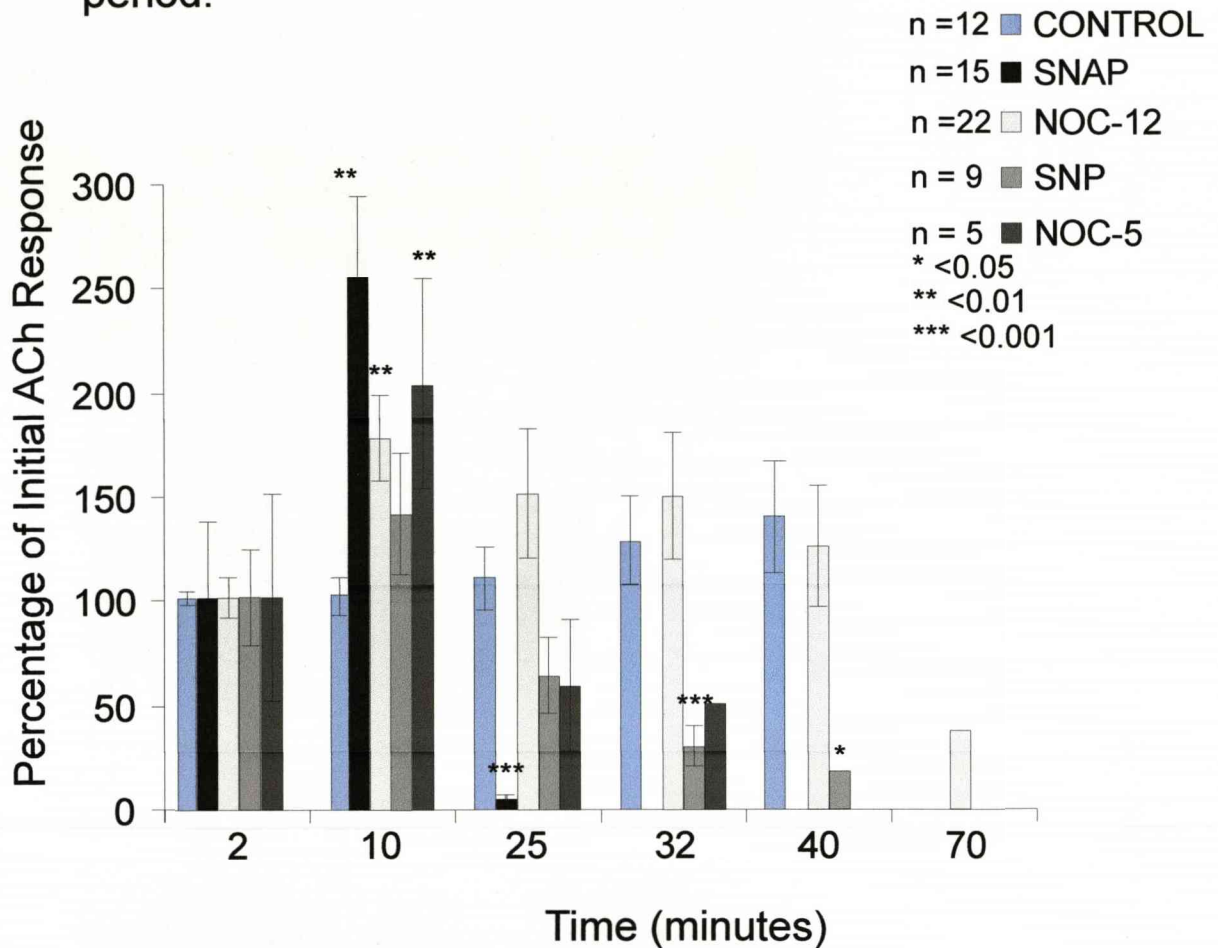
Change in $[Ca^{2+}]_i$ in response to 50nM ACh in the presence of 200 μ M NOC-5 initially increases but then gradually decreases with repeated application over the experimental time period.



Time course showing cumulative data for 50nM ACh in the presence of 200 μ M NOC-5 in mouse submandibular acinar cells. The data show the series of experimental time points where responses to 50nM ACh in the presence of 200 μ M NOC-5 occurred. Final time point error bar absent due to a lack of sample size. Statistical significance compared to control.

Figure 3.1.11 Trace A

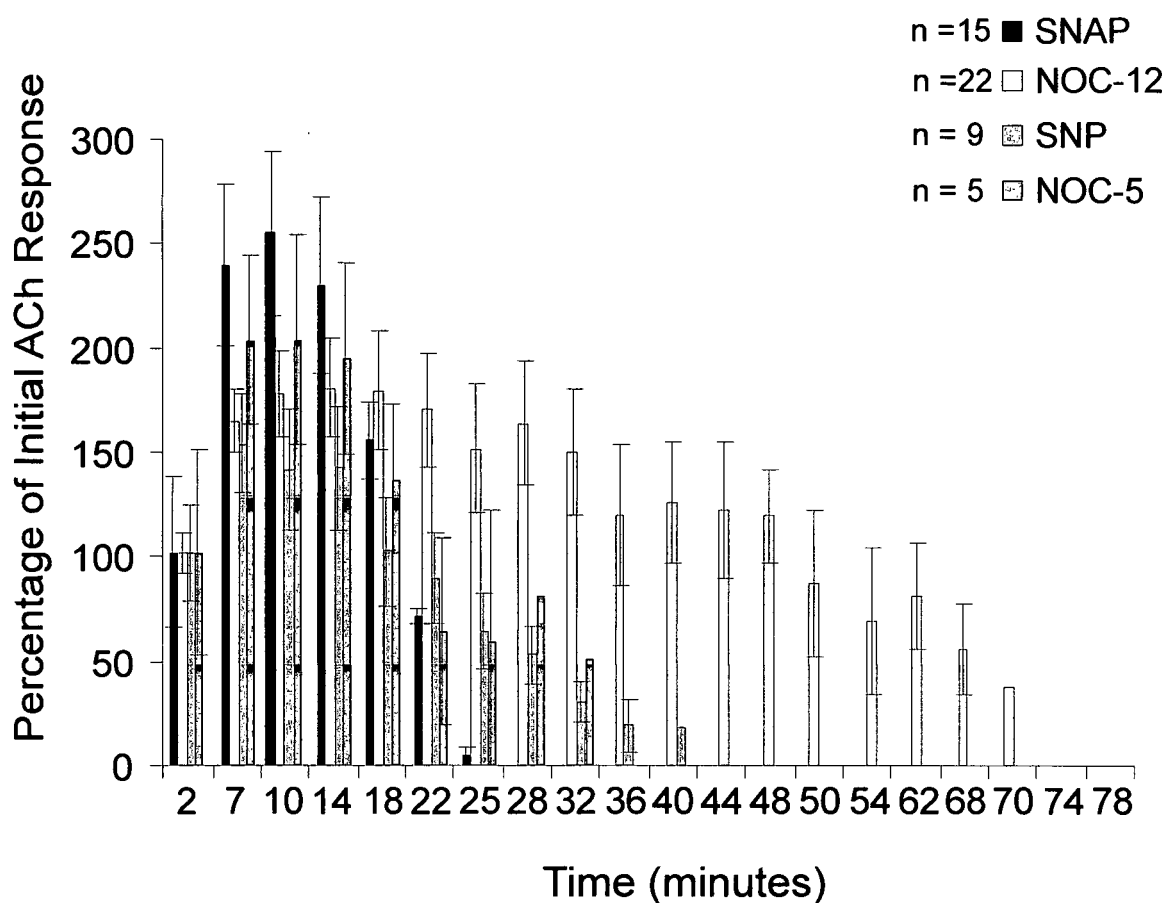
Change in $[Ca^{2+}]_i$ in response to 50nM ACh only and in the presence of 100 μ M SNAP, 200 μ M NOC-12, 100 μ M SNP and 200 μ M NOC-5 respectively over the experimental time period.



Bar chart showing cumulative data for 100 μ M SNAP (end point 32 minutes), 200 μ M NOC-12 (end point 78 minutes), 100 μ M SNP (end point 40 minutes) and 200 μ M NOC-5 (end point 32 minutes) in mouse submandibular acinar cells. Specific time points selected to best illustrate the effect of all four NO donors on the ACh induced response in mouse submandibular acinar cells. The ACh only experiments had an end point of approximately 50 minutes and any statistical significance shown is experimental sample compared to control.

Figure 3.1.11 Trace B

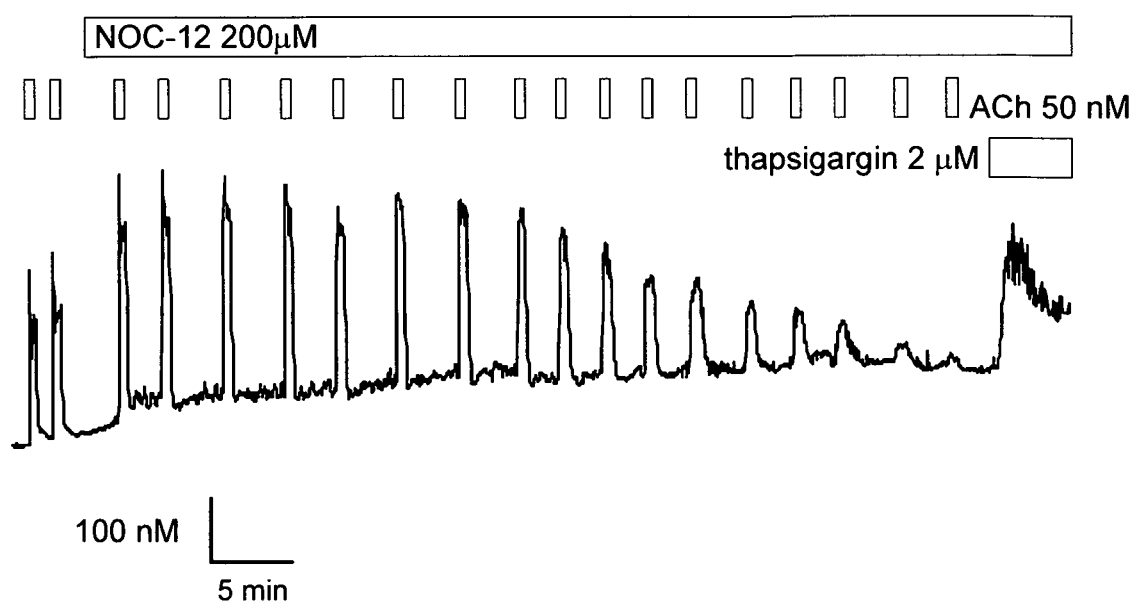
Change in $[Ca^{2+}]_i$ in response to 50nM ACh in the presence of 100 μ M SNAP, 200 μ M NOC-12, 100 μ M SNP and 200 μ M NOC-5 respectively over the experimental time period.



Bar chart showing cumulative data for 100 μ M SNAP (end point 32 minutes), 200 μ M NOC-12 (end point 78 minutes), 100 μ M SNP (end point 40 minutes) and 200 μ M NOC-5 (end point 32 minutes) in mouse submandibular acinar cells.

Figure 3.1.12

Change in $[Ca^{2+}]_i$ in response to 50nM ACh, illustrating how 200 μ M NOC-12 induced amplification and inhibition of $[Ca^{2+}]_i$ signal but how cells were still able to respond to Thapsigargin.



ACh (50 nM) stimulated increased $[Ca^{2+}]_i$ measured in mouse submandibular acinar cells maintained in primary tissue culture fluid for 24 and 48 hours respectively.

Trace shows responses with repeated stimulation with 50nM ACh before and after application of both NO donor NOC-12 chronically followed by exposure to SERCA pump inhibitor Thapsigargin post experimental run down (see scale bar).

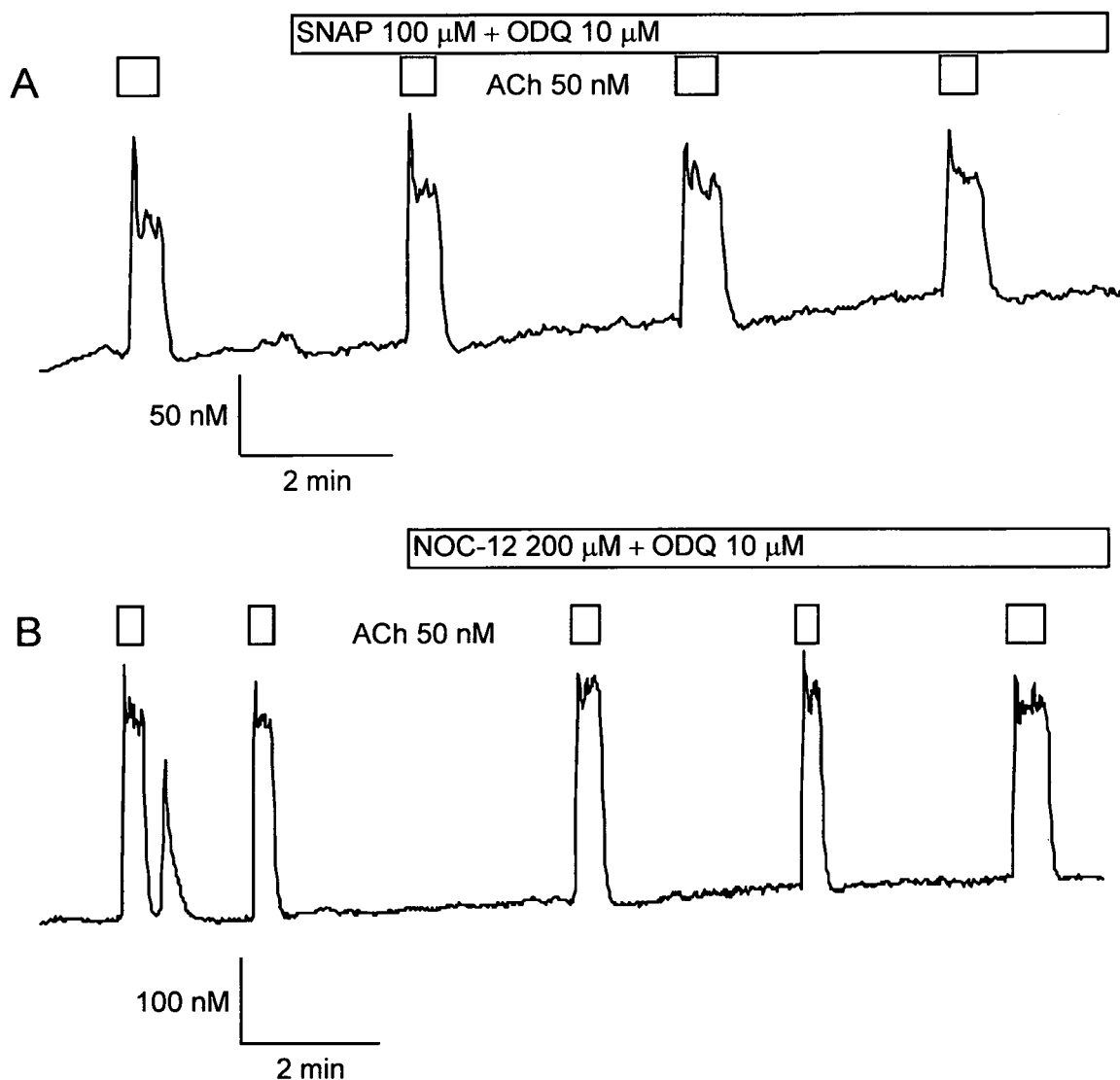
Inhibitors – ODQ

Following the results achieved through use of all four NO donors (SNAP, NOC-12, SNP and NOC-5) the mode of action of NO had to be determined. As discussed previously, (Chapter 1 Introduction 1.2 Nitric oxide section) the most likely pathway involved in the activity of NO is the cADPr pathway so to investigate this hypothesis two inhibitors of this pathway were selected. The first inhibitor selected was ODQ as this blocks the initial, sGC, step of the pathway. SNAP and NOC-12 were selected to use with NO pathway inhibitors ODQ as they were both consistent in the initial experiments and SNAP was the original NO donor and both have relatively long half lives.

Figure 3.1.13 parts A and B shows representative traces demonstrating the affect of soluble Guanylate Cyclase (sGC) inhibitor 1H-[1,2,4]oxadiazolo[4,3-a]quinoxalon-1-one (ODQ) on the ACh-evoked increase in $[Ca^{2+}]_i$ in mouse submandibular acinar cells of the NO donors SNAP and NOC-12 respectively. Trace A shows a series of $[Ca^{2+}]_i$ responses to ACh (50nM) in the presence of SNAP (100 μ M) and also ODQ (10 μ M) over the protocol defined time points. Trace B shows the $[Ca^{2+}]_i$ responses to ACh (50nM) in the presence of NOC-12 (200 μ M) and ODQ (10 μ M) over the same protocol defined time points. Comparison of the $[Ca^{2+}]_i$ responses in figures A and B, shows that exposure of the mouse submandibular acinar cells to NO in the presence of ODQ removed the significant increase in response to ACh observed previously from an average SNAP response of $235.8 \pm 35.39 \%$ (n=15) to $113.6 \pm 3.83 \%$ (n=5) and an average NOC-12 response of $162.5 \pm 10.4\%$ (n=22) to $103.3 \pm 2.23 \%$ (n=5) respectively. In the presence of ODQ and SNAP or NOC-12 the Ca^{2+} signal did not increase significantly greater than control.

Figure 3.1.13

Change in $[Ca^{2+}]_i$ in response to 50nM ACh in the presence of 100 μ M SNAP and 200 μ M NOC-12 respectively in the presence 10 μ M ODQ acutely.



ACh (50 nM) stimulated increased $[Ca^{2+}]_i$ measured in mouse submandibular acinar cells maintained in primary tissue culture fluid for 24 and 48hours respectively.

Trace A shows responses with repeated stimulation with 50nM ACh before and after application of both NO donor SNAP and NO inhibitor ODQ acutely (see scale bar).

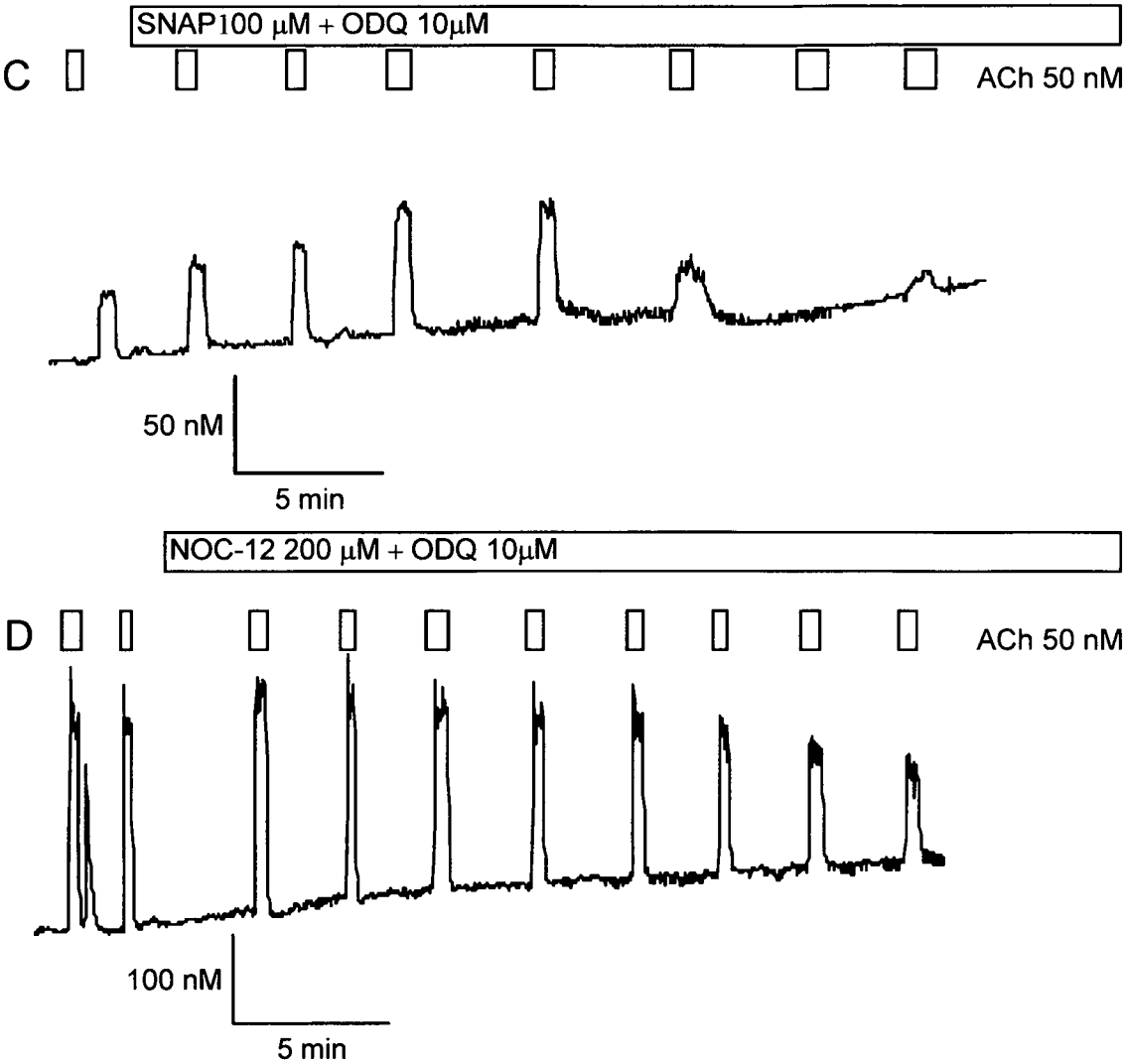
Trace B shows responses with repeated stimulation with 50nM ACh before and after application of both NO donor NOC-12 and NO inhibitor ODQ acutely (see scale bar).

However, more prolonged experiments were required to demonstrate what effect inhibitors of the cADPr pathway would have on the desensitisation of acinar cells to ACh induced previously by the NO donors, SNAP and NOC-12 respectively.

Figure 3.1.13 parts C and D shows representative traces demonstrating the effect of ODQ on the ACh-evoked increase in $[Ca^{2+}]_i$ in mouse submandibular acinar cells following chronic exposure in either SNAP and NOC-12. Trace C shows a prolonged series of $[Ca^{2+}]_i$ responses to ACh (50nM) in the presence of both SNAP (100 μ M) and ODQ (10 μ M) over the protocol defined time points. Trace D shows the $[Ca^{2+}]_i$ responses to ACh (50nM) in the presence of both NOC-12 (200 μ M) and ODQ (10 μ M) over the same protocol defined time points. Comparison of traces C and D shows that exposure of the mouse submandibular acinar cells to either NO donor in the presence of ODQ removed the significant increase in response to ACh observed previously. However, in spite of the presence of ODQ the inhibition of the ACh induced $[Ca^{2+}]_i$ response by NO still occurred with either SNAP or NOC-12. At 28 minutes the ACh stimulated increase in $[Ca^{2+}]_i$ response in the presence of SNAP and ODQ was not significantly different from zero. Whereas the time point at which the ACh stimulated increase in $[Ca^{2+}]_i$ response in the presence of NOC-12 and ODQ was not significantly different from zero was 36 minutes. The data in figure 3.1.14 parts C and D shows that over a prolonged period of time the cells still become less sensitive to ACh and finally stop responding to stimulus even in the presence of sGC inhibitor ODQ. Therefore the results suggest that the induced hypofunction may be independent of the NO pathway.

Figure 3.1.13

Change in $[Ca^{2+}]_i$ in response to 50nM ACh in the presence of 100 μ M SNAP and 200 μ M NOC-12 respectively in the presence 10 μ M ODQ chronically.

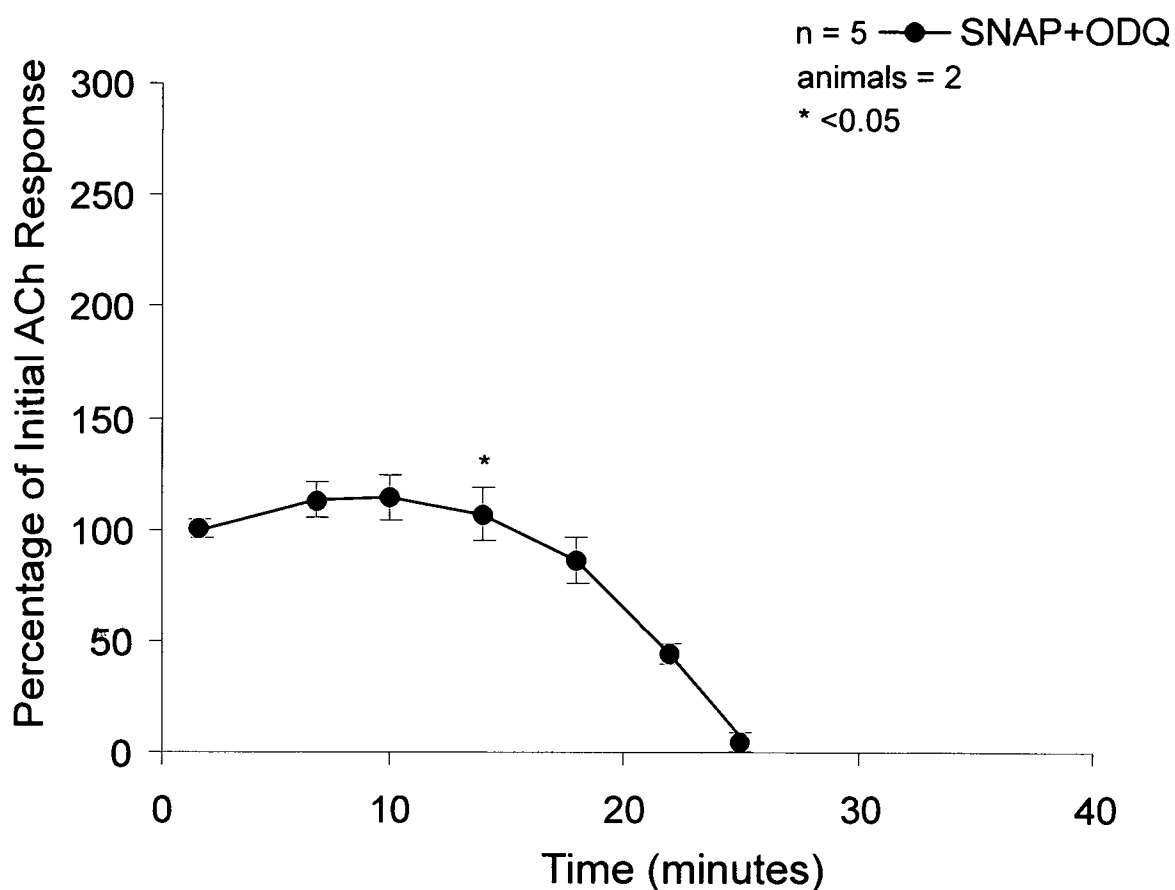


ACh (50 nM) stimulated increased $[Ca^{2+}]_i$ measured in mouse submandibular acinar cells maintained in primary tissue culture fluid for 24 hours. Trace C shows responses with repeated stimulation with 50nM ACh before and after application of both NO donor SNAP and NO inhibitor ODQ chronically (see scale bar). Trace D shows responses with repeated stimulation with 50nM ACh before and after application of the NO donor NOC-12 and NO inhibitor ODQ chronically (see scale bar).

The data in figures 3.1.14 and 3.1.15 show the cumulative average responses achieved using SNAP and NOC-12 in the presence of the NO pathway inhibitor ODQ respectively. Upon observation of these average data in figure 3.1.14 and 3.1.15 the chronic pattern of response induced by the presence of NO was clearly maintained even in the presence of ODQ. So ODQ does not inhibit the long term effect of NO and the induced reduction of the ACh-evoked $[Ca^{2+}]_i$ response, so ODQ is only effective in the short term which suggests that the rundown induced by NO is independent of the cADPr pathway. The average data in figure 3.1.16 shows all average results represented as a bar chart to allow direct comparison between control and experimental conditions.

Figure 3.1.14

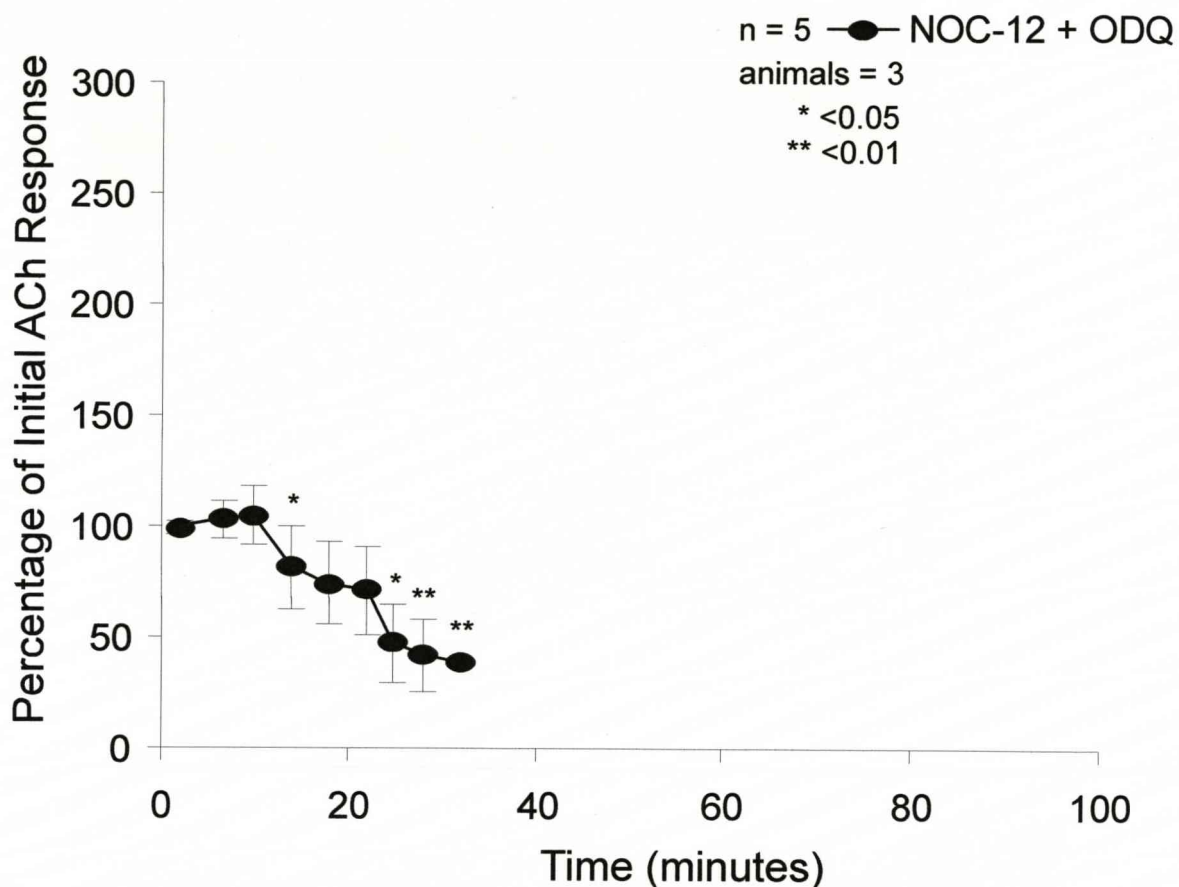
Change in $[Ca^{2+}]_i$ in response to 50nM ACh in the presence of 100 μ M SNAP and 10 μ M ODQ showing the gradual decrease in response over the experimental time period.



Time course showing cumulative data for 50nM ACh in the presence of 100 μ M SNAP and 10 μ M ODQ in mouse submandibular acinar cells. The data show the series of experimental time points where responses to 50nM ACh in the presence of 100 μ M SNAP and 10 μ M ODQ occurred. Any statistical significance indicated is compared to control

Figure 3.1.15

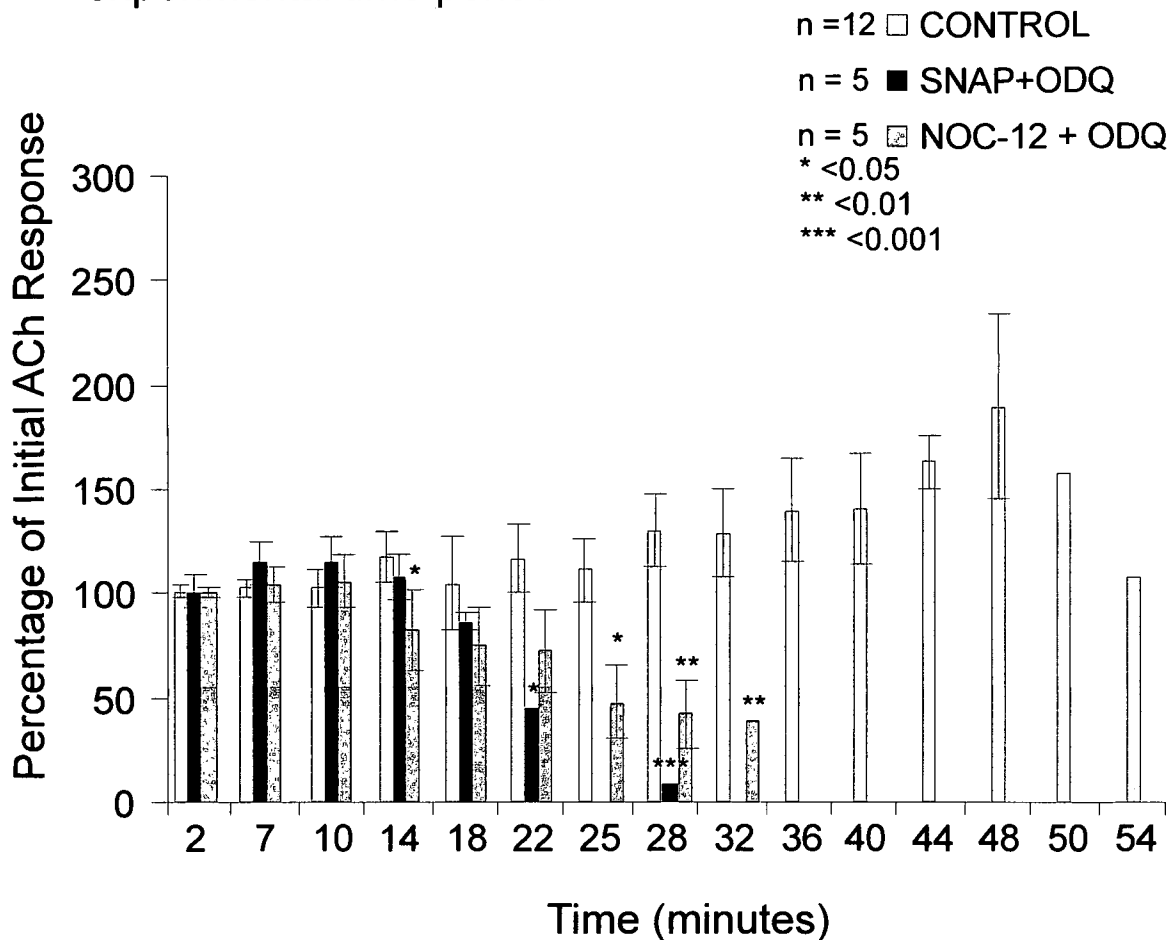
Change in $[Ca^{2+}]_i$ in response to 50nM ACh in the presence of 200 μ M NOC-12 and 10 μ M ODQ showing the gradual decrease in response over the experimental time period.



Time course showing cumulative data for 50nM ACh in the presence of 200 μ M NOC-12 and 10 μ M ODQ in mouse submandibular acinar cells. The data show the series of experimental time points where responses to 50nM ACh in the presence of 200 μ M NOC-12 and 10 μ M ODQ occurred. Any statistical significance indicated is compared to control.

Figure 3.1.16

Change in $[Ca^{2+}]_i$ in response to 50nM ACh and 50nM ACh in the presence of 100 μ M SNAP with 10 μ M ODQ and 200 μ M NOC-12 with 10 μ M ODQ respectively over the experimental time period.



Bar chart showing cumulative data for 50nM ACh control (end point 50 minutes), 100 μ M SNAP with 10 μ M ODQ (end point 28 minutes, no response stimulated at 25 minutes) and 200 μ M NOC-12 with 10 μ M ODQ (end point 32 minutes) in mouse submandibular acinar cells. Any statistical significance indicated is compared to control.

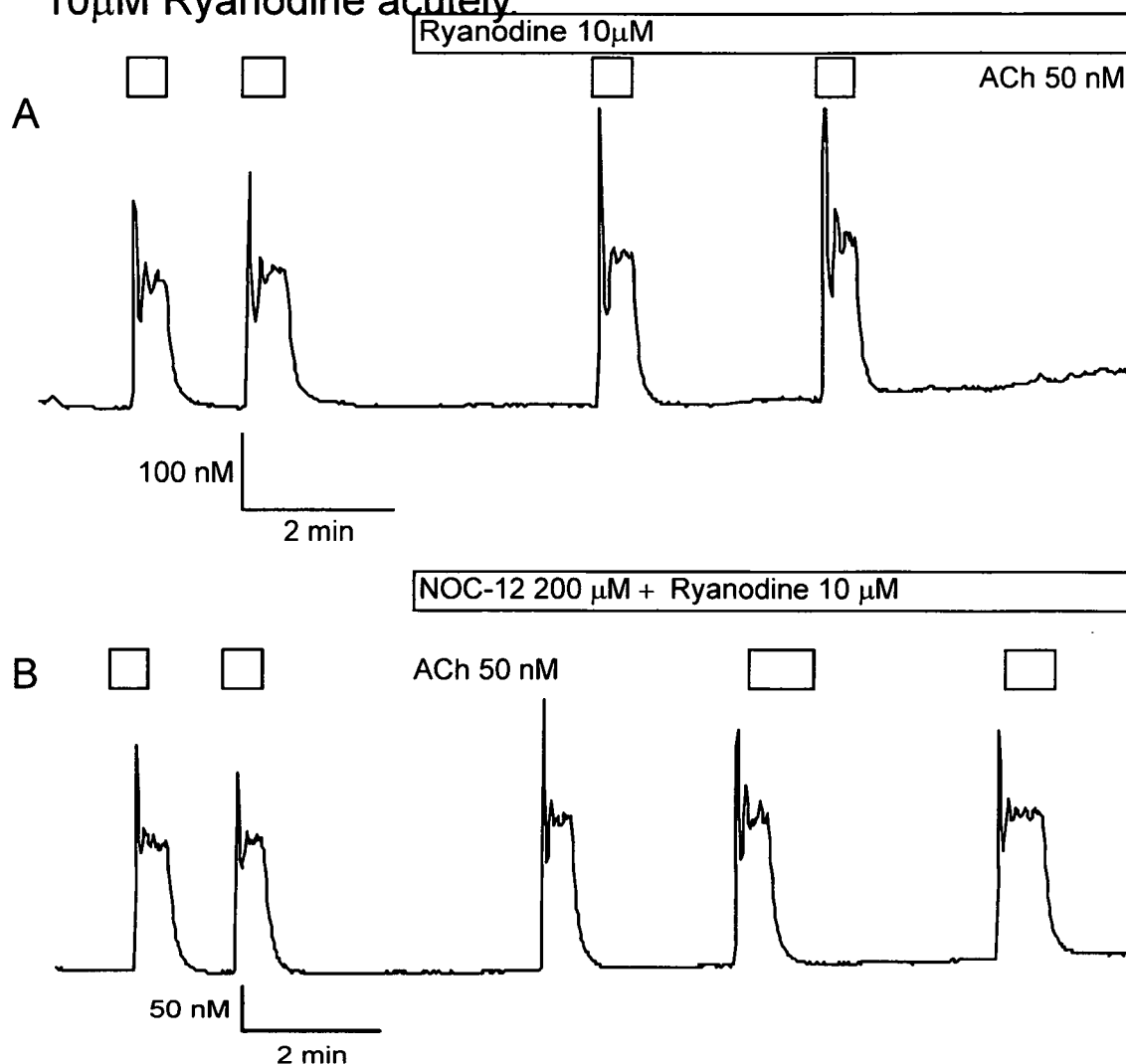
Inhibitors - Ryanodine

Following the results achieved using ODQ a second inhibitor of the cADPr pathway, Ryanodine, was used. Ryanodine acts on the RyR directly and so blocks the cADPr pathway at the final step whereas ODQ acts on sGC which is the initial step of the cADPr pathway as discussed earlier (Chapter 1 Introduction 1.2 Nitric Oxide section). NOC-12 was selected for use with Ryanodine to allow direct comparison with the ODQ data and NOC-12 produced much more consistent results and proved less problematic to use than SNAP.

Figure 3.1.17 parts A and B shows representative traces demonstrating the effect of the Ryanodine receptor inhibitor Ryanodine on NOC-12 on the ACh-evoked increase in $[Ca^{2+}]_i$ in mouse submandibular acinar cells. Trace A shows a series of control $[Ca^{2+}]_i$ responses to ACh (50nM) in the presence of Ryanodine (10 μ M) only over the protocol defined time points. Trace B shows the $[Ca^{2+}]_i$ responses to ACh in the presence of both NOC-12 (200 μ M) and Ryanodine (10 μ M) over the same protocol defined time points. By comparing the $[Ca^{2+}]_i$ response of cells to ACh under Ryanodine only control conditions (A) to those obtained following combined exposure to both NOC-12 and Ryanodine (B) at equivalent time points, the data show that exposure of the mouse submandibular acinar cells to NOC-12 during exposure to Ryanodine significantly ($P < 0.05$) removes the previous increased response to ACh from an average NOC-12 response of $162.5 \pm 10.4 \%$ ($n=22$) to $121.3 \pm 10.84 \%$ ($n=8$). Therefore the data in figure 3.1.17 demonstrate the inhibition of NO induced amplification of the ACh-evoked increase in $[Ca^{2+}]_i$ by the Ryanodine receptor inhibitor Ryanodine.

Figure 3.1.17

Change in $[Ca^{2+}]_i$ in response to 50nM ACh in the presence of 10 μ M Ryanodine and 200 μ M NOC-12 in the presence 10 μ M Ryanodine acutely.



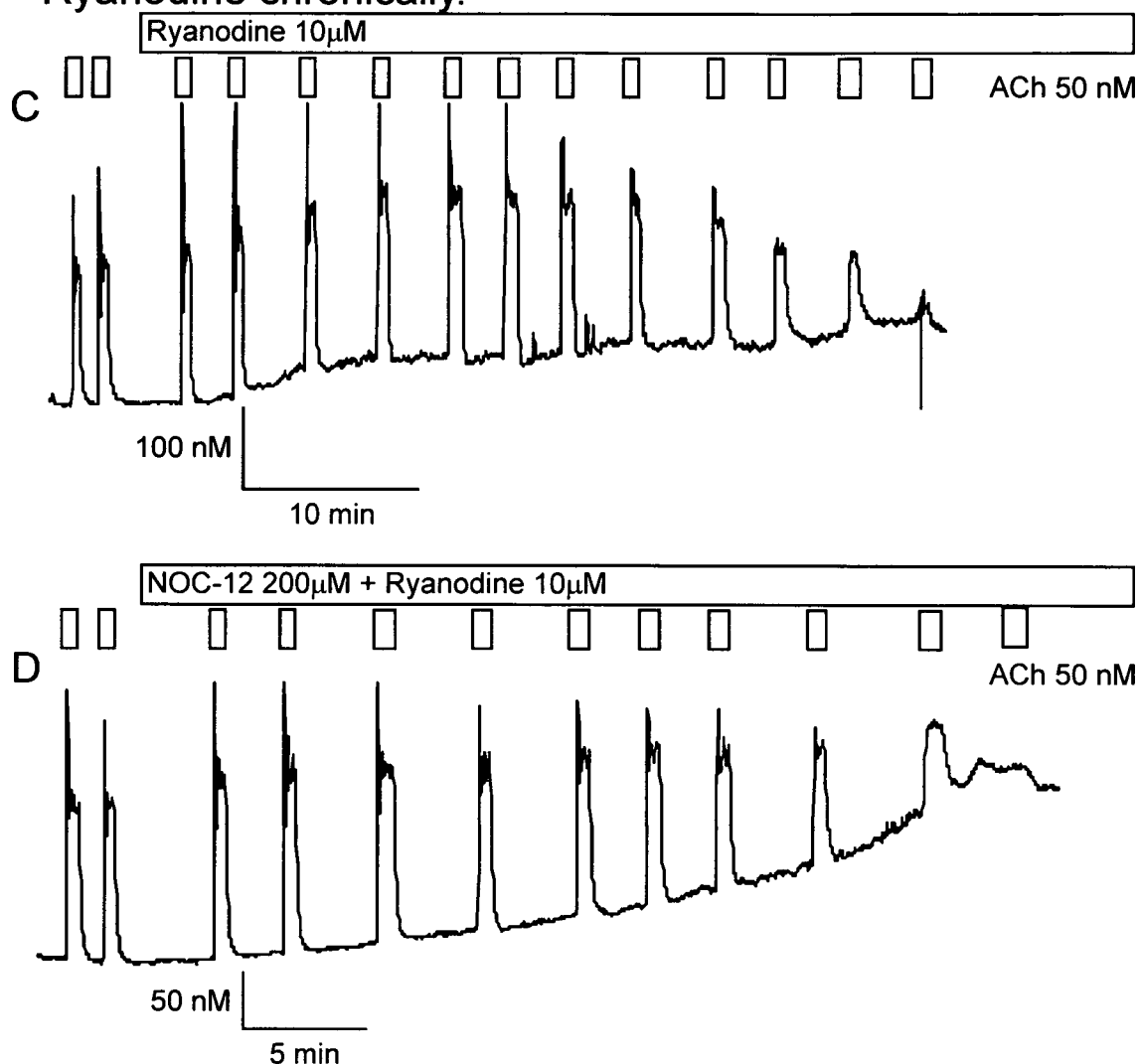
ACh (50 nM) stimulated increased $[Ca^{2+}]_i$ measured in mouse submandibular acinar cells maintained in primary tissue culture fluid for 24 hours.

Trace A shows responses with repeated stimulation with 50nM ACh before and after application of NO pathway inhibitor Ryanodine only acutely (see scale bar).

Trace B shows responses with repeated stimulation with 50nM ACh before and after application of the NO donor NOC-12 and NO pathway inhibitor Ryanodine acutely (see scale bar).

Figure 3.1.17

Change in $[Ca^{2+}]_i$ in response to 50nM ACh in the presence of 10 μ M Ryanodine and 200 μ M NOC-12 with 10 μ M Ryanodine chronically.



ACh (50 nM) stimulated increased $[Ca^{2+}]_i$ measured in mouse submandibular acinar cells maintained in primary tissue culture fluid for 24 hours.

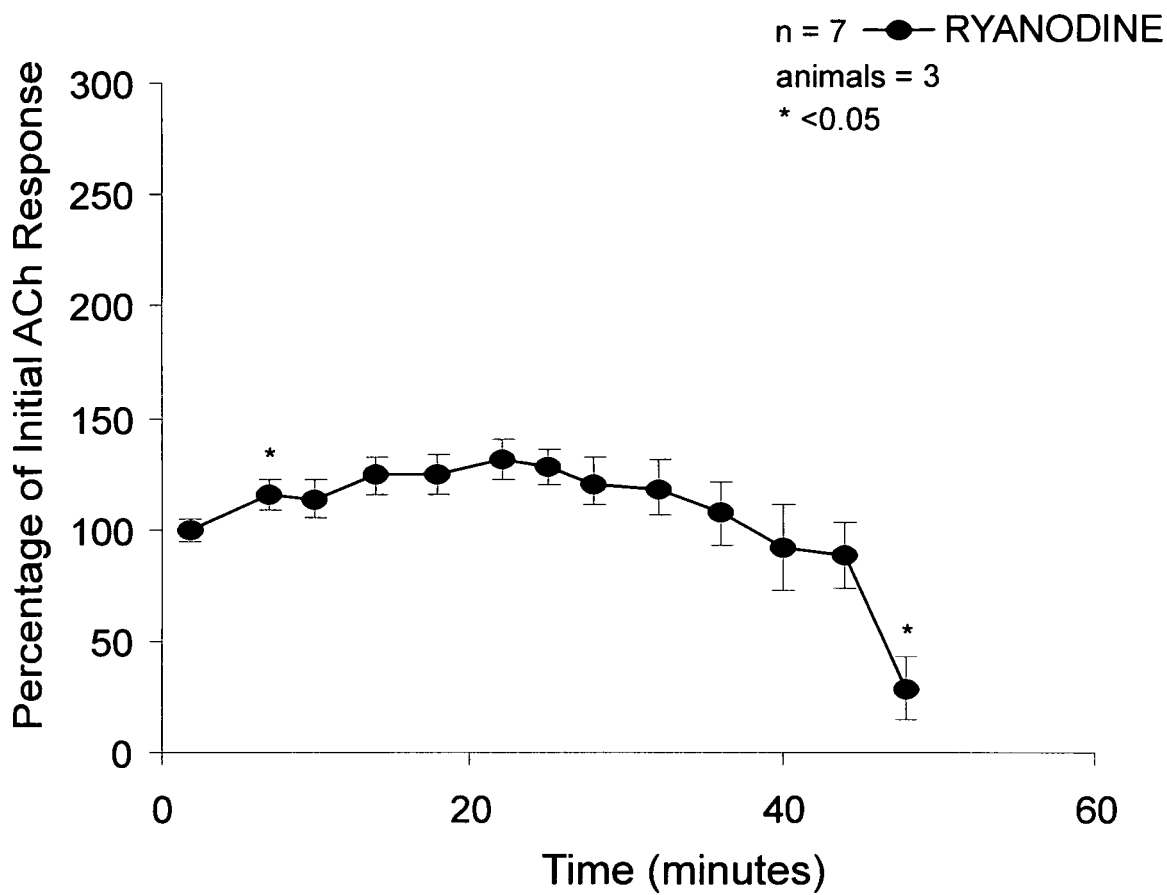
Trace C shows responses with repeated stimulation with 50nM ACh before and after application of Ryanodine chronically (see scale bar).

Trace D shows responses with repeated stimulation with 50nM ACh before and after application of the NO donor NOC-12 and NO pathway inhibitor Ryanodine chronically (see scale bar).

Figure 3.1.17 parts C and D shows representative traces demonstrating the chronic effect of Ryanodine on the effect of NOC-12 on the ACh-evoked increase in $[Ca^{2+}]_i$ in mouse submandibular acinar cells. Trace C shows a series of control $[Ca^{2+}]_i$ responses to ACh (50nM) in the presence of Ryanodine (10 μ M) only over the protocol defined time points. Trace D shows the $[Ca^{2+}]_i$ responses to ACh (50nM) in the presence of both NOC-12 (200 μ M) and Ryanodine (10 μ M) over the same protocol defined time points.

The data in figures 3.1.18 and 3.1.19 show the cumulative average responses achieved, using Ryanodine alone and NOC-12 in the presence of Ryanodine. The cumulative data in figure 3.1.18 show that Ryanodine itself induces run-down by blocking the Ryanodine receptors directly. The data in figure 3.1.20 allows direct comparison between control, Ryanodine only and Ryanodine and NOC-12 together and demonstrates the very similar patterns of response with the only major variation being the maintained level of response under control conditions. As a result of these findings the usefulness of Ryanodine as an inhibitor of the effect of NO activity is limited as in the short term it functions to stop the amplification of response but use in chronic experiments is problematic. There is also no obvious additive effect between Ryanodine and NOC-12 as the use of NOC-12 in the presence of Ryanodine doesn't induce further run-down than Ryanodine alone or vice-versa. Figure 3.1.21 is a simple bar chart which allows the degree of initial amplification to be observed and compared between control and experimental conditions.

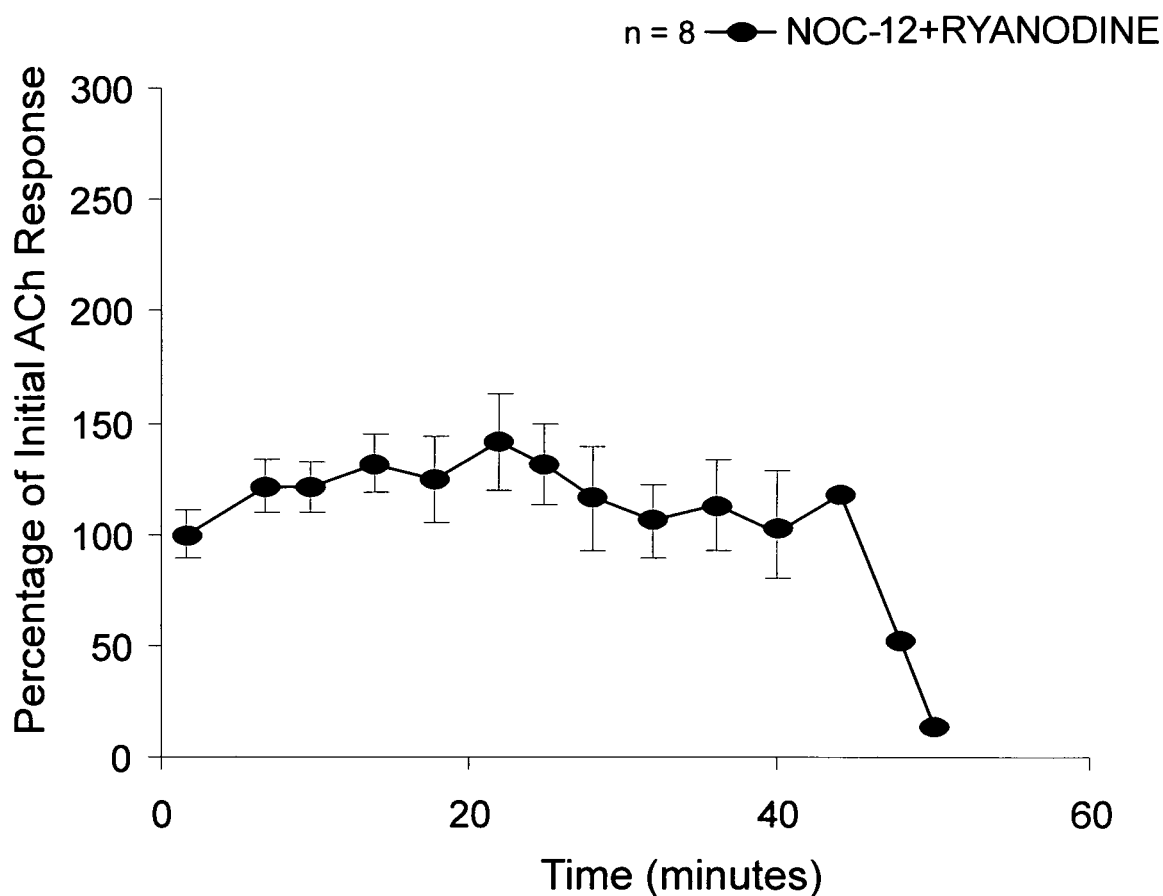
Figure 3.1.18
Change in $[Ca^{2+}]_i$ in response to 50nM ACh in the presence of 10 μ M Ryanodine showing decrease with repeated application.



Time course showing cumulative data for 50nMACh in the presence or absence of 10 μ M Ryanodine in mouse submandibular acinar cells. The data show the series of experimental time points where responses to 50nM ACh in the presence of 10 μ M Ryanodine occurred. Any statistical significance shown is compared to control.

Figure 3.1.19

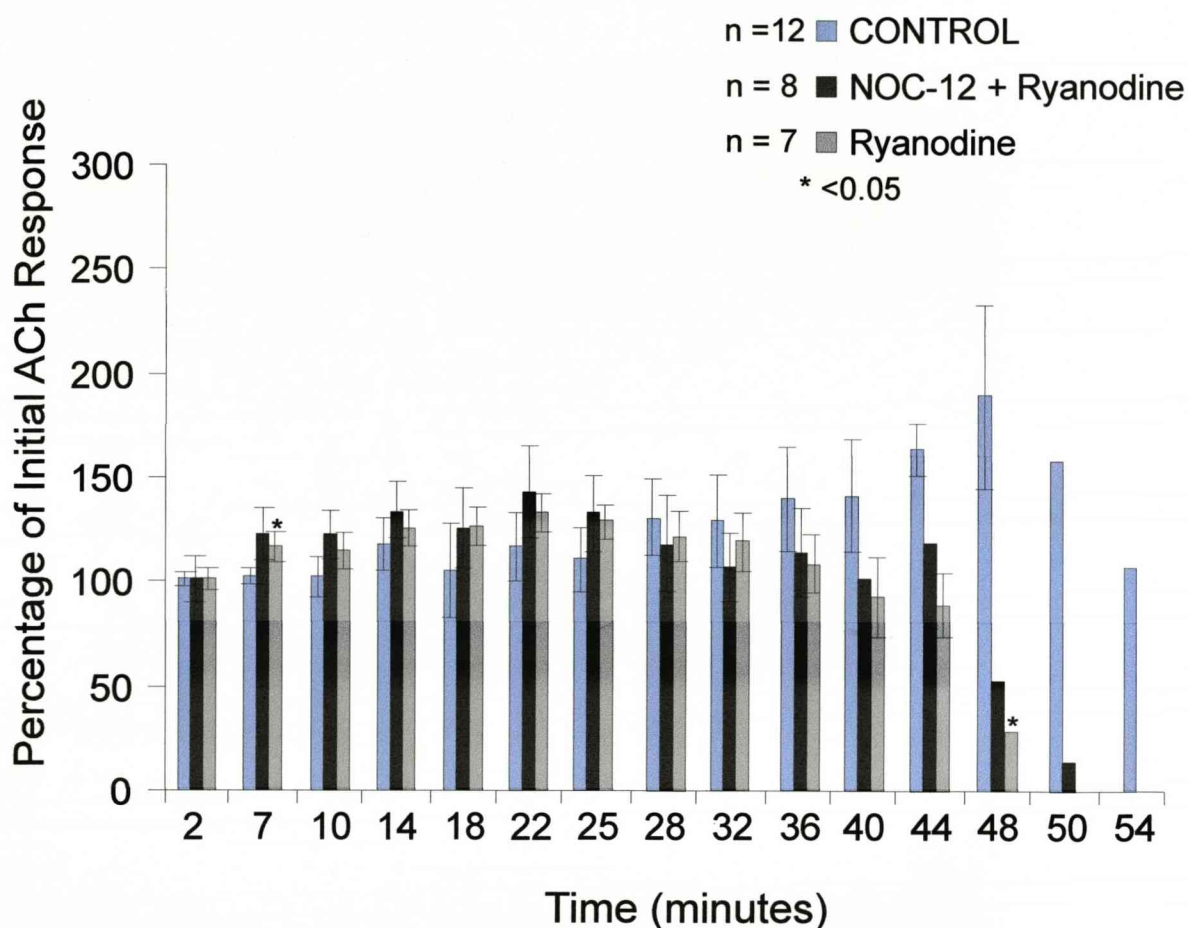
Change in $[Ca^{2+}]_i$ in response to 50nM ACh in the presence of both 10 μ M Ryanodine and 200 μ M NOC-12 showing gradual decrease in response.



Time course showing cumulative data for 50nMACh in the presence or absence of both 10 μ M Ryanodine and 200 μ M NOC-12 in mouse submandibular acinar cells. The data show the series of experimental time points where responses to 50nM ACh in the presence of both 10 μ M Ryanodine and 200 μ M NOC-12 occurred. Final three time points have no error bars present due to a lack of sample number.

Figure 3.1.20

Change in $[Ca^{2+}]_i$ in response to 50nM ACh and 50nM ACh in the presence of 200 μ M NOC-12 with 10 μ M Ryanodine and 10 μ M Ryanodine respectively over the experimental time period.



Bar chart showing cumulative data for 50nM ACh control (end point 50 minutes), 100 μ M SNAP with 10 μ M ODQ (end point 28 minutes, no response stimulated at 25 minutes) and 200 μ M NOC-12 with 10 μ M ODQ (end point 32 minutes) in mouse submandibular acinar cells. Any statistical significance shown is compared to control. There were statistically significant (<0.05) variations between NOC-12 only and Ryanodine and NOC-12 together at the 7, 10 and 25 minute time points and also statistically significant (<0.05) variations between Ryanodine only and NOC-12 only at the 7, 10 and 48 minute time points.

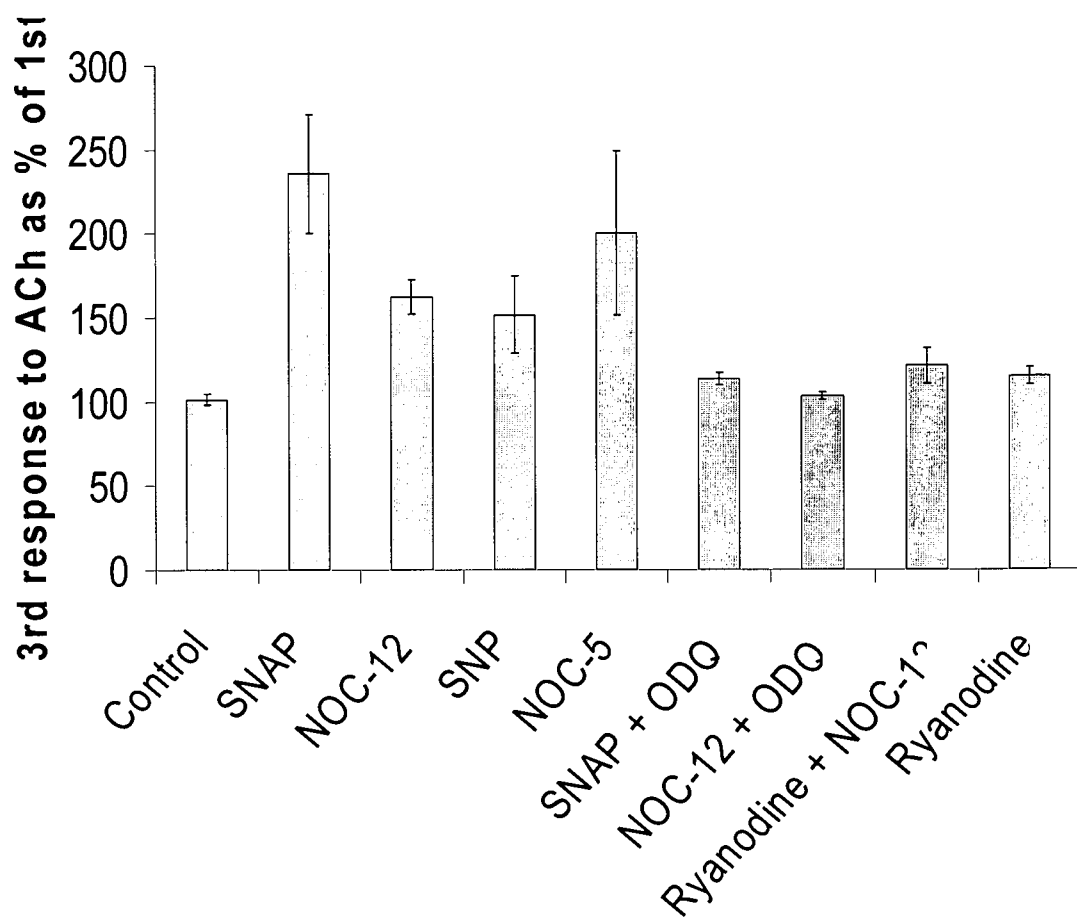


Figure 3.1.21: Data presented as a bar chart to allow direct comparison between all average results for all experimental conditions for the level of amplification induced at the third ACh stimulation compared to control

Conclusion

The data in figure 3.1.4 parts A to D and figure 3.1.5 show how exposure of the mouse submandibular acinar cells to SNAP, NOC-12, SNP or NOC-5 respectively, changes the pattern of response and how NO initially induced amplification of the ACh-evoked increase in $[Ca^{2+}]_i$ followed by NO induced inhibition of the ACh-evoked increase in $[Ca^{2+}]_i$ over the experimental time period with NOC-12 exhibiting a more prolonged period of time but traces B and D in figure 3.1.4 and both traces in 3.1.5 show cells becoming less sensitive to ACh and finally being unresponsive to ACh stimulus.

The cumulative normalised data in figures 3.1.7 to 3.1.11 demonstrate the chronic pattern of $[Ca^{2+}]_i$ response induced following prolonged NO exposure. The data in figures 3.1.6 to 3.1.11 allow direct comparison between control responses and those responses achieved under experimental conditions with all experiments performed in accordance with the devised experimental protocol stated previously. The data overall shows that exposure of the mouse submandibular acinar cells to NOC-12 inhibited the response to ACh but the rate of inhibition was not comparable to SNAP, SNP or NOC-5 as NOC-12 took far longer to induce inhibition of the response, NOC-12 demonstrated an alternative response pattern compared to SNAP, SNP and NOC-5 as the average values in figures 3.1.7 to 3.1.10 show. Variations in time course between the four is most likely a result of variations in the rate of NO release which varied between the four donors. Figure 3.1.12 demonstrates that the reduction in responsiveness to ACh following exposure to NO are not a result of decreased calcium stores as may be suggested as thapsigargin post NO inhibition still induces a considerable mobilisation of Ca^{2+} which goes some way to prove that the cells still contain considerable Ca^{2+} stores. These post NO exposures to thapsigargin ensure

that a lack of $[Ca^{2+}]_i$ is not responsible for the inhibition of response observed following exposure of the acinar cells to NO.

As described previously, (Chapter 1 Introduction 1.2 Nitric Oxide section) NO was selected for investigation as a possible cause of salivary hypofunction in SjS. These data would suggest that NO does have the ability to induce acinar hypo-function but only after prolonged time periods. However, the results were achieved over relatively short time periods when compared to the SjS patients likely NO exposure duration. Therefore, NO was able to induce healthy acinar cells to behave like SjS acinar cells. The chronic experiments were therefore compatible with the hypothesised role of NO in SjS. Another important result achieved over the duration of these experiments was that prolonged incubation of the acinar cells with the NO donors did not produce inhibition of response. Inhibition only occurred when cells were repeatedly stimulated with ACh, however, the responses to ACh which were achieved post NO donor incubation were smaller in magnitude compared to those which were not incubated. The response to 50nM ACh stimulation following prolonged pre-incubation (2-5 hours) in the presence of NOC-12 was on average $49.7 \pm 24.3\%$ (n=9) of the averaged first response to ACh without pre-incubation.

In the presence of ODQ and SNAP or NOC-12 the Ca^{2+} signal did not increase significantly greater than control. Therefore these data support the concept that NO is causing an amplification in the $[Ca^{2+}]_i$ response through the cADPr pathway as acute amplification induced by any either NO donor is prevented by addition of ODQ.

The average data in figures 3.1.14 to 3.1.16 shows that exposure of the mouse submandibular acinar cells to SNAP or NOC-12 still induces inhibition of response in the presence of ODQ which dose not vary significantly from the induced inhibition of response in the absence of ODQ for SNAP. However, although the degree of

desensitisation of response to ACh does not change the rate of desensitisation does increase for NOC-12 in the presence of ODQ. This was previously noted by Takuma and colleagues who observed that the cytotoxic effect of NOC-12 was exacerbated by ODQ (Takuma, Phuagphong et al. 2002). We might speculate that ODQ amplifies the NOC-12 by increasing the rate of release of NO by NOC-12 but this effect of ODQ on NOC-12 was not investigated further.

The use of two cADPr pathway inhibitors allows validation and a clearer insight into where NO functions within the pathway as the two inhibitors function at opposite ends of the pathway as ODQ prevents the initial step and Ryanodine blocks the receptor directly so the use of both inhibitors greatly strengthens the NO/cADPr argument.

The data in figure 3.1.17 parts A and B shows that the use of NOC-12 in combination with Ryanodine prevented the induced amplification of the ACh-evoked increase in $[Ca^{2+}]_i$. These data confirm that NO is mediating its effects through the cADPr pathway. Further experiments were required to demonstrate what effect inhibitors of the cADPr pathway would have on the de-sensitisation to ACh induced previously by the NO donor NOC-12.

The de-sensitisation observed in figure 3.1.17 trace C with Ryanodine only was expected as Ryanodine blocks the RyR in a sub-conductance state so would be expected to de-sensitise the RyR to ACh when used alone. The data in figure 3.1.20 allows direct comparison between control, Ryanodine only and Ryanodine and NOC-12 together and demonstrates that the results produced from NOC-12 and Ryanodine were indistinguishable from the results produced using Ryanodine alone. The Use of Ryanodine produces results consistent with ODQ and confirms that the amplification induced by NO is mediated through the cADPr pathway. However, the

chronic data produced from use of the ODQ and Ryanodine with the NO donors would suggest that NO induces desensitisation and inhibition of the ACh response independently of the cADPr pathway as neither inhibitor of this pathway blocked the NO induced inhibition. There was no significant difference observed between NOC-12 and Ryanodine and Ryanodine alone. Figure 3.1.21 allows direct comparison between the third response for all conditions compared to control.

So in summary all four donors were able to induce amplification and inhibition of the $[Ca^{2+}]_i$ response. The degree of amplification and the rate of desensitisation induced by the NO donors varied between donors but was most likely relative to the individual donors rates of release of NO. The use of four donors removed the likelihood of the results achieved being an artefact of any one donor as all four donors gave similar patterns of response. The control data show that the mouse submandibular acinar cells ability to respond to stimulus did not diminish over the experimental time period. The NO exposed data demonstrate that the mouse submandibular acinar cells initially become hyper-responsive to 50nM ACh but then gradually become hypo-responsive over the experimental time period in the presence of any of the four NO donors.

The use of two inhibitors of the cADPr pathway demonstrated that the amplification induced was mediated through the cADPr pathway. However, the induced desensitisation persisted in the presence of both cADPr pathway inhibitors which indicates that the reduction in $[Ca^{2+}]_i$ response to ACh is in-dependent of the cADPr pathway. The sum of these data suggest a role for NO in glandular hypofunction in SjS as the cells were desensitised to ACh following chronic exposure to NO.

Chapter Four

Results

Nitric Oxide

Human Submandibular Acinar Cells



UNIVERSITY OF
LIVERPOOL

Introduction

Following the work performed using mouse submandibular acinar cells subsequent experiments were performed on acinar cells from human submandibular tissue obtained, following ethical approval, from head and neck cancer operations. Tissue used was histologically normal and from non-irradiated patients. Experiments from such cells are much more valuable and would give a better insight when examining the pathological processes of the disease.

The two NO donors selected were NOC-12 and SNP. These two donors were selected as they were relatively easy to use and produced good results in the mouse submandibular acinar cells. Both NO pathway inhibitors were used but only in conjunction with NOC-12 as that gave the most reliable and consistent results. The human submandibular acinar cells appeared much more sensitive than the mouse submandibular acinar cells and as a result the control responses did demonstrate some degree of reduction over the experimental time period but the final results proved consistent with those achieved using the mouse submandibular acinar cells.

All experiments were performed in accordance with the strict protocol described previously (Chapter 2 materials and methods section 2.8, figure 2.8.2). The response of human submandibular acinar cells to ACh follows the same typical pattern as the mouse submandibular acinar cells as discussed previously (Chapter 2 materials and methods section 2.8, figure 2.8.1 trace A).

Results - Acute Experiments

The initial experiments were performed acutely using NOC-12 and SNP to show the effect of NO on ACh-evoked Ca^{2+} signal in human submandibular acinar cells.

Table 4.1.1: Table of results for human submandibular acinar cells

Number of samples	Type of Response	Degree of Response (Mean \pm SE) as a Percentage	Time Taken to decrease to zero (where applicable)
n=9	Control	94.7 \pm 3.43%	N/A
n=3	SNP	1066.7 \pm 260.34%	40
n=5	NOC-12	112.4 \pm 11.84%	62
n=3	NOC-12 + ODQ	108.5 \pm 1.06%	32
n=4	NOC-12 + Ryanodine	101 \pm 2.09%	44
n=3	Ryanodine	73.4 \pm 6.02%	N/A

Figure 4.1.1 parts A and B shows representative traces demonstrating the effect of the NO donor SNP on the ACh-evoked increase in $[\text{Ca}^{2+}]_i$ in human submandibular acinar cells. Trace A shows a series of control responses to ACh (50nM) over the protocol defined time points. Trace B shows the responses to ACh (50nM) in the presence of NO donor SNP (75 μ M) over the same protocol defined time points. Comparison of the response of cells to ACh (50nM) under control conditions (A) to that obtained following exposure to NO donor SNP (B) at equivalent time points, shows that exposure of the human submandibular acinar cells to an NO donor SNP significantly ($P<0.001$) increased the $[\text{Ca}^{2+}]_i$ response to ACh (50nM) compared to control. When the data for all the experiments was gathered and expressed as

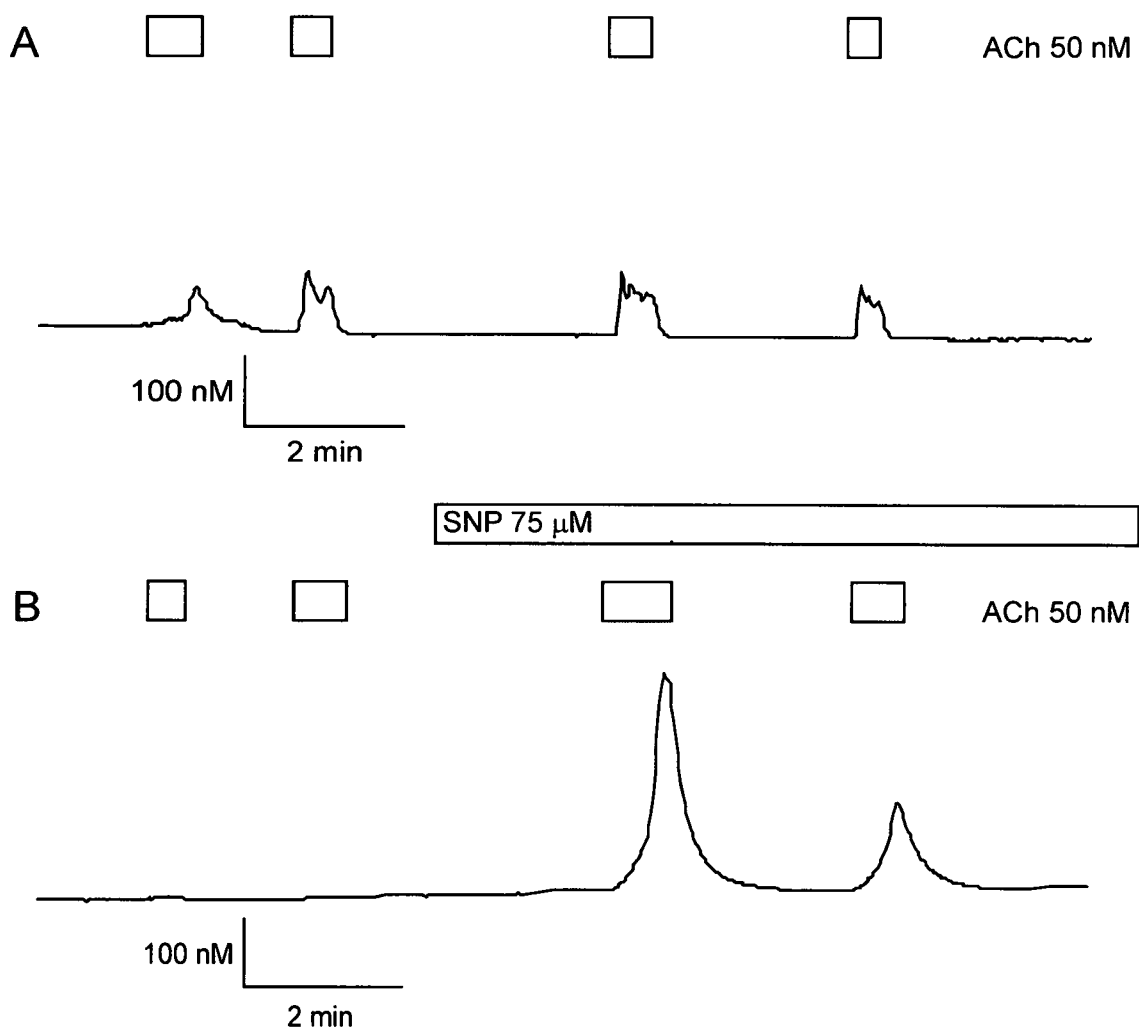
percentages the average control response was $94.7 \pm 3.43\%$ (n=9) compared to $1066.7 \pm 260.34\%$ (n=3) in the presence of SNP.

Figure 4.1.1 parts C and D shows representative traces which demonstrate the effect of the NO donor NOC-12 on the ACh-evoked increase in $[Ca^{2+}]_i$ in human submandibular acinar cells. Trace C shows a series of control $[Ca^{2+}]_i$ responses to ACh (50nM) over the protocol defined time points. Trace D shows the $[Ca^{2+}]_i$ responses to ACh (50nM) in the presence of the NO donor NOC-12 (200 μ M) over the same protocol defined time points. Comparison of the $[Ca^{2+}]_i$ response of cells to ACh under control conditions (C) to that obtained following exposure to NO donor NOC-12 (D) at equivalent time points, shows that exposure of the human submandibular acinar cells to NO donor NOC-12 did not significantly increase the response to ACh compared to control. When the data for all the experiments was gathered and expressed as percentages the average control response was $94.7 \pm 3.43\%$ (n=9) compared to $112.4 \pm 11.84\%$ (n=5) in the presence of NOC-12.

As stated previously (Chapter 1 Introduction 1.2 Nitric oxide) elevated levels of NO have been observed in SjS patients and NO has been suggested to have a role in the progression of the disease and the resulting salivary gland hypo-function. Unfortunately this preliminary data would suggest that NO induces hyper, not hypo-function as it enhanced the cells responses to ACh. However, these initial experiments only determined the acute effect of NO on acinar cells and in the salivary glands of SjS patients the acinar cells would be exposed to NO long-term so these experiments are less relevant to SjS patients. Extended duration experiments were required to determine the effect of NO long term.

Figure 4.1.1

Change in $[Ca^{2+}]_i$ in response to 50nM ACh, illustrating how 75 μ M SNP induced amplification of $[Ca^{2+}]_i$ signal.

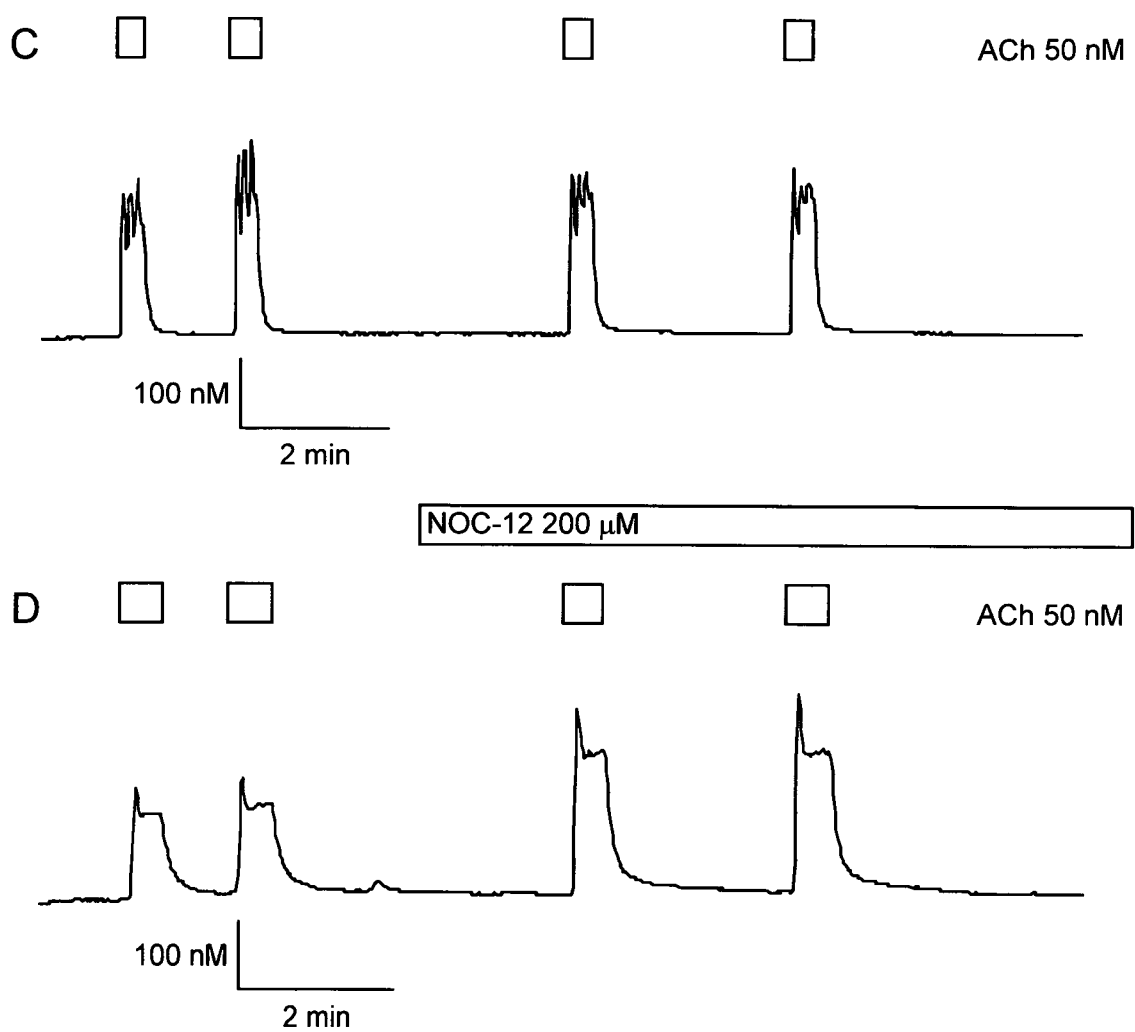


ACh (50nM) stimulated increased $[Ca^{2+}]_i$ measured in human submandibular acinar cells maintained in primary tissue culture fluid for 72 (control) and 48 (SNP) hours respectively.

Trace A shows response to repeated stimulation with 50nM ACh only (see bar).

Trace B shows responses to repeated stimulation with 50nM ACh before and after application of the NO donor SNP (see bar).

Figure 4.1.1
Change in $[Ca^{2+}]_i$ in response to 50nM ACh, illustrating how 200 μ M NOC-12 induced amplification of $[Ca^{2+}]_i$ signal.



ACh (50nM) stimulated increased $[Ca^{2+}]_i$ measured in human submandibular acinar cells maintained in primary tissue culture fluid for 72 (control) and 24 (NOC-12) hours respectively. Trace C shows response to repeated stimulation with 50nM ACh only (see bar). Trace D shows responses to repeated stimulation with 50nM ACh before and after application of the NO donor NOC-12 (see bar).

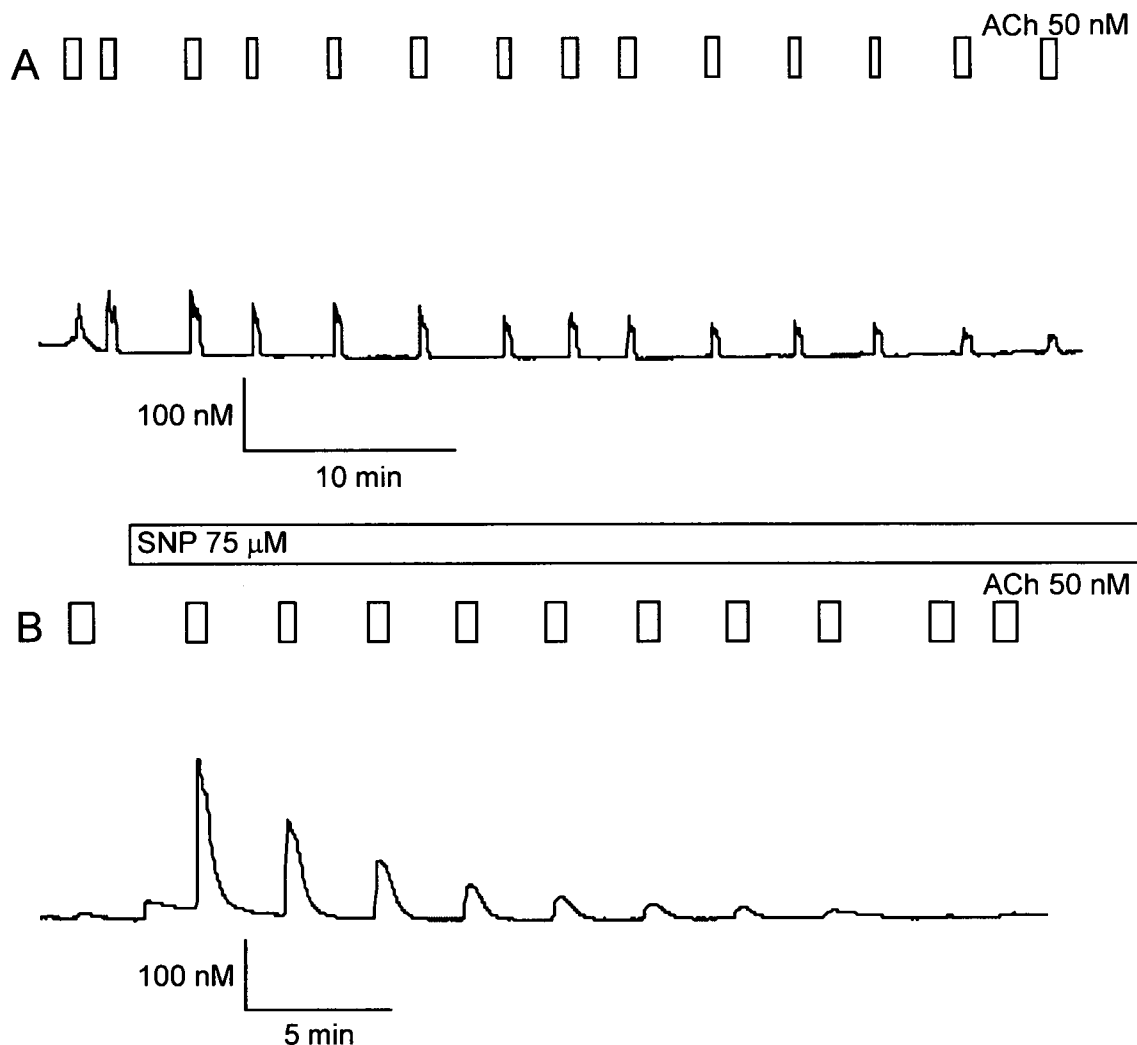
Chronic Experiments

Following the initial results achieved a second set of experiments were conducted which exposed the human submandibular acinar cells more chronically to NO. These more chronic experiments were performed to determine the effect of NO exposure more long term and would be more relevant to the NO exposure in SjS patients. The results of this work could give a more accurate insight into the effect induced on the response of acinar cells to ACh following prolonged NO exposure.

Figure 4.1.2 parts A and B shows representative traces demonstrating the chronic effect of the NO donor SNP on the ACh-evoked increase in $[Ca^{2+}]_i$ in human submandibular acinar cells. Trace A shows a prolonged series of control $[Ca^{2+}]_i$ responses to ACh (50nM) over the protocol defined time period. Trace A also shows that the cells under control conditions maintain their ability to respond over the expanded experimental protocol. Trace B shows the $[Ca^{2+}]_i$ responses to ACh (50nM) in the presence of NO donor SNP (75 μ M) over the same protocol defined time points. As described previously comparison of the acinar cell $[Ca^{2+}]_i$ response to ACh under control conditions (A) to that which was obtained following exposure to NO donor SNP (B), shows that exposure of the human submandibular acinar cells to an NO donor SNP initially increased the level of response to ACh. The control response in figure 4.1.2 trace A shows some degree of run-down over the duration of the experiment. However, the data in figure 4.1.2 part B show that over a prolonged period of time the cells become less sensitive to ACh and finally stop responding to stimulus. At 40 minutes the ACh stimulated increase in $[Ca^{2+}]_i$ response in the presence of SNP was not significantly different from zero.

Figure 4.1.2

Change in $[Ca^{2+}]_i$ in response to 50nM ACh, illustrating how 75 μ M SNP induced amplification and inhibition of $[Ca^{2+}]_i$ signal.



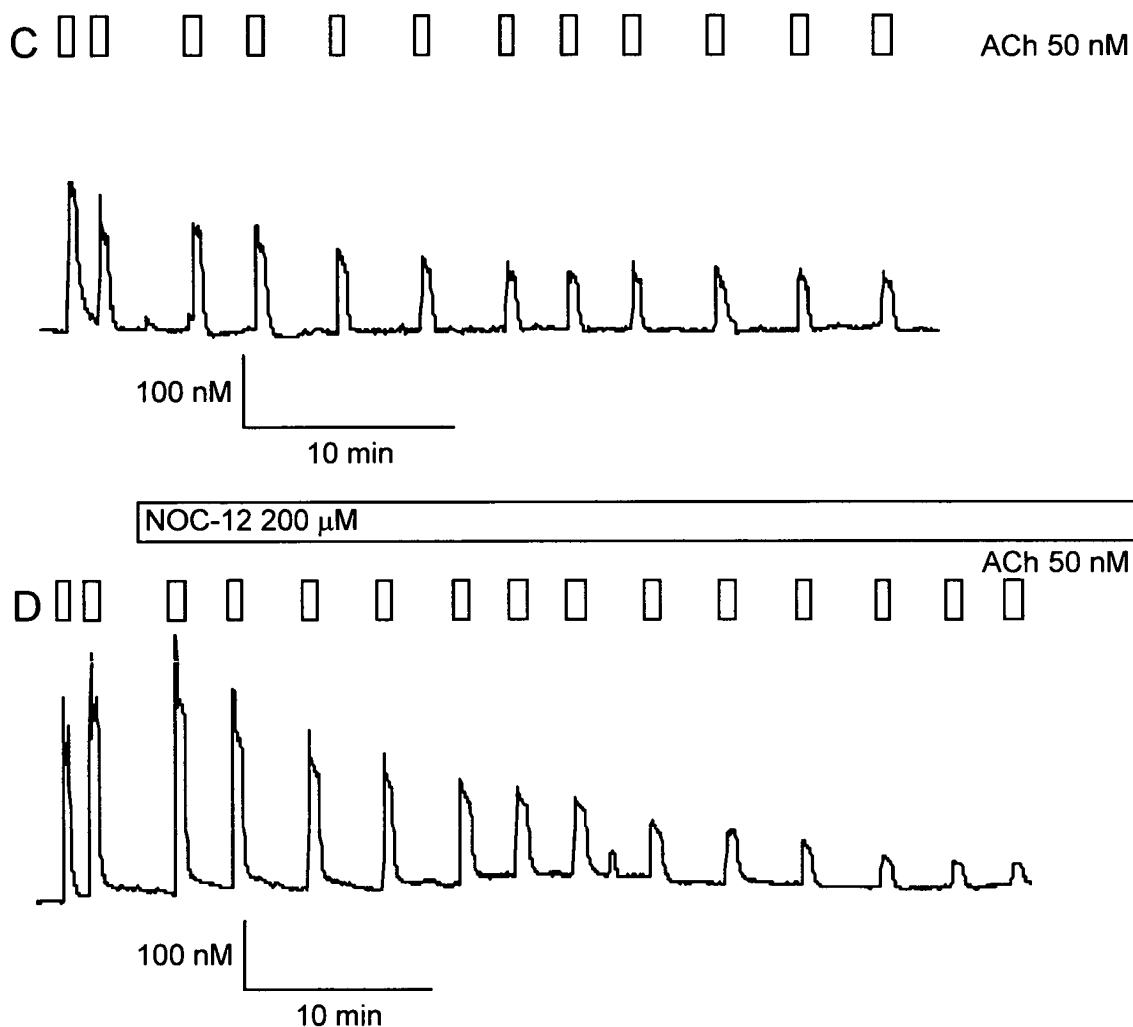
ACh (50nM) stimulated increased $[Ca^{2+}]_i$ measured in human submandibular acinar cells maintained in primary tissue culture fluid for 24 hours.

Trace A shows response to repeated stimulation with 50nM ACh only (see bar).

Trace B shows responses to repeated stimulation with 50nM ACh before and after application of the NO donor SNAP (see bar).

Figure 4.1.2

Change in $[Ca^{2+}]_i$ in response to 50nM ACh, illustrating how 200 μ M NOC-12 induced amplification and inhibition of $[Ca^{2+}]_i$ signal.



ACh (50nM) stimulated increased $[Ca^{2+}]_i$ measured in human submandibular acinar cells maintained in primary tissue culture fluid for 48 (control) and 24 (NOC-12) hours respectively.

Trace C shows response to repeated stimulation with 50nM ACh only (see bar).

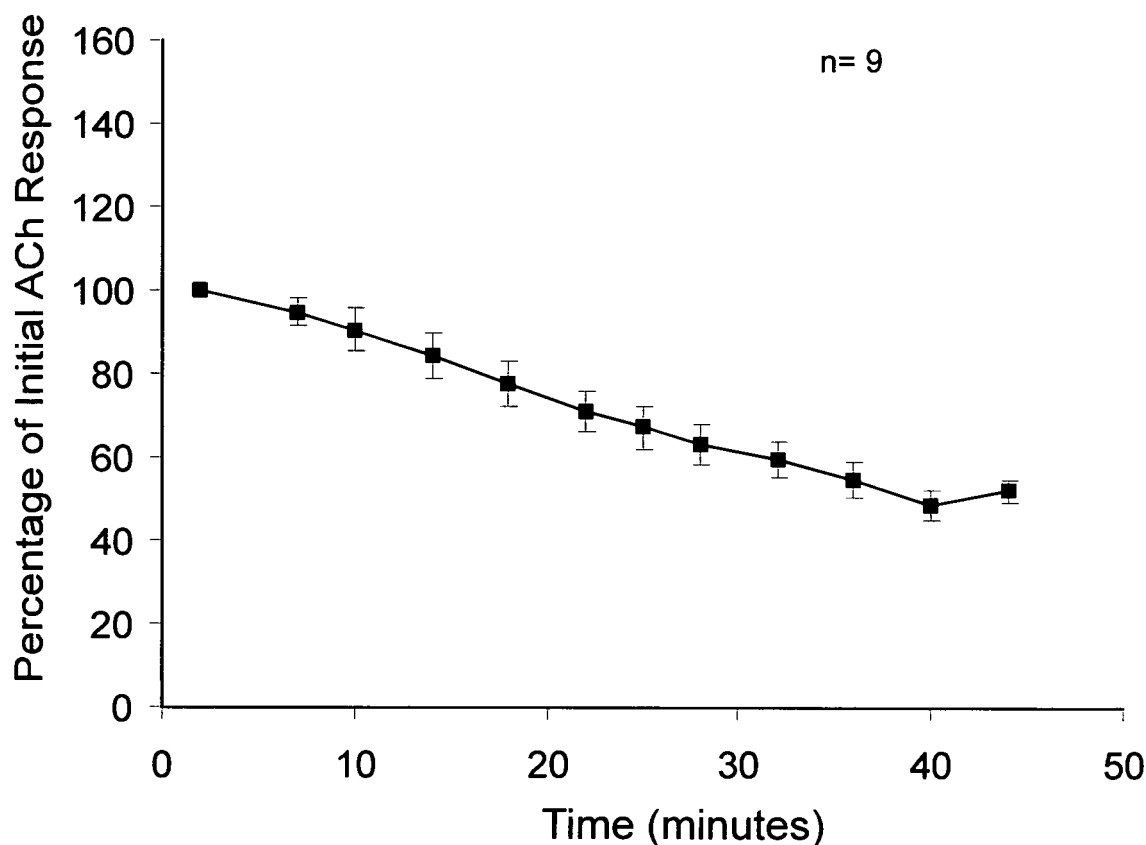
Trace D shows responses to repeated stimulation with 50nM ACh before and after application of the NO donor NOC-12 (see bar).

Figure 4.1.2 parts C and D shows representative traces demonstrating the chronic effect of NO donor NOC-12 on the ACh-evoked increase in $[Ca^{2+}]_i$ in human submandibular acinar cells. Trace C shows a prolonged series of control $[Ca^{2+}]_i$ responses to ACh (50nM) over the protocol defined time points, with cells maintaining the level of response. Trace D shows the $[Ca^{2+}]_i$ responses to ACh (50nM) in the presence of NO donor NOC-12 (200 μ M) over the same protocol defined time points. Comparison of the $[Ca^{2+}]_i$ response of cells to ACh under control conditions (C) to those obtained following exposure to NO donor NOC-12 (D) at equivalent time points, shows that exposure of the human submandibular acinar cells to an NO donor NOC-12 slightly increased the level of response to ACh. However, the data in figure 4.1.2 part D also show that over a prolonged period of time the cells become less sensitive to ACh and finally stop responding to stimulus. At 62 minutes the ACh stimulated increase in $[Ca^{2+}]_i$ response in the presence of NOC-12 was not significantly different from zero.

The data in figures 4.1.3 to 4.1.5 show the cumulative average responses achieved under control conditions, those achieved using NO donor SNP and those achieved using NO donor NOC-12 respectively. Upon review of the average data in figures 4.1.4 and 4.1.5 the chronic pattern of response of NO is clearly observable. The cumulative average data in figures 4.1.3 to 4.1.5 also allow direct comparison between control and experimental conditions. Figure 4.1.6 shows cumulative data presented as a bar chart to allow direct comparison between control and experimental conditions.

Figure 4.1.3

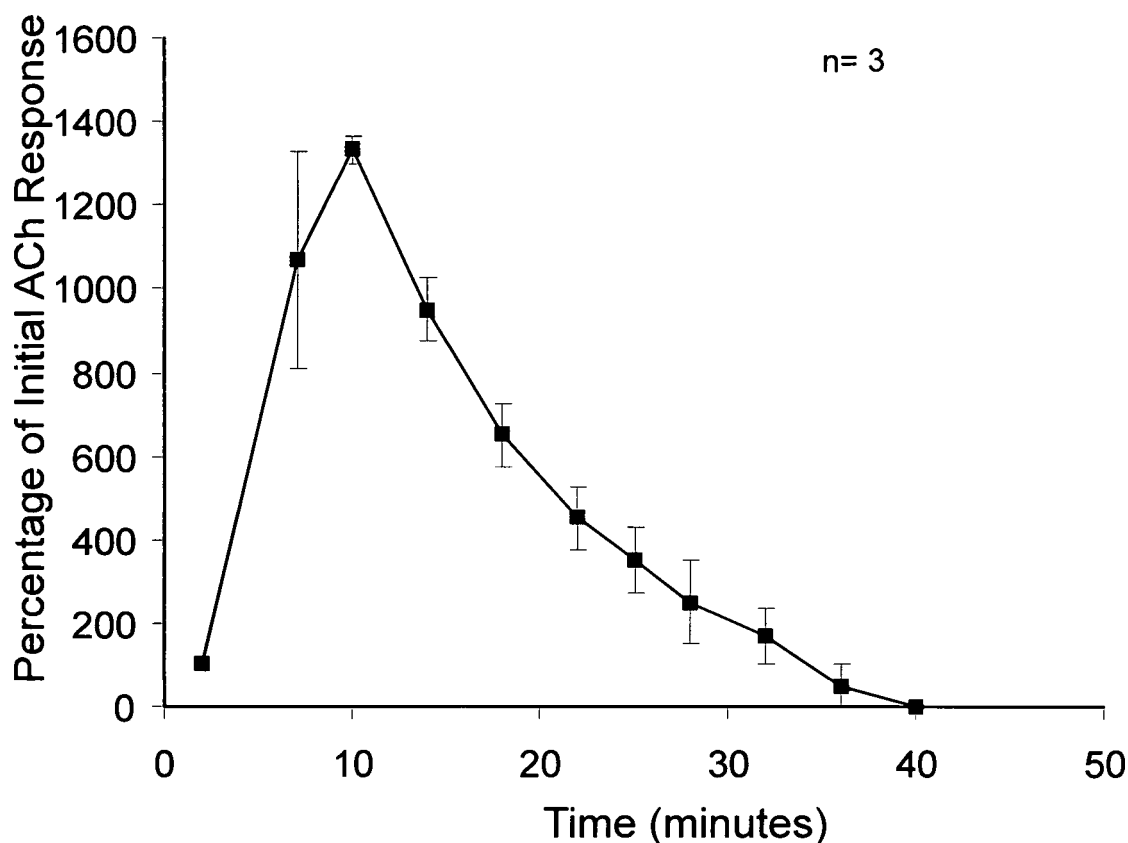
Change in $[Ca^{2+}]_i$ in response to 50nM ACh did not totally diminish with repeated application over the experimental time period.



Time course showing cumulative data for 50nM ACh in human submandibular acinar cells. The data show the series of experimental time points where responses to 50nM ACh occurred. These data show the standard response of human submandibular acinar cells to 50nM ACh under control conditions.

Figure 4.1.4

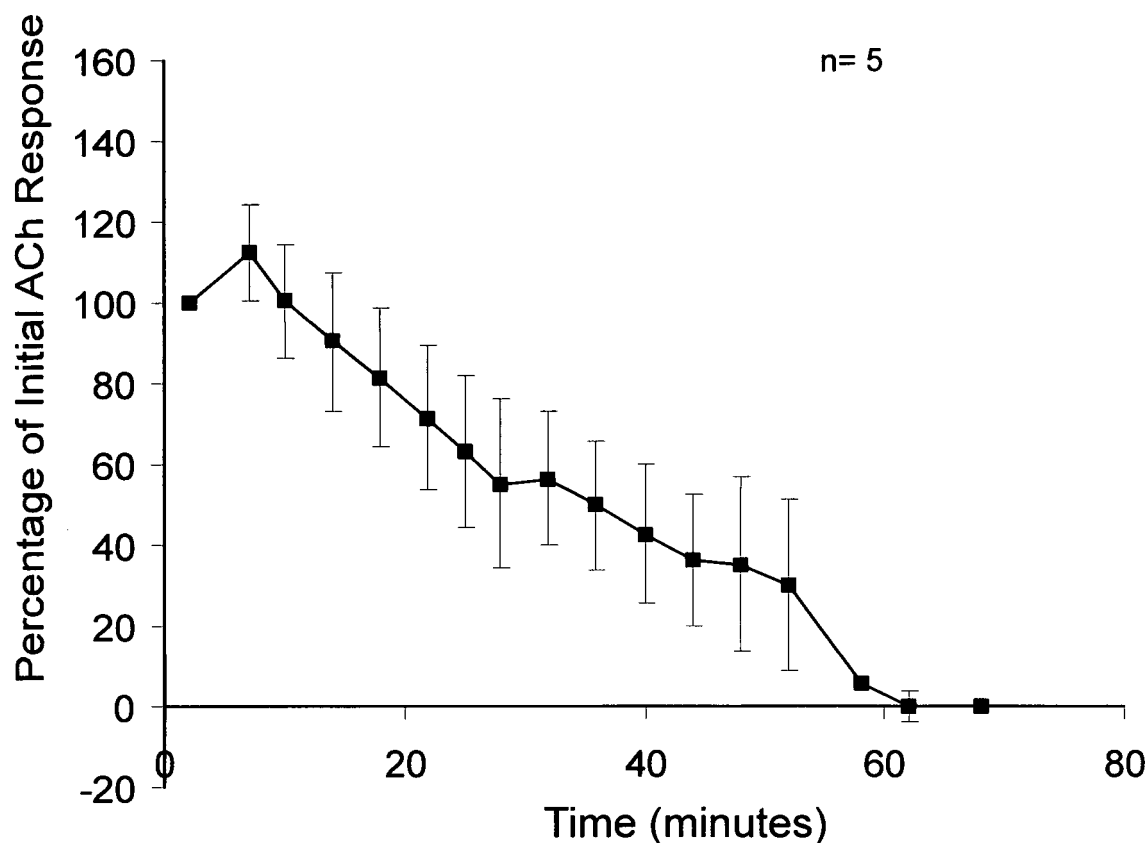
Change in $[Ca^{2+}]_i$ in response to 50nM ACh in the presence of 75 μ M SNP initially increases but then gradually decreases with repeated application over the experimental time period.



Time course showing cumulative data for 50nM ACh in the presence of 75 μ M SNP in human submandibular acinar cells. The data show the series of experimental time points where responses to 50nM ACh in the presence of 75 μ M SNP occurred. The cumulative data was produced from a relatively small sample size due to the small amount of human tissue available but this significant increase in response was observed in each experiment.

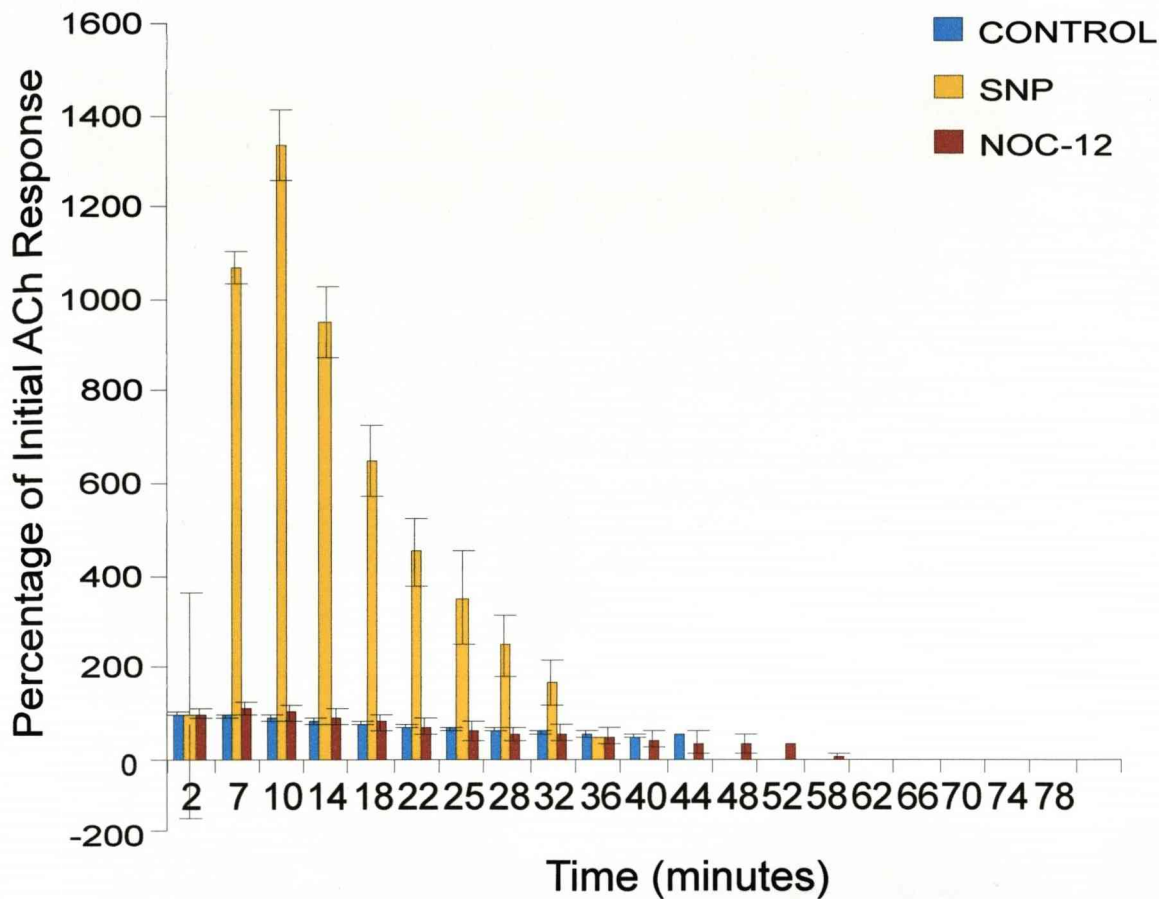
Figure 4.1.5

Change in $[Ca^{2+}]_i$ in response to 50nM ACh in the presence of 200 μ M NOC-12 initially marginally increases but then gradually decreases with repeated application over the experimental time period.



Time course showing cumulative data for 50nM ACh in the presence of 200 μ M NOC-12 in human submandibular acinar cells. The data show the series of experimental time points where responses to 50nM ACh in the presence of 200 μ M NOC-12 occurred.

Figure 4.1.6
Change in $[Ca^{2+}]_i$ in response to 50nM ACh only and 50nM ACh in the presence of 75 μ M SNP and 200 μ M NOC-12 respectively over the experimental time period.



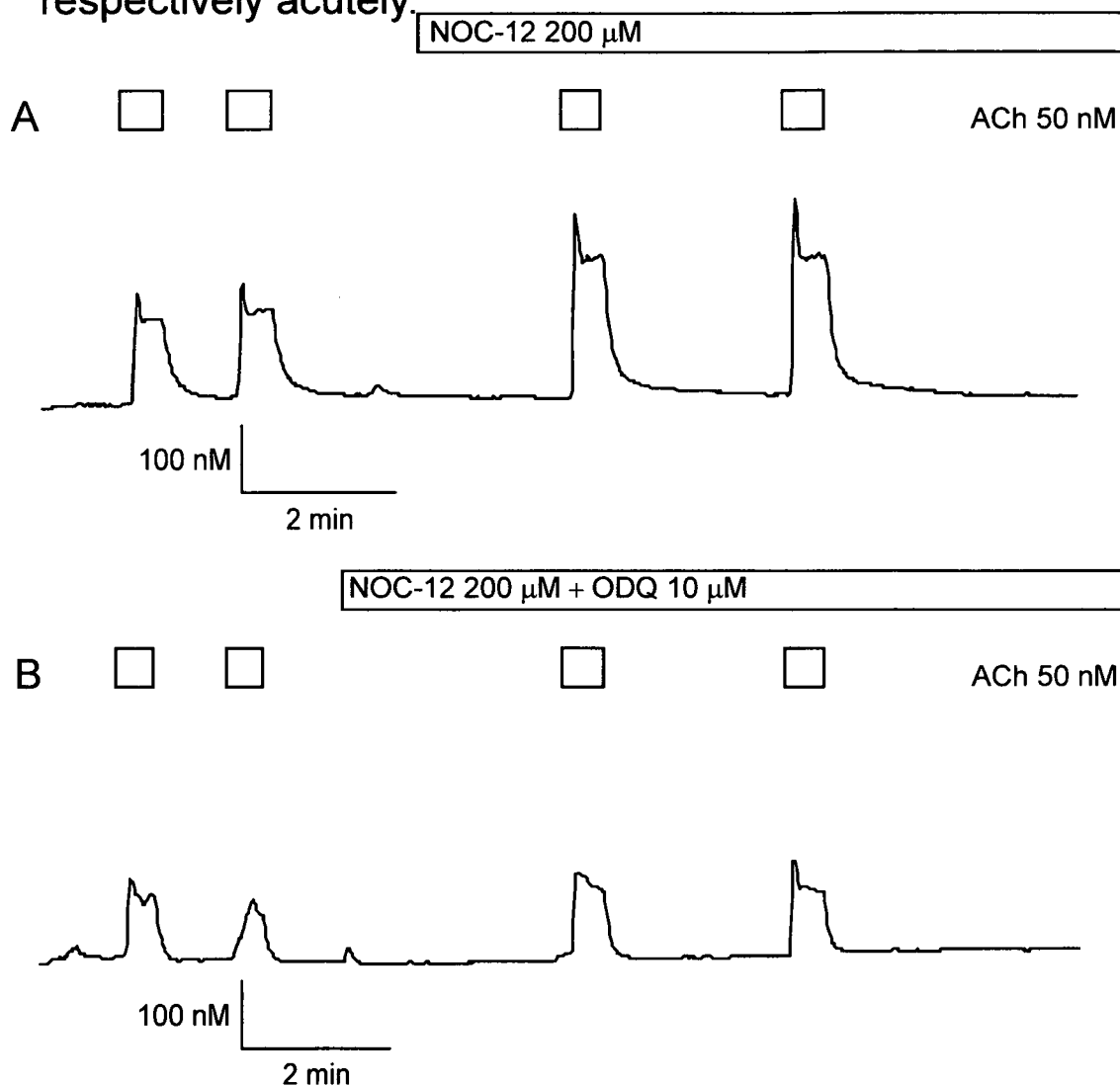
Inhibitors - ODQ

Following the results achieved through use of the NO donors SNP and NOC-12, the mode of action of NO in human submandibular acinar cells had to be determined. As discussed previously, (Chapter 1 Introduction 1.2 nitric oxide section) NO is considered to act through the cADPr pathway so to investigate this hypothesis inhibitors of this pathway were once again used. NOC-12 was selected for use with the NO pathway inhibitors as it gave good results and proved much more consistent than SNP. ODQ was again selected as the first NO pathway inhibitor.

Figure 4.1.7 parts A and B shows representative traces demonstrating the affect of sGC inhibitor ODQ on the affect of NO donor NOC-12 on the ACh-evoked increase in $[Ca^{2+}]_i$ in human submandibular acinar cells. Trace A shows a series of $[Ca^{2+}]_i$ responses to ACh (50nM) in the presence of the NO donor NOC-12 (200 μ M) only over the protocol defined time points. Trace B shows the $[Ca^{2+}]_i$ responses to ACh (50nM) in the presence of NO donor NOC-12 (200 μ M) and ODQ (10 μ M) over the same protocol defined time points. Comparison of the $[Ca^{2+}]_i$ responses in figures A and B, shows that exposure of the human submandibular acinar cells to NO in the presence of ODQ slightly reduced the increase in response to ACh observed previously from an average NOC-12 response of $112.4 \pm 11.84\%$ (n=5) to $108.5 \pm 1.06\%$ (n=3) for NOC-12 in the presence of ODQ. The data in figure 4.1.7 parts A and B demonstrate inhibition of the NO induced amplification of the ACh-evoked increase in $[Ca^{2+}]_i$ by ODQ.

Figure 4.1.7

Change in $[Ca^{2+}]_i$ in response to 50nM ACh in the presence of 200 μ M NOC-12 and 200 μ M NOC-12 with 10 μ M ODQ respectively acutely.



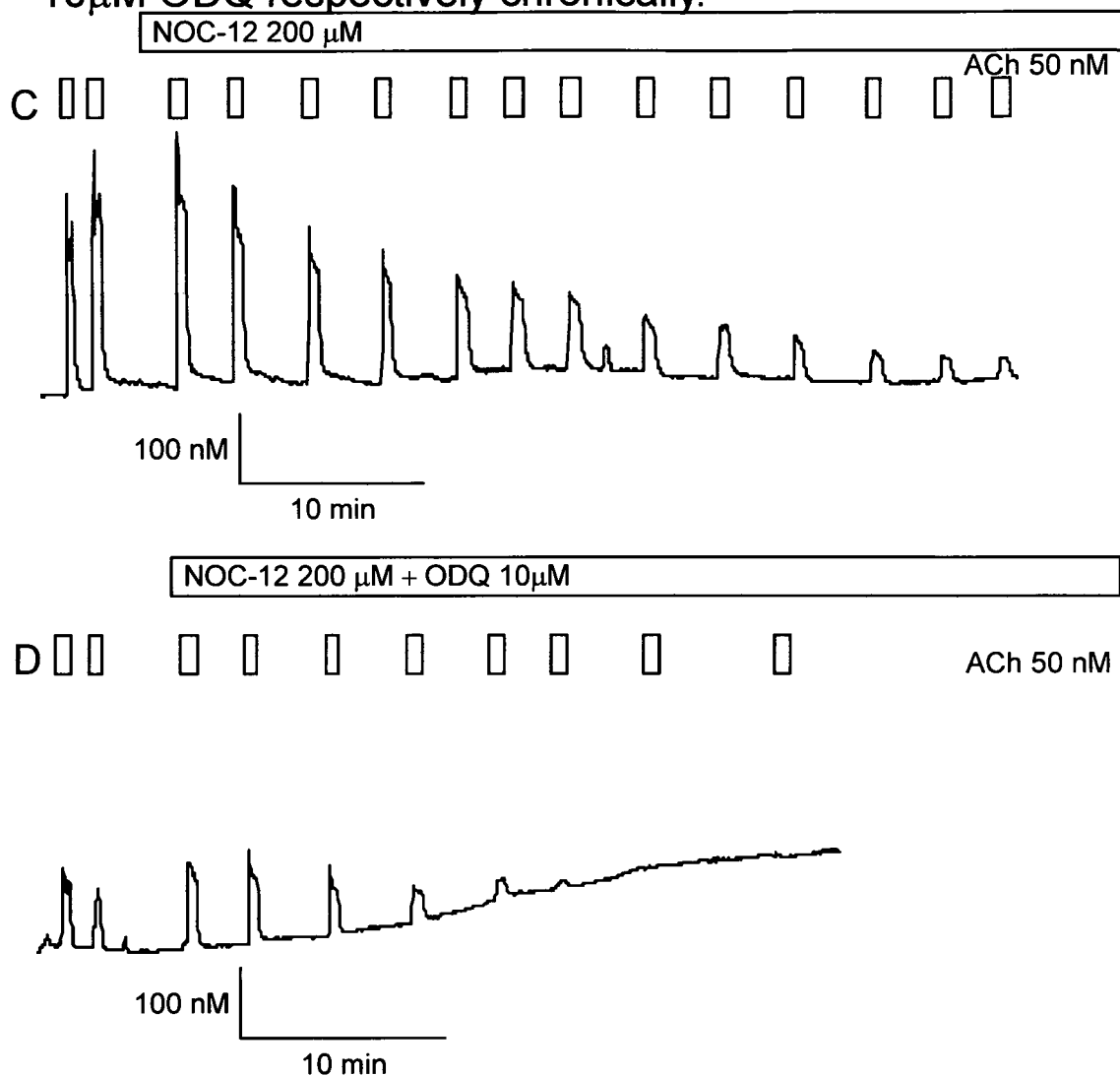
ACh (50nM) stimulated increased $[Ca^{2+}]_i$ measured in human submandibular acinar cells maintained in primary tissue culture fluid for 24 (NOC-12) and 48 (NOC-12/ODQ) hours respectively.

Trace A shows responses to repeated stimulation with 50nM ACh before and after application of NO donor NOC-12 (see bar).

Trace B shows responses to repeated stimulation with 50nM ACh before and after application of the NO donor NOC-12 with NO pathway inhibitor ODQ (see bar).

Figure 4.1.7

Change in $[Ca^{2+}]_i$ in response to 50nM ACh in the presence of 200 μ M NOC-12 and 200 μ M NOC-12 in the presence 10 μ M ODQ respectively chronically.



ACh (50nM) stimulated increased $[Ca^{2+}]_i$ measured in human submandibular acinar cells maintained in primary tissue culture fluid for 24 hours.

Trace C shows responses to repeated stimulation with 50nM ACh before and after application of NO donor NOC-12 (see bar).

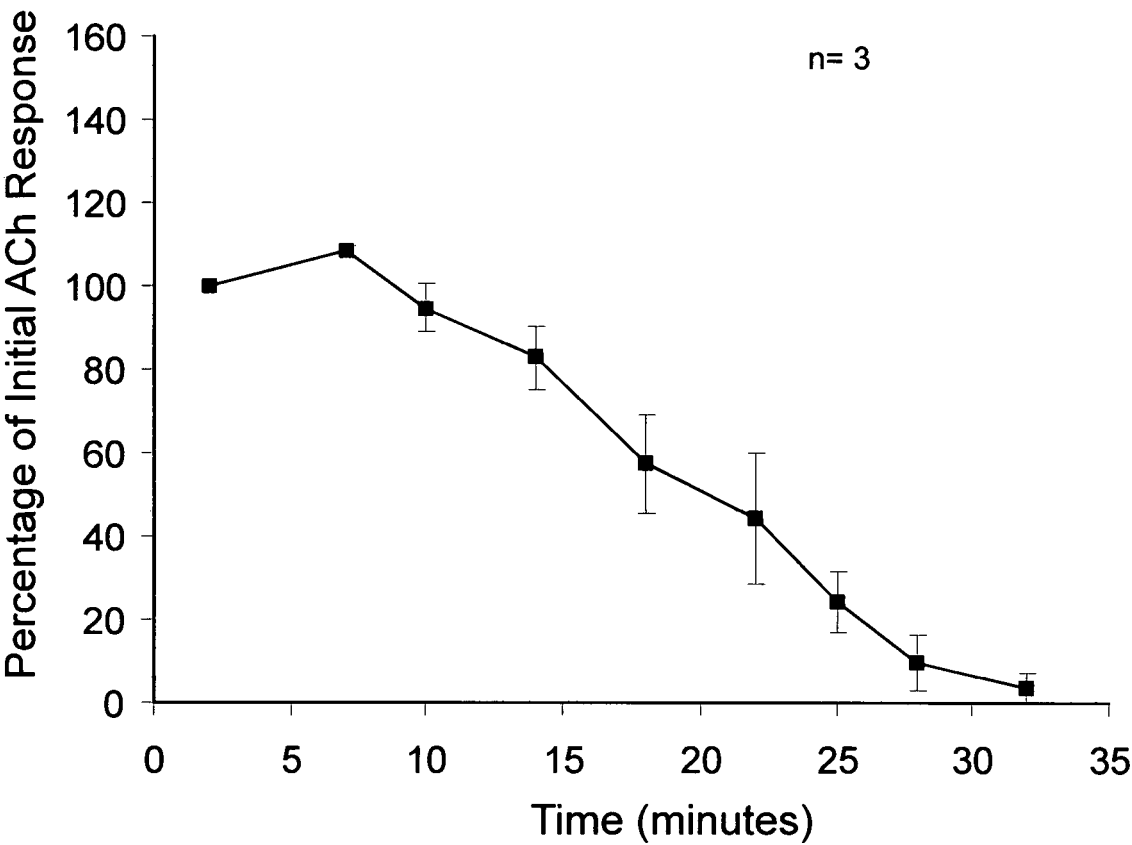
Trace D shows responses to repeated stimulation with 50nM ACh before and after application of the NO donor NOC-12 and NO inhibitor ODQ (see bar).

However, more prolonged experiments were required to demonstrate what effect inhibitors of the cADPr pathway would have on the de-sensitisation of acinar cells to ACh induced previously by the NO donor NOC-12.

Figure 4.1.7 parts C and D shows representative traces demonstrating the chronic effect of ODQ on the effect of NO donor NOC-12 on the ACh-evoked increase in $[Ca^{2+}]_i$ in human submandibular acinar cells. Trace C shows a prolonged series of $[Ca^{2+}]_i$ responses to ACh (50nM) in the presence NO donor NOC-12 (200 μ M) only over the protocol defined time points. Trace D shows the $[Ca^{2+}]_i$ responses to ACh (50nM) in the presence of NO donor NOC-12 (200 μ M) and also ODQ (10 μ M) over the same protocol defined time points. Comparison of traces C and D shows that exposure of the human submandibular acinar cells to the NO donor NOC-12 in the presence of ODQ removed the significant increase in response but the de-sensitisation of the acinar cells to ACh still occurred so ODQ does not prevent the rundown occurring. At 32 minutes the ACh stimulated increase in $[Ca^{2+}]_i$ response in the presence of NOC-12 and ODQ was not significantly different from zero. As was observed in the mouse submandibular acinar cells the rate of inhibition induced by NOC-12 in the presence of ODQ appeared to be increased compared to NOC-12 only as NOC-12 only took 62 minutes to induce total inhibition of the response to ACh.

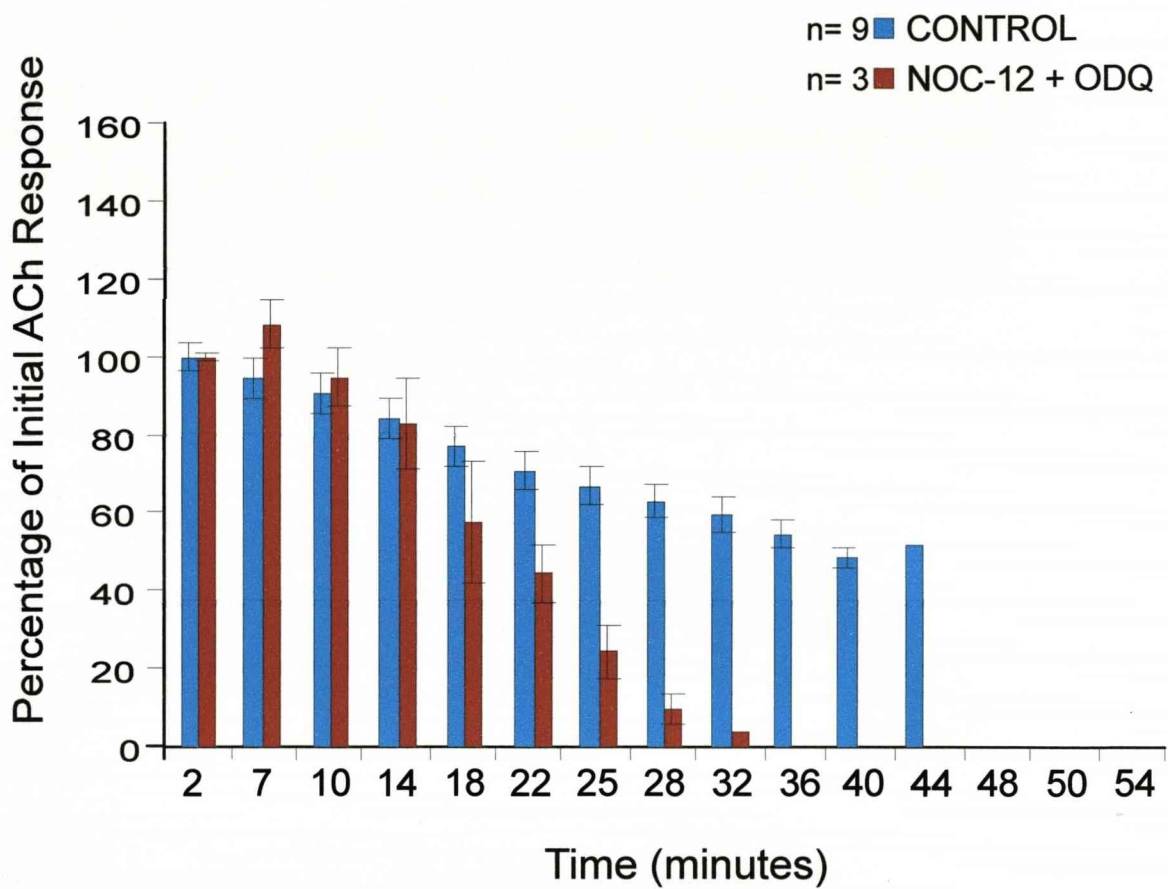
The data in figures 4.1.8 and 4.1.9 show the cumulative average responses achieved using the NO donor NOC-12 in the presence of ODQ. The average data in figure 4.1.9 is presented as a bar chart to allow direct comparison between control conditions and those involving the NO donor NOC-12 in the presence of ODQ.

Figure 4.1.8
Change in $[Ca^{2+}]_i$ in response to 50nM ACh in the presence of 200 μ M NOC-12 and 10 μ M ODQ gradually decreases with repeated application over the experimental time period.



Time course showing cumulative data for 50nM ACh in the presence of 200 μ M NOC-12 and 10 μ M ODQ in human submandibular acinar cells. The data show the series of experimental time points where responses to 50nM ACh in the presence of 200 μ M NOC-12 and 10 μ M ODQ occurred.

Figure 4.1.9
Change in $[Ca^{2+}]_i$ in response to 50nM ACh and 50nM ACh in the presence of 200 μ M NOC-12 with 10 μ M ODQ respectively over the experimental time period.



Bar chart showing cumulative data for 50nMACh control (end point 44 minutes) and 200 μ M NOC-12 with 10 μ M ODQ (end point 32 minutes) in human submandibular acinar cells.

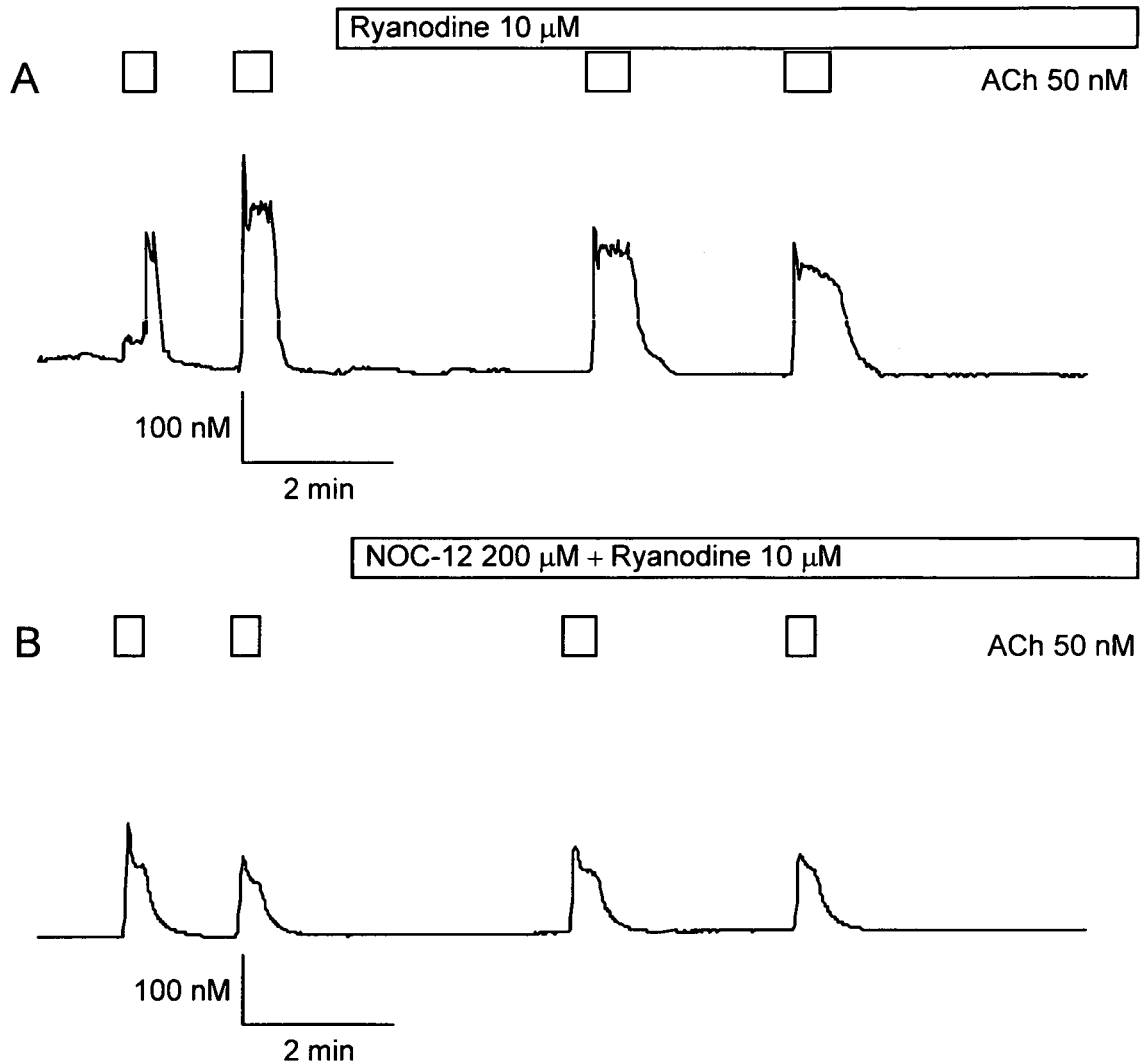
Inhibitor - Ryanodine

Following the results obtained with ODQ the second cADPr pathway inhibitor Ryanodine was again used. NOC-12 was again used as the NO donor to allow direct comparison with the ODQ data.

Figure 4.1.10 parts A and B show representative traces demonstrating the effect of the Ryanodine receptor inhibitor Ryanodine on the effect of NO donor NOC-12 on the ACh-evoked increase in $[Ca^{2+}]_i$ in human submandibular acinar cells. Trace A shows a series of control $[Ca^{2+}]_i$ responses to ACh (50nM) in the presence of Ryanodine (10 μ M) only over the protocol defined time points. Trace B shows the $[Ca^{2+}]_i$ responses to ACh in the presence of both NO donor NOC-12 (200 μ M) and Ryanodine (10 μ M) over the same protocol defined time points. By comparing the $[Ca^{2+}]_i$ response of cells to ACh under control Ryanodine only conditions (A) to those obtained following combined exposure to NO donor NOC-12 and Ryanodine (B) at equivalent time points, the data show that exposure of human submandibular acinar cells to NOC-12 in combination with Ryanodine demonstrate a significant ($P<0.01$) variation in response when compared to those with Ryanodine only.

Figure 4.1.10

Change in $[Ca^{2+}]_i$ in response to 50nM ACh in the presence of 10 μ M Ryanodine and 200 μ M NOC-12 in the presence of 10 μ M Ryanodine respectively acutely.



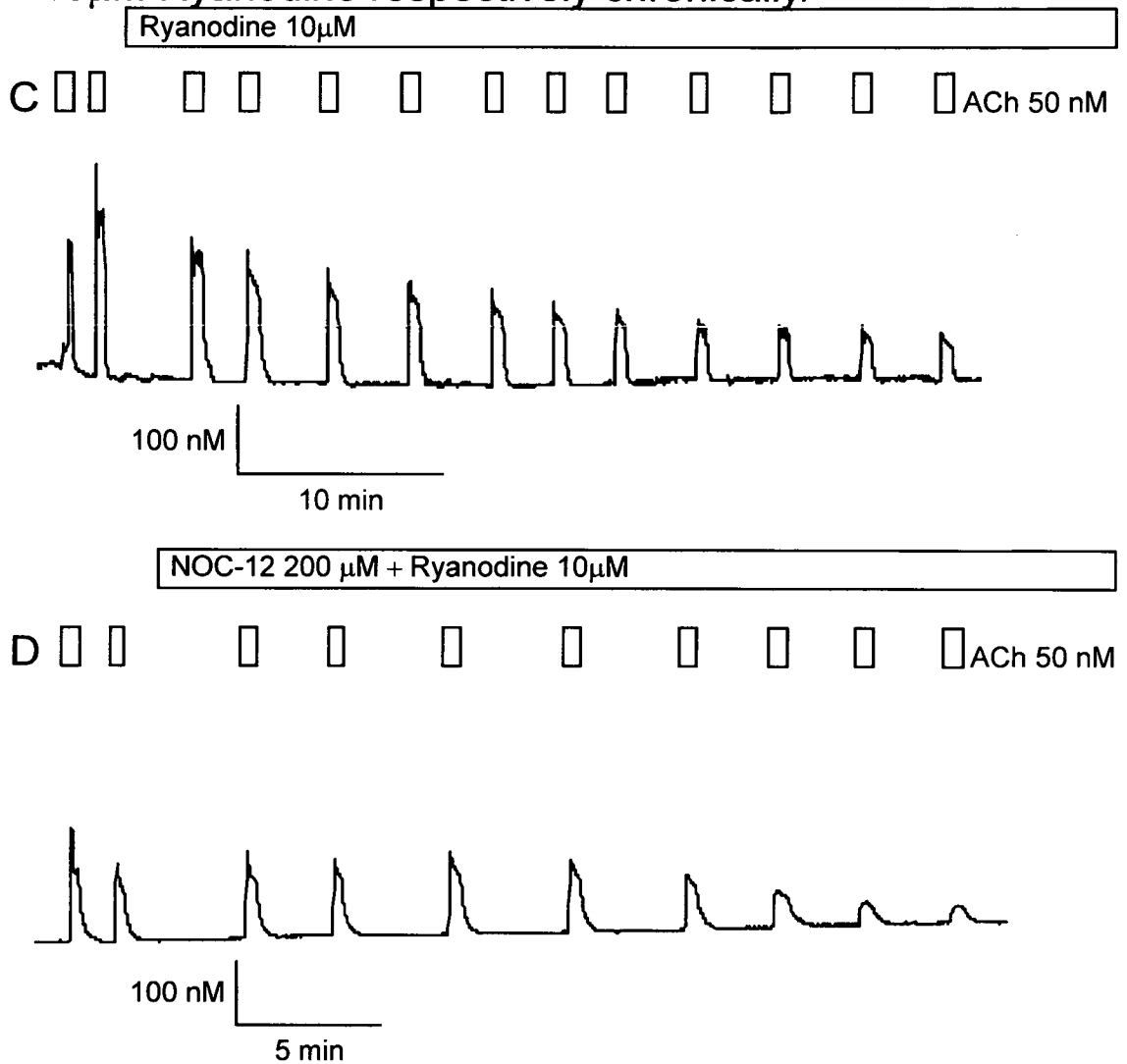
ACh (50 nM) stimulated increased $[Ca^{2+}]_i$ measured in human submandibular acinar cells maintained in primary tissue culture fluid for 24 hours. Trace A shows responses to repeated stimulation with 50nM ACh before and after application of NO pathway inhibitor Ryanodine (see bar). Trace B shows responses to repeated stimulation with 50nM ACh before and after application of the NO donor NOC-12 and NO pathway inhibitor Ryanodine (see bar).

More prolonged experiments were again required to demonstrate what effect this inhibitor of the cADPr pathway would have on the de-sensitisation to ACh induced previously by the NO donor NOC-12.

Figure 4.1.10 parts C and D shows representative traces demonstrating the chronic effect of Ryanodine on the effect of NO donor NOC-12 on the ACh-evoked increase in $[Ca^{2+}]_i$ in human submandibular acinar cells. Trace C shows a series of control $[Ca^{2+}]_i$ responses to ACh (50nM) in the presence of Ryanodine (10 μ M) only over the protocol defined time points. Trace D shows the $[Ca^{2+}]_i$ responses to ACh (50nM) in the presence of both NO donor NOC-12 (200 μ M) and Ryanodine (10 μ M) over the same protocol defined time points. By comparing the $[Ca^{2+}]_i$ response of cells to ACh under control Ryanodine conditions (C) to those obtained following combined exposure to NO donor NOC-12 and Ryanodine (D) at equivalent time points, shows that exposure to NOC-12 in the presence of Ryanodine over a prolonged time period does not prevent de-sensitisation of the acinar cells to ACh. At 44 minutes the ACh stimulated increase in $[Ca^{2+}]_i$ response in the presence of NOC-12 and Ryanodine together was not significantly different from zero and the average data for NOC-12 and Ryanodine together was significantly ($P < 0.05$) different from control. However, at 40 minutes the ACh stimulated increase in $[Ca^{2+}]_i$ response in the presence of Ryanodine only was still significantly above zero. Ryanodine alone induces some degree of inhibition of the $[Ca^{2+}]_i$ responses to ACh (50nM) over the duration of the experiment but not as great as that induced by NOC-12 and Ryanodine together.

Figure 4.1.10

Change in $[Ca^{2+}]_i$ in response to 50nM ACh in the presence of 10 μ M Ryanodine and 200 μ M NOC-12 in the presence of 10 μ M Ryanodine respectively chronically.



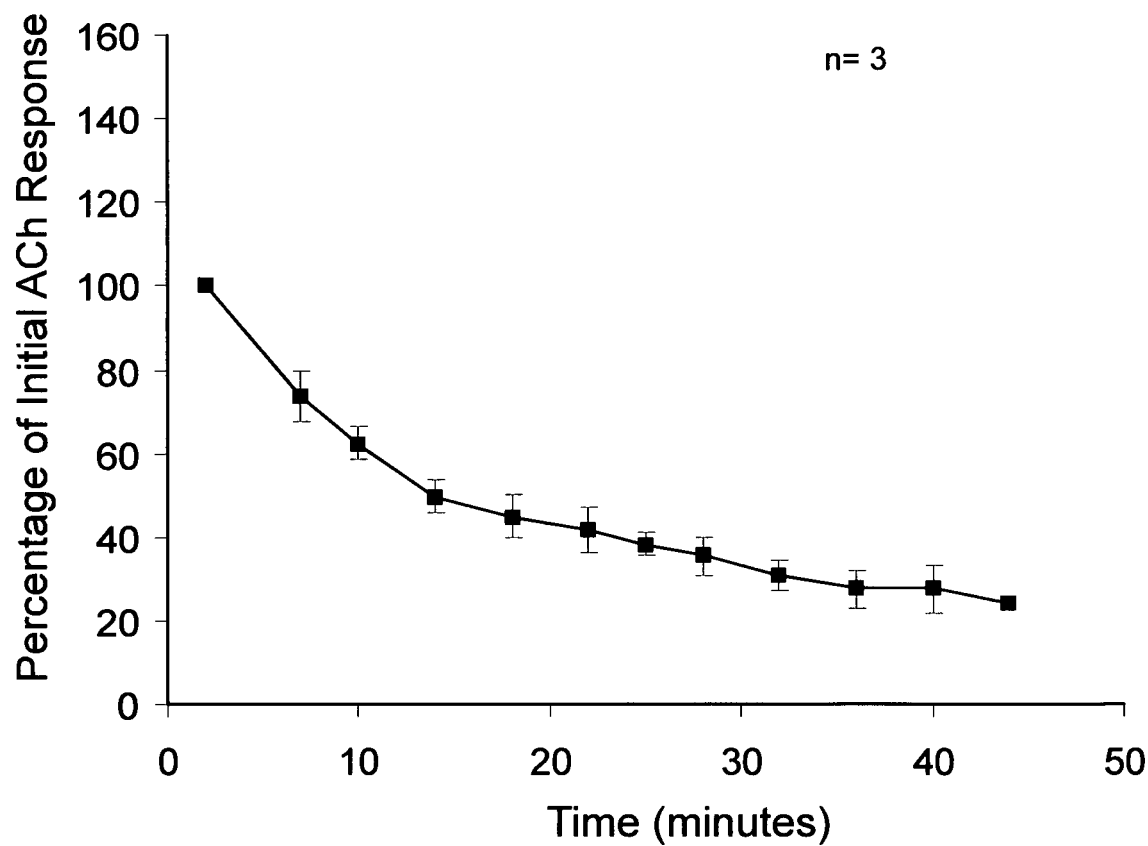
ACh (50 nM) stimulated increased $[Ca^{2+}]_i$ measured in human submandibular acinar cells maintained in primary tissue culture fluid for 24 hours.

Trace C shows responses to repeated stimulation with 50nM ACh before and after application of NO pathway inhibitor Ryanodine (see bar).

Trace D shows responses to repeated stimulation with 50nM ACh before and after application of the NO donor NOC-12 and NO inhibitor Ryanodine (see bar).

Figure 4.1.11

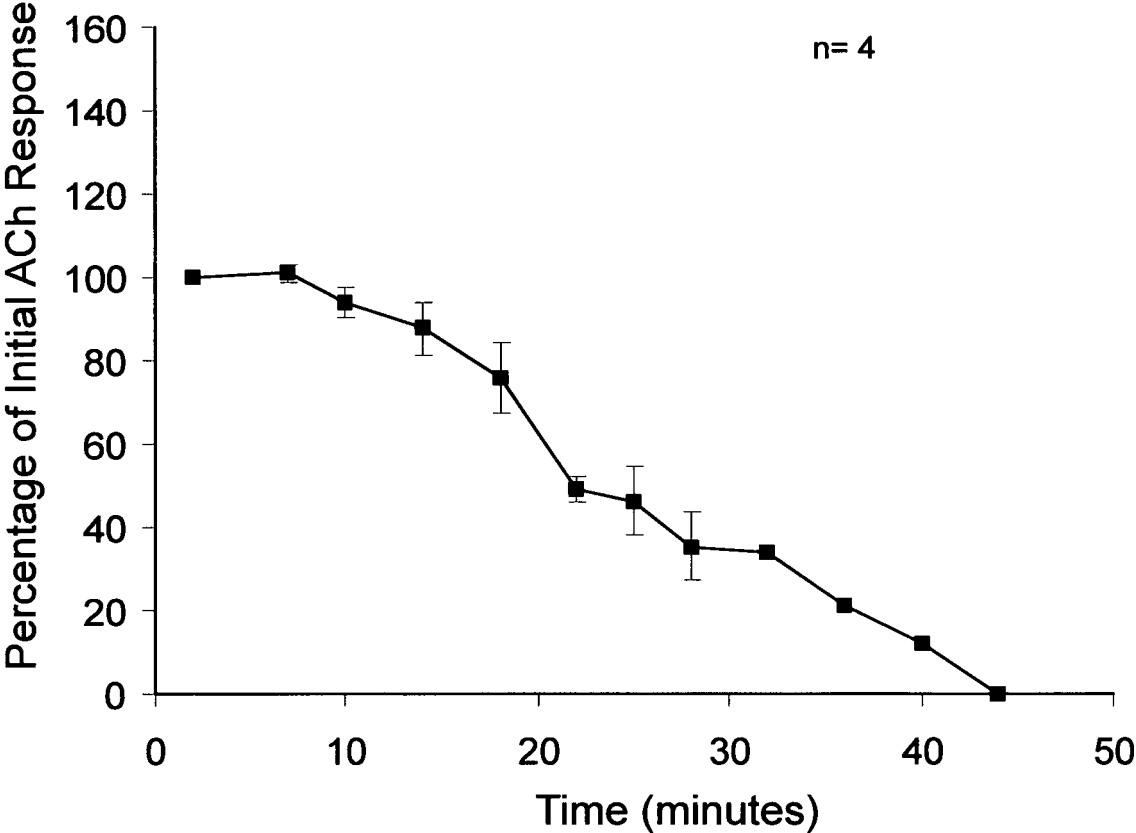
Change in $[Ca^{2+}]_i$ in response to 50nM ACh in the presence of 10 μ M Ryanodine decreases with repeated application over the experimental time period.



Time course showing cumulative data for 50nM ACh in the presence of 10 μ M Ryanodine in human submandibular acinar cells. The data show the series of experimental time points where responses to 50nM ACh in the presence of 10 μ M Ryanodine occurred.

Figure 4.1.12

Change in $[Ca^{2+}]_i$ in response to 50nM ACh in the presence of 10 μ M Ryanodine and 200 μ M NOC-12 over the experimental time period.



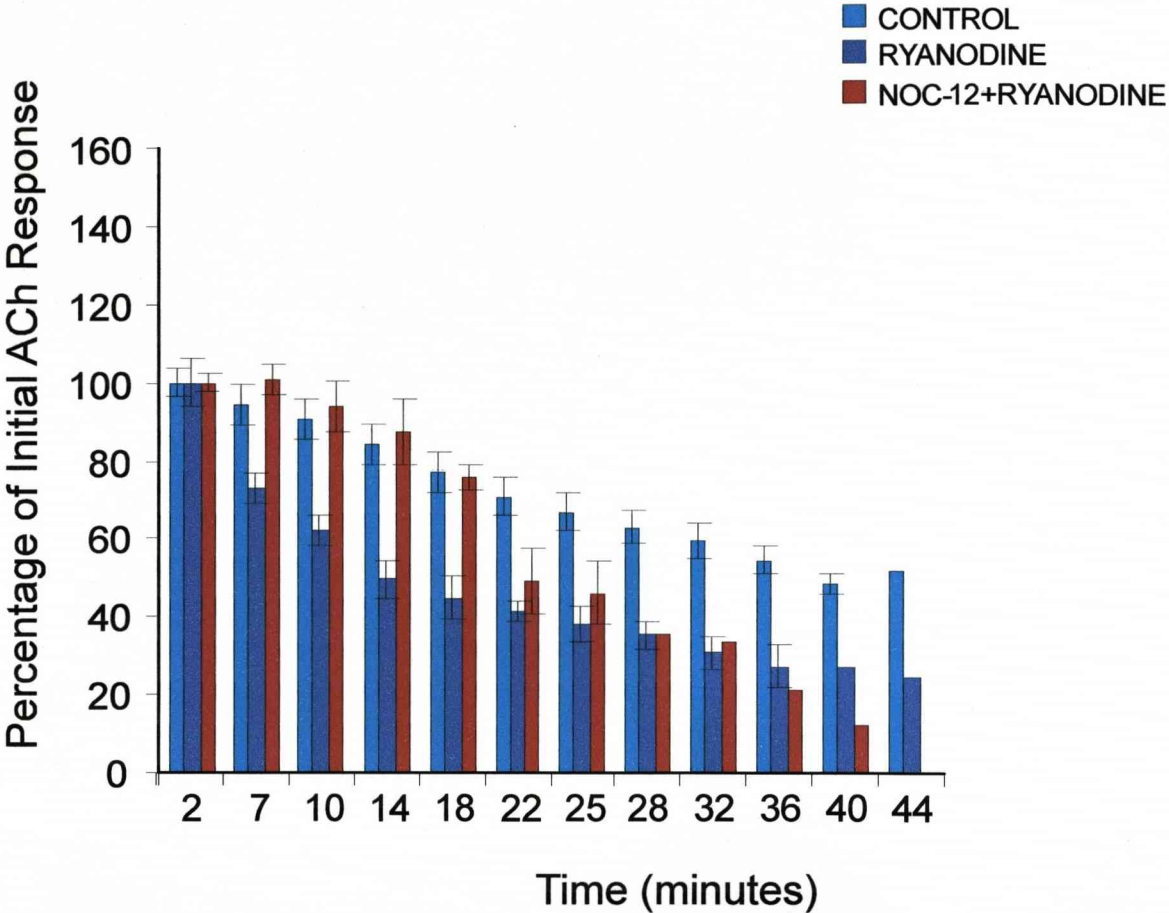
Time course showing cumulative data for 50nM ACh in the presence of 10 μ M Ryanodine and 200 μ M NOC-12 in human submandibular acinar cells. The data show the series of experimental time points where responses to 50nM ACh in the presence of 10 μ M Ryanodine and 200 μ M NOC-12 occurred.

When the three data sets were compared between NOC-12 only, Ryanodine only and NOC-12 in the presence of Ryanodine there was some degree of variation between data sets. When the data for all the experiments was gathered and expressed as percentages the average NOC-12 response was $112.4 \pm 11.84\%$ (n=5) compared to $101 \pm 2.09\%$ (n=4) for NOC-12 in the presence of Ryanodine whereas Ryanodine only had an average response of $73.4 \pm 6.02\%$ (n=3).

There was no statistically significant difference between NOC-12 only and NOC-12 in the presence of Ryanodine or Ryanodine only but there was a significant ($P < 0.01$) difference when NOC-12 in the presence of Ryanodine was compared to Ryanodine only. There was also a statistically significant variation between NOC-12 and Ryanodine together and Ryanodine only ($P < 0.05$) compared to control conditions. The data in figure 4.1.10 demonstrate the inhibition of the NO induced amplification of the ACh-evoked increase in $[Ca^{2+}]_i$ by Ryanodine and also show initial inhibition induced by Ryanodine only.

Figure 4.1.13

Change in $[Ca^{2+}]_i$ in response to 50nM ACh only and 50nM ACh in the presence of 10 μ M Ryanodine only and 10 μ M Ryanodine and 200 μ M NOC-12 together respectively over the experimental time period.



Bar chart showing cumulative data for 50nMACh control (end point 44 minutes), 10 μ M RYANODINE (end point 44 minutes) and 200 μ M NOC-12 with 10 μ M RYANODINE (end point 44 minutes) in human submandibular acinar cells.

The data in figures 4.1.11 and 4.1.12 show the cumulative average responses achieved, using Ryanodine alone and NO donor NOC-12 in the presence of Ryanodine respectively. When compared with figure 4.1.5 for NOC-12 alone the only observable variations between data sets were that NOC-12 decreases more rapidly when used in combination with Ryanodine compared to NOC-12 only. In all instances where NOC-12 is present the level decreases to zero which does not occur when Ryanodine alone is used. The average data in figures 4.1.11 and 4.1.12 also allow direct comparison of experimental data with those achieved under control conditions in figure 4.1.3. Figure 4.1.13 is the cumulative data presented as a bar chart to allow direct comparison between control and experimental conditions.

Conclusions

The data in figure 4.1.1 demonstrate that the use of either NO donor, SNP or NOC-12, induced amplification of the ACh-evoked increase in $[Ca^{2+}]_i$, the results were not comparable as NOC-12 only induced a marginal increase in response. There was some degree of reduction with the control trace which explains why the percentage decreased to 94.7% as opposed to being maintained at 100%. One notable problem with trace B of figure 4.1.1 is the lack of responses to ACh only. This particular trace was only selected because there was a lack of SNP runs and this particular experiment gave the most suitable presentation of data. SNP proved difficult to use with the human submandibular cells due to their sensitivity.

Comparison of data in figure 4.1.2 shows that the use of either NO donor, SNP or NOC-12, initially induced amplification of the ACh-evoked increase in $[Ca^{2+}]_i$ but the responses were not comparable as the increase induced by NOC-12 was only marginal compared to control. However, the data also show that both NO donors

induced inhibition of the ACh-evoked increase in $[Ca^{2+}]_i$ when compared to control. Trace B in figure 4.1.2 is not ideal as it only shows one stimulation with ACh prior to NO donor exposure but was the most suitable from the data available as the data set was very small due to the sensitivity of the Human submandibular acinar cells and problems with SNP usage.

The average cumulative data presented in figures 4.1.3 to 4.1.6 demonstrate that the desensitisation induced by ACh in the presence of both SNP and NOC-12 was more significant than that induced by ACh alone, so both NO donors were able to induce inhibition of the response to ACh in human submandibular acinar cells.

As described previously (Chapter 1 Introduction 1.2 nitric oxide section), NO was selected for investigation as a possible cause of salivary hypofunction in SjS. The chronic data could suggest that NO does have the ability to induce acinar hypofunction but only after prolonged time periods. Therefore NO induces healthy acinar cells to behave like SjS acinar cells. The chronic experiments are therefore compatible with the hypothesised role of NO in SjS.

The data in figure 4.1.7 parts A and B demonstrate inhibition of NO induced amplification of the ACh-evoked increase in $[Ca^{2+}]_i$ by ODQ. Therefore these data support the hypothesis that NO is acting through the cADPr pathway. The acute amplification previously observed with NOC-12 is decreased by the addition of ODQ which may suggest that the acute amplification induced by NO is functioning through the cADPr pathway.

The data in figure 4.1.7 parts C and D show that over a prolonged period of time the cells still become less sensitive to ACh and finally stop responding to stimulus even in the presence ODQ. Therefore the results suggest that the hypofunction induced by

NO is independent of the cADPr pathway. So in spite of the presence of the sGC inhibitor ODQ use of the NO donor NOC-12 still resulted in inhibition of the acinar cells response to ACh.

As observed previously in the mouse submandibular acinar cells the cumulative average data presented in figures 4.1.8 and 4.1.9 show that using the NO donor NOC-12 in the presence of ODQ causes an enhancement of response. There appears to be some degree of additive effect between ODQ and NOC-12 as the use of NOC-12 in the presence of ODQ induces a more rapid de-sensitisation of the acinar cells to ACh but the level of inhibition is no greater. This amplification of the effect of NOC-12 by ODQ has been observed previously by Takuma and colleagues who noted that ODQ appeared to exacerbate the cytotoxic effect of NOC-12 as opposed to blocking it (Takuma, Phuagphong et al. 2002). We may speculate that this is due to ODQ accelerating the rate of release of NO from NOC-12 but further work is required to determine how ODQ amplifies the response of NOC-12.

The data in figure 4.1.10 parts A and B show that the use of NOC-12 with Ryanodine removed the induced amplification of the ACh-evoked increase in $[Ca^{2+}]_i$. The use of Ryanodine with NOC-12 suggests that NO is acting through the cADPr pathway. The data in figure 4.1.10 parts C and D also show that over a prolonged period of time the cells still become less sensitive to ACh and finally stop responding to stimulus in the presence of both NO donor NOC-12 only and NOC-12 and Ryanodine together. The de-sensitisation observed in trace C with Ryanodine only would be expected as the mode of action of Ryanodine, which was determined previously, is direct blocking of the Ryanodine receptor so Ryanodine would gradually inhibit ACh stimulated responses.

The cumulative data in figure 4.1.11 also shows that Ryanodine itself induces run-down by blocking the Ryanodine receptors directly. As a result of these findings the usefulness of Ryanodine as a marker of NO pathway activity is limited as in the short term it functions to stop the induced amplification of the response to ACh but use in chronic experiments is problematic.

The cumulative data presented in figures 4.1.11 to 4.1.13 demonstrate the responses achieved using NOC-12 or Ryanodine alone and those using NOC-12 and Ryanodine together were hard to differentiate between as the average response patterns were very similar. There is no obvious additive effect between Ryanodine and NOC-12 with regard to the degree of desensitisation induced as NOC-12 only and NOC-12 and Ryanodine together both induce total inhibition of the response to ACh. However, the rate of desensitisation of the response to ACh in the presence of NOC-12 does seem to occur more rapidly when Ryanodine is also present which might add strength to the argument that the desensitisation induced by NO is independent of the cADPr pathway as both NOC-12 and Ryanodine alone induced a degree of desensitisation but the rate of desensitisation appears increased when both Ryanodine and NOC-12 are present as the combined experiment took less time to induce total inhibition of the response to ACh.

The inhibitory data from both ODQ and Ryanodine suggests that the hypofunction induced by NO most likely occurs independently of the cADPr pathway but more work is required to elucidate how NO induces inhibition of the response..

In summary the human submandibular acinar cells appeared more sensitive to ACh compared to the mouse submandibular acinar cells which may explain the observed decrease in response to ACh under control conditions. This increased sensitivity to ACh might also explain the modest increase in response to ACh in the presence of

NOC-12 as the rate of release of NO is much slower from NOC-12 compared to other NO donors so it was unable to induce as great an effect in the human submandibular cells. There were also problems with the use of SNP which may be due to its more rapid rate of release of NO and may have influenced the outcome of the results due to the limited data set produced. The acute effects observed when either SNP or NOC-12 were used with human submandibular acinar cells did vary from the data achieved with mouse submandibular acinar cells, however, the chronic effects observed proved consistent and the final response pattern was the same regardless of NO donor as the chronic NO effect occurred with both NO donors.

The use of either inhibitor of the cADPr pathway removed the previously observed marginal amplification of the ACh-evoked increase in $[Ca^{2+}]_i$. However, the NO pathway inhibitors had no effect on the run down induced by NO which would suggest that inhibition is independent of the cADPr pathway. The use of two cADPr pathway inhibitors allows validation of where NO functions within the pathway as ODQ prevents the initial sGC step and Ryanodine blocks the RyR directly so the use of both inhibitors greatly strengthens the NO/cADPr argument. The results presented here suggest a possible role for NO in glandular hypofunction.

Chapter Five

Results

Nitric Oxide

Mouse Lacrimal Acinar Cells



UNIVERSITY OF
LIVERPOOL

Introduction

All experiments were performed in accordance with the strict protocol described previously (Chapter 2 materials and methods section 2.8, figure 2.8.2). The response of mouse lacrimal acinar cells to ACh follows the same typical pattern as the mouse submandibular acinar cells as discussed previously (Chapter 2 materials and methods section 2.8, figure 2.8.1 trace A).

Following the work performed using mouse and human submandibular acinar cells subsequent experiments were performed on mouse lacrimal acinar cells. These experiments would to determine if the effects observed in the submandibular acinar cells was specific to that cell type or if the responses also occurred in lacrimal cells.

The NO donor selected was NOC-12 to allow continuity of results between data sets. This donor was also selected as it was relatively easy to use and produced good results in the mouse submandibular acinar cells. Both NO pathway inhibitors ODQ and Ryanodine were again used in conjunction with NOC-12. The only variation was that Ryanodine only experiments were not conducted in a number great enough to provide valid interpretable results but the few that were performed did produce a similar pattern of response to that observed in mouse and human submandibular acinar cells.

Results

Acute Experiments

The initial experiments were performed acutely using NOC-12 to show the effect of NO on ACh-evoked Ca^{2+} signal in mouse lacrimal acinar cells.

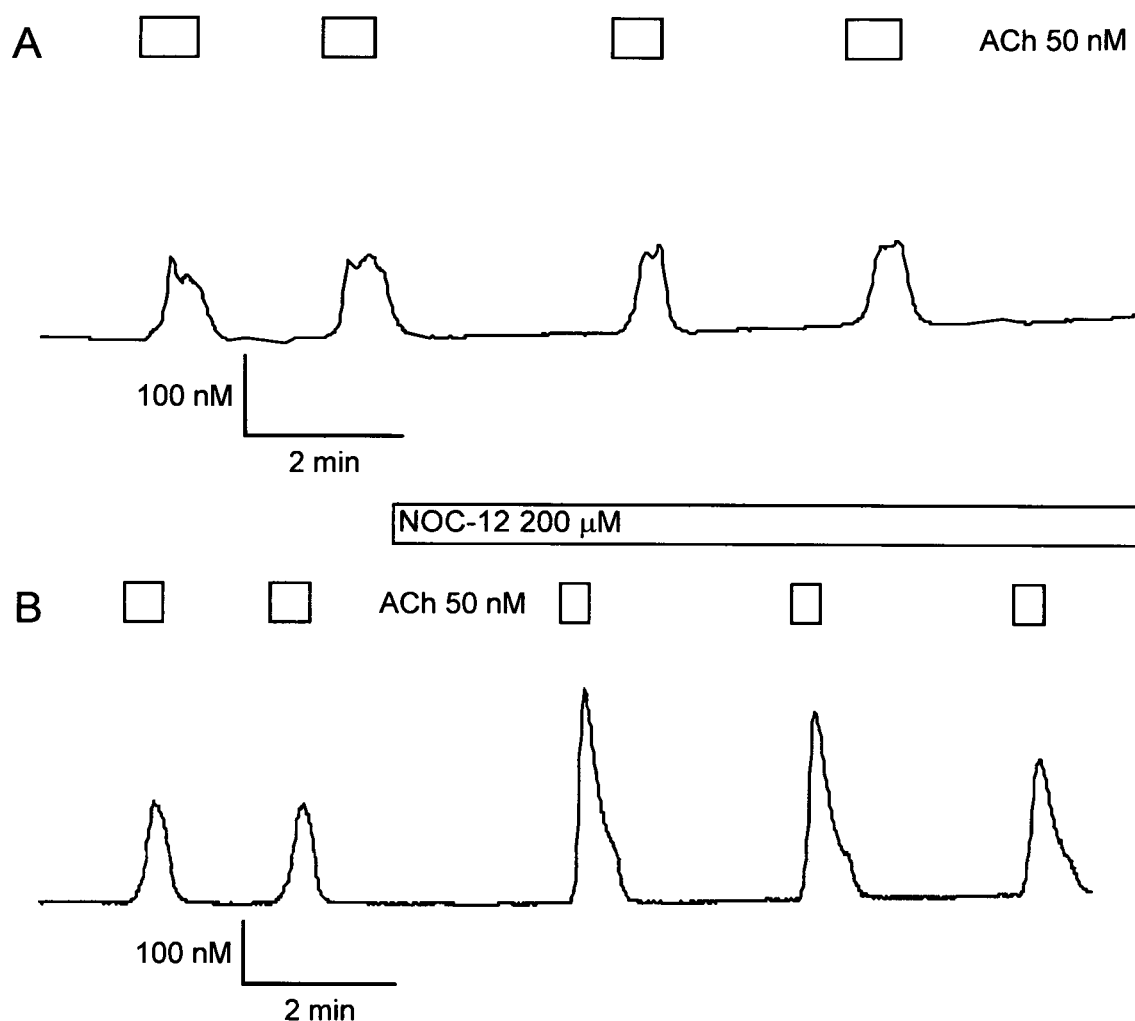
Table 5.1.1: Table of results for human submandibular acinar cells

Number of samples	Type of Response	Degree of Response (Mean \pm SE) as a Percentage	Time Taken to decrease to zero (where applicable)
n=7	Control	102.8 \pm 4.87%	N/A
n=9	NOC-12	178.1 \pm 28.89%	36
n=7	NOC-12 + ODQ	102.1 \pm 3.76%	36
n=9	NOC-12 + Ryanodine	104.1 \pm 5.97%	48

Figure 5.1.1 parts A and B shows representative traces which demonstrate the effect of the NO donor NOC-12 on the ACh-evoked increase in $[\text{Ca}^{2+}]_i$ in mouse lacrimal acinar cells. Trace A shows a series of control $[\text{Ca}^{2+}]_i$ responses to ACh (50nM) over the protocol defined time points. Trace B shows the $[\text{Ca}^{2+}]_i$ responses to ACh (50nM) in the presence of the NO donor NOC-12 (200 μ M) over similar protocol defined time points. Comparison of the $[\text{Ca}^{2+}]_i$ response of cells to ACh under control conditions (A) to that obtained following exposure to NO donor NOC-12 (B) at equivalent time points, shows that exposure of the mouse lacrimal acinar cells to NOC-12 significantly ($P<0.05$) increased the response to ACh from an average control response of 102.8 \pm 4.87% (n=7) to 178.1 \pm 28.89% (n=9) in the presence of NOC-12. The data in figure 5.1.1 parts A and B demonstrate NO induced amplification of the ACh-evoked increase in $[\text{Ca}^{2+}]_i$.

Figure 5.1.1

Change in $[Ca^{2+}]_i$ in response to 50nM ACh, illustrating how 200 μ M NOC-12 induced amplification of the $[Ca^{2+}]_i$ signal.



ACh (50nM) stimulated increased $[Ca^{2+}]_i$ measured in mouse lacrimal acinar cells maintained in primary tissue culture fluid for 24 hours (control) and 2 hours (NOC-12) respectively.

Trace A shows response to repeated stimulation with 50nM ACh only (see bar).

Trace B shows responses to repeated stimulation with 50nM ACh before and after application of the NO donor NOC-12 (see bar).

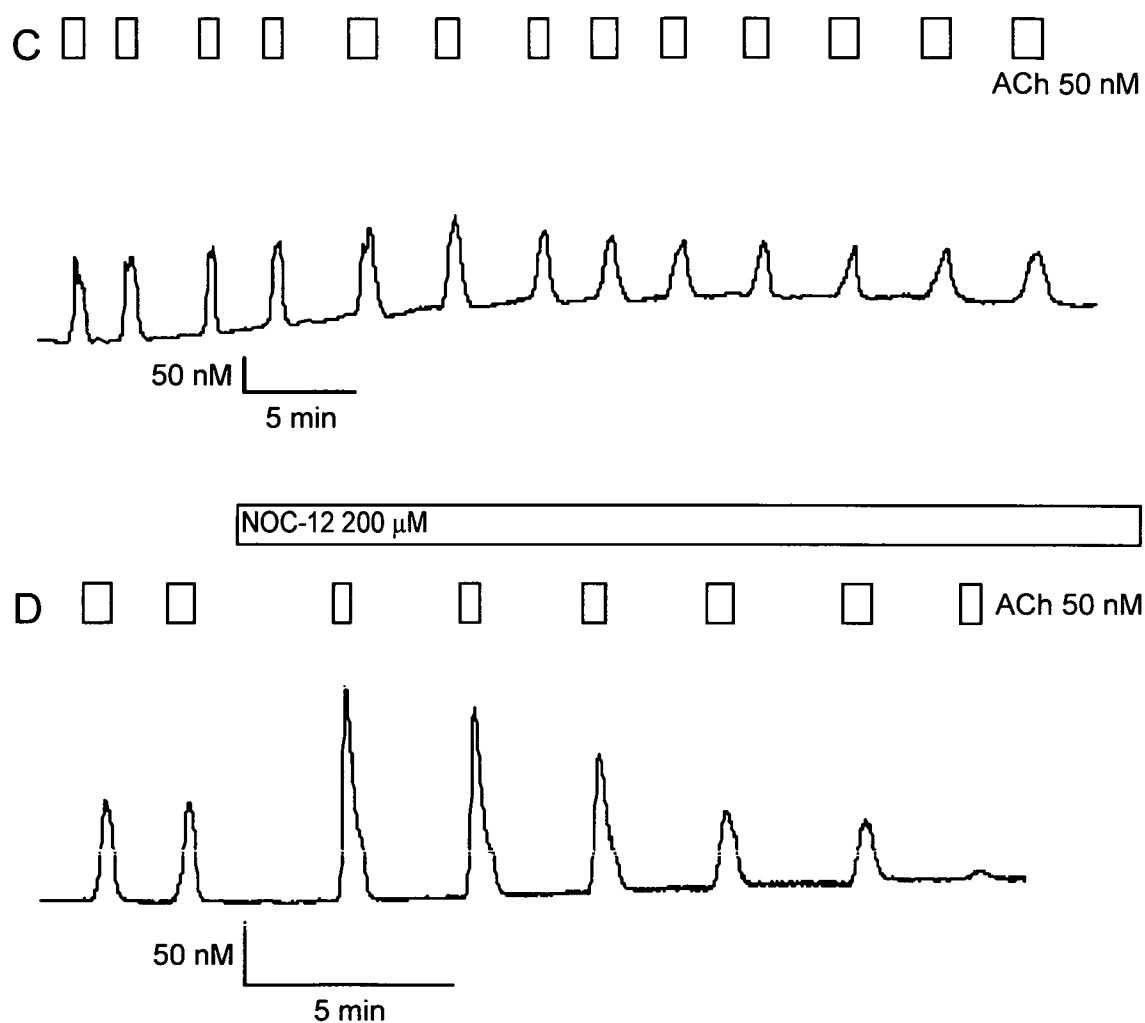
Chronic Experiments

Figure 5.1.1 parts C and D shows representative traces demonstrating the chronic effect of NO donor NOC-12 on the ACh-evoked increase in $[Ca^{2+}]_i$ in mouse lacrimal acinar cells. Trace C shows a prolonged series of control $[Ca^{2+}]_i$ responses to ACh (50nM) over the protocol defined time points, with cells maintaining the level of response. Trace D shows the $[Ca^{2+}]_i$ responses to ACh (50nM) in the presence of NO donor NOC-12 (200 μ M) over similar protocol defined time points. Comparison of the $[Ca^{2+}]_i$ response of cells to ACh under control conditions (C) to those obtained following exposure to NO donor NOC-12 (D) at equivalent time points, shows that exposure of the mouse lacrimal acinar cells to an NO donor NOC-12 increased the level of response to ACh. However, the data in figure 5.1.1 also show that over a prolonged period of time the cells become less sensitive to ACh and gradually stop responding to stimulus. At the end of the experimental time period the ACh stimulated increase in $[Ca^{2+}]_i$ in the presence of NOC-12 was significantly ($P < 0.001$) different from control.

The data in figure 5.1.1 parts A and B demonstrate NO induced amplification of the ACh-evoked increase in $[Ca^{2+}]_i$ and parts C and D demonstrate NO induced inhibition of the ACh-evoked increase in $[Ca^{2+}]_i$.

Figure 5.1.1

Change in $[Ca^{2+}]_i$ in response to 50nM ACh, illustrating how 200 μ M NOC-12 induced amplification and inhibition of the $[Ca^{2+}]_i$ signal.



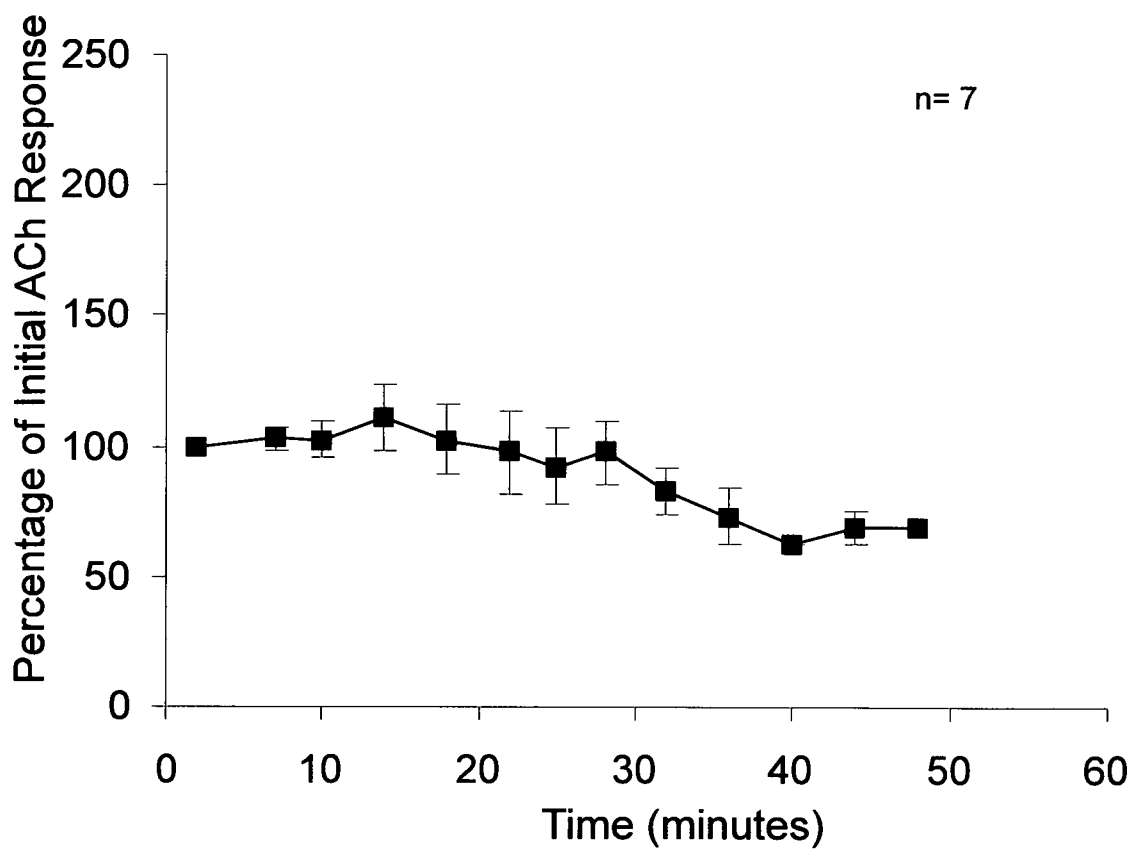
ACh (50nM) stimulated increased $[Ca^{2+}]_i$ measured in mouse lacrimal acinar cells maintained in primary tissue culture fluid for 24 hours and 2 hours respectively.

Trace C shows response to repeated stimulation with 50nM ACh only (see bar).

Trace D shows responses to repeated stimulation with 50nM ACh before and after application of the NO donor NOC-12 (see bar).

The data in figures 5.1.2 and 5.1.3 show the cumulative average responses achieved under control conditions and those achieved using the NO donor NOC-12 and allow direct comparison between control and NO donor affected conditions. Upon review of the cumulative data in figure 5.1.3 the chronic pattern of response of NO is clearly observable. The data presented in figure 5.1.4 allows direct comparison between control and experimental conditions and shows the variation in response pattern.

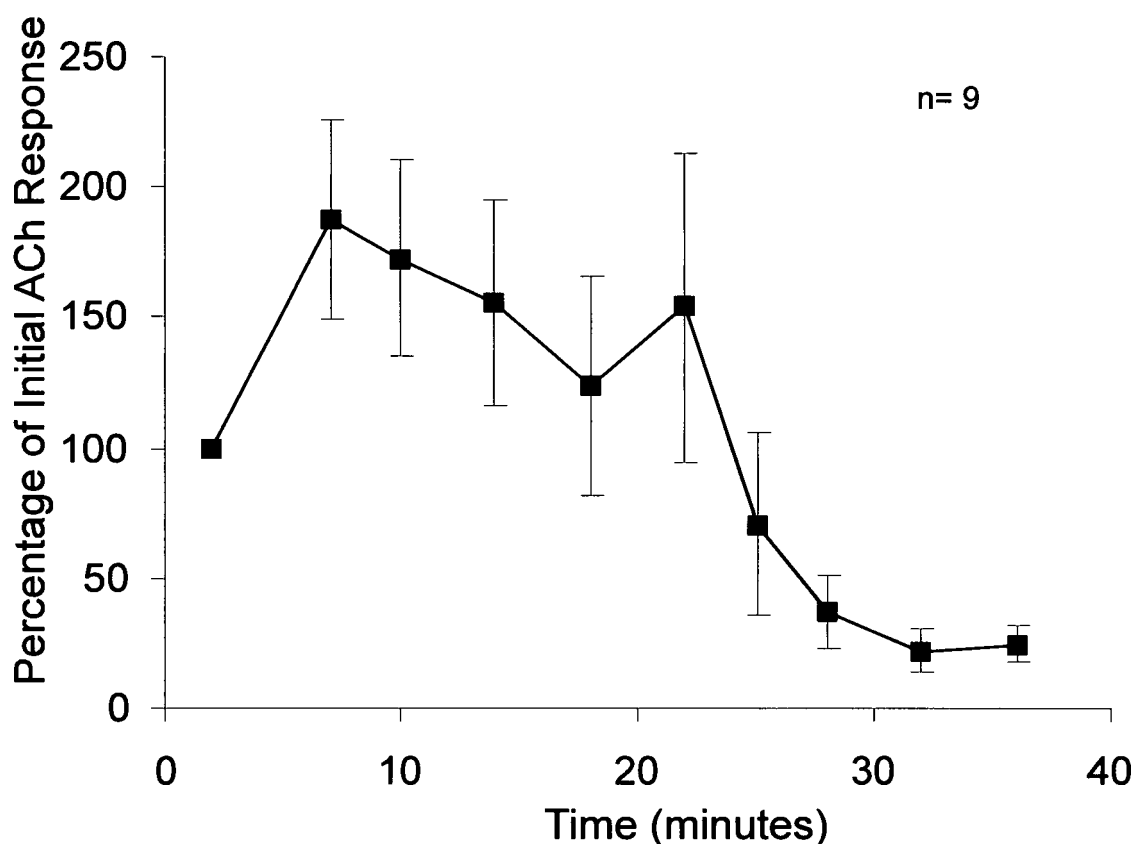
Figure 5.1.2
Change in $[Ca^{2+}]_i$ in response to 50nM ACh did not diminish with repeated application over the experimental time period.



Time course showing cumulative data for 50nM ACh in mouse lacrimal acinar cells. The data show the series of experimental time points where responses to 50nM ACh occurred. These data show the standard response of mouse lacrimal acinar cells to 50nM ACh under control conditions.

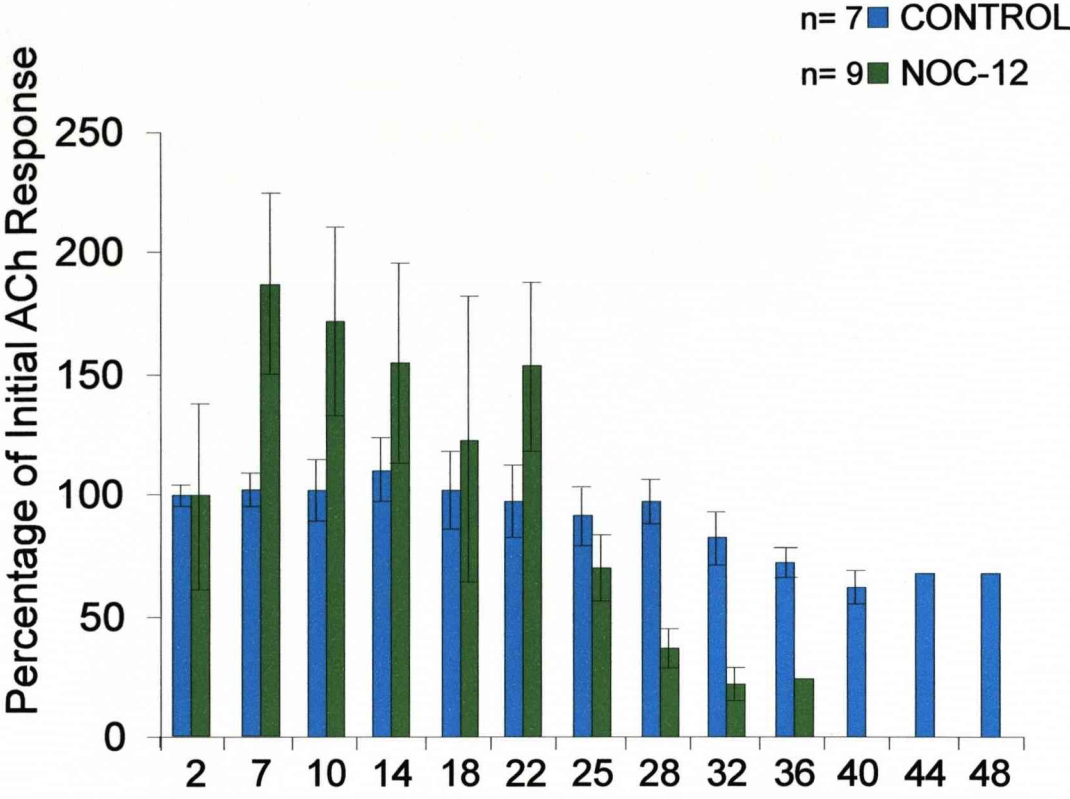
Figure 5.1.3

Change in $[Ca^{2+}]_i$ in response to 50nM ACh in the presence of 200 μ M NOC-12 initially increases but then gradually decreases with repeated application over the experimental time period.



Time course showing cumulative data for 50nM ACh in the presence of 200 μ M NOC-12 in mouse lacrimal acinar cells. The data show the series of experimental time points where responses to 50nM ACh in the presence of 200 μ M NOC-12 occurred.

Figure 5.1.4
Change in $[Ca^{2+}]_i$ signal in response to 50nM ACh and 50nM ACh in the presence of 200 μ M NOC-12 respectively over the experimental time period.



Bar chart showing cumulative data for 50nM ACh control (end point 48 minutes), 200 μ M NOC-12 (end point 36 minutes) in mouse lacrimal acinar cells.

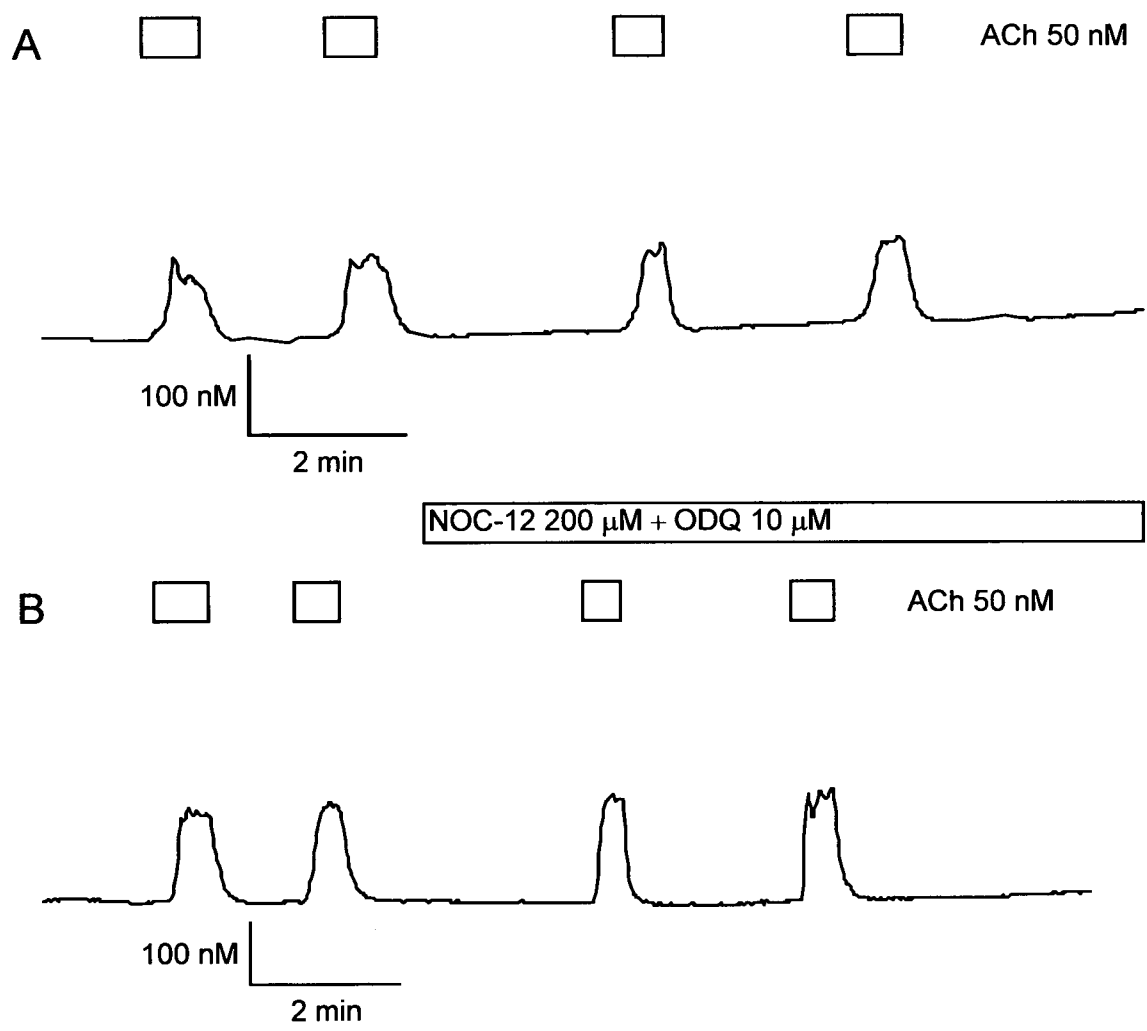
Inhibitor - ODQ

Upon completion of the NOC-12 experiments and the observed inhibition induced under chronic conditions the mode of action of NO had to be determined in this alternative cell type. As discussed previously, (Chapter 1 Introduction 1.2 nitric oxide section) NO is considered to act through the cADPr pathway. To investigate this hypothesis the two inhibitors of this pathway, ODQ and Ryanodine, were again used. The use of both NO pathway inhibitors also allowed direct comparison with the results obtained from the other two cell types.

Figure 5.1.5 parts A and B shows representative traces demonstrating the affect of sGC inhibitor ODQ on the affect of the NO donor NOC-12 on the ACh-evoked increase in $[Ca^{2+}]_i$ in mouse lacrimal acinar cells. Trace A shows a series of $[Ca^{2+}]_i$ responses to ACh (50nM) only. Trace B shows the $[Ca^{2+}]_i$ responses to ACh (50nM) in the presence of NO donor NOC-12 (200 μ M) and ODQ (10 μ M) over the same protocol defined time points. Comparison of the $[Ca^{2+}]_i$ responses in figures A and B, shows that exposure of the mouse lacrimal acinar cells to NO in the presence of sGC inhibitor ODQ removed the significant increase in response to ACh observed previously from an average NOC-12 only response of $178.1 \pm 28.89\%$ (n=9) to $102.1 \pm 3.76\%$ (n=7) for NOC-12 in the presence of ODQ. The data in figure 5.1.5 parts A and B demonstrate significant ($P < 0.05$) inhibition of NO induced amplification of the ACh-evoked increase in $[Ca^{2+}]_i$ by the sGC inhibitor ODQ.

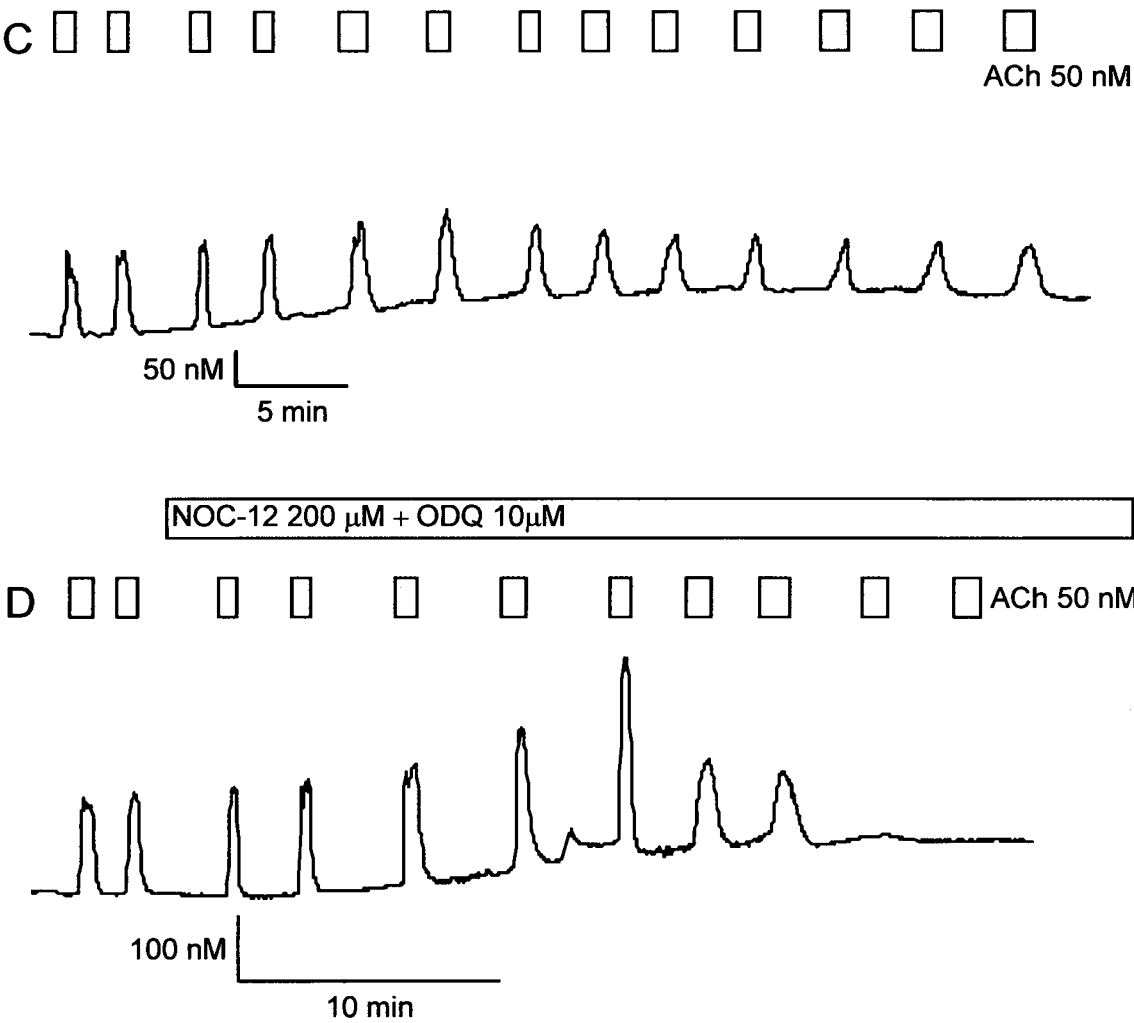
However, more prolonged experiments were required to demonstrate what effect inhibitors of the cADPr pathway would have on the de-sensitisation of acinar cells to ACh induced previously by the NO donor NOC-12.

Figure 5.1.5
 Change in $[Ca^{2+}]_i$ in response to 50nM ACh and 50nM ACh in the presence of 200 μ M NOC-12 in the presence of 10 μ M ODQ acutely.



ACh (50 nM) stimulated increased $[Ca^{2+}]_i$ measured in mouse lacrimal acinar cells maintained in primary tissue culture fluid for 24 (control) and 48hours NOC-12/ODQ) respectively .
 Trace A shows responses to repeated stimulation with 50nM ACh only (see bar).
 Trace B shows responses to repeated stimulation with 50nM ACh before and after application of the NO donor NOC-12 and NO pathway inhibitor ODQ (see bar).

Figure 5.1.5
 Change in $[Ca^{2+}]_i$ in response to 50nM ACh and 50nM ACh in the presence of 200 μ M NOC-12 in the presence of 10 μ M ODQ chronically

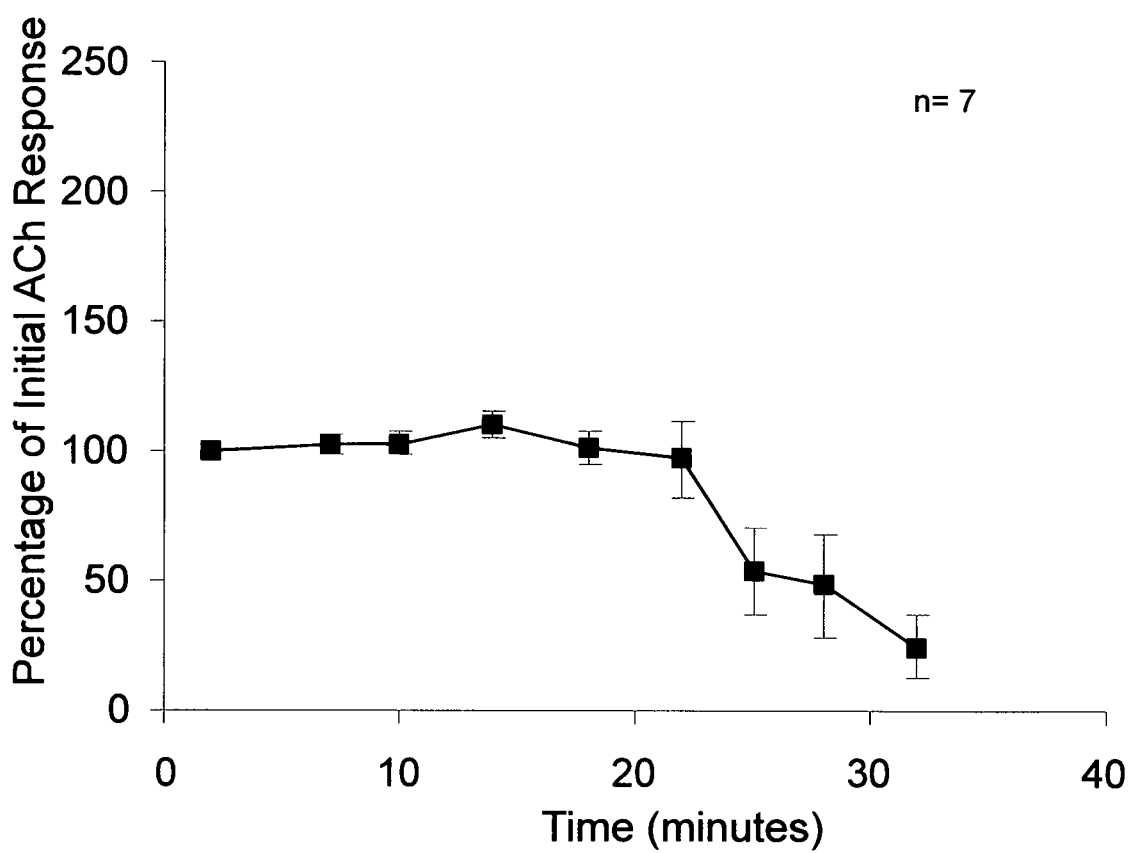


ACh (50 nM) stimulated increased $[Ca^{2+}]_i$ measured in mouse lacrimal acinar cells maintained in primary tissue culture fluid for 24 hours. Trace C shows responses to repeated stimulation with 50nM ACh only (see bar). Trace D shows responses to repeated stimulation with 50nM Ach before and after application of the NO donor NOC-12 and NO inhibitor ODQ(see bar).

Figure 5.1.5 parts C and D shows representative traces demonstrating the chronic effect of ODQ on the effect of the NO donor NOC-12 on the ACh-evoked increase in $[Ca^{2+}]_i$ in mouse lacrimal acinar cells. Trace C shows a prolonged series of $[Ca^{2+}]_i$ responses to ACh (50nM) only over the protocol defined time points. Trace D shows the $[Ca^{2+}]_i$ responses to ACh (50nM) in the presence of NO donor NOC-12 (200 μ M) and also sGC inhibitor ODQ (10 μ M) over the same protocol defined time points. Comparison of traces C and D shows that exposure of the mouse lacrimal acinar cells to the NO donor NOC-12 in the presence of sGC inhibitor ODQ removed the significant increase observed with the NO donor NOC-12 only. However, the more prolonged experiment shows that the cells still become de-sensitised to ACh in the presence of ODQ. At 36 minutes the ACh stimulated increase in $[Ca^{2+}]_i$ response in the presence of NOC-12 and ODQ was not significantly different from zero.

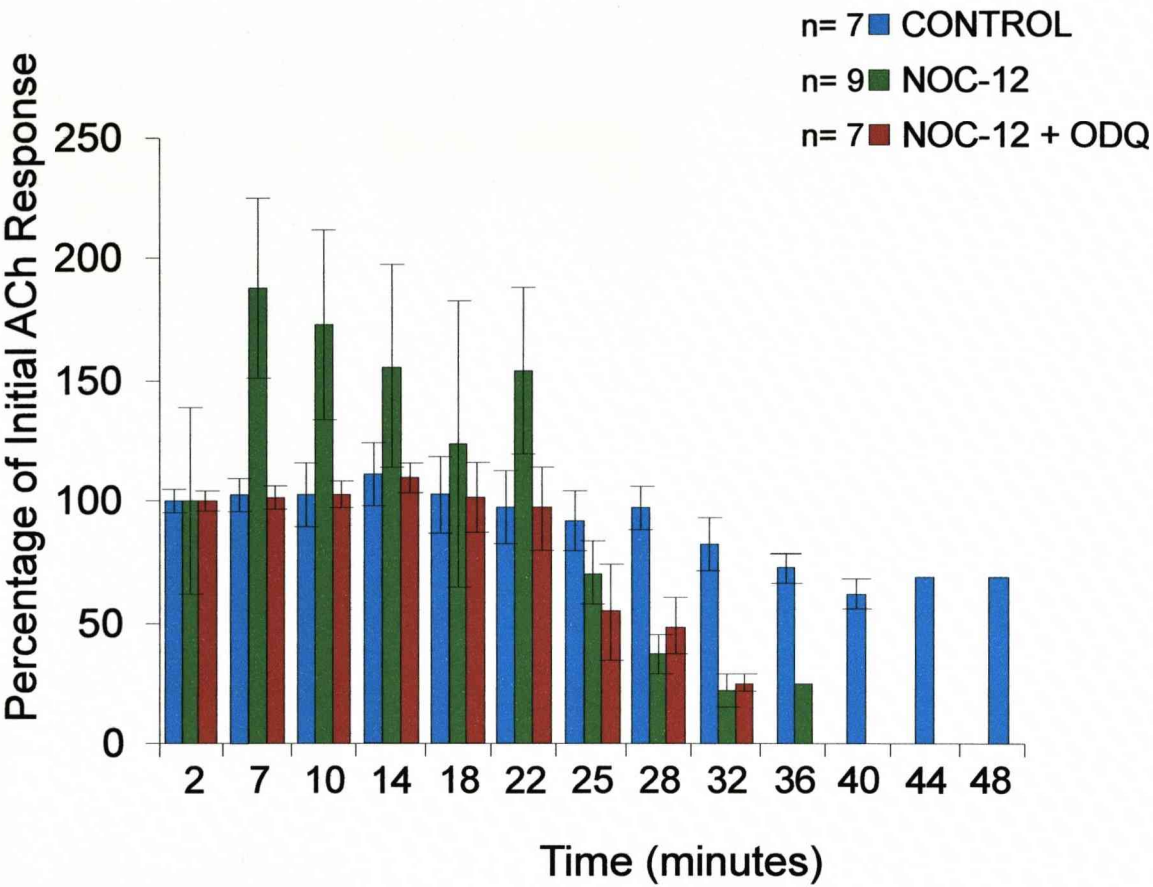
The data in figure 5.1.6 show the cumulative average responses achieved using the NO donor NOC-12 in the presence of the cADPr pathway inhibitor ODQ. Upon observation of the average data presented in figure 5.1.6 the chronic pattern of response is clearly observable. The average data in figure 5.1.7 shows all responses represented as a bar chart to allow direct comparison between ACh induced $[Ca^{2+}]_i$ signal results obtained under control conditions, under NOC-12 only conditions and those obtained using NOC-12 in the presence of ODQ and demonstrates the clear chronic pattern of response in the absence or presence of ODQ. However, the presence of ODQ does not appear to enhance the effect of NOC-12 as was observed with the human and mouse submandibular acinar cells but this may simply be because the lacrimal acinar cells are more sensitive to NO in the first instance as they had the most rapid desensitisation rate to NOC-12.

Figure 5.1.6
Change in $[Ca^{2+}]_i$ in response to 50nM ACh in the presence of 200 μ M NOC-12 and 10 μ M ODQ gradually decreases with repeated application over the experimental time period.



Time course showing cumulative data for 50nM ACh in the presence of 200 μ M NOC-12 and 10 μ M ODQ in mouse lacrimal acinar cells. The data show the series of experimental time points where responses to 50nM ACh in the presence of 200 μ M NOC-12 and 10 μ M ODQ occurred.

Figure 5.1.7
 Change in $[Ca^{2+}]_i$ signal in response to 50nM ACh and 50nM ACh in the presence of 200 μ M NOC-12 and 200 μ M NOC-12 with 10 μ M ODQ respectively over the experimental time period.



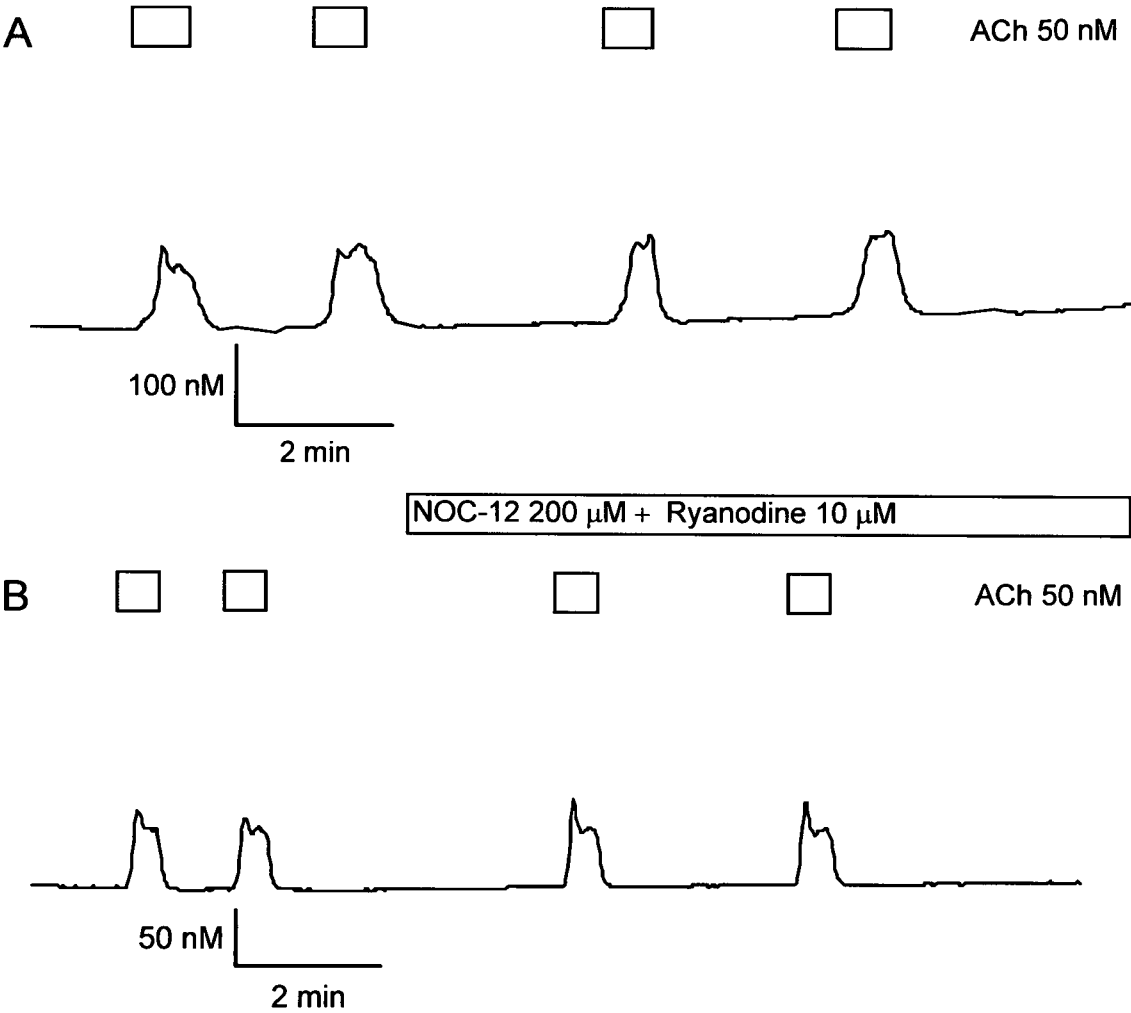
Bar chart showing cumulative data for 50nMACh control (end point 48 minutes), 100 μ M NOC-12 (end point 36 minutes) and 200 μ M NOC-12 with 10 μ M ODQ (end point 36 minutes) in mouse lacrimal acinar cells.

Inhibitor - Ryanodine

As with the submandibular acinar cells following the work conducted with ODQ the second cADPr pathway inhibitor Ryanodine was again used to try and determine the mode of action of NO.

Figure 5.1.8 parts A and B shows representative traces demonstrating the effect of the Ryanodine receptor inhibitor Ryanodine on the effect of NO donor NOC-12 on the ACh-evoked increase in $[Ca^{2+}]_i$ in mouse lacrimal acinar cells. Trace A shows a series of control $[Ca^{2+}]_i$ responses to ACh (50nM) only over the protocol defined time points. Trace B shows the $[Ca^{2+}]_i$ responses to ACh in the presence of both NO donor NOC-12 (200 μ M) and Ryanodine (10 μ M) over the same protocol defined time points. By comparing the $[Ca^{2+}]_i$ response of cells to ACh under control conditions (A) to those obtained following combined exposure to NO donor NOC-12 and Ryanodine receptor Ryanodine (B) at equivalent time points, the data show that exposure of the mouse lacrimal acinar cells to an NO donor NOC-12 during exposure to Ryanodine inhibitor Ryanodine significantly ($P < 0.05$) removes the previously observed increased in response to ACh from an average NOC-12 only response of $178.1 \pm 28.89\%$ ($n=9$) to $104.1 \pm 5.97\%$ ($n=9$) to NOC-12 in the presence of Ryanodine. The two traces are very similar and the cumulative data (figure 5.1.9) shows that the use of Ryanodine with NOC-12 reduces the level of response to one which is equal to the average control response of $102.8 \pm 4.87\%$ ($n=7$) and shows no significant variation between the average response of these two data sets.

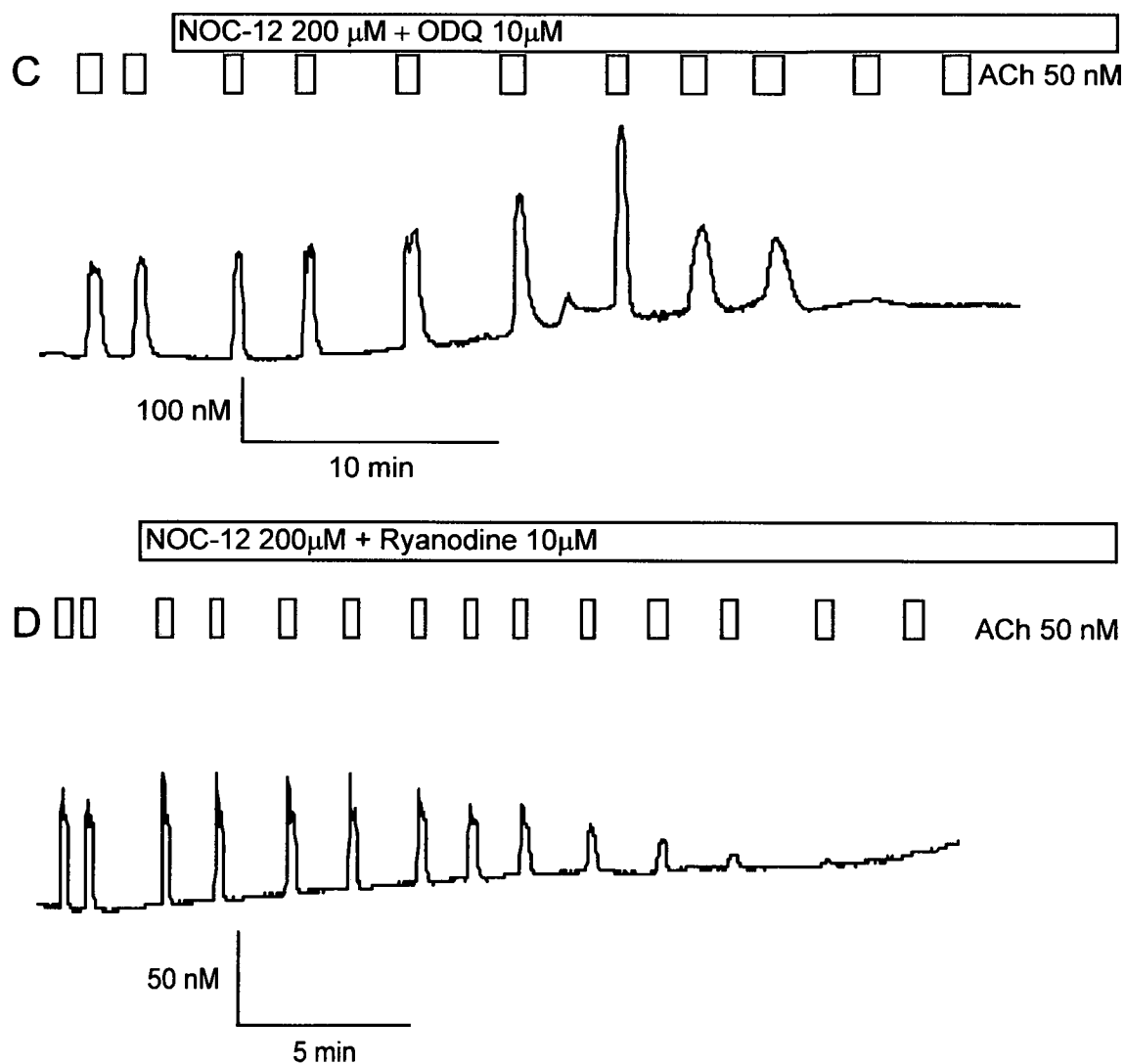
Figure 5.1.8
Change in $[Ca^{2+}]_i$ in response to 50nM ACh and 50nM ACh
the presence of 200 μ M NOC-12 in the presence of 10 μ M
Ryanodine acutely.



ACh (50 nM) stimulated increased $[Ca^{2+}]_i$ measured in mouse lacrimal acinar cells maintained in primary tissue culture fluid for 24 hours.
Trace A shows responses to repeated stimulation with 50nM ACh only (see bar).
Trace B shows responses to repeated stimulation with 50nM ACh before and after application of the NO donor NOC-12 and NO pathway inhibitor Ryanodine (see bar).

Figure 5.1.8

Change in $[Ca^{2+}]_i$ in response to 50nM ACh in the presence of 200 μ M NOC-12 in the presence of 10 μ M ODQ and 10 μ M Ryanodine respectively over the experimental time period.



ACh (50 nM) stimulated increased $[Ca^{2+}]_i$ measured in mouse lacrimal acinar cells maintained in primary tissue culture fluid for 24 hours.

Trace C shows responses to repeated stimulation with 50nM ACh before and after application of NO donor NOC-12 and NO pathway inhibitor ODQ (see bar).

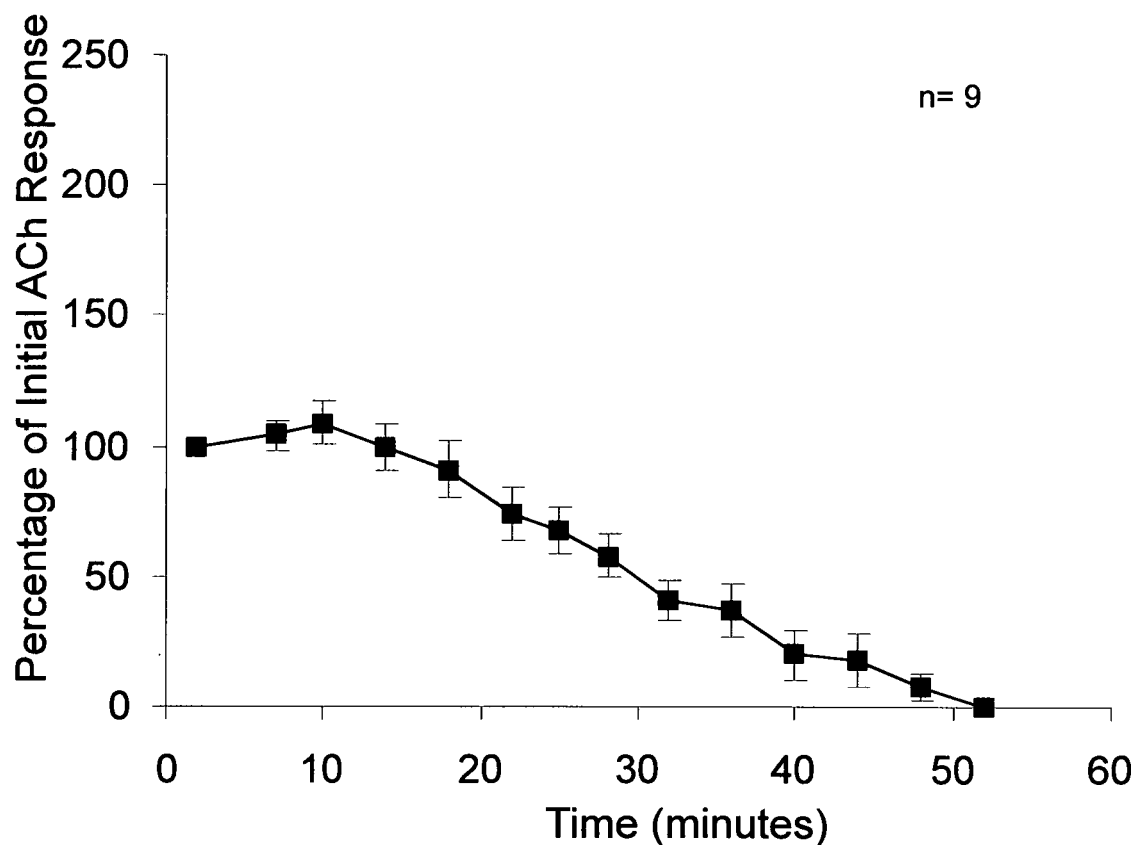
Trace D shows responses to repeated stimulation with 50nM ACh before and after application of the NO donor NOC-12 and NO pathway inhibitor Ryanodine (see bar).

Figure 5.1.8 parts C and D show representative traces demonstrating the chronic effect of NOC-12 in the presence of ODQ or Ryanodine respectively, on the ACh-evoked increase in $[Ca^{2+}]_i$ in mouse lacrimal acinar cells. Trace C shows a series of $[Ca^{2+}]_i$ responses to ACh (50nM) in the presence of both NOC-12 (200 μ M) and ODQ (10 μ M) over the protocol defined time points. Trace D shows the $[Ca^{2+}]_i$ responses to ACh (50nM) in the presence of both NOC-12 (200 μ M) and Ryanodine (10 μ M) over the same protocol defined time points. By comparing the $[Ca^{2+}]_i$ response of cells to ACh under combined exposure to ODQ and NOC-12 conditions (C) to those obtained following combined exposure to NOC-12 and Ryanodine (D) at equivalent time points, we can show that exposure of the mouse lacrimal acinar cells to NOC-12 during exposure to either ODQ or Ryanodine removes the increase observed when NOC-12 only is used. However, the observed rundown in response and desensitisation of the cells to ACh still occurs in the presence of either ODQ or Ryanodine which could suggest that the hypofunction induced by NO occurs independent of the cADPr pathway.

At 48 minutes the ACh stimulated increase in $[Ca^{2+}]_i$ response in the presence of NOC-12 and Ryanodine was not significantly different from zero. When the average values of the chronic experiments for NOC-12 in the presence of ODQ or Ryanodine are compared there is very little variation in the response pattern. They are both significantly ($P < 0.01$) different compared to control but show no significant variation when compared to each other or when compared to NOC-12 only.

Figure 5.1.9

Change in $[Ca^{2+}]_i$ signal in response to 50nM ACh in the presence of 10 μ M Ryanodine and 200 μ M NOC-12 initially maintained but then rapidly decreases with repeated application over the experimental time period.

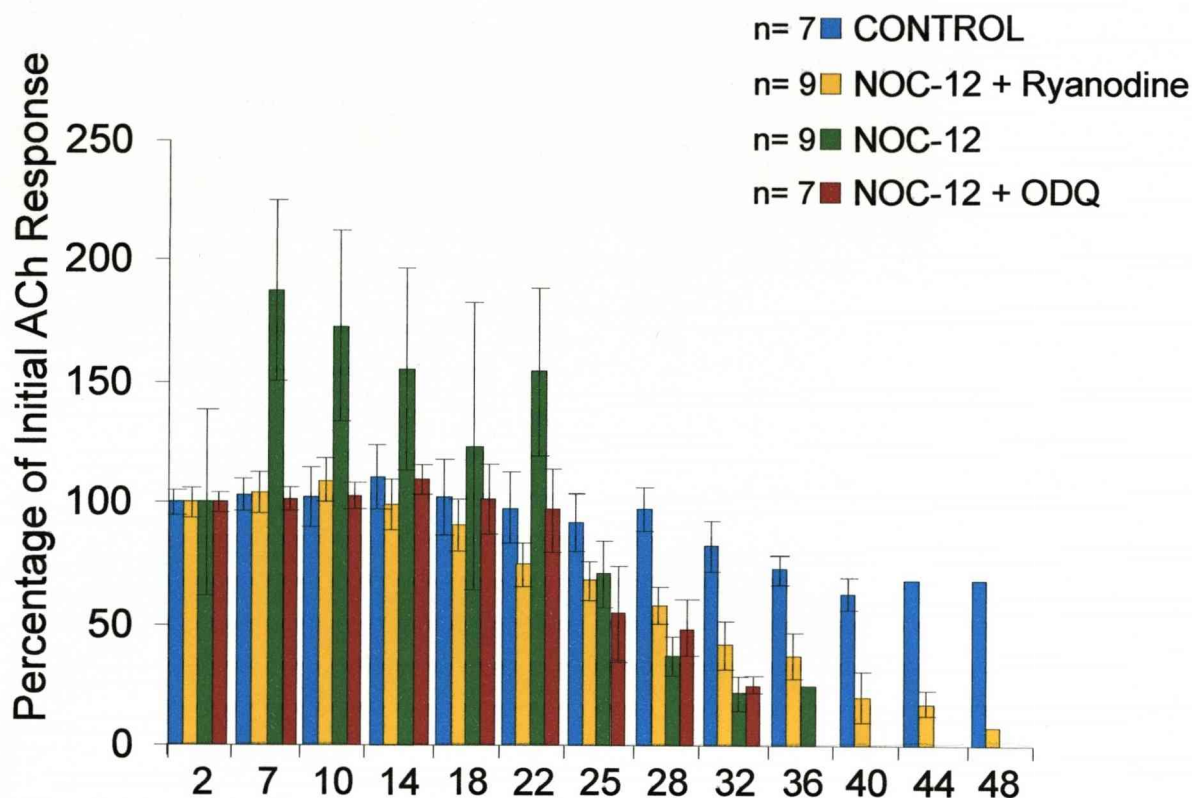


Time course showing cumulative data for 50nM ACh in the presence of 10 μ M Ryanodine and 200 μ M NOC-12 in mouse lacrimal acinar cells. The data show the series of experimental time points where responses to 50nM ACh in the presence of 10 μ M Ryanodine and 200 μ M NOC-12 occurred.

The data in figure 5.1.9 show the cumulative average responses achieved, using NOC-12 in the presence of Ryanodine. The cumulative data in figure 5.1.10 allows direct comparison between control conditions and those involving NOC-12 alone and NOC-12 in the presence of either Ryanodine or ODQ respectively. The key variations between the four data sets presented in figure 5.1.10 are the initial amplification observed when NOC-12 alone was used, the maintained level of response under control conditions. However, the pattern of reduction and gradual hypo-function of the cells was relatively equal under chronic conditions and there was little variation in the rundown between NOC-12 only and NOC-12 in the presence of either Ryanodine or ODQ.

Figure 5.1.10

Change in $[Ca^{2+}]_i$ signal in response to 50nM ACh and 50nM ACh in the presence of 200 μ M NOC-12 and 200 μ M NOC-12 with either 10 μ M Ryanodine or 10 μ M ODQ respectively over the experimental time period.



Bar chart showing cumulative data for 50nM ACh control (end point 48 minutes), 200 μ M NOC-12 (end point 36 minutes) and 200 μ M NOC-12 with 10 μ M Ryanodine (end point 48 minutes) in mouse lacrimal acinar cells.

Conclusions

The data in figure 5.1.1 parts A and B demonstrate that the use of the NO donor NOC-12 induced amplification of the ACh-evoked increase in $[Ca^{2+}]_i$, so this preliminary data suggests NO would induce hyper-function of response. This data is in opposition to NO being implicated in the pathogenesis of salivary gland hypo-function in SjS as discussed previously (Chapter 1 Introduction 1.2 Nitric oxide section). However, these initial experiments only determine the acute effect of NO in lacrimal acinar cells. In the salivary glands of SjS patients the acinar cells would be exposed to NO much more long-term so these experiments are less relevant.

Comparison of data in figure 5.1.1 parts C and D show that although the use of the NO donor NOC-12 did initially induce amplification of the ACh-evoked increase in $[Ca^{2+}]_i$, it did ultimately induce inhibition of the ACh-evoked increase in $[Ca^{2+}]_i$ when compared to control. These chronic experiments would be more relevant to the NO exposure in SjS patients and would give a more accurate insight into the effect on acinar cell response to ACh following prolonged exposure to NO.

As described previously (Chapter 1 Introduction 1.2 nitric oxide section), NO was selected for investigation as a possible cause of salivary hypo-function in SjS. These data would suggest that NO does have the ability to induce acinar hypofunction but only after prolonged periods of time. Therefore NO has the capacity to induce healthy acinar cells to behave like SjS acinar cells. The chronic experiments are therefore compatible with the hypothesised role of NO in SjS.

The average data observed with NOC-12 in the presence of ODQ acutely was comparable to control ACh only conditions and showed no significant variation in

results. The acute amplification is prevented by the addition of sGC inhibitor ODQ so the acute amplification activity of NO appears to be mediated through the cADPr pathway. The chronic data for NOC-12 and ODQ together is comparable to NOC-12 only and total inhibition of the response occurs at approximately the same time point as NOC-12 only. The chronic data therefore suggests that inhibition of the response is occurring independently of the cADPr pathway.

So in spite of the presence of ODQ the NOC-12 induced inhibition still occurred over the duration of the experimental time period. The data in figure 5.1.5 part D show that over a prolonged period of time the cells still become less sensitive to ACh and finally stop responding to stimulus even in the presence of sGC inhibitor ODQ. Therefore the results suggest that the induced hypo-function may occur independently of the proposed NO pathway.

The average data observed with NOC-12 in the presence of Ryanodine acutely was comparable to control ACh only conditions and showed no significant variation in results. The presence of Ryanodine removed the induced amplification of the ACh-evoked increase in $[Ca^{2+}]_i$ which would suggest that the NO induced amplification is mediated through the cADPr pathway. However, the chronic data for NOC-12 and Ryanodine together show that Ryanodine did not prevent the NO induced inhibition of the ACh-evoked increase in $[Ca^{2+}]_i$ which would suggest that the NO induced inhibition is not mediated through the Ryanodine receptor and NO may induce hypofunction independently of the cADPr pathway..

The use of two cADPr pathway inhibitors provide better insight as to if and where NO functions within the pathway as ODQ prevents the initial step and Ryanodine blocks the Ryanodine receptor directly so the use of both inhibitors could greatly strengthen the NO/cADPr argument. Both inhibitors of the cADPr pathway remove the previously

observed amplification of the ACh-evoked increase in $[Ca^{2+}]_i$ induced by NOC-12. The desensitisation patterns observed with either ODQ or Ryanodine with NOC-12 respectively are highly similar to each other and both are similar to the inhibition induced by NOC-12 only. As with the mouse and human submandibular acinar cells the chronic results from both cADPr pathway inhibitors suggest that the hypofunction is independent of the cADPr pathway.

Figure 5.1.10 shows cumulative data which allows direct comparison between control conditions, NOC-12 only and NOC-12 in the presence of ODQ and Ryanodine respectively. The two main points of variation are the initial amplification observed when NOC-12 only was used and the response level maintained by ACh only. The rundown for all three sets of experimental data are relatively equal. Both inhibitors of the NO pathway were able to remove the NOC-12 induced amplification but neither had any effect on the rundown and the desensitisation of the acinar cells to ACh by NO.

In summary the lacrimal cells produced a set of response patterns similar to those observed previously with the human and mouse submandibular acinar cells. The NOC-12 induced amplification when acutely applied and desensitisation when chronically applied. Both inhibitors of the cADPr pathway inhibited the initial amplification but had no effect on the desensitisation induced by NO which once again suggested that the amplification was mediated through the cADPr pathway but that the desensitisation was most likely independent of the cADPr pathway. The results again suggest that NO has the ability to mediate acinar cell hypofunction and demonstrate that lacrimal cells respond in the same manner as submandibular cells.

Chapter Six

Results

Adenosine Tri-phosphate As a Stress signal inducer



UNIVERSITY OF
LIVERPOOL

Introduction

Following the experiments conducted with nitric oxide other factors which may be up-regulated under stress conditions were identified. Adenosine tri-phosphate (ATP) has been suggested to function as a stress signal and we wanted to determine how it might mediate a stress response. We observed responses to ATP in human and mouse submandibular acinar cells and also mouse lacrimal acinar cells.

We hypothesised that ATP would stimulate a pattern of response alternative to ACh which would be clearly visualised using Microfluorimetry techniques. However, we were unable to visualise any variation in response pattern which may suggest that either the variations induced by stimulations from either ACh or ATP occur much more subtly or that our rate of sampling was not great enough to identify any variations which may occur. Although we were unable to visualise variations in response pattern between ACh and ATP we did observe a degree of addition of response when ACh and ATP were used together and this varied from simply increasing the concentration of ACh which may suggest that ATP mobilises Ca^{2+} from stores which are unreceptive to ACh. This data was consistent with previous work conducted but we did not investigate this further.

Figure 6.1.1

3 separate traces showing the change in $[Ca^{2+}]_i$ signal in response to 50nM ACh and 100 μ M ATP stimulation respectively.

Trace A shows $[Ca^{2+}]_i$ response to two separate single stimulations by 50nM ACh and 100 μ M ATP respectively (see scale bar) measured in mouse submandibular acinar cells maintained in primary culture for 2 hours.

Trace B shows $[Ca^{2+}]_i$ response to 100 μ M ATP stimulation during constant 50nM ACh stimulation (see scale bar) measured in mouse submandibular acinar cells maintained in primary culture for 2 hours.

Trace C shows $[Ca^{2+}]_i$ response to 50nM ACh stimulation during constant 100 μ M ATP stimulation (see scale bar) measured in mouse submandibular acinar cells maintained in primary culture for 2 hours.

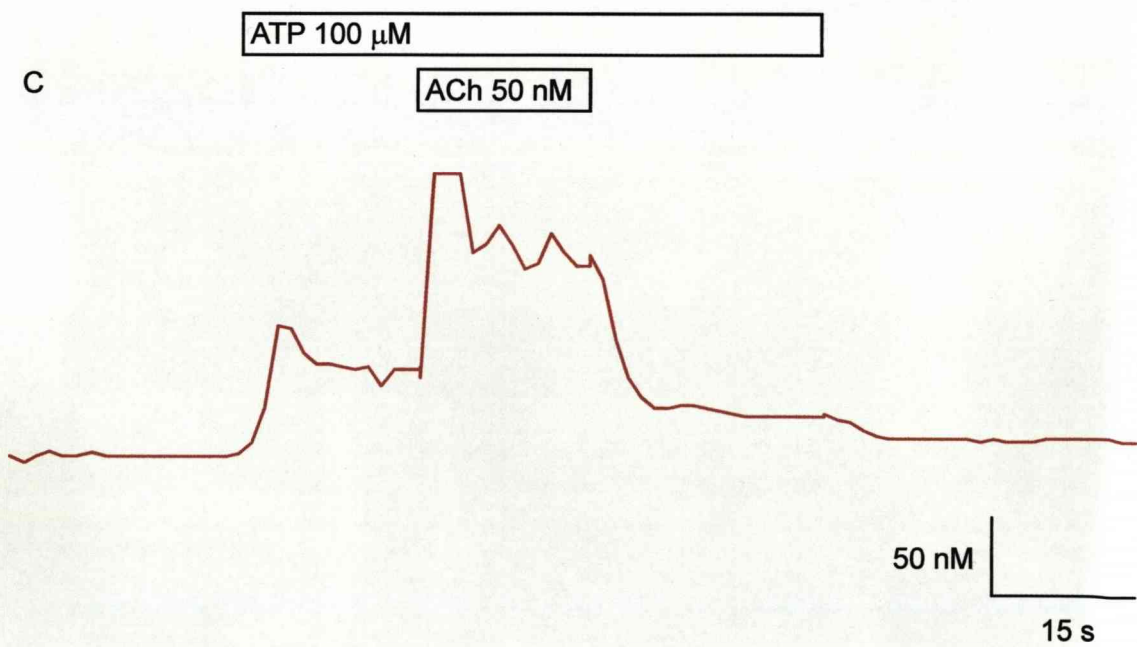
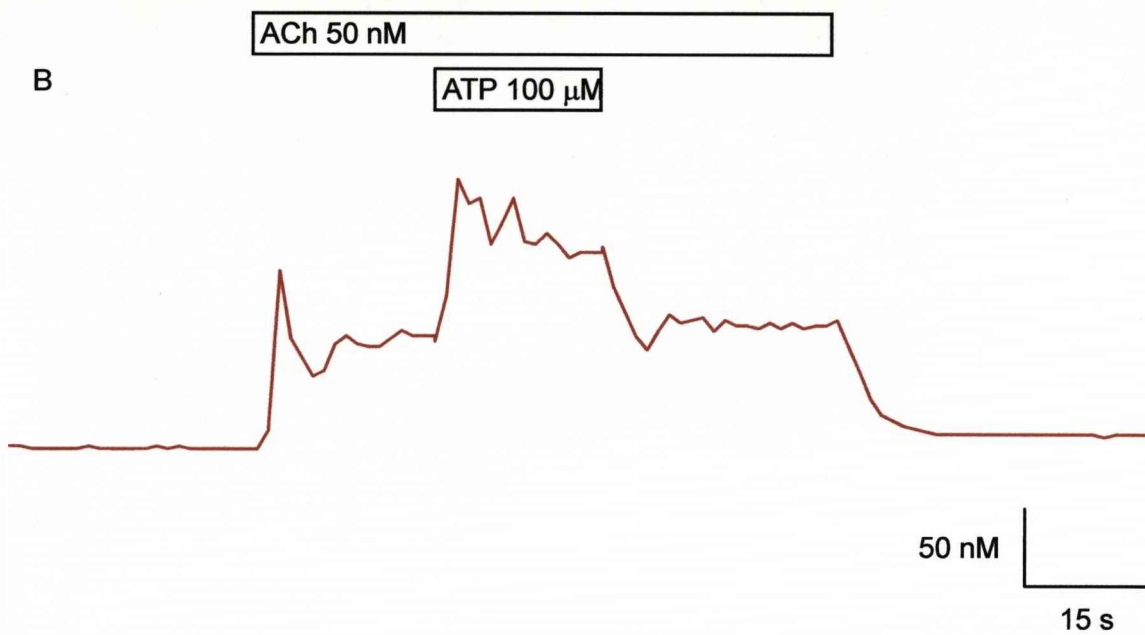
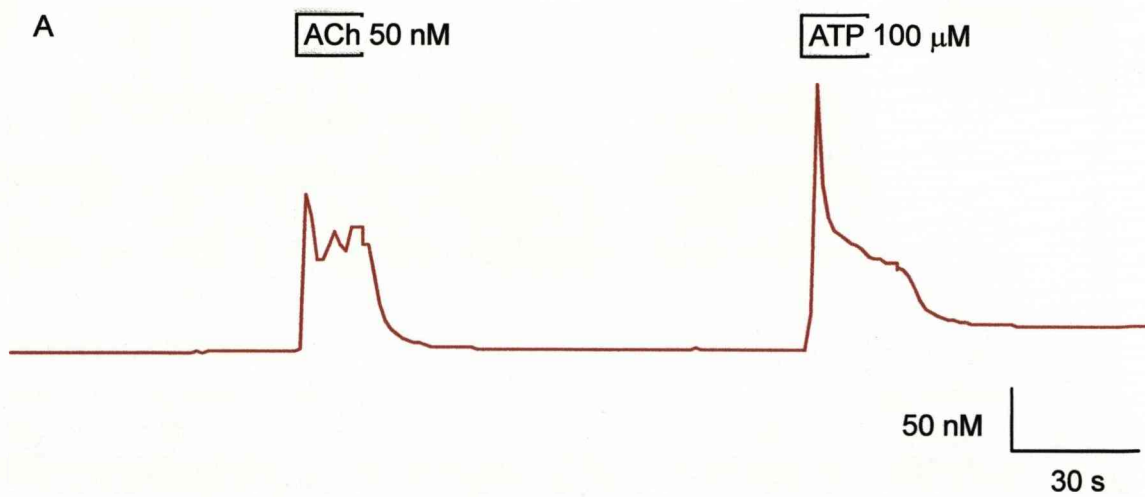


Figure 6.1.1 Part D: shows the average dose responses to 100μM, 250μM and 500μM ATP plus the average response to 500nM ACh in mouse submandibular acinar cells.

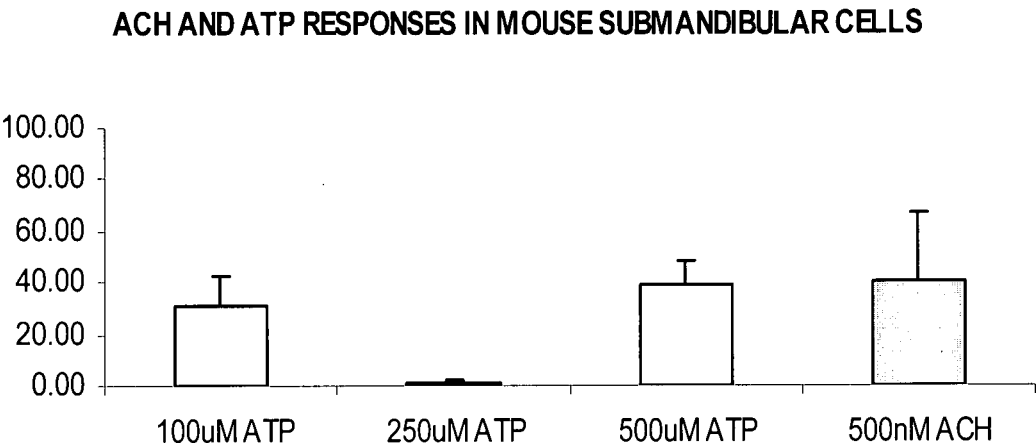


Figure 6.1.1 Part E: shows the average dose responses to 100μM, 250μM and 500μM ATP plus the average response to 500nM ACh in human submandibular acinar cells.

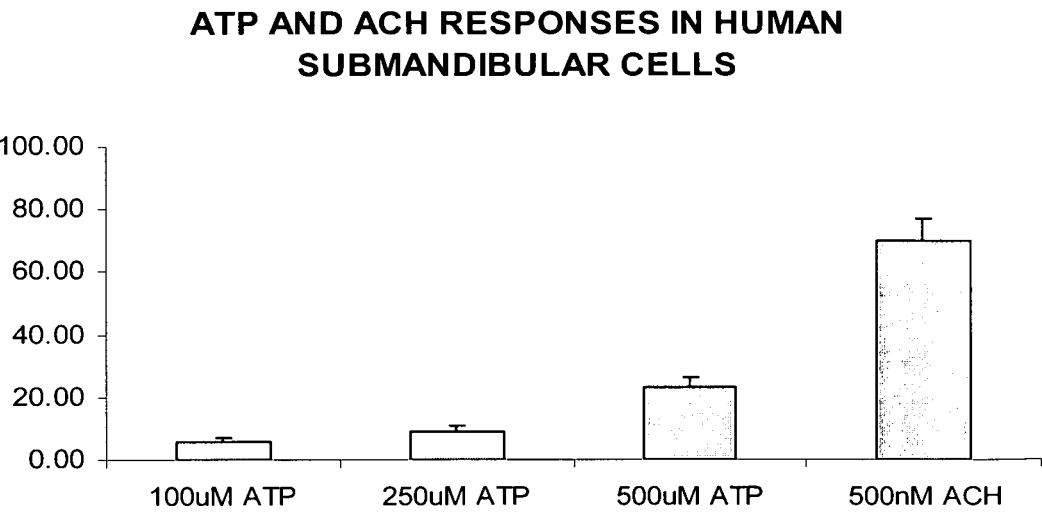


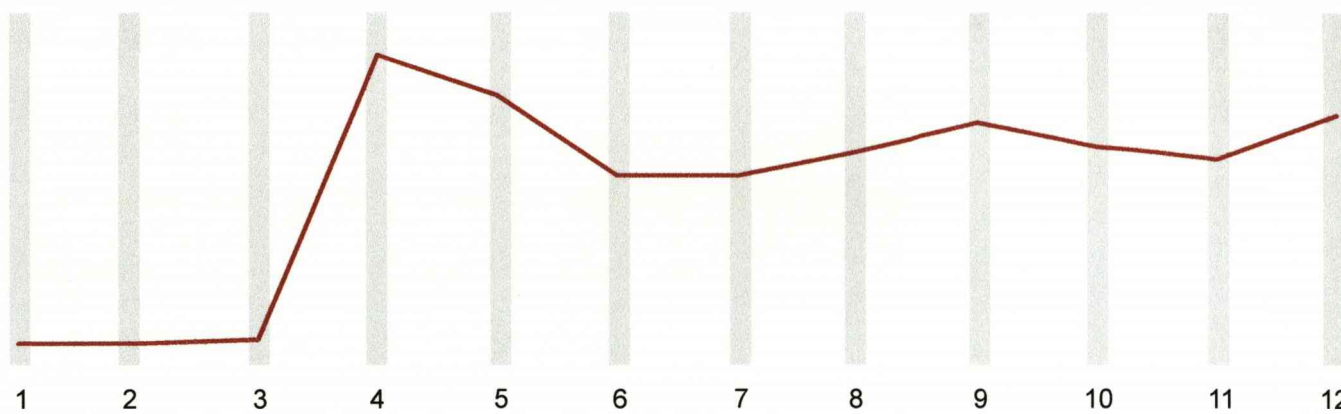
Figure 6.1.2

Change in $[Ca^{2+}]_i$ in response to 50nM ACh.

Part A shows the $[Ca^{2+}]_i$ signal in response to 50nM ACh stimulation as seen in the initial response in figure 6.1.1 trace A but expanded out to allow more clear observation of response pattern (see scale bar).

Part B shows a series of TIF images showing the actual acinar cell increased $[Ca^{2+}]_i$ response to 50nM ACh stimulation in real time, with each numbered TIF image equating exactly to the numbered vertical shaded lines on the trace shown in figure 6.1.2 part A.

A ACh 50 nM



10 % |
2.5 s

B

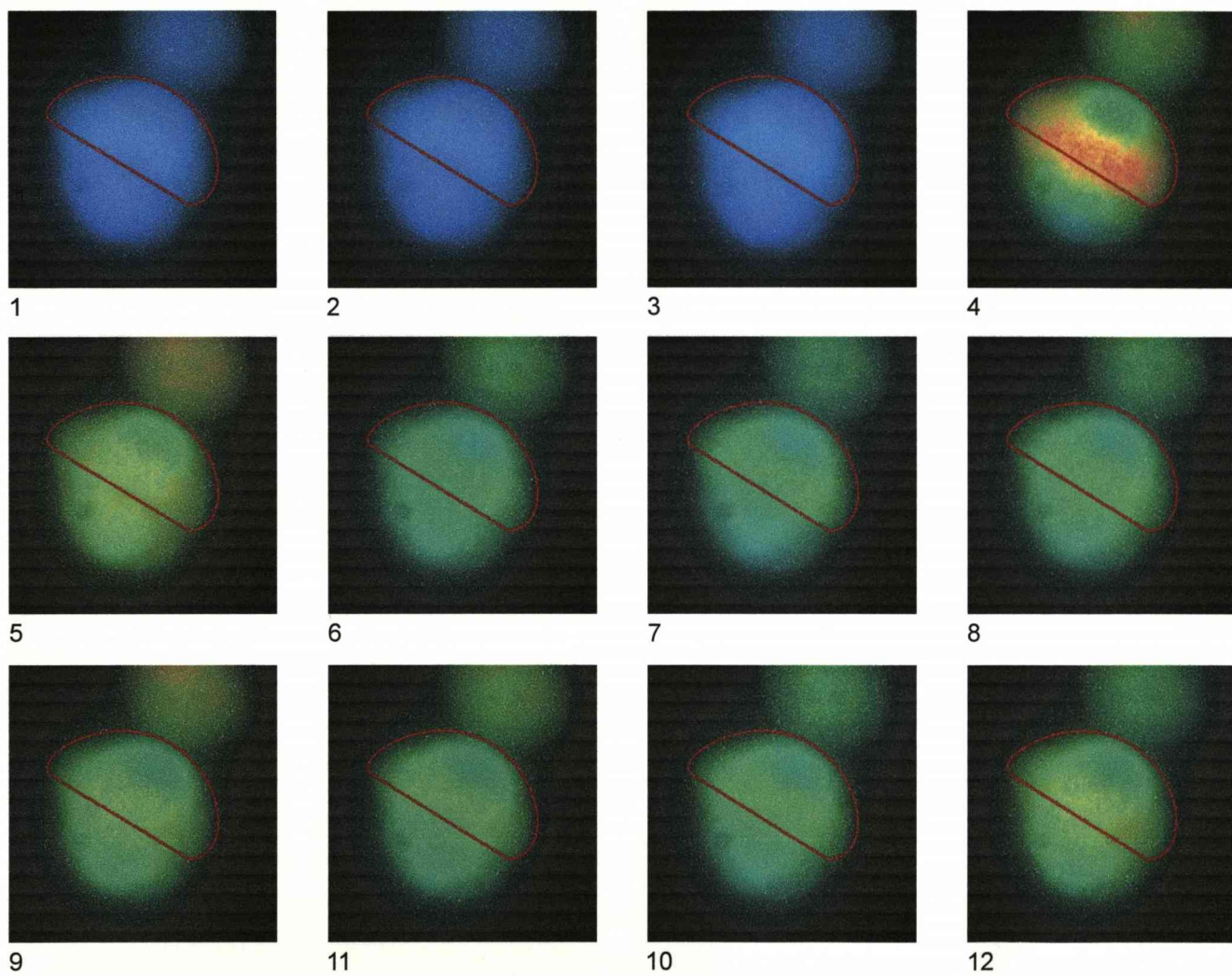


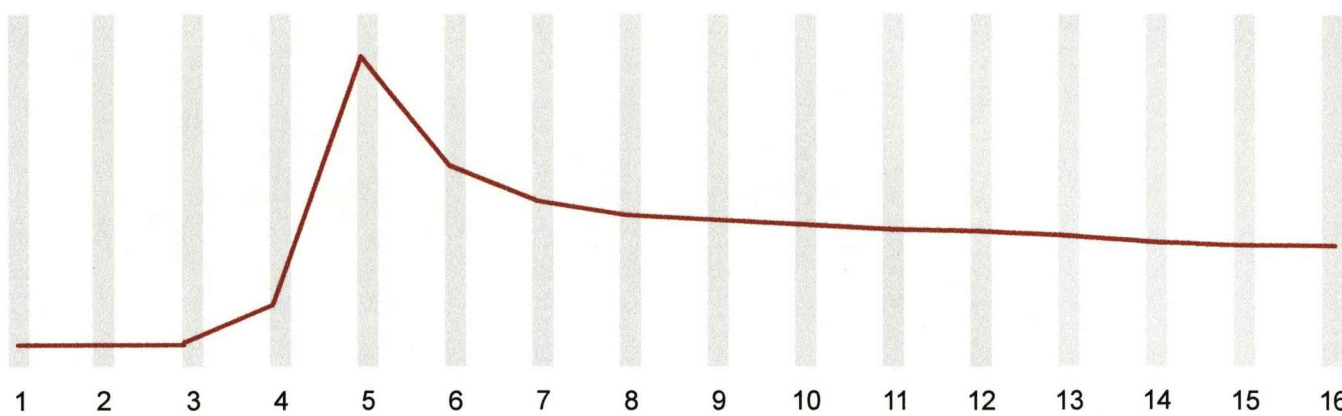
Figure 6.1.3

Change in $[Ca^{2+}]_i$ signal in response to 100 μ M ATP.

Part A shows the $[Ca^{2+}]_i$ signal in response to 100 μ M ATP stimulation as seen in the second response in figure 6.1.1 trace A expanded out to allow more clear observation of response pattern (see scale bar).

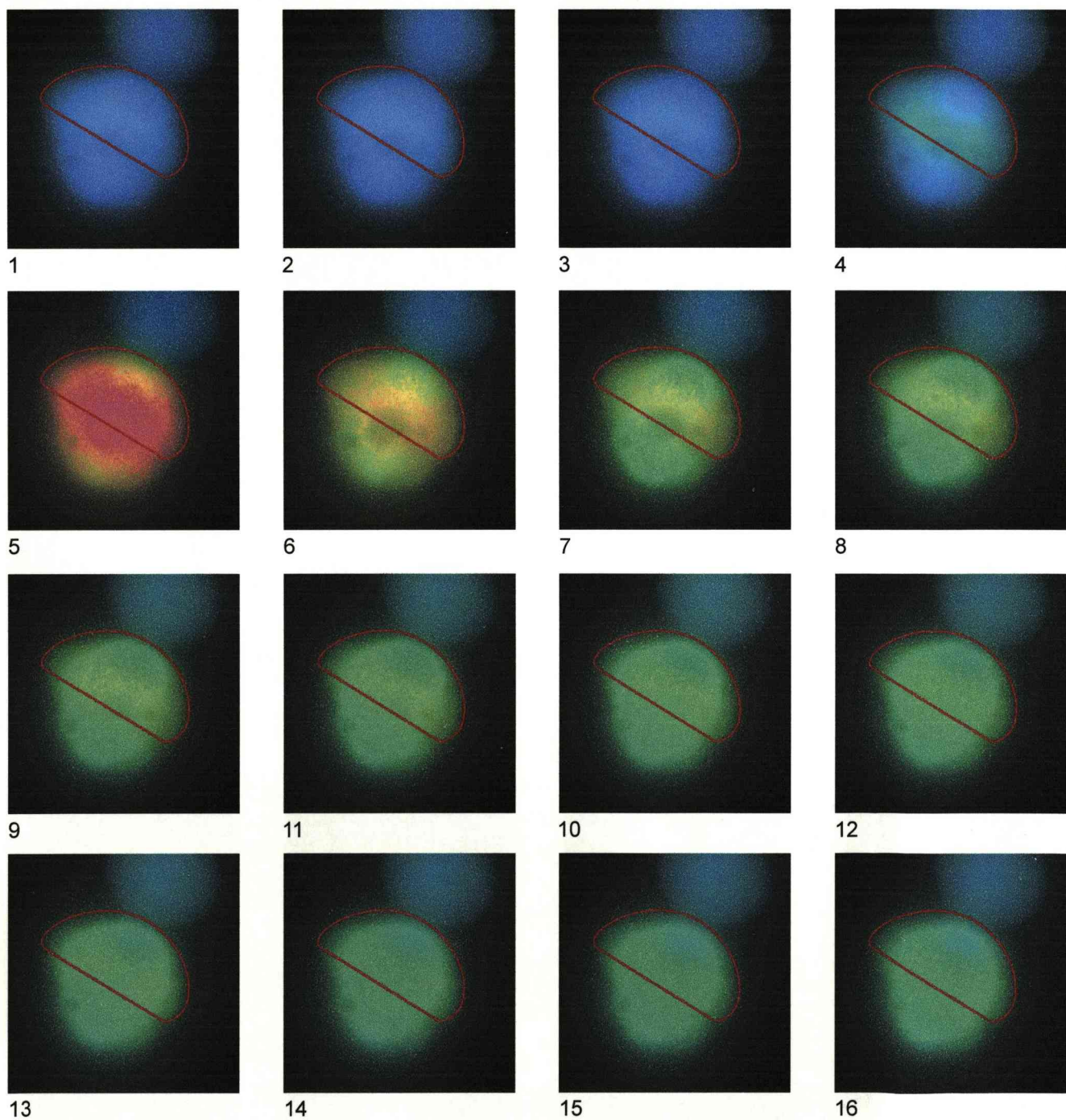
Part B shows a series of TIF images showing the actual acinar cell increased $[Ca^{2+}]_i$ response to 100 μ M ATP stimulation in real time, with each numbered TIF image equating exactly to the numbered vertical shaded lines on the trace shown in figure 6.1.3 part A.

A ATP 100 μ M



10 % |
3 s

B



ATP was selected for investigation based on its activity as a marker of stress as receptors with which it interacts are known to be up-regulated under conditions of stress. The traces in figure 6.1.1 demonstrate how mouse submandibular acinar cells increase $[Ca^{2+}]_i$ in response to stimulation with 50nM ACh and 100 μ M ATP respectively. The mouse submandibular acinar cells were able to mobilise Ca^{2+} in response to either agonist but the responses varied between agonists. This may be due to the suggested variation in function between ACh and ATP as ACh is released to stimulate fluid secretion whereas ATP is released under conditions of stress so the response stimulated by each agonist might vary based on their individual function.

The initial response in figure 6.1.1 part A shows a typical ACh response, similar to the one described previously in Chapter 3 Results Nitric oxide mouse submandibular acinar cells figure 3.1.1: trace A. The most obvious variation between the responses in figure 3.1.1 trace A is the large initial response 'spike' observed with 100 μ M ATP which does not occur with 50nM ACh. This is unlikely to be due to the variations in concentration as the presence, absence, or size of the 'spike' is largely independent of the agonist concentration. The second important variation is the oscillatory nature of the response. As shown in figure 6.1.1. part A first response which demonstrates a clear oscillatory pattern when cells were stimulated with ACh. This type of response pattern was commonly but not universally observed with ACh but was not observed on any occasion with ATP as shown by figure 6.1.1 part A second response. This might simply be due to the variation in function between ACh and ATP but was not investigated further.

Both responses initiate immediately upon exposure to stimulus which is characterized by a rapid rise in $[Ca^{2+}]_i$, observed as an upward "spike" in the trace from resting $[Ca^{2+}]_i$ level. Both responses have an initial spike but the ATP response has a much larger initial spike. Both responses then stabilize to a sustained plateau

in the $[Ca^{2+}]_i$, at a level below that of the "spike". The magnitude of the plateau phase of the response increased in proportion with agonist concentration. The initial ACh response has an oscillatory plateau whereas the second ATP response has a level plateau. The ATP response does not hold as level as the ACh response which may be relative to the variation in stimulation type as appears to very gradually decrease following the initial spike while the cell is still exposed to stimulus which is not observable in the ACh response. In both responses once the stimulus was removed there was a return to the resting $[Ca^{2+}]_i$ level.

We conducted ATP stimulation experiments in both mouse and human submandibular acinar cells and also mouse lacrimal acinar cells and all were able to mobilize Ca^{2+} in response to ATP stimulation. Mouse lacrimal acinar cells did appear to give a larger response to ATP compared to mouse and human submandibular acinar cells but this might simply be due to an increased sensitivity to ATP in lacrimal acinar cells. However, the lacrimal acinar cells experimental number (n=5) was relatively small, experiments were conducted using only one concentration of ATP (100 μ M) and ATP responses only occurred subsequent to ACh responses so the data was of only limited value but did demonstrate clearly the ability of mouse lacrimal acinar cells to respond to ATP. The human submandibular acinar cell data set demonstrated a clear dose response which was not as clearly observable in the data set from the mouse submandibular acinar cells, but, both sets of data showed a deviation in the dose response pattern at 250 μ M ATP (figures 6.1.1 part D is the mouse dose data and figure 6.1.1 part E is the human ATP dose data).

These data suggest that ATP stimulates activation of the same processes as ACh as the cells produced a similar response following stimulation with ATP as they did following stimulation with ACh. So ATP would most likely be functioning through the P2Y receptors which are known to be associated with G-protein activation

(Abbracchio and Burnstock 1994) and are known to be present in the salivary glands (Turner, Landon et al. 1999) as discussed earlier (Chapter 1 Introduction 1.3 ATP section).

The data presented in figure 6.1.1 traces B and C demonstrates an additive effect between ACh and ATP as the combination of the two appears to be increased when compared to either individually. This type of response pattern was observed a number of times in both human (n=20) and mouse (n=60) submandibular acinar cells.

Figure 6.1.1 part B shows an initial increase in $[Ca^{2+}]_i$ in response to 50nM ACh stimulation followed by a further increase in $[Ca^{2+}]_i$ when the mouse submandibular acinar cells were subsequently stimulated with 100 μ M ATP also. Once ATP stimulation was removed the $[Ca^{2+}]_i$ response level reduced to a $[Ca^{2+}]_i$ response level marginally higher than the previous ACh $[Ca^{2+}]_i$ response level. The $[Ca^{2+}]_i$ response to ACh was maintained until ACh stimulation was removed. The cells maintained an oscillatory response pattern throughout the duration of the stimulus exposure but the response became more oscillatory when the cells were exposed to both ACh and ATP. Once ACh stimulation was removed the $[Ca^{2+}]_i$ response level reduced further but did not return to the original base line.

Figure 6.1.1 part C shows an initial increase in $[Ca^{2+}]_i$ in response to 100 μ M ATP stimulation followed by a further increase in $[Ca^{2+}]_i$ when the mouse submandibular acinar cells were subsequently stimulated with 50nM ACh also. Once ACh stimulation was removed the $[Ca^{2+}]_i$ response level reduced to a $[Ca^{2+}]_i$ response level marginally lower than the previous ATP $[Ca^{2+}]_i$ response level. The $[Ca^{2+}]_i$ response to ATP appeared to constantly reduce back to base line throughout the duration of ATP only exposure but reduced further once ATP stimulation was

removed but did not return to the original base line. The oscillatory response pattern varies throughout the experimental time frame. When the cells were initially stimulated with ATP only they have no observable oscillatory response pattern but once stimulated with ATP and ACh together the cells have a clearly observable oscillatory response pattern. However, when the ACh stimulation was removed the response again becomes a sustained plateau with no observable oscillatory response pattern.

When parts B and C from figure 6.1.1 are compared the order of the addition of ACh and ATP does not appear to affect the outcome as both traces show similar patterns of response. The addition of ACh in figure 6.1.1 part C appears to induce some degree of oscillation to the response pattern which does not persist once ACh is removed and ATP appears to induce a sustained plateau with no observable oscillations. However, the addition of ATP to figure 6.1.1 part B does appear to make the oscillatory response more intense which might be a direct result of increased Ca^{2+} mobilisation and the oscillations reduce once ATP is removed. The degree of oscillation might be connected to the response induced by the agonist but was not investigated further.

Following the observations made on response traces like figure 6.1.1 parts B and C a series of experiments were conducted to demonstrate the additive effect between ACh and ATP. A series of response stimulations were selected which produced an interesting set of data and clearly demonstrated an additive effect between ACh (50nM) and ATP (100 μ M). This series of experiments were conducted in mouse submandibular acinar cells (n=45) and consisted of the cells being exposed to ACh only, ACh and ATP together and ATP only. The average results for these experiments were: ACh only $32.71 \pm 4.17\%$; ACh and ATP together $44.44 \pm 4.77\%$; ATP only $8.97 \pm 2.30\%$. This data series show significant ($P < 0.001$) differences

between ATP only and stimulation with ACh and ATP together and also the ACh only stimulation. The data are presented as mean \pm standard error as a percentage and the value relates to the increase above base line.

The occurrence of an additive effect between ACh and ATP may indicate the mobilization of Ca^{2+} through an alternative pathway such as other types of purinergic receptors (P2X) or from alternative Ca^{2+} stores as discussed earlier (Chapter 1 Introduction 1.3 ATP section). The original work conducted by Gallacher in 1982 demonstrated the presence of purinergic receptors in parotid acinar cells from mice but it was also observed during these original experiments that the response patterns of ACh and ATP were indistinguishable (Gallacher 1982).

Following the determination that ACh and ATP demonstrate some degree of additive effect we speculated that ACh and ATP may stimulate different patterns of response. Experiments were then conducted to elucidate if ATP and ACh initiated their responses at separate points within the acinar cell. These experiments were conducted following the suggestion that ACh and ATP would initiate at different points based on the suggestion that ATP acts as a stress signal and P2Y_2 receptors are known to be up-regulated in the SjS animal model NOD.B10 mice (Schrader, Camden et al. 2005). We speculated that stimulation by ATP could produce a different pattern of response in the acinar cell compared to ACh, which would distinguish between fluid secretion stimulation and stress. It was considered that the point of initiation would be the key as a variation in initiation point might induce a variation in response pattern and ACh and ATP would induce responses at different points in the cell.

The data presented in figures 6.1.2 and 6.1.3 show a series of cell images in real time and allow the pattern of response to be studied and compared between ACh

and ATP. The signal appears to originate at approximately the same place following stimulation by ACh and ATP as seen in image number 4 in figure 6.1.2 and image number 5 in figure 6.1.3. The data show that the initiation point of ATP does not vary from the initiation point of ACh and there appears to be no variation in the response pattern. So the two sets of TIF images presented in figures 6.1.2 and 6.1.3 part B show that the response initiates at approximately the same region of the cell following stimulation with ACh and ATP and proceeds in the same manner around the cell regardless of stimulus. The section of experimental trace presented in part A of figures 6.1.2 and 6.1.3 demonstrate the presence (ACh) or absence (ATP) of an oscillatory response pattern, most likely due to variations in Ca^{2+} mobilisation. Based on this series of experiments ATP does not appear to stimulate a response in the opposite direction to ACh as was speculated so the data could not substantiate our speculation that ATP initiates a response pattern alternative to that induced by ACh.

We were unable to visualise a variation in response pattern between ACh and ATP from the series of experiments conducted as both appeared to follow the same pattern of response which initiated at the apical pole and moved to the basolateral pole. ACh produces a well known spatial/temporal pattern of Ca^{2+} signal which moves clearly from the apical to the basolateral pole (Harmer, Smith et al. 2005) and we speculated that ATP may induce a signal at the basolateral pole which might move to the apical pole and so move in a totally opposite direction compared to ACh. Both responses appear to follow the same approximate pattern of response and move to approximately the same areas of the cell which would suggest that there is no variation in the response between ACh and ATP. So ACh and ATP demonstrated very similar patterns of response overall.

So in summary this data would suggest that ATP does induce a variation in response compared to ACh with respect to Ca^{2+} stores mobilized based on the observed

additive effect of response between ACh and ATP. We cannot explain how cells may use ATP as part of a stress signal or how cells may differentiate between ACh and ATP when the responses appear indistinguishable. We speculated that ACh and ATP would produce different Ca^{2+} signals but we observed no variation in movement of the responses induced by ACh and ATP as ATP appeared to initiate at the same point as ACh and apparently follows the same pattern of response with the exception of the lack of oscillation induced by ATP. Further experiments would be required to elucidate the effect of elevated ATP levels in acinar cells.

Chapter Seven

Results

Cell – Cell Coupling and the Effects of Nitric Oxide



UNIVERSITY OF
LIVERPOOL

Introduction

The aim of these experiments was to determine if acinar cells communicate at an intercellular level and how this may occur. We hypothesised that some degree of cell to cell communication must occur within salivary glands and would be vital for salivary secretion. A key feature in Sjögrens syndrome is infiltration of lymphocytes at specific loci within the salivary and lacrimal glands. Based on this fact we hypothesised that the main reason for this may be due to specific cells within the salivary and lacrimal glands attracting the lymphocytes and suggested that such cells may function as so called 'pacemaker' cells. The existence of such cells would go some way to explain why a whole gland may be inhibited by the presence of a limited number of lymphocytes.

We determined that the level of synergy between cells may be demonstrated by the degree of synchrony observed between specific cells. The level observed is the cells Ca^{2+} response to ACh with or without the presence of NO. Cells were selected under specific conditions, where cell to cell communication may or may not occur, and the degree of synchrony analysed. The level of synchrony was determined by how in phase or out of phase the cells were i.e. how similar their patterns of response were. We also tried to identify if any cell within specific groups of cells appeared to regulate the responses of other cells i.e. controlling their response pattern and determining when they would respond.

The experiments with NO were selected to determine what effect NO may have at the multiple cell level based on its effect at the single cell level.

Figure 7.1.1

Change in $[Ca^{2+}]_i$ signal in response to 50nM ACh in the absence and presence of 200 μ M NOC-12 demonstrating no degree of synchronisation.

Part A: Change in $[Ca^{2+}]_i$ signal in response to a series of 50nM ACh stimulations in the absence and presence of 200 μ M NOC-12 in mouse submandibular acinar cells maintained in primary culture for 2 hours and presented as a specific section of an experimental trace (see scale bar).

Part B: The section of experimental trace taken from part A and broken down into the two specific selected cells responses at each time point with each stimulation point of interest given as an individual figure at each time point and then shown in relation to one another (see scale bar).

Cell one is designated by red and cell two is designated by green.

The cells presented here are in different acini and are therefore not connected so there is little chance of cell to cell communication occurring.

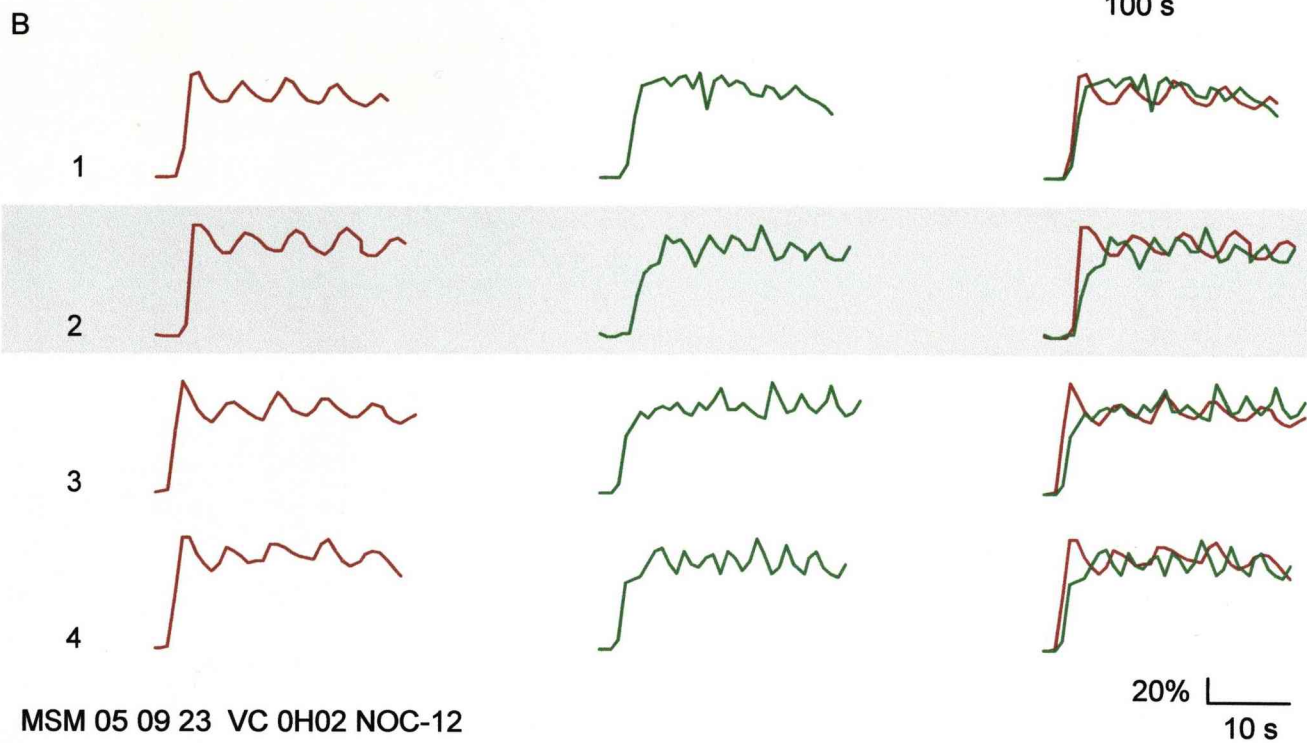
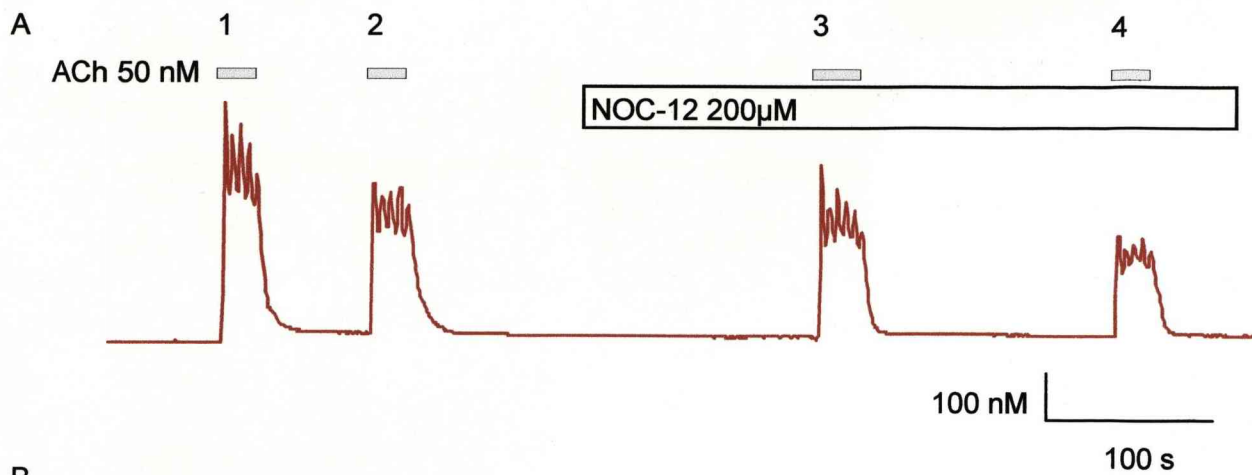


Figure 7.1.2

Change in $[Ca^{2+}]_i$ signal in response to 50nM ACh demonstrating no degree of synchronisation.

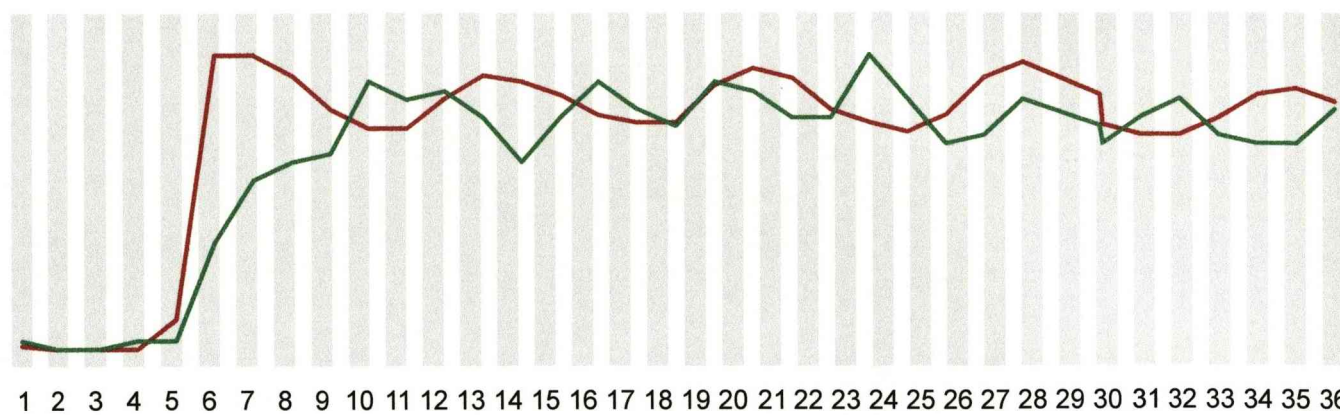
Part A: Change in $[Ca^{2+}]_i$ signal in response to a single 50nM ACh stimulation in mouse submandibular acinar cells maintained in primary culture for 2 hours, taken from the 2nd application point from figure 7.1.1 and presented as a specific section of the experimental trace and marked in figure 7.1.1 part B by the single shaded strip (see scale bar).

Part B: A sequence of TIF images illustrating the cells responding in real time. The sequence of TIF images equate exactly to each numbered vertical shaded area presented on the trace in part A.

Cell one designated as red, cell two designated as green.

The cells presented here are in different acini and are therefore not connected so there is little chance of cell to cell communication occurring.

A ACh 50 nM 2nd Application



10 % |
5 s

B

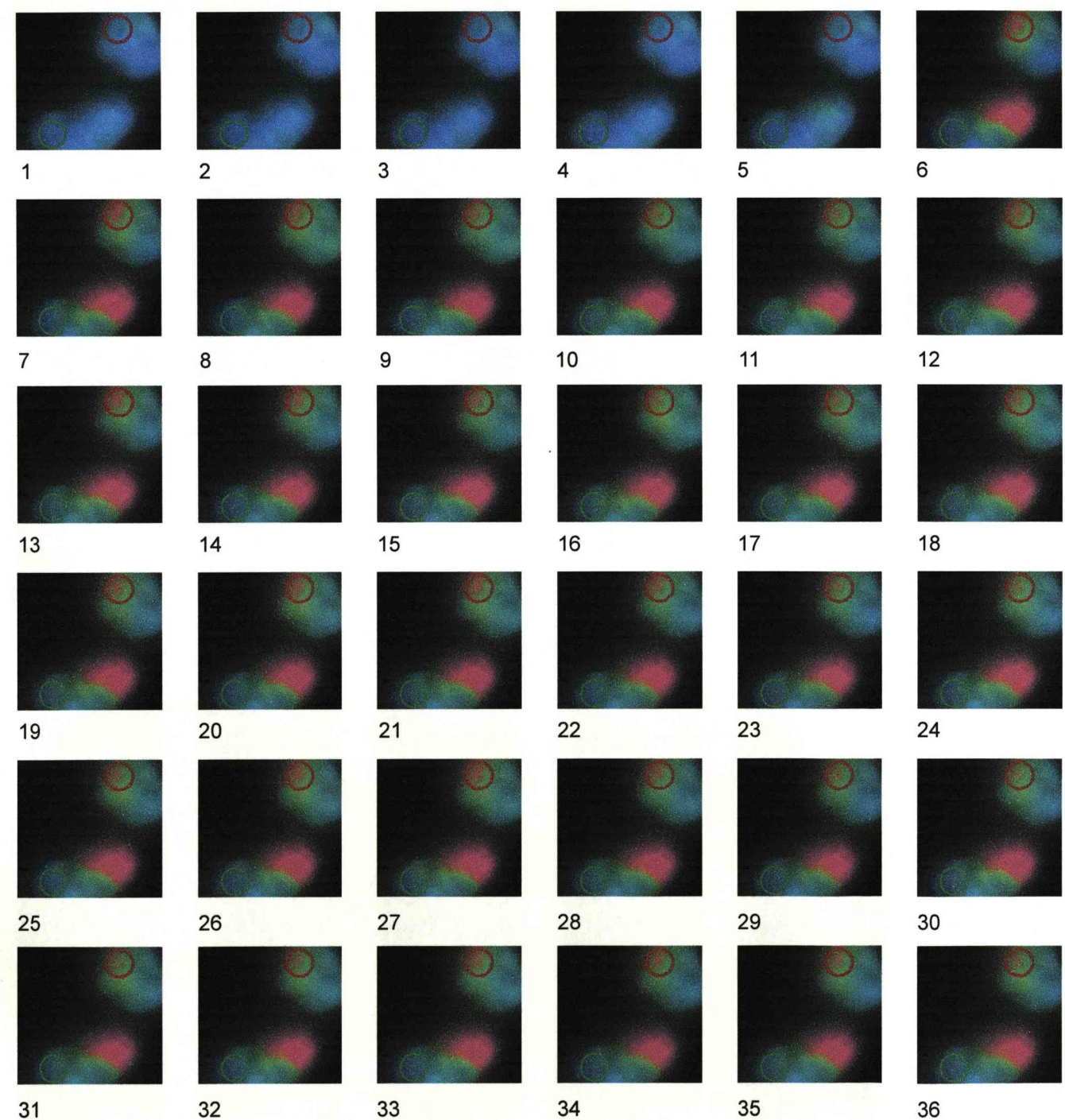


Figure 7.1.3

Change in $[Ca^{2+}]_i$ signal in response to 50nM ACh demonstrating lack of synchronisation.

Part A: Change in $[Ca^{2+}]_i$ signal in response to repeated 50nM ACh stimulation in mouse submandibular acinar cells maintained in primary culture for 24 hours and presented as a whole experimental trace (see scale bar).

Part B: The whole experimental trace from part A broken down into each specific response time point and with each stimulation point presented as an individual figure for each of the three selected cells and then shown in relation to one another (see scale bar).

Cell one designated as red, cell two designated as green and cell three designated as blue.

The cells presented here are within the same acini.

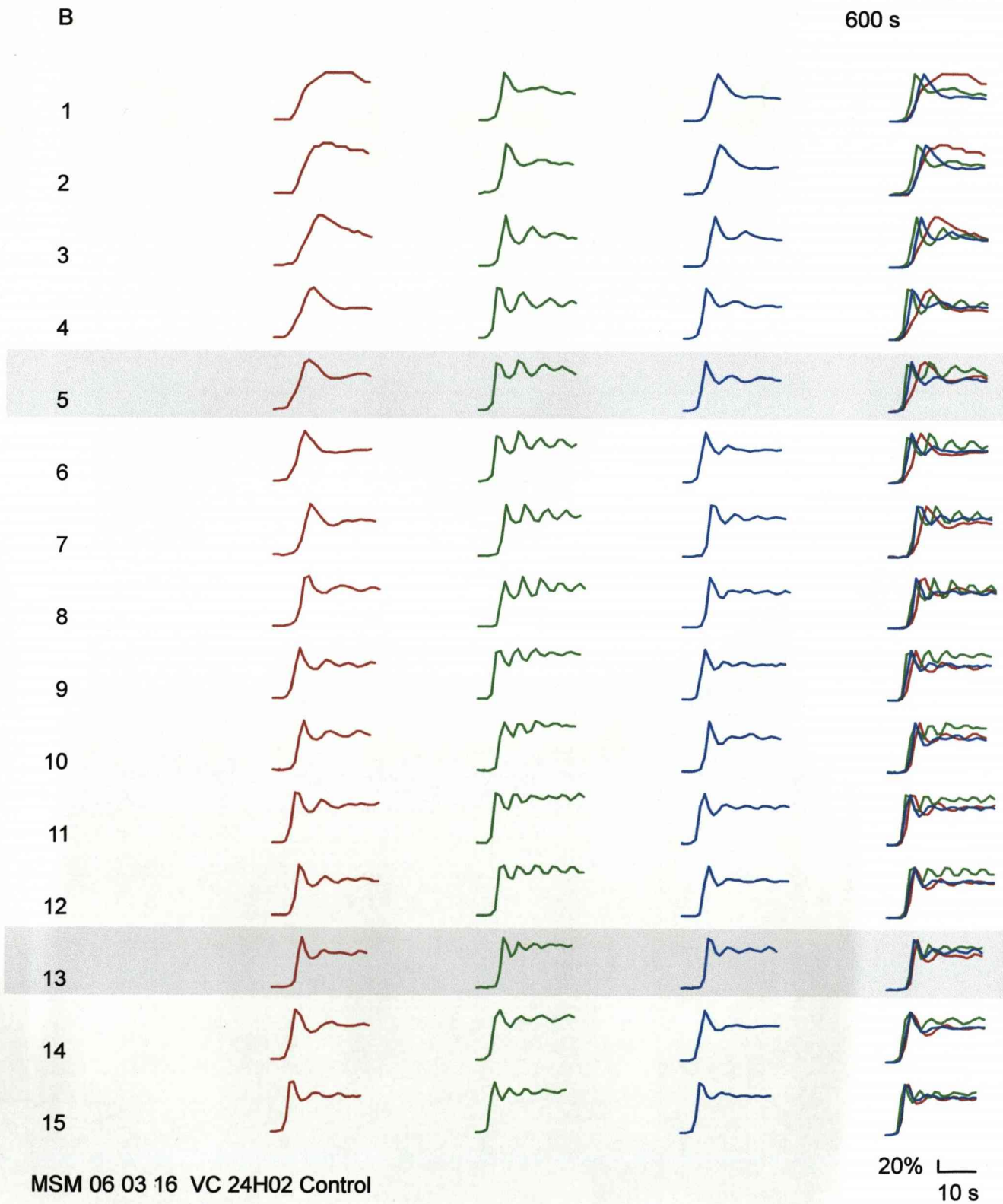
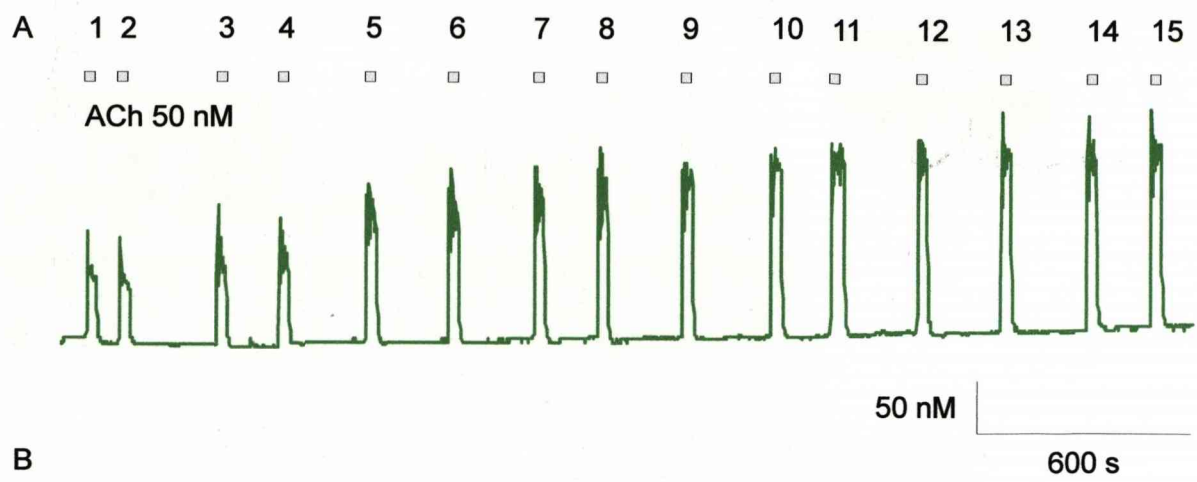


Figure 7.1.4

Change in $[Ca^{2+}]_i$ signal in response to 50nM ACh demonstrating lack of synchronisation at 5th stimulation point.

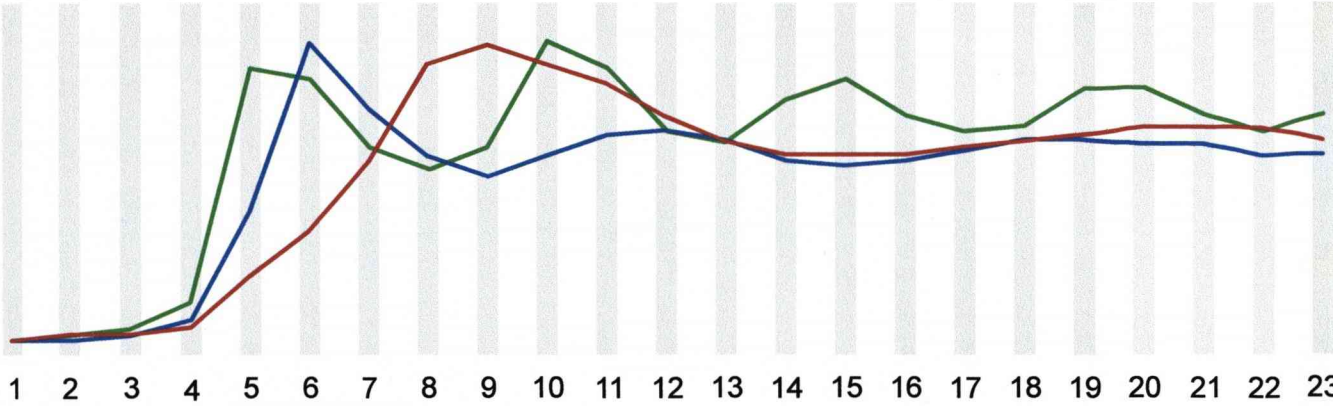
Part A: Change in $[Ca^{2+}]_i$ signal in response to a single 50nM ACh stimulation in mouse submandibular acinar cells maintained in primary culture for 24 hours produced at the 5th application point given as a specific section of the experimental trace illustrated in figure 7.1.3 part A and marked by the first horizontal shaded strip in figure 7.1.3 part B (see scale bar).

Part B: A sequence of TIF images illustrating the cells responding in real time. The sequence of TIF images equate exactly to each vertical shaded line given on the trace in part A.

Cell one designated as red, cell two designated as green and cell three designated as blue.

The cells presented here are within the same acini.

A ACh 50 nM 5th Application



B

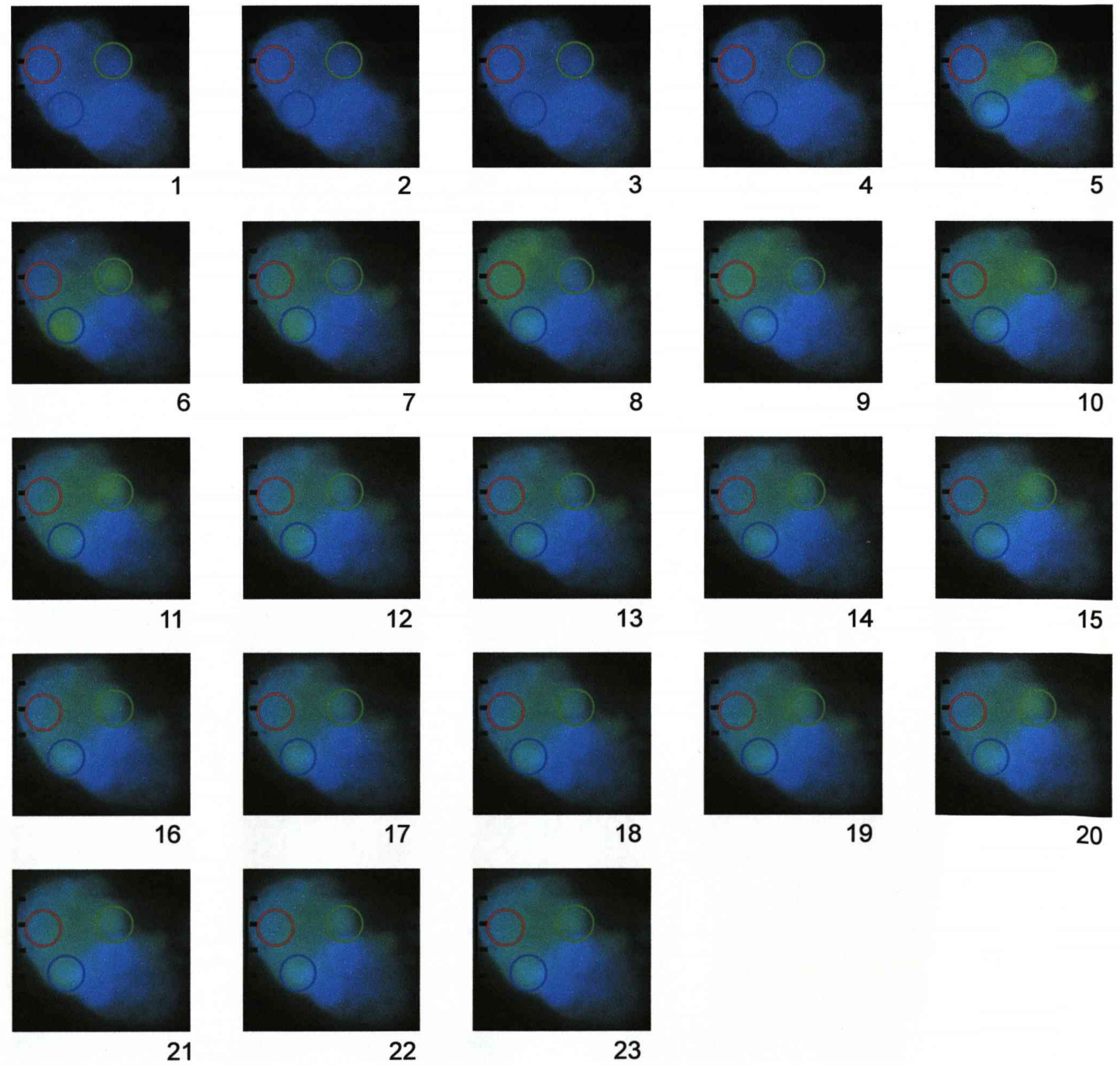


Figure 7.1.5

Change in $[Ca^{2+}]_i$ signal in response to 50nM ACh demonstrating lack of synchronisation at 13th stimulation point.

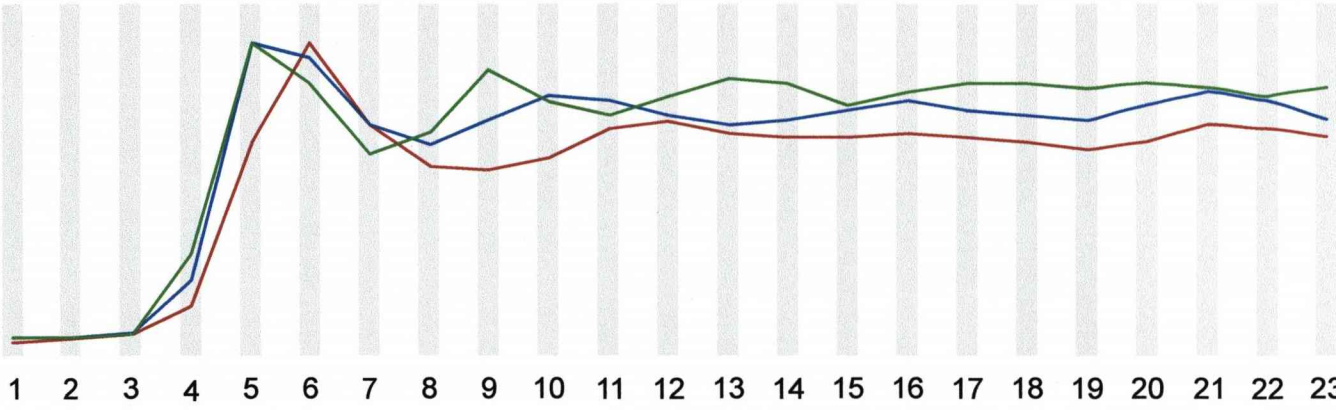
Part A: Change in $[Ca^{2+}]_i$ signal in response to a single 50nM ACh stimulation in mouse submandibular acinar cells maintained in primary culture for 24 hours produced at the 13th application point given as a specific section of the experimental trace illustrated in figure 7.1.3 part A and marked by the second horizontal shaded line in figure 7.1.3 part B (see scale bar).

Part B: A sequence of TIF images illustrating the cells responding in real time. The sequence of TIF images equate exactly to each vertical numbered shaded line given on the trace in part A.

Cell one designated as red, cell two designated as green and cell three designated as blue.

The cells presented here are in the same acini.

A ACh 50 nM 13th Application



10 % |
5 s

B

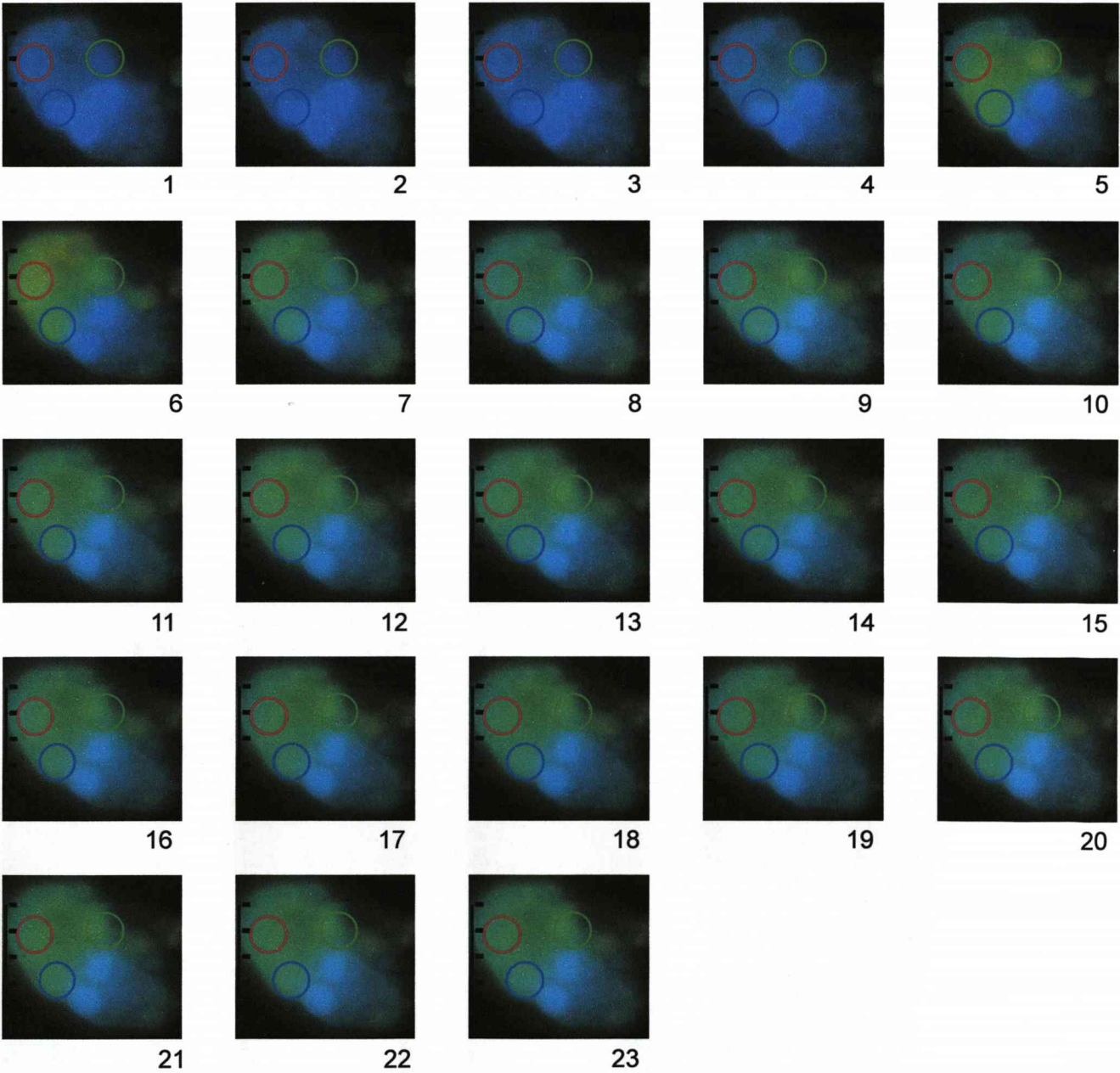


Figure 7.1.6

Change in $[Ca^{2+}]_i$ signal in response to 50nM ACh demonstrating cell – cell communication.

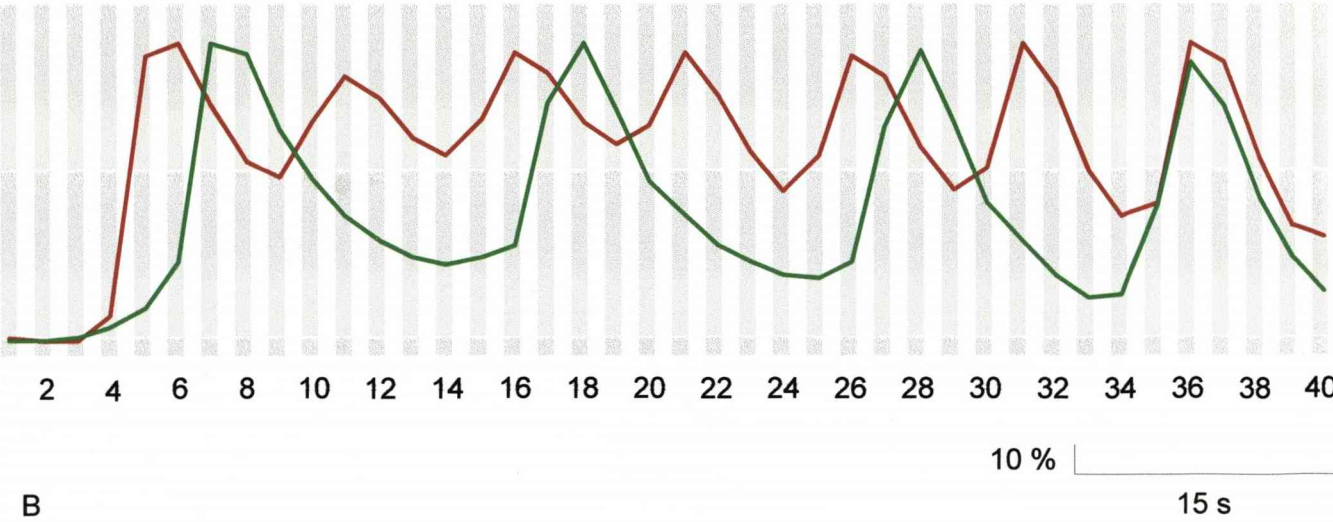
Part A: Change in $[Ca^{2+}]_i$ signal in response to 50nM ACh stimulation in human submandibular acinar cells maintained in primary culture for 48 hours, given as a specific section of trace (see scale bar).

Part B: A sequence of TIF images illustrating the cells responding in real time. The sequence of TIF images equate exactly to the vertical grey lines presented on the trace in part A.

Cell one designated as red, cell two designated as green.

Cells are within the same acini and in direct contact with one another.

A ACh 50 nM



B

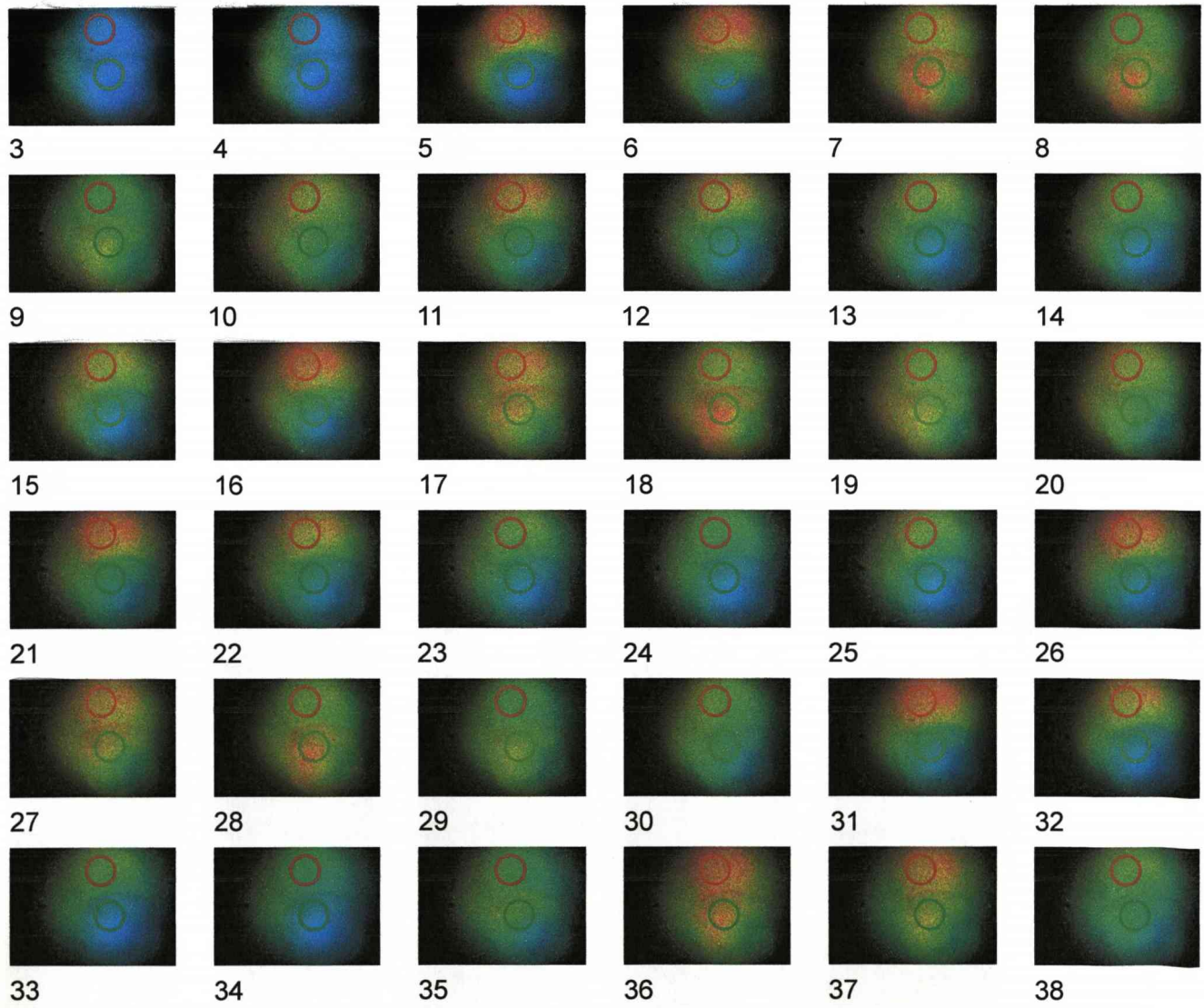


Figure 7.1.7

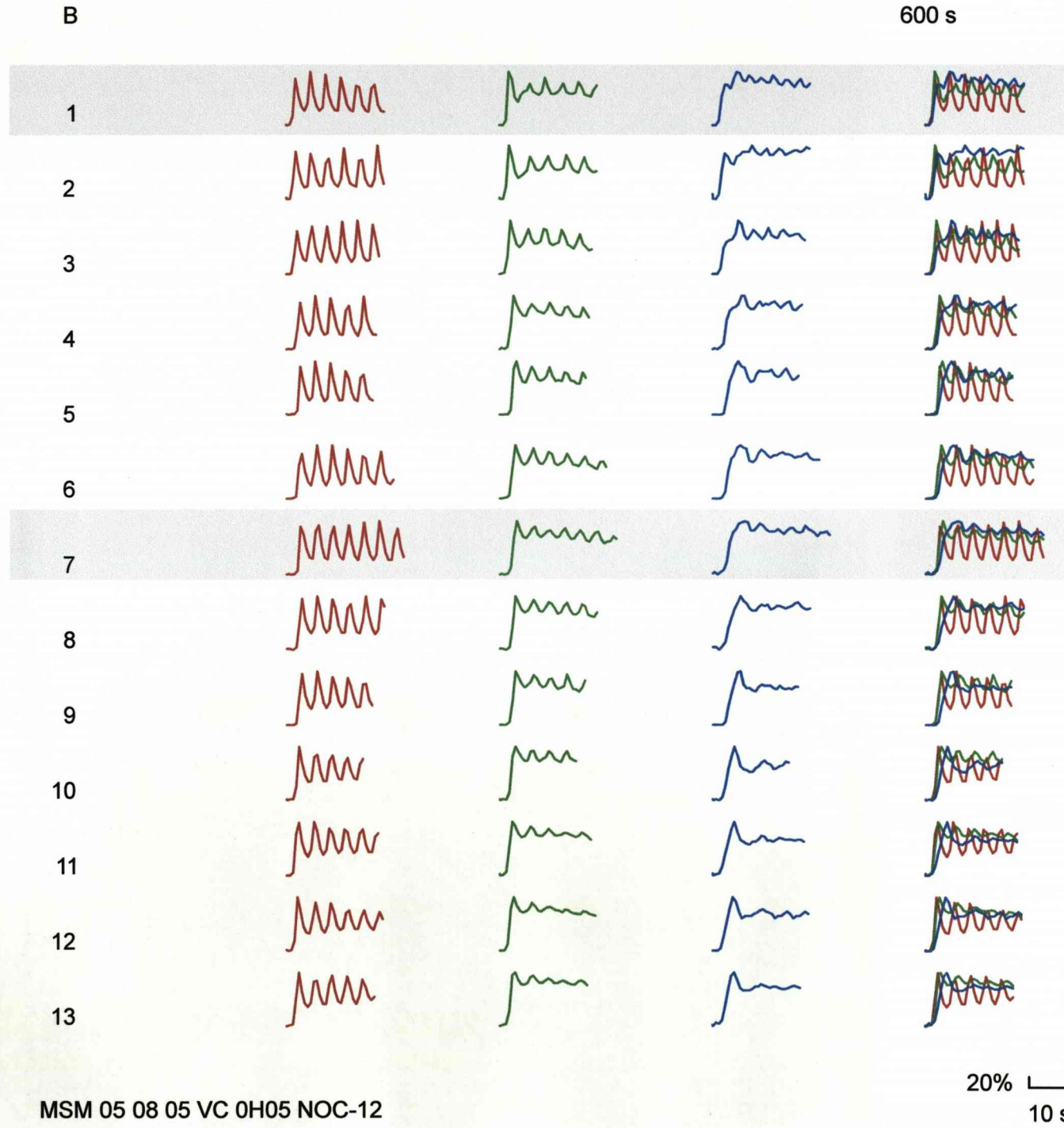
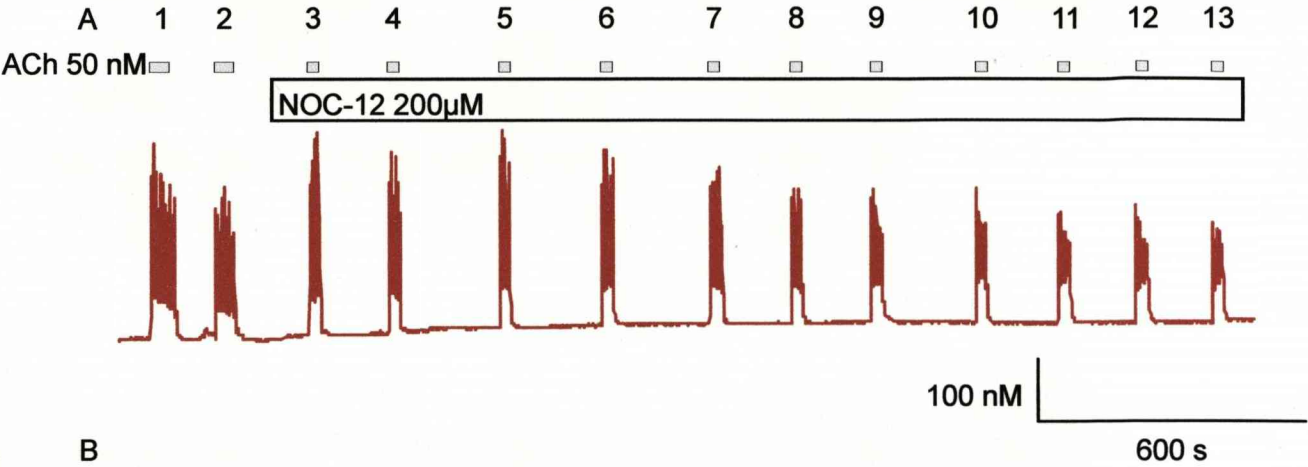
Change in $[Ca^{2+}]_i$ signal in response to 50nM ACh in the absence and presence of 200 μ M NOC-12 demonstrating synchronisation.

Part A: Change in $[Ca^{2+}]_i$ signal in response to repeated 50nM ACh stimulation in the presence of 200 μ M NOC-12 in mouse submandibular acinar cells maintained in primary culture for 2 hours and presented as a whole experimental trace (see scale bar).

Part B: The whole experimental trace from part A broken down into each specific response time point for each of the three selected cells and with each stimulation point presented as an individual figure at each time point and then shown in relation to one another (see scale bar).

Cell one designated as red, cell two designated as green and cell three designated as blue.

The cells presented here are in the same acini.



MSM 05 08 05 VC 0H05 NOC-12

Figure 7.1.8

Change in $[Ca^{2+}]_i$ signal in response to 50nM ACh demonstrating synchronisation at the 1st stimulation point.

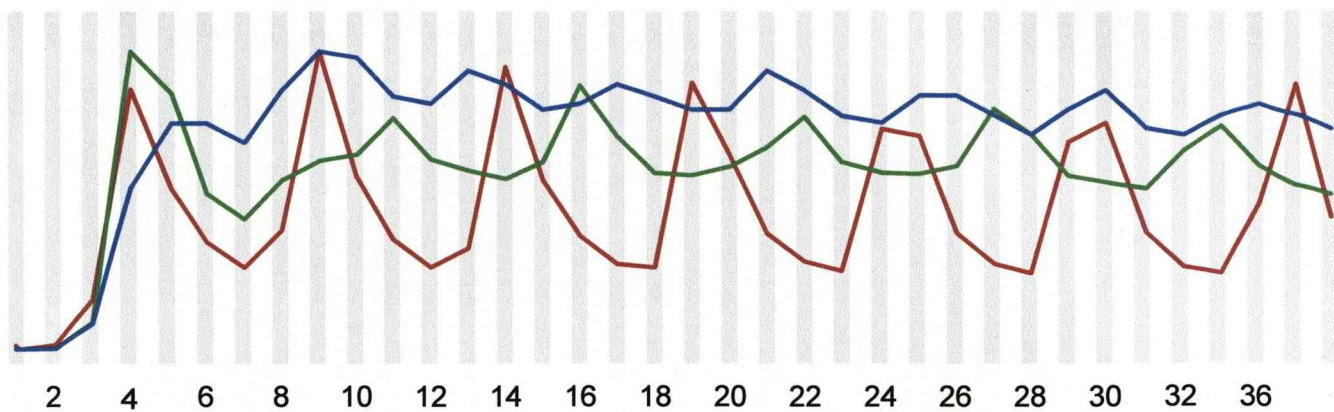
Part A: Change in $[Ca^{2+}]_i$ signal in response to a single 50nM ACh stimulation in mouse submandibular acinar cells maintained in primary culture for 2 hours produced at the 1st application point given as a section of the experimental trace taken from a specific stimulation point from figure 7.1.7 part A and marked by the first horizontal shaded strip in figure 7.1.7 part B (see scale bar).

Part B: A sequence of TIF images illustrating the cells responding in real time. The sequence of TIF images equate exactly to the numbered vertical shaded lines presented on the trace in part A.

Cell one designated as red, cell two designated as green and cell three designated as blue.

The cells presented here are in the same acini.

A ACh 50 nM 1st Application



10 %
5 s

B

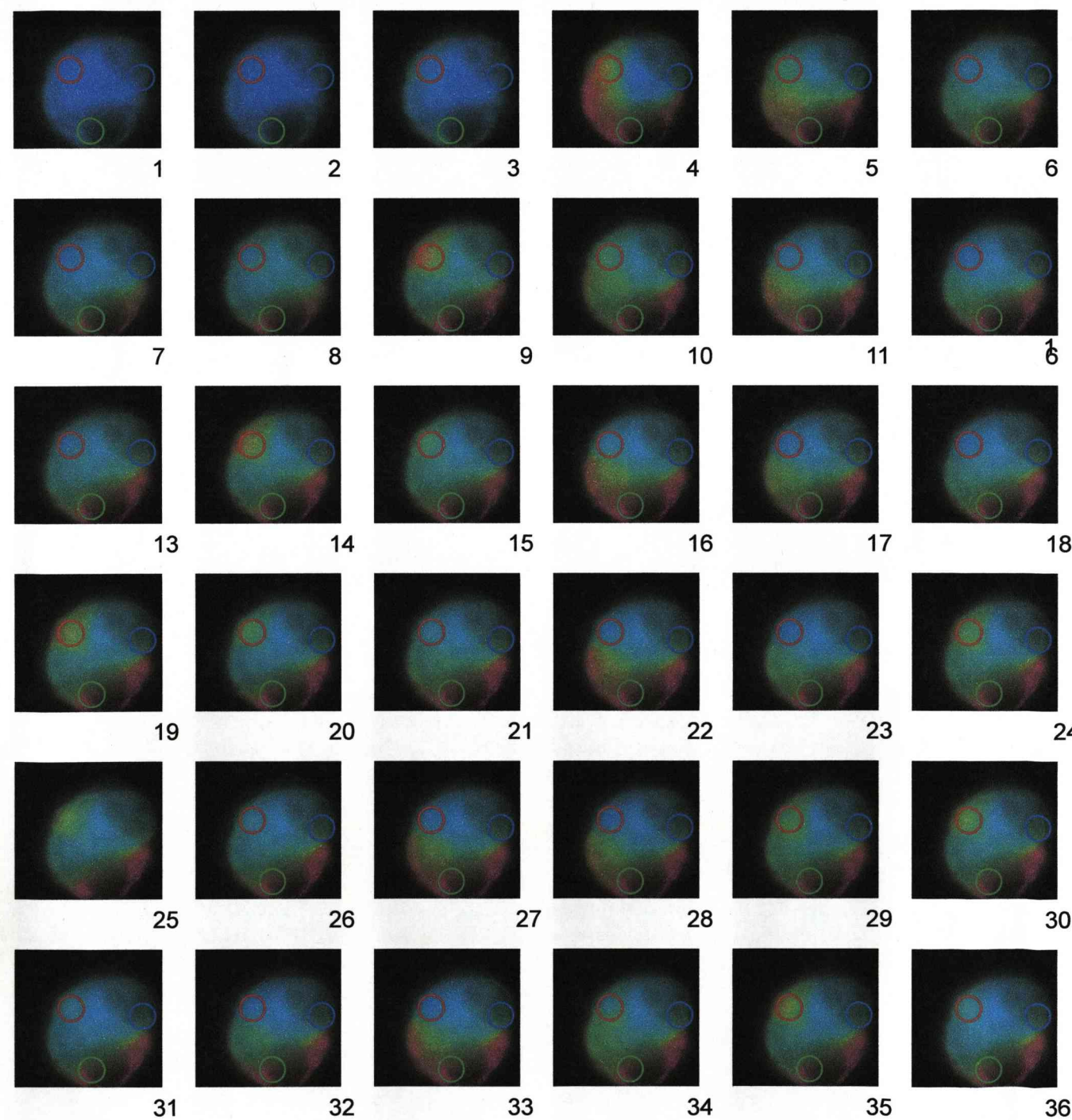


Figure 7.1.9

Change in $[Ca^{2+}]_i$ signal in response to 50nM ACh in the presence of 200 μ M NOC-12 demonstrating synchronisation at the 7th stimulation point.

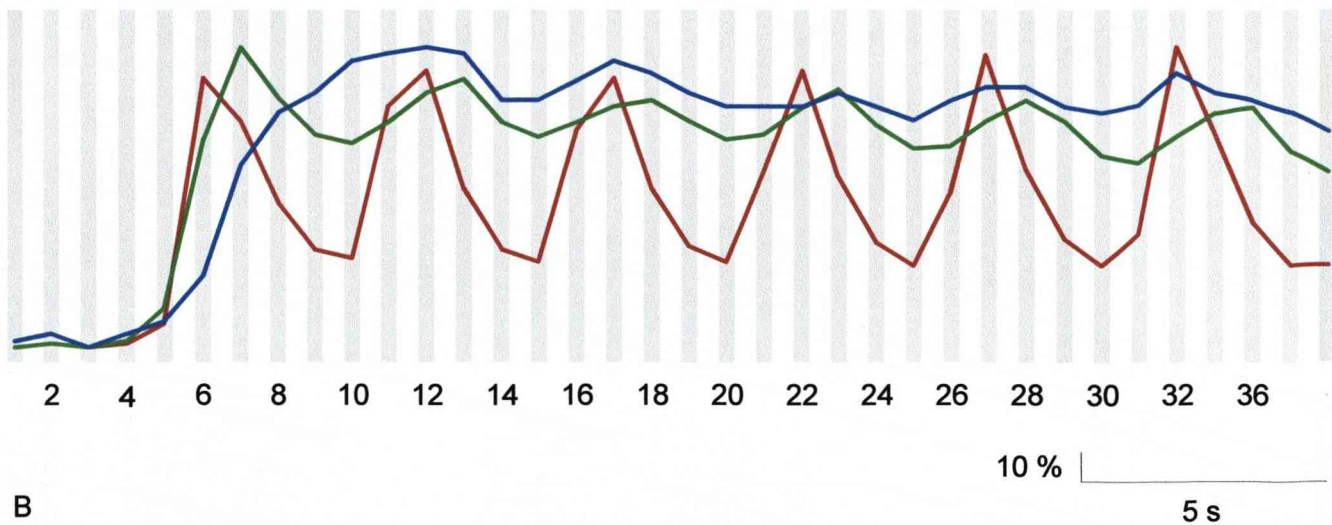
Part A: Change in $[Ca^{2+}]_i$ signal in response to a single 50nM ACh stimulation in the presence of 200 μ M NOC-12 in mouse submandibular acinar cells maintained in primary culture for 2 hours produced at the 7th application point given as a section of the experimental trace and taken from a specific stimulation point from figure 7.1.7 part A and marked by the second horizontal shaded strip in figure 7.1.7 part B (see scale bar).

Part B: A sequence of TIF images illustrating the cells responding in real time. The sequence of TIF images equate exactly to the numbered vertical shaded lines presented on the trace in part A.

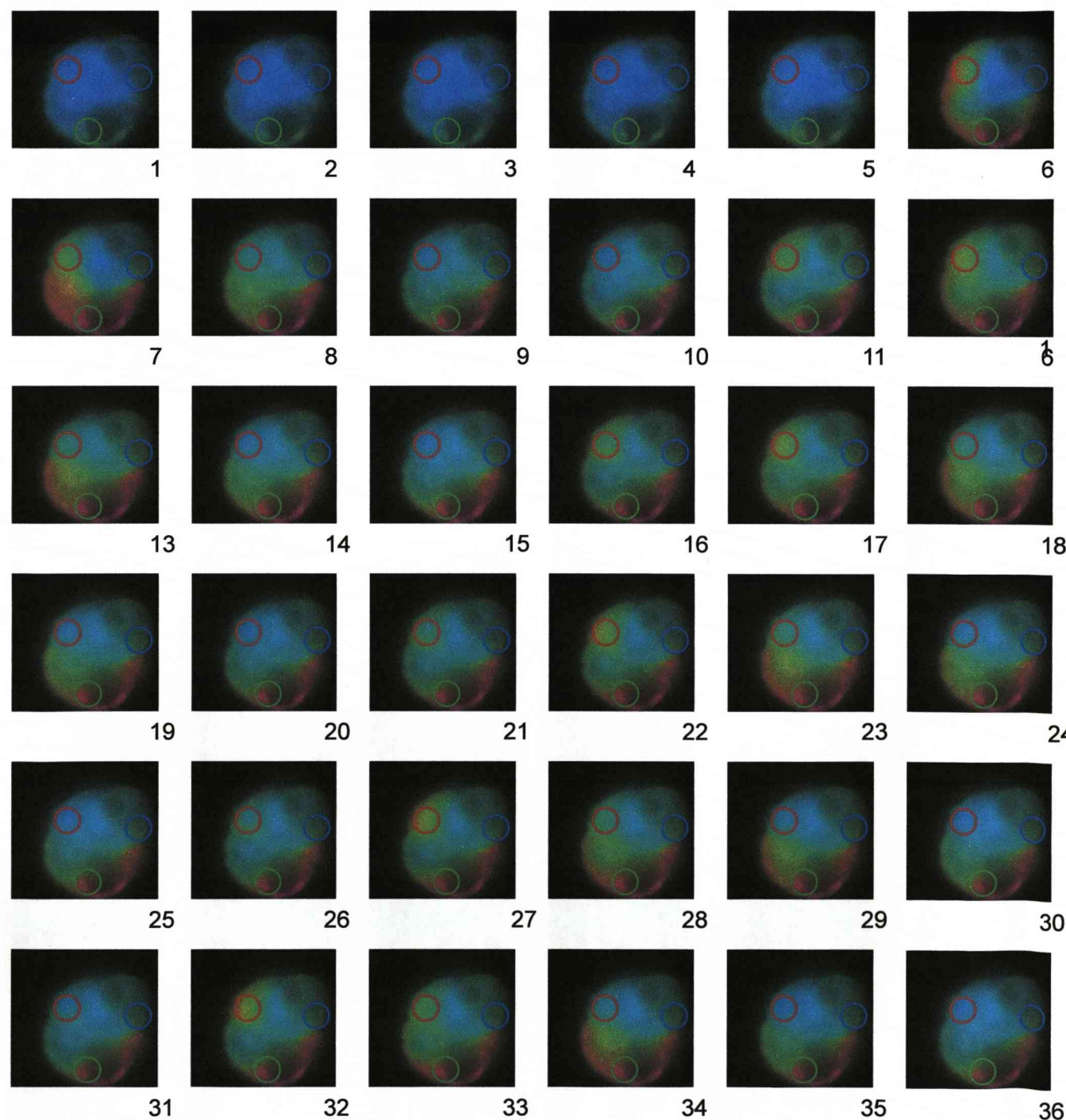
Cell one designated as red, cell two designated as green and cell three designated as blue.

The cells presented here are in the same acini.

A ACh 50 nM in the presence of NOC-12 200 μ M 7th Application



B



Following the results achieved using nitric oxide on submandibular and lacrimal acinar cells the degree of cell to cell communication was investigated. Acinar cells were selected dependent on the degree of oscillation and the number of cells present. As mentioned in earlier sections (Chapter 3 results nitric oxide and mouse submandibular acinar cells) the cells selected responded typically to ACh and gave good oscillations in $[Ca^{2+}]_i$ response signal. The preliminary measure of how well coupled cells are is the extent to which the Ca^{2+} oscillations are synchronised. This pattern of response offered an opportunity to study the progression of the Ca^{2+} waves across individual cells and the communication of Ca^{2+} signals from one cell to another. Cells which demonstrated no degree of contact were initially observed during stimulation to determine the degree of cell to cell communication and what effect this may have on the pattern of response. The data in figure 7.1.1 part A show the series of experimental time points where responses to 50nM ACh occurred in the presence or absence of 200 μ M NOC-12. Figure 7.1.1 part A shows a section of experimental trace demonstrating a series of nice oscillatory responses to stimulation in the presence and absence of 200 μ M NOC-12.

The data in figure 7.1.1 part B show the individual stimulation points which occurred in figure 7.1.1 part A numbered 1 to 4 with cell one designated by red and cell two designated by green and the experimental trace from part A broken down into the two individual responses at each specific response time point. These two individual illustrations at each time point in figure 7.1.1 part B show the two separate cells $[Ca^{2+}]_i$ signal responses to stimulation with ACh 50nM in the absence and presence of 200 μ M NOC-12 in mouse submandibular acinar cells.

The first cell designated by the red trace in figure 7.1.1 part B which is presented as the first column of responses appears to maintain a good oscillatory response pattern which varies very little at each stimulation point. The second cell designated by the

green trace and presented as the second column of responses has a much more random oscillatory pattern compared to cell one. Both have obvious oscillations and cell one has a good initial response spike whereas cell two does not appear to have a response initiation spike. The data show how the oscillatory responses of the two acinar cells changed over this specific experimental time period. Cell one has a nice regular oscillatory pattern whereas cell two has a much more random response pattern. The two traces in figure 7.1.1 part B do not demonstrate any degree of synchronisation when compared to one another.

The data presented in figure 7.1.2 show a specific time point selected from figure 7.1.1. This specific stimulation point is marked by the single horizontal shaded region on figure 7.1.1 part B and is the 2nd stimulation of the mouse submandibular acinar cells by 50nM ACh and occurs in the absence of 200µM NOC-12. Figure 7.1.2 part A is the two individual illustrations from the 2nd ACh stimulation placed together as a section of experimental trace to allow analysis of synchronisation between the two cells. Figure 7.1.2 part B is a series of TIFS numbered 1 to 36 which equate to the series of vertical shadings presented in figure 7.1.2 part A and show the real time responses of the two selected mouse submandibular acinar cells and allow the pattern of response to be observed.

The data in figure 7.1.2 would suggest that there is no degree of synchronisation between these cells at this experimental time point as the cells have no obvious response pattern with relation to one another and have independent oscillatory patterns. This could suggest that the cells require direct cell to cell contact to induce a unified oscillatory pattern. This particular experiment shows the two clearly disconnected cells responding with totally random patterns with relation to one another. The data appears to confirm that acinar cells require cell to cell contact to allow synchronisation of the oscillatory pattern and that synchronisation is not a result

of the cells natural rhythm. The acinar cells would have no direct reason to oscillate together. So any observed synchronous oscillations would be the result of cells communicating cell to cell so acinar cells would not naturally oscillate at roughly the same frequency. The data in figures 7.1.1 and 7.1.2 demonstrate the lack of oscillatory rhythm between two disconnected cells so no direct contact between cells means no synchronisation of oscillatory rhythm.

The data in cell to cell figure 7.1.3 part A shows a whole experimental trace with repeated 50nM ACh stimulation in mouse submandibular acinar cells. The stimulations occurred at specific time points numbered 1 to 15. The data in figure 7.1.3 part B shows the whole experimental trace from part A broken down into each specific response time point and each point is subsequently broken down into three individual illustrations of response. These three individual illustrations at each time point in figure 7.1.3 part B show the three separate cells change in $[Ca^{2+}]_i$ signal in response to stimulation with ACh 50nM in mouse submandibular acinar cells. The data show how the oscillatory responses of the three acinar cells changed over the experimental time course.

The first cell designated by the red traces and shown as the first of the three illustration sets initially has no obvious oscillations and the two other cells are designated by green for the second cell and blue for the third cell and green and blue only appear to have initial spikes of response and no overly obvious oscillations. The patterns of oscillations gradually increase for all three selected cells at each further experimental time point. The cell two is also the first to initiate a response and is observed to increase its level of oscillations more rapidly and the oscillations are much more obvious in this particular cell. The levels of oscillations also seem to decrease over time towards the end of the experimental time frame for cell three and

is reduced in cell two but cell one seems to maintain its oscillatory level relatively well.

The data presented in cell to cell figures 7.1.4 and 7.1.5 show specific time points selected from figure 7.1.3. These specific stimulation points are marked by two horizontal shaded bands on figure 7.1.3 part B and are the 5th and 13th stimulation of the mouse submandibular acinar cells by 50nM ACh. Figure 7.1.4 part A is the three individual illustrations from the 5th ACh stimulation placed together as a section of experimental trace to allow analysis of synchronisation between the three cells. Figure 7.1.4 part B is a series of TIFS numbered 1 to 23 which equate exactly to the series of vertical bands present on figure 7.1.4 part A and show the real time responses of the mouse submandibular acinar cells. The data in figure 7.1.4 would suggest that there is no degree of synchronisation between these cells at this experimental time point as the cells have no obvious response pattern with relation to one another and have apparently independent oscillatory patterns.

The data in figure 7.1.5 part A is the three individual illustrations from the 13th ACh stimulation placed together as a section of experimental trace to allow analysis of synchronisation between the three cells. Figure 7.1.5 part B is a series of TIFS numbered 1 to 23 which equate exactly to the series of vertical bands present on figure 7.1.5 part A and show the real time responses of the mouse submandibular acinar cells. The data in figure 7.1.5 would suggest that there is no degree of synchronisation between these cells at this experimental time point as the cells have no obvious response pattern with relation to one another and have independent oscillatory patterns. The cells do not appear to be coupled and no cross talk between cells is apparent.

The data in figures 7.1.4 and 7.1.5 suggest that the designated cells do not demonstrate any degree of synchronisation initially and do not become more synchronous over the duration of the experiment. The only apparent variation in response over time is the change in time delay between the individual cells initiation of responses which appears to reduce. Cell one and cell three have much more similar patterns of response when all three cells are directly compared. Cell two has a much more obvious oscillatory pattern and always responds first to ACh 50nM stimulation. The cells do not appear to demonstrate any degree of cell to cell communication and these data also suggest that acinar cells do not have a natural oscillatory rhythm at which they respond as the cells were not synchronous so synchronicity appears to be dependent on cell to cell communication.

However, the data in figure 7.1.6 part A demonstrates clear cell to cell coupling as one cell controls the initiation of the $[Ca^{2+}]_i$ response in the other cell in a small clump of human submandibular acinar cells. The responses demonstrate a clear oscillatory response pattern which is maintained throughout the duration of the $[Ca^{2+}]_i$ response to 50nM ACh. The first cell designated by red always initiates a $[Ca^{2+}]_i$ response which is followed by a $[Ca^{2+}]_i$ response in the other cell designated by green. The red cell has an oscillatory frequency that is exactly twice that of the frequency of the other cell but keeps the other cell in the same phase. This data suggests that the first cell is acting as a pacemaker cell as discussed earlier (Chapter 1 Introduction 1.4 cell-cell coupling section). The series of TIF images presented in figure 7.1.6 part B show the clear pattern of response in the acinar cells in real time and allow the transmission of the response $[Ca^{2+}]_i$ signal to be followed from cell to cell and it is clear from these sequence of images numbered 5 to 8 that the Ca^{2+} signal in the red designated cell is driving that in the green designated cell. The cells in figure 7.1.6 demonstrate spontaneous cell to cell communication and give the appearance of cell to cell communication. The data in figure 7.1.6 demonstrates a very clear example of

cell to cell Ca^{2+} signalling. These data suggest that there may be a role for pacemaker cells in submandibular cells and subsequently a role in glandular hypofunction in SjS.

Based on these responses we then wanted to know what effect NO had on cell to cell coupling and whether NO altered Ca^{2+} signalling between acinar cells. The data in figure 7.1.7 part A shows a whole experimental trace with repeated 50nM ACh stimulation in the presence of 200 μM NOC-12 in mouse submandibular acinar cells. The stimulations occurred at specific time points numbered 1 to 13. The data in figure 7.1.7 part B shows the whole experimental trace from part A broken down into each specific response time point and each point is subsequently broken down into three individual illustrations of response. These three individual illustrations at each time point in figure 7.1.7 part B represent the three separate selected cells change in $[\text{Ca}^{2+}]_i$ signal in response to stimulation with ACh 50nM in the absence and presence of 200 μM NOC-12 in mouse submandibular acinar cells. The data show how the oscillatory responses of the three acinar cells changed over the experimental time course.

All three selected cells (designated by red for cell one, green for cell two and blue for cell three) regions initially have good obvious oscillations and cell one appears to maintain its pattern of response relatively well over the experimental duration. Cell two and cell three do become slightly less oscillatory over the duration of the experiment. Cell three designated by the blue traces also seems to develop a large response spike upon initiation of the $[\text{Ca}^{2+}]_i$ response signal over the duration of the experiment but conversely the size of the response spike upon initiation of the $[\text{Ca}^{2+}]_i$ signal in the cell two designated by the green traces decreases. Cells one and two maintain their response initiation pattern throughout the duration of the experiment but the time lag between the initiation of response between these two cells and cell

three increases over the experimental time period. Cell one designated by the red traces maintains its oscillatory pattern throughout the duration of the experiment and the cells designated two and three also maintain their oscillatory patterns relatively well.

The data presented in figures 7.1.8 and 7.1.9 show specific time points selected from figure 7.1.7. These specific stimulation points are marked by two horizontal shaded regions on figure 7.1.7 part B and are the 1st and 7th stimulation of the mouse submandibular acinar cells by 50nM ACh in the presence of 200µM NOC-12. Figure 7.1.8 part A is the three individual illustrations from the 1st ACh stimulation placed together as a section of experimental trace to allow analysis of synchronisation between the three cells. Figure 7.1.8 part B is a series of TIFS numbered 1 to 36 which equate exactly to the series of vertical numbered lines present on figure 7.1.8 part A and show the real time responses of the mouse submandibular acinar cells. The data in figure 7.1.8 would suggest that there is a degree of synchronisation between these cells at this experimental time point as the cells have an obvious response pattern with relation to one another and appear to have a relatively synchronous oscillatory pattern. There appears to be a degree of order with relation to response which the cells follow throughout the duration of this particular stimulation with 50nM ACh in the presence of 200µM NOC-12.

Figure 7.1.9 part A is the three individual illustrations from the 7th ACh stimulation placed together as a section of experimental trace to allow analysis of synchronisation between the three cells. Figure 7.1.9 part B is a series of TIFS numbered 1 to 36 which equate exactly to the series of vertical lines present on figure 7.1.9 part A and show the real time responses of the mouse submandibular acinar cells. The data in figure 7.1.9 would suggest that the degree of synchronisation observed in figure 7.1.8 has been enhanced. The cells appear to be

more synchronous at this time point and still follow a specific response order so the cells do appear to be coupled in this instance. The data presented in figures 7.1.7 to 7.1.9 would suggest that cross talk between the cells is occurring as the cells seem to be further synchronised in figure 7.1.9 compared to figure 7.1.8 so the cells are more synchronous at the 7th time point than at the 1st time point but show synchronicity throughout the duration of the experiment.

The data in figures 7.1.8 and 7.1.9 suggest that the designated cells are synchronous and become more synchronous over the duration of the experimental time period. The cells appear to follow a specific response pattern with relation to one another and maintain this pattern throughout the duration of the experiment. The data in figures 7.1.8 and 7.1.9 demonstrate that the cells are relatively synchronous throughout the duration of the experiment. The first response to ACh shown in figure 7.1.8 occurs in the absence of 200 μ M NOC-12 and the cells are still obviously synchronous so the synchronicity is not a result of the NOC-12. However, the cells do seem to become more synchronous over the duration of the experimental time period as is clear in figure 7.1.9 so NOC-12 may enhance synchronicity but does not appear to induce it based on these data.

So in summary when acinar cells oscillate there is a tendency for the oscillatory signals to adopt very similar periodicity and phase. This tendency increases with the application of repeated stimulation with ACh but in contrast cells that are not touching show no evidence of synchronisation and have varying periodicity and phase. The data presented here show that the Ca²⁺ signal may serve to integrate the secretory responses of individual acinar cells into a functional unit. Furthermore, prolonged exposure to NO did not affect the aspect of cell to cell signalling which is very important as NO did induce desensitisation at the single cell level. When the cells are not in direct contact there is not opportunity for cell to cell communication and as a

result there is no cell to cell communication. These data suggest that when cells are in direct contact they do appear to talk and NO seems to increase the degree of synchronisation over the experimental time period. However, in these experiments it is hard to determine whether any one cell is acting to direct the function of those near based on the use of primary perfusion which bathes all cells equally. But the data presented in figure 7.1.6 does suggest cell to cell communication and shows clear periodicity and the ability of one cell to drive the response in other neighbouring cells. So the existence of cell to cell communication in acinar cells would provide an opportunity to understand how limiting factors may induce hypofunction of the whole gland in SjS.

Chapter Eight

Discussion, Conclusion & Future Work



UNIVERSITY OF
LIVERPOOL

8.1 Introduction

Sjögren's syndrome (SjS) is one of the three most common autoimmune disorders (Pillemer, Matteson et al. 2001), which has been demonstrated to have a population prevalence similar to that of rheumatoid arthritis (Hazes and Silman 1990). Individuals with SjS have been noted to have features which predispose them to development of the disease. Evidence shows that sufferers have specific genetic similarities in relation to HLA-linkages and in particular there is a prevalence of HLA-DR2, DR3, DR5 and HLA-B8 (Scully 1986; Fox, Tornwall et al. 1999; Jonsson, Haga et al. 2000). It is also likely that there is a hormone related factor which may contribute to the disease in SjS based on the strong sexual dimorphism with female prevalence at a ratio of 9:1 compared to males (Scully 1986). Depending on genetic predisposition any immune response which affects homeostasis of the glandular environment may give rise to glandular dysregulation and result in the development of autoimmunity.

It was originally assumed that the lack of saliva produced by SjS patients was the direct result of glandular atrophy as a consequence of immune mediated destruction of the acinar cells (Scully 1986). However, it was more recently observed that most SjS patients have large quantities of residual acinar tissue which appears histologically normal but simply does not function (Fox and Maruyama 1997; Fox, Tornwall et al. 1999; Humphreys-Beher, Brayer et al. 1999). Following the realisation that many SjS patients have residual tissue, Dawson and colleagues conducted experiments on human labial acinar cells taken from SjS patients and demonstrated that the cells have the ability to respond to stimulation in vitro (Dawson, Field et al. 2001). However, the cells do exhibit decreased sensitivity to ACh which was shown as a right shift in concentration dependence. Such findings suggest that the lack of

fluid secretion observed in SjS is not a direct result of glandular atrophy but more likely a result of glandular hypofunction. Advancements in the understanding of SjS and the identification of the underlying mechanisms involved give greater scope for the development of future treatments and future hope for SjS patients.

One factor which is clear is that when salivary glands respond to an insult they always induce inflammation regardless of the source of the initial challenge. Inflammation of the salivary glands is associated with increases in capillary permeability which would most likely be mediated by NO. NO is a known potent vasodilator and was originally identified based on its relaxation of endothelial tissue.

Desensitisation of the acinar cells and the stress conditions induced are the primary focus of the research presented in this thesis and may go some way to explain the glandular hypofunction observed in SjS.

The determination that NO is elevated in SjS may have important implications as the data strongly suggest that NO may have the ability to modulate the magnitude of the $[Ca^{2+}]_i$ subsequent to salivary acinar cell stimulation by agonist. In Sjögren's syndrome sources of NO include not only that produced by invading immune cells but also NO may be produced by the salivary and lacrimal acinar cells themselves as NOS activity and cGMP production were significantly increased following activation of muscarinic receptors by antimuscarinic antibodies or carbachol (Bacman, Berra et al. 1998; Perez Leiros, Sterin-Borda et al. 1999; Bacman, Berra et al. 2001) in a Ca^{2+} -dependent manner. Any increased permeability induced by NO would allow inflammatory bodies such as lymphocytes and macrophages to enter the glandular interstitium and these are also known to release NO so could in theory increase the problem induced by NO as they allow more NO to become available which in turn would allow more lymphocytes to enter the salivary glands.

8.2 A Possible role for nitric oxide in acinar hypofunction

The primary focus of this investigation was the identification of the physiological roles of NO in the fluid secretion pathway.

The sum of the data presented here could indicate that NO may have a physiological role under normal conditions and may function acutely to induce an increased rate of secretion by sensitising the acinar cells to ACh. It is impossible to determine the actual physiological levels of NO as it is rapidly broken down so we do not know the actual levels present *in vivo* as they would be difficult to determine so we cannot say how accurately the levels we used *in vivo* compare to those found *in vitro*. My findings also highlighted a possible role for NO in the development of acinar hypofunction through desensitisation of the acinar cells to ACh following chronic exposure to NO. The NO induced desensitisation could suggest a role for NO in SjS.

This interest in NO is based on the knowledge that increased levels of NO have been demonstrated in both the saliva (Konttinen, Platts et al. 1997) and the expired air from patients with SjS (Ludviksdottir, Janson et al. 1999). It has also been reported that the levels of NOS are elevated in the labial glands of patients with SjS (Konttinen, Platts et al. 1997) and evidence suggests that SjS IgG may have the capacity to increase levels of NOS and cGMP in both salivary and lacrimal acinar cells (Bacman, Berra et al. 1998; Perez Leiros, Sterin-Borda et al. 1999; Bacman, Berra et al. 2001).

NO donors have previously been used to stimulate salivary acinar cells to mobilise Ca^{2+} (Looms, Tritsaris et al. 2001), which was suggested to most likely occur through activation of the RyR. Previous work conducted in other cell types (Galione, McDougall et al. 1993; Galione, White et al. 1993) determined that the formation of

cADPr was linked to the formation of cGMP, which in turn is produced in response to cell stimulation with NO (Denninger and Marletta 1999) and this was confirmed by the 2001 study by Looms and colleagues (Looms, Tritsarlis et al. 2001). We initially found that higher concentrations of NO donor were able to induce spontaneous Ca^{2+} release, in the absence of agonist stimulation (Figure 3.1.1). In this study it was demonstrated that exposure of mouse submandibular acinar cells to NO initially increased the acinar cells sensitivity to ACh. This initial amplification of the response induced by NO may be explained by the normal secretory pathway involving cADPr (Galione, McDougall et al. 1993; Galione and White 1994); (Guse 1999); (Galione and Churchill 2000; Galione and Churchill 2002). We understand how hypersecretion may be induced by NO and the amplification induced by acute application of NO observed in my data makes sense in relation to current knowledge. This type of phenomenon has previously been reported in mouse submandibular acinar cells that were exposed to cADPr prior to stimulation with ACh (Harmer, Gallacher et al. 2001). In acinar cells the release of Ca^{2+} through the RyR is not considered to be the point of initiation of the Ca^{2+} signal but these results are consistent with data which demonstrated that high concentrations of cADPr, which is now known to be the endogenous RyR agonist, induced mobilisation of Ca^{2+} (Galione and White 1994); (Harmer, Smith et al. 2001).

The most likely role of cADPr and RyR is modulation of the ACh-evoked Ca^{2+} signal but it must also be noted that mobilisation of Ca^{2+} following cADPr stimulation of RyR is not necessarily coupled to activation of an extracellular receptor. My experimental protocol was designed to be as close as possible to physiological conditions in order to determine whether NO had the capacity to function in a regulatory role with regard to RyR, however the concentrations selected were levels which we believed would be most appropriate to levels found in SjS patients but as stated previously it is

impossible to determine this accurately due to the very nature of NO. My data show that, in both human and mouse submandibular cells and also mouse lacrimal cells, exposure to NO donor enhanced the subsequent response to agonist stimulation. This is most likely the direct result of NO release rather than an artefact of a particular NO donor because similar enhancement was observed using three chemically unrelated NO donors, SNAP, SNP and NOC-12 and also a second type of NOC, NOC-5. The increased levels of cADPr induced by NO would be expected to induce increased acinar cell sensitivity to ACh and may also account for findings in MRL/lpr mice whose cells exhibited hypersensitivity to ACh in vitro (Zoukhri, Hodges et al. 1998).

The amplification of the ACh response was suggested to be induced through the cADPr pathway and the use of two inhibitors of this pathway, ODQ and Ryanodine, demonstrated that this was most likely the case. Both inhibitors removed the previously observed NO induced amplification. These two inhibitors were selected as ODQ blocks the activation of sGC and so acts at the initiation of the pathway and Ryanodine blocks the RyR directly and so acts at the termination of the pathway. These two inhibitors prove that the NO induced amplification of the ACh response in acinar cells is acting in a cGMP-dependent manner. However, in SjS we observe hypofunction not hyperfunction and so proposed that the hypofunction which may be induced by NO must occur over a more prolonged time period so more chronic experiments were conducted.

When the acinar cells were exposed to NO chronically the major observation was the induced inhibition of response to ACh over time. This was again proved to be independent of the NO donor type used as all NO donors exhibited a similar pattern of response. The type of cell used also had no effect on outcome as all three cell types exhibited a similar pattern of response to NO donor. The sum of these findings

may suggest a possible universal mechanism which is conserved between cell types and also between species.

The cause of the inhibition was suggested to be most likely the direct result of Ca^{2+} store depletion which would be logical as if the stores are depleted there is no Ca^{2+} to mobilise which would result in a lack of response to ACh. However, this was proved not to be the case as the use of Thapsigargin, an inhibitor of the SERCA pump (Smith and Gallacher 1994); (Smith and Reed 1996), induced an observable Ca^{2+} response (Figure 3.1.12) and so demonstrated that stores were still able to function and inhibition is not the result of a lack of Ca^{2+} . This then suggested that the inhibition could be related to the cGMP pathway but the use of ODQ disproved this as the reduction in response to ACh still occurred in the presence of ODQ so the inhibition is independent of the cGMP pathway.

The next suggested cause was desensitisation of the RyR directly, but inhibition of the ACh response still occurred when Ryanodine was used following prolonged exposure to NO. These data were more problematic than ODQ as the use of Ryanodine in the absence of NO donor induced a significant inhibition of the ACh response in all three cell types, this is understandable as Ryanodine acts to block the RyR directly. There appeared to be no observable additive effect between ryanodine and NO donor together in the mouse submandibular and lacrimal acinar cells. However, there was some degree of additive effect observed in the human submandibular acinar cells as the level decreased more rapidly when NOC-12 and Ryanodine were used together than when NOC-12 was used alone and when only Ryanodine was used an increased level of inhibition was also observed in this cell type. This suggests that the human submandibular cells are more sensitive to Ryanodine than the mouse cells but the human cells were generally more sensitive. The sum of these findings suggests that the inhibition induced by NO was

independent of the cGMP pathway but as figure 3.1.12 proved it was not a result of Ca^{2+} store depletion which led to the suggestion that the inhibition may be the result of nitrosylation.

Until relatively recently it was thought that the only outcome of nitrosylation was apoptosis as apoptosis occurred when proteins were nitrosylated (Sarih, Souvannavong et al. 1993) and other evidence showed that local high concentrations of NO may induce nitrosylation of aa residues which could cause cellular dysfunction and possibly promote cell death (Denninger and Marletta 1999). However, it has since been determined that apoptosis is not the only consequence of nitrosylation as it has been shown that the nitrosylation of cysteine residues could regulate the function of a broad spectrum of proteins (Stamler, Lamas et al. 2001); (Dickinson and Forman 2002); (Brune 2005). Most recently there is evidence demonstrating the presence of signature residues or motifs within proteins that have the potential to act as targets for nitrosylation. Such motifs have been identified and extensively studied in RyR (Dulhunty, Gage et al. 2001); (Sun, Xu et al. 2003). However, these motifs are also found in the IP_3R (Khan, Wagner et al. 2006), which is unsurprising based on their homology. We have no evidence to indicate that RyR are being down-regulated through nitrosylation and other components of the stimulus-secretion pathway may be the target of nitrosylation not RyR. There is also evidence to suggest that the targets of nitrosylation include muscarinic receptors and upon nitrosylation, the distribution of receptors at the cells surface may be affected (Maggio, Barbier et al. 1995); (Wang, Moniri et al. 2006), which is another possible explanation for the desensitisation of the acinar cells to ACh. However, inhibition induced by nitrosylation of some component of the stimulus secretion pathway, perhaps RyR may provide the basis for a mechanism to explain the observed right shift in dose dependence in the labial glands of SjS patients (Dawson, Field et al. 2001) and also explain the desensitisation induced by NO observed in the experiments presented here.

So in summary, although the best understood mechanism by which NO exerts its effects on cellular function is cGMP-dependent through the activation of sGC (Denninger and Marletta 1999), there are many ways in which NO is thought to mediate its biological effects both directly and indirectly such as nitrosylation (reviewed (Blaise, Gauvin et al. 2005)). The evidence presented from the chronic experiments is consistent with a role for NO in glandular hypofunction by a cGMP independent mechanism. This is possibly through s-nitrosylation of a key component of the stimulus-secretion pathway which is as yet unidentified. All four NO donors (SNAP, SNP, NOC-12 and NOC-5) produced similar patterns of response with the only variation being the degree of the response to ACh which was most likely related to the rate of NO release of the individual NO donors but was not investigated further. Acinar cells were also incubated with NO donors to determine the effect of NO following longer term chronic exposure, however, this appeared to have no obvious effect as hypofunction did not occur in the absence of repeated ACh stimulation but it was noted that when cells were stimulated with ACh the observed change in $[Ca^{2+}]_i$ was much lower than the previous control responses which were not pre-incubated and as stated previously were reduced by approximately 50% compared to control.

So these data could certainly go some way towards explaining the observed right shift in the ACh concentration dependence in human labial glands from SjS patients (Dawson, Field et al. 2001) based on the knowledge that NO is known to be elevated in SjS (Konttinen, Platts et al. 1997); (Ludviksdottir, Janson et al. 1999); (Wanchu, Khullar et al. 2000); (Pertovaara, Antonen et al. 2007). It may be the chronic NO exposure of the salivary acinar cells of SjS patients *in vivo* which causes the reduced sensitivity of the acinar cells to ACh. We were able to re-produce this outcome *in vitro* by chronically exposing healthy acinar cells, from both human and mouse sources, to NO which led to the production of SjS like cells from previously healthy acinar cells. We have demonstrated that nitric oxide from four different nitric oxide

donors is capable of significantly reducing or totally abolishing the acinar $[Ca^{2+}]_i$ response to ACh and so has the capacity to induce glandular hypofunction. NO therefore fits into the proposed alternative non-apoptotic SjS model (Dawson, Fox et al. 2006).

8.3 A Possible role for adenosine tri-phosphate in acinar hypofunction

The key theme of this thesis is desensitisation and the occurrence of stressful conditions in acinar cells. ACh is not the only Ca^{2+} mobilising agonist to which acinar tissue may be exposed *in vitro*. The other Ca^{2+} mobilising agonist which has been implicated under stressful conditions is ATP and ATP is suggested to act as a possible stress mediator. We wanted to see if time course and progression of a Ca^{2+} signal in response to ATP differed significantly from ACh. ACh has a specific and well characterised response pattern which initiates at the apical pole and spreads from there to the basolateral pole. We speculated that an ATP mediated signal may originate at a different point in the cell. Such variations in initiation point would allow a clear distinction between Ca^{2+} mediated fluid secretion and a Ca^{2+} mediated stress signal. My data (figure 6.1.1 part A) demonstrated the ability of mouse and human submandibular acinar cells and mouse lacrimal acinar cells to respond to ATP.

The ability to mobilise Ca^{2+} in response to stimulation by ATP has previously been demonstrated in both rat submandibular (McMillian, Soltoff et al. 1987; McMillian, Soltoff et al. 1988); (Dehaye, Moran et al. 1999) and mouse parotid gland (Gallacher 1982) and data have suggested that the ability to secrete in response to ATP may be mediated by P2X and P2Y. More recent data demonstrated the ability of isolated human labial glands to respond to ATP (Pedersen, Dissing et al. 2000). My data (figure 6.1.1 parts B and C) also demonstrated a degree of additive effect between

ACh and ATP. Based on the responses observed we may speculate that the response to both agonists is likely to occur through the same pathway and using the same G-protein coupled receptors. The ATP activity is likely to be through the P2Y which are known to be associated with G-protein activation. When the two agonists were used in conjunction there was an obvious additive effect, this was observed as an increased response as the level increased by approximately the same level as the ATP response when ATP was used in conjunction with ACh. If ATP and ACh mobilised Ca^{2+} from the same intracellular stores then this additive effect would not be observed.

At first sight it appears that the additive nature of the Ca^{2+} signal would suggest that at least some of the Ca^{2+} is mobilised by an alternative subset of Ca^{2+} stores by ATP. ACh may have a certain specific Ca^{2+} pool and ATP possibly has an alternative Ca^{2+} pool (Berridge, Lipp et al. 2000); (Petersen, Tepikin et al. 2001); (Berridge 2006); (Petersen and Tepikin 2008). This variation in pool may be the key to the variation in response that ACh and ATP induce as the mobilisation of Ca^{2+} from different stores may produce a different Ca^{2+} signal and this stimulates the variation in response of the acinar cells. My data also demonstrated the lack of an oscillatory response pattern following stimulation with ATP but an oscillatory response pattern was frequently observed when cells were stimulated with ACh which may also suggest that a possible variation in response pattern between these two agonists may be the factor which results in a variation in outcome and how Ca^{2+} may regulate two totally different signal types.

Following the initial observation that the response patterns induced by ACh and ATP where apparently the same response pattern across the cell was tracked to produce an experimental time course for each agonist (figures 6.1.2 and 6.1.3). The results suggested no variation in response between ACh and ATP as the images show that

the response initiates at approximately the same point following stimulation with either agonist. This may possibly be due to limitations in the sampling system that was used as the resolution may not be adequate to visualise such variations in initiation point. The sum of these results suggested that there may not be differences in the initiation point of the signal between ACh and ATP but there could be variations in the Ca^{2+} pool that is mobilised following agonist stimulation but the data also suggests that the Ca^{2+} signal in response to ATP may be carried in the same manner as an ACh induced signal. This would mean that the same mechanisms are involved and the signal would also initiate at the apical pole and like a response to ACh would move from the apical pole to the basolateral (Thorn, Lawrie et al. 1993); (Harmer, Smith et al. 2005). This would explain the lack of variation in initiation point and may explain why signals induced by ACh and ATP appear to be the same.

8.4 A Possible role for cell - cell coupling in acinar hypofunction

The results so far have focussed on the factors which may induce acinar cell hypofunction at the single cell level. The functional unit of the salivary gland is more likely to be the acinus not the individual acini. The results presented in this section aim to shift the focus from the individual cell to the response of the cell as part of a group. The nature of the epilemmal arrangement of the nerves and the limited innervation within the salivary glands (Garrett and Kidd 1993) would be explained by cell to cell coupling as all cells within the salivary gland are unlikely to be exposed to the same stimulus. Cell to cell communication could function to propagate the signal to those cells which are less directly exposed to stimulus. So the organisation of the gland must allow signals to perpetuate throughout the gland with only a relatively limited nerve/acinar cell interface. If there is no actual variation between the

individual acinar cells within an acinus then there will automatically be variations in the level of stimulation that each cell receives based on glandular innervation as some cells will always receive higher doses of stimulant simply due to their position with relation to the nerves. Communication between acinar cells would allow for unification of the response signal following stimulation. It would be pointless for cells to just signal randomly or for only one cell to be stimulated so there must be some degree of communication present in salivary acinar cells.

The experiments that we conducted in vitro were unable to mimic the exact effects experienced by the cells in vivo. The primary perfusion system stimulated all cells simultaneously which made the process of determining cell to cell coupling more difficult. The $[Ca^{2+}]_i$ was inclined to rise simultaneously in all acinar cells within the small clumps investigated. However, there were occasions when agonist stimulation gave rise to a series of oscillations in $[Ca^{2+}]_i$ and not prolonged plateau. When such responses occurred it presented the opportunity to observe the pattern of response and the progression of signal between cells. It became evident that in cells where communication was absent the oscillatory pattern was similar but there was no suggestion that the basic frequency was the same. Figures 7.1.1 and 7.1.2 were produced from cells situated in separate acini and so could not possibly be in direct contact and shared oscillatory pattern was observed which is what we anticipated as this lack of contact removes the cells ability to communicate directly with one another. These cells have no apparent natural frequency at which they respond and the lack of contact suggests that the lack of synchrony is due to a lack of cell to cell communication.

These data show that acinar cells do not appear to have the same fundamental frequency and there was no evidence to suggest that acinar cells have a natural basic frequency at which to oscillate. Cells respond at a similar frequency but are

never synchronous as only tiny variations in the frequency will deter the cells from hitting and assuming the same phase if cells do not communicate cell to cell as shown in figures 7.1.3 to 7.1.5, which are situated within the same acini but do not appear to be communicating.

There is no direct reason why cells should be synchronous if they are not communicating because if they are not communicating they should never be synchronous. These data suggests two things: (i) cells do appear to communicate under normal circumstances; (ii) acinar cells must be in direct contact with one another for communication to occur.

The data in figure 7.1.9 shows that 1 cell appears to be in charge of the oscillation frequency. This would suggest the presence of pacemaker cells like those found in cardiac tissue (Bers 1991); (Katz 1992) which fire first in response to stimulation, as the pacemaker cells are those with the highest natural frequency and this frequency drives the response. So in acinar cells the cell which drives the frequency would be assumed to be the one with the highest natural frequency which would then produce a co-ordinated output like that observed in cardiac tissue. This type of response is observable in figure 7.1.6 which shows cells responding synchronously but cell one appears to drive the response and has an oscillatory pattern which is twice the frequency of the other cell. So this driving cell has a base frequency which is twice that of the other cell and as a result proceeds to induce the other cell to respond in the same phase and although the other cell is not as active it is still able to respond in exactly the same phase as the driving cell.

The results suggest that acinar cells do talk to each other and this may be a way of synchronising the cells of an acinus in a co-ordinated way to nerve stimulation. NO was observed to desensitise the cells at a single cellular level and if it also has the

ability to inhibit cell to cell coupling then it may give rise to desensitisation at the level of the acinus. However, the data suggested that NO does not have an effect on cell to cell coupling and does not induce reduced synchronisation as shown in figures 7.1.7 to 7.1.9 which show cells which are synchronised and responding together in phase and period in both the absence and presence of NO. Over the experimental time course of these experiments we did not observe any reduction in the level of cell to cell synchronisation of signalling. The data indicate that NO might actually enhance the level of synchronisation as the response in figure 7.1.9 is more synchronous than that observed in 7.1.8. So in summary we had expected to see reduced synchronisation in response to the presence of NO based on the desensitisation induced by NO at the single cell level which would make the gland less functional, but NO does not appear to affect synchronisation and does not appear to induce inhibition of response at the acinus level so the role of NO in cell to cell coupling is unclear.

So in summary the results presented in this study suggest that acinar cells do communicate in an intercellular manner and there is likely to be cellular coupling within the salivary glands. Intercellular signalling has been observed previously in acinar cells from rat parotid tissue using ATP and CCh (Segawa, Takemura et al. 2002). Their data demonstrated a variation in synchronicity of signalling between acini and duct cells and also more importantly that acinar cells within an acinus respond synchronously and behave as a functional unit (Segawa, Takemura et al. 2002). My data would suggest that this may also occur in mouse submandibular acinar cells. The presence or absence of synchronisation is most likely due to variations between cells as observed in the variation between results from apparently similar groups of cells (figures 7.1.3 to 7.1.5 and 7.1.7 to 7.1.9). Cells must be in direct contact with one another to communicate as shown by figure 7.1.1 and 7.1.2 as these cells exhibited no signs of synchronicity.

These data also suggest that NO acts to increase the sensitivity of the cells to ACh and so make the cells more able to respond in a synchronous manner, so NO may act to prime the cells to ACh and enhance cellular coupling under normal conditions. However, in SjS the levels of NO are elevated which may lead to an excessive level of activation and unlike under normal conditions the level of enhancement induced by NO may be detrimental to cellular coupling which may reduce the level of synchronicity and therefore enhance the glandular hypo-function. In order for the whole acinus to function as a single unit there must be cell to cell communication as although individual cells function in response to stimulation the whole acinus will respond as a functional unit without cell to cell communication. These data also suggest that some cells do appear to have slightly increased frequencies of response and cells do appear to communicate which would be all that is required to make the acinus function as a unit.

So the theory of cell coupling in salivary glands could provide a suitable explanation as to why the individual cells within the salivary glands function as a whole unit and if these so called 'pacemaker' cells do exist it could go some way to explain why the infiltrating lymphocytes occur at such specific areas of the gland and have the ability to disable a whole gland through inhibition of a few cells. In summary the theory of cell to cell coupling with relation to SjS is extremely intriguing as it would provide a viable link between glandular hypofunction and the observable key features in SjS.

8.5 A mechanism to account for acinar hypofunction in Sjögren's syndrome

When you consider the vast number of interactions that are necessary for fluid secretion and the complexity of the process as a whole numerous factors could be responsible or involved in the SGH exhibited in SjS patients. The results from this study suggest that one of the most likely factors is de-sensitisation of the acinar cells to ACh and it would be expected that over time the lack of sensitivity to ACh and lack of function of the salivary glands would lead to glandular atrophy which would account for the classical model of destruction being the cause of SGH in SjS. The data from this study also show that cell coupling is likely to play an enormous part in SGH and would offer a viable explanation for the specificity of the lymphocytic infiltration points and how a relatively small number of lymphocytes may elicit inhibition in a whole gland. The progression of the disease is still unclear and even the initiating event is open to debate as the events which lead to the development of many autoimmune diseases such as SjS are still poorly understood.

We hypothesise based on the evidence presented in this study that the focal infiltration may be directed by the cellular organisation of the gland and the infiltrating cells may be attracted to the suggested 'pace-maker' cells. The elevated levels of NO may act to enhance this situation further by both allowing increased capillary permeability and by also de-sensitising individual acinar cells, which in combination could explain hypo-function of the whole gland.

It is highly likely that many factors are involved in the desensitisation of the acinar tissue in SjS which eventually leads to SGH. NO is produced following activation of NOS and the concentration of NO surrounding the acinar cells would be further increased by secretion of NO from the surrounding nerves but the greatest amount

would be produced by the invading lymphocytes and macrophages, as NO is known to be produced at high concentrations by specialised immune cells such as macrophages and lymphocytes (Forstermann, Gath et al. 1995); (Lomniczi, Suburo et al. 1998). As the local concentration of NO increases there would be increased activation of sGC which would result in a subsequent increase in the intracellular concentration of cGMP. My data demonstrates that NO either directly or through activation of the RyR via cADPr alters acinar sensitivity to ACh. Following long term exposure to NO the cell changes state from hyper-excited to hypo-excited as it becomes less sensitive to ACh and as my data also suggested a process that may be mediated by a loss of muscarinic receptors based on inhibitory data. My study demonstrated that chronic exposure to NO did affect the ability of an acinar cell to respond to agonist. The acinar cells used in these experiments were isolated primary cells. My data also demonstrated that although NO did not induce cell coupling and synchronisation of the oscillatory pattern of the response it did appear to enhance the oscillatory pattern and made the cells more synchronised and so may also act as an intercellular messenger.

These ideas for the development of acinar hypofunction in SjS are still speculative, but we do appear to be getting closer to understanding the development of the disease and ultimately the cause of SGH in SjS following the initial attempts made to explain the novel finding of acinar desensitisation in SjS. The evidence suggesting the presence of synchronisation in acinar cells and the idea of cell coupling would go some way to explain and connect the many separate areas of research in SjS.

Conclusion

Following chronic exposure to NO the acinar cells become desensitised in response to ACh. This desensitisation is seen in both submandibular and lacrimal and both human and mouse cells. My belief is that this desensitisation would be an important general mechanism that could possibly amplify the effects of other antiseecretory agents such as the M3R antibodies found in some SjS individuals and so may account for the glandular hypofunction which is observed in SjS. So NO is suggested as a unifying feature and is likely to have a primary role in the development of glandular hypofunction in SjS as the results presented here demonstrate how chronic exposure to NO induced healthy acinar cells to become SjS like and much less sensitive to ACh. The presence of cell to cell communication may also provide a plausible explanation as to why in the case of SjS patients a small number of invading lymphocytes may inhibit a whole gland.

Future work

In order to further explore the cause of acinar desensitisation to agonist in SjS, the point of NO activity must be determined as it appears to work independently of the cGMP pathway to induce hypo-function. The use of Biotinylation may prove useful to identify points of nitrosylation (Jaffrey, Erdjument-Bromage et al. 2001; Jaffrey and Snyder 2001) in acinar cells. The process identifies points of nitrosylation using the biotin switch method and visualises using immunoblotting techniques which may prove useful for mapping the effect of NO in acinar cells.

Further work conducted using more specific application of ATP may demonstrate variations in signal initiation points. A Patch clamp pipette could be used to administer ATP more directly to specific regions of a cell or the sampling rate may be increased to allow improved visualisation of the response initiation points.

Further work on cell to cell coupling including the use of patch clamp pipette on specific individual cells within a small cell clump to identify signal propagation between cells and how external factors may affect cell to cell coupling such as the use of IP₃ which has previously been suggested as a possible intercellular signalling molecule (Rottingen and Iversen 2000).

The aim of this work is to provide hope for patients with SjS and also to allow the future development of treatments at least for those still in the early stages of the disease and hopefully to offer some alleviation of symptoms in most.

Bibliography



UNIVERSITY OF

LIVERPOOL

- Abbracchio, M. P. and G. Burnstock (1994). "Purinoreceptors: are there families of P2X and P2Y purinoreceptors?" Pharmacol Ther 64(3): 445-75.
- Abi-Gerges, N., L. Hove-Madsen, et al. (1997). "A comparative study of the effects of three guanylyl cyclase inhibitors on the L-type Ca²⁺ and muscarinic K⁺ currents in frog cardiac myocytes." Br J Pharmacol 121(7): 1369-77.
- Ahn, J. S., J. M. Camden, et al. (2000). "Reversible regulation of P2Y(2) nucleotide receptor expression in the duct-ligated rat submandibular gland." Am J Physiol Cell Physiol 279(2): C286-94.
- Al-Sa'doni, H. and A. Ferro (2000). "S-Nitrosothiols: a class of nitric oxide-donor drugs." Clin Sci (Lond) 98(5): 507-20.
- Al-Sa'doni, H. H., I. Y. Khan, et al. (2000). "A novel family of S-nitrosothiols: chemical synthesis and biological actions." Nitric Oxide 4(6): 550-60.
- Ambudkar, I. S. (2000). "Regulation of calcium in salivary gland secretion." Crit Rev Oral Biol Med 11(1): 4-25.
- Ayling, L. J., G. S. Whitley, et al. (2006). "Dimethylarginine dimethylaminohydrolase (DDAH) regulates trophoblast invasion and motility through effects on nitric oxide." Hum Reprod 21(10): 2530-7.
- Bacman, S., A. Berra, et al. (2001). "Muscarinic acetylcholine receptor antibodies as a new marker of dry eye Sjogren syndrome." Invest Ophthalmol Vis Sci 42(2): 321-7.
- Bacman, S. R., A. Berra, et al. (1998). "Human primary Sjogren's syndrome autoantibodies as mediators of nitric oxide release coupled to lacrimal gland muscarinic acetylcholine receptors." Curr Eye Res 17(12): 1135-42.
- Baker, O. J., J. M. Camden, et al. (2008). "P2Y2 nucleotide receptor activation up-regulates vascular cell adhesion molecular-1 expression and enhances lymphocyte adherence to a human submandibular gland cell line." Mol Immunol 45(1): 65-75.
- Baum, B. J. and R. B. Wellner (1999). "Receptors in Salivary Glands." In: Garrett, J.R., Ekstrom, J., Anderson, L.C. (Eds.), Neural Mechanisms of Salivary Secretion 3: 44-58.
- Bell, M., A. Askari, et al. (1999). "Sjogren's syndrome: a critical review of clinical management [published erratum appears in J Rheumatol 1999 Dec;26(12):2718]." J Rheumatol 26(9): 2051-61.
- Bergfeld, G. R. and T. Forrester (1992). "Release of ATP from human erythrocytes in response to a brief period of hypoxia and hypercapnia." Cardiovasc Res 26(1): 40-7.
- Berridge, M. J. (1993). "Inositol trisphosphate and calcium signalling." Nature 361(6410): 315-25.
- Berridge, M. J. (1994). "The biology and medicine of calcium signalling." Mol Cell Endocrinol 98(2): 119-24.
- Berridge, M. J. (1995). "Capacitative calcium entry." Biochem J 312(Pt 1): 1-11.
- Berridge, M. J. (1997). "Elementary and global aspects of calcium signalling." J Exp Biol 200(Pt 2): 315-9.

- Berridge, M. J. (1998). "Neuronal calcium signaling." Neuron 21(1): 13-26.
- Berridge, M. J. (2005). "Unlocking the secrets of cell signaling." Annu Rev Physiol 67: 1-21.
- Berridge, M. J. (2006). "Calcium microdomains: organization and function." Cell Calcium 40(5-6): 405-12.
- Berridge, M. J., P. Lipp, et al. (2000). "The versatility and universality of calcium signalling." Nat Rev Mol Cell Biol 1(1): 11-21.
- Bers, D. M. (1991). "Excitation coupling and cardiac contractile force " Kluwer Academic Publishers 119-148, 171-204.
- Berstein, G., J. L. Blank, et al. (1992). "Phospholipase C-beta 1 is a GTPase-activating protein for Gq/11, its physiologic regulator." Cell 70(3): 411-8.
- Bezprozvanny, I. (2005). "The inositol 1,4,5-trisphosphate receptors." Cell Calcium 38(3-4): 261-72.
- Bezprozvanny, I., J. Watras, et al. (1991). "Bell-shaped calcium-response curves of Ins(1,4,5)P₃- and calcium-gated channels from endoplasmic reticulum of cerebellum." Nature 351(6329): 751-4.
- Blaise, G. A., D. Gauvin, et al. (2005). "Nitric oxide, cell signaling and cell death." Toxicology 208(2): 177-92.
- Bloch, K. J., W. W. Buchanan, et al. (1956). "Sjogrens Syndrome: a clinical, pathological and serological study of 62 cases." Medicine (Baltimore) 44: 187-231.
- Boarder, M. R. and S. M. Hourani (1998). "The regulation of vascular function by P2 receptors: multiple sites and multiple receptors." Trends Pharmacol Sci 19(3): 99-107.
- Bodin, P. and G. Burnstock (2001). "Purinergic signalling: ATP release." Neurochem Res 26(8-9): 959-69.
- Boitano, S., E. R. Dirksen, et al. (1992). "Intercellular propagation of calcium waves mediated by inositol trisphosphate." Science 258(5080): 292-5.
- Bowman, S. J. (2002). "Collaborative research into outcome measures in Sjogren's syndrome. Update on disease assessment." Scand J Rheumatol Suppl(116): 23-7.
- Bowman, S. J., G. H. Ibrahim, et al. (2004). "Estimating the prevalence among Caucasian women of primary Sjogren's syndrome in two general practices in Birmingham, UK." Scand J Rheumatol 33(1): 39-43.
- Boyer, J. L., G. L. Waldo, et al. (1992). "Beta gamma-subunit activation of G-protein-regulated phospholipase C." J Biol Chem 267(35): 25451-6.
- Bredt, D. S., P. M. Hwang, et al. (1991). "Cloned and expressed nitric oxide synthase structurally resembles cytochrome P-450 reductase." Nature 351(6329): 714-8.
- Brennan, P. A., T. Umar, et al. (2000). "Expression of nitric oxide synthase in pleomorphic adenomas of the parotid." Br J Oral Maxillofac Surg 38(4): 338-42.

- Brown, D. A., J. I. Bruce, et al. (2004). "cAMP potentiates ATP-evoked calcium signaling in human parotid acinar cells." J Biol Chem 279(38): 39485-94.
- Brune, B. (2005). "The intimate relation between nitric oxide and superoxide in apoptosis and cell survival." Antioxid Redox Signal 7(3-4): 497-507.
- Brunner, F., H. Stessel, et al. (1995). "Novel guanylyl cyclase inhibitor, ODC reveals role of nitric oxide, but not of cyclic GMP in endothelin-1 secretion." FEBS Lett 376(3): 262-6.
- Burnstock, G. (1981). "Review lecture. Neurotransmitters and trophic factors in the autonomic nervous system." J Physiol 313: 1-35.
- Caulfield, M. P. (1993). "Muscarinic receptors--characterization, coupling and function." Pharmacol Ther 58(3): 319-79.
- Caulfield, M. P. and N. J. Birdsall (1998). "International Union of Pharmacology. XVII. Classification of muscarinic acetylcholine receptors." Pharmacol Rev 50(2): 279-90.
- Chahwala, S. B. and L. C. Cantley (1984). "Extracellular ATP induces ion fluxes and inhibits growth of Friend erythroleukemia cells." J Biol Chem 259(22): 13717-22.
- Charest, R., P. F. Blackmore, et al. (1985). "Characterization of responses of isolated rat hepatocytes to ATP and ADP." J Biol Chem 260(29): 15789-94.
- Chaulet, H., C. Desgranges, et al. (2001). "Extracellular nucleotides induce arterial smooth muscle cell migration via osteopontin." Circ Res 89(9): 772-8.
- Chow, S. C., G. E. Kass, et al. (1997). "Purines and their roles in apoptosis." Neuropharmacology 36(9): 1149-56.
- Chung, H. T., H. O. Pae, et al. (2001). "Nitric oxide as a bioregulator of apoptosis." Biochem Biophys Res Commun 282(5): 1075-9.
- Ciccarelli, R., P. Ballerini, et al. (2001). "Involvement of astrocytes in purine-mediated reparative processes in the brain." Int J Dev Neurosci 19(4): 395-414.
- Ciccarelli, R., P. Di Iorio, et al. (1999). "Rat cultured astrocytes release guanine-based purines in basal conditions and after hypoxia/hypoglycemia." Glia 25(1): 93-8.
- Cimaz, R., A. Casadei, et al. (2003). "Primary Sjogren syndrome in the paediatric age: a multicentre survey." Eur J Pediatr 162(10): 661-5.
- Collo, G., R. A. North, et al. (1996). "Cloning OF P2X5 and P2X6 receptors and the distribution and properties of an extended family of ATP-gated ion channels." J Neurosci 16(8): 2495-507.
- Conti, A., L. Gorza, et al. (1996). "Differential distribution of ryanodine receptor type 3 (RyR3) gene product in mammalian skeletal muscles." Biochem J 316 (Pt 1): 19-23.
- Cooke, J. P. and V. J. Dzau (1997). "Derangements of the nitric oxide synthase pathway, L-arginine, and cardiovascular diseases." Circulation 96(2): 379-82.
- Cooke, J. P. and V. J. Dzau (1997). "Nitric oxide synthase: role in the genesis of vascular disease." Annu Rev Med 48: 489-509.

Cotton, S. A., A. L. Herrick, et al. (1999). "Endothelial expression of nitric oxide synthases and nitrotyrosine in systemic sclerosis skin." J Pathol 189(2): 273-8.

Coutinho-Silva, R., M. Parsons, et al. (2003). "P2X and P2Y purinoceptor expression in pancreas from streptozotocin-diabetic rats." Mol Cell Endocrinol 204(1-2): 141-54.

Culp, D. J., W. Luo, et al. (1996). "Both M1 and M3 receptors regulate exocrine secretion by mucous acini." Am J Physiol 271(6 Pt 1): C1963-72.

Dale, H. H. (1914). "The occurrence in ergot and action of acetylcholine." Journal of Physiology LXVIII(iii-iv).

Damas, J. (1994). "Pilocarpine-induced salivary secretion, kinin system and nitric oxide in rats." Arch Int Physiol Biochem Biophys 102: 103-5.

Daniels, T. E. (1984). "Labial salivary gland biopsy in Sjogren's syndrome. Assessment as a diagnostic criterion in 362 suspected cases." Arthritis Rheum 27(2): 147-56.

Daniels, T. E. and P. C. Fox (1992). "Salivary and oral components of Sjogren's syndrome." Rheum Dis Clin North Am 18(3): 571-89.

Dargie, P. J., M. C. Agre, et al. (1990). "Comparison of Ca²⁺ mobilizing activities of cyclic ADP-ribose and inositol trisphosphate." Cell Regul 1(3): 279-90.

Dash, P. R., J. E. Cartwright, et al. (2003). "Nitric oxide protects human extravillous trophoblast cells from apoptosis by a cyclic GMP-dependent mechanism and independently of caspase 3 nitrosylation." Exp Cell Res 287(2): 314-24.

Dawson, L. J., E. A. Field, et al. (2001). "Acetylcholine-evoked calcium mobilisation and ion channel activation in human labial gland acinar cells from patients with primary Sjögren's syndrome." Clinical and Experimental Immunology 124: 480-485.

Dawson, L. J., P. C. Fox, et al. (2006). "Sjogrens syndrome--the non-apoptotic model of glandular hypofunction." Rheumatology (Oxford) 45(7): 792-8.

Dawson, L. J., D. J. Holt, et al. (2001). "A comparison of salivary gland hypofunction in primary and secondary Sjogren's syndrome." Oral Dis 7(1): 28-30.

Dawson, L. J., P. M. Smith, et al. (2000). "Sjogren's syndrome-time for a new approach." Rheumatology (Oxford) 39(3): 234-7.

Dayoub, H., V. Achan, et al. (2003). "Dimethylarginine dimethylaminohydrolase regulates nitric oxide synthesis: genetic and physiological evidence." Circulation 108(24): 3042-7.

Dehay, J. P., A. Moran, et al. (1999). "Purines, a new class of agonists in salivary glands?" Arch Oral Biol 44 Suppl 1: S39-43.

Denninger, J. W. and M. A. Marletta (1999). "Guanylate cyclase and the .NO/cGMP signaling pathway." Biochim Biophys Acta 1411(2-3): 334-50.

Dewey, M. M. and L. Barr (1964). "A Study of the Structure and Distribution of the Nexus." J Cell Biol 23: 553-85.

- Dickinson, D. A. and H. J. Forman (2002). "Glutathione in defense and signaling: lessons from a small thiol." Ann N Y Acad Sci 973: 488-504.
- Dorner, T. and P. E. Lipsky (2002). "Abnormalities of B cell phenotype, immunoglobulin gene expression and the emergence of autoimmunity in Sjogren's syndrome." Arthritis Res 4(6): 360-71.
- Dubyak, G. R., D. S. Cowen, et al. (1988). "Activation of inositol phospholipid breakdown in HL60 cells by P2-purinergic receptors for extracellular ATP. Evidence for mediation by both pertussis toxin-sensitive and pertussis toxin-insensitive mechanisms." J Biol Chem 263(34): 18108-17.
- Dulhunty, A., P. Gage, et al. (2001). "The glutathione transferase structural family includes a nuclear chloride channel and a ryanodine receptor calcium release channel modulator." J Biol Chem 276(5): 3319-23.
- Edwards, A. V., M. E. Brelen, et al. (1999). "Effects of reducing submandibular blood flow on secretory responses to parasympathetic stimulation in anaesthetized cats." Exp Phys 84: 677-687.
- Edwards, A. V., A. P. Harrison, et al. (2002). "Effects of endothelin on submandibular responses to parasympathetic stimulation in anaesthetised sheep." Auto Neuro 99: 47-53.
- Edwards, A. V., A. S. Thakor, et al. (2003). "Effects of prolonged reduction in blood flow on submandibular secretory function in anaesthetised sheep." J Appl Physiol 95: 751-757.
- Ekstrom, J. (1999). "Role of nonadrenergic, noncholinergic autonomic transmitters in salivary glandular activities in vivo." In: Garrett, J.R., Ekstrom, J., Anderson, L.C. (Eds.), Neural Mechanisms of Salivary Secretion 6: 94-130.
- Ennion, S. J. and R. J. Evans (2002). "Conserved cysteine residues in the extracellular loop of the human P2X(1) receptor form disulfide bonds and are involved in receptor trafficking to the cell surface." Mol Pharmacol 61(2): 303-11.
- Eugenin, E. A., H. Gonzalez, et al. (1998). "Gap junctional communication coordinates vasopressin-induced glycogenolysis in rat hepatocytes." Am J Physiol 274(6 Pt 1): G1109-16.
- Faraci, F. M., C. D. Sigmund, et al. (1998). "Responses of carotid artery in mice deficient in expression of the gene for endothelial NO synthase." Am J Physiol 274(2 Pt 2): H564-70.
- Feher, E., T. Zelles, et al. (1999). "Immunocytochemical localisation of neuropeptide-containing nerve fibres in human labial glands." Arch Oral Biol 44(Suppl 1): S33-7.
- Fickling, S. A., D. P. Holden, et al. (1999). "Regulation of macrophage nitric oxide synthesis by endothelial cells: a role for NG,NG-dimethylarginine." Acta Physiol Scand 167(2): 145-50.
- Filippov, G., D. B. Bloch, et al. (1997). "Nitric oxide decreases stability of mRNAs encoding soluble guanylate cyclase subunits in rat pulmonary artery smooth muscle cells." J Clin Invest 100(4): 942-8.

- Finch, E. A., T. J. Turner, et al. (1991). "Calcium as a coagonist of inositol 1,4,5-trisphosphate-induced calcium release." Science 252(5004): 443-6.
- Fitzsimonds, R. M. and M. M. Poo (1998). "Retrograde signaling in the development and modification of synapses." Physiol Rev 78(1): 143-70.
- Fleischer, S. (2008). "Personal recollections on the discovery of the ryanodine receptors of muscle." Biochem Biophys Res Commun 369(1): 195-207.
- Forstermann, U., I. Gath, et al. (1995). "Isoforms of nitric oxide synthase. Properties, cellular distribution and expressional control." Biochem Pharmacol 50(9): 1321-32.
- Fox, P. C. (2007). "Autoimmune diseases and Sjogren's syndrome: an autoimmune exocrinopathy." Ann N Y Acad Sci 1098: 15-21.
- Fox, P. C. and P. M. Speight (1996). "Current concepts of autoimmune exocrinopathy: immunologic mechanisms in the salivary pathology of Sjogren's syndrome." Crit Rev Oral Biol Med 7(2): 144-58.
- Fox, R. I. (2005). "Sjogren's syndrome." Lancet 366(9482): 321-31.
- Fox, R. I., F. V. Howell, et al. (1984). "Primary Sjogren syndrome: clinical and immunopathologic features." Semin Arthritis Rheum 14(2): 77-105.
- Fox, R. I. and T. Maruyama (1997). "Pathogenesis and treatment of Sjogren's syndrome." Curr Opin Rheumatol 9(5): 393-9.
- Fox, R. I., P. Michelson, et al. (2000). "Sjogren's syndrome." Clin Dermatol 18(5): 589-600.
- Fox, R. I., C. A. Robinson, et al. (1986). "Sjogren's syndrome. Proposed criteria for classification." Arthritis Rheum 29(5): 577-85.
- Fox, R. I. and I. Saito (1994). "Criteria for diagnosis of Sjogren's syndrome." Rheum Dis Clin North Am 20(2): 391-407.
- Fox, R. I., M. Stern, et al. (2000). "Update in Sjogren syndrome." Curr Opin Rheumatol 12(5): 391-8.
- Fox, R. I., J. Tornwall, et al. (1999). "Current issues in the diagnosis and treatment of Sjogren's syndrome." Curr Opin Rheumatol 11(5): 364-71.
- Francois, M. and G. Kojda (2004). "Effect of hypercholesterolemia and of oxidative stress on the nitric oxide-cGMP pathway." Neurochem Int 45(6): 955-61.
- Fredholm, B. B. and P. Hedqvist (1980). "Modulation of neurotransmission by purine nucleotides and nucleosides." Biochem Pharmacol 29(12): 1635-43.
- Furchgott, R. F. and J. V. Zawadzki (1980). "The obligatory role of endothelial cells in the relaxation of arterial smooth muscle by acetylcholine." Nature 288(5789): 373-6.
- Galione, A. and G. C. Churchill (2000). "Cyclic ADP ribose as a calcium-mobilizing messenger." Sci STKE 2000(41): PE1.
- Galione, A. and G. C. Churchill (2002). "Interactions between calcium release pathways: multiple messengers and multiple stores." Cell Calcium 32(5-6): 343-54.

- Galione, A., H. C. Lee, et al. (1991). "Ca²⁺-induced Ca²⁺ release in sea urchin egg homogenates: modulation by cyclic ADP-ribose." Science 253(5024): 1143-6.
- Galione, A., A. McDougall, et al. (1993). "Redundant mechanisms of calcium-induced calcium release underlying calcium waves during fertilization of sea urchin eggs." Science 261(5119): 348-52.
- Galione, A. and A. White (1994). "Ca²⁺ release induced by cyclic ADP-ribose." Trends Cell Biol 4(12): 431-6.
- Galione, A., A. White, et al. (1993). "cGMP mobilizes intracellular Ca²⁺ in sea urchin eggs by stimulating cyclic ADP-ribose synthesis." Nature 365(6445): 456-9.
- Gallacher, D. V. (1982). "Are there purinergic receptors on parotid acinar cells?" Nature 296(5852): 83-6.
- Gallacher, D. V. and P. M. Smith (1999). Autonomic transmitters and Ca²⁺-activated cellular responses in salivary glands in vitro. Neural mechanisms of salivary secretion. J. R. Garret, J. Ekstrom and L. C. Anderson. Basel, Karger. 11: 80-93.
- Garcia-Carrasco, M., S. Fuentes-Alexandro, et al. (2006). "Pathophysiology of Sjogren's syndrome." Arch Med Res 37(8): 921-32.
- Garrett, J. R. (1967). "The innervation of normal human submandibular and parotid salivary glands. Demonstrated by cholinesterase histochemistry, catecholamine fluorescence and electron microscope." Arch Oral Biol 12: 1417-36.
- Garrett, J. R. and A. Kidd (1993). "The innervation of salivary glands as revealed by morphological methods." Microsc Res Tech 26(1): 75-91.
- Garrett, M., T. Kerr, et al. (1999). "Phase-dependent inhibition of H-reflexes during walking in humans is independent of reduction in knee angular velocity." J Neurophysiol 82(2): 747-53.
- Garthwaite, J., E. Southam, et al. (1995). "Potent and selective inhibition of nitric oxide-sensitive guanylyl cyclase by 1H-[1,2,4]oxadiazolo[4,3-a]quinoxalin-1-one." Mol Pharmacol 48(2): 184-8.
- Gautam, D., T. S. Heard, et al. (2004). "Cholinergic stimulation of salivary secretion studied with M1 and M3 muscarinic receptor single- and double-knockout mice." Mol Pharmacol 66(2): 260-7.
- Giaume, C. and L. Venance (1998). "Intercellular calcium signaling and gap junctional communication in astrocytes." Glia 24(1): 50-64.
- Gordon, J. L. (1986). "Extracellular ATP: effects, sources and fate." Biochem J 233(2): 309-19.
- Gordon, T. P., A. I. Bolstad, et al. (2001). "Autoantibodies in primary Sjogren's syndrome: new insights into mechanisms of autoantibody diversification and disease pathogenesis." Autoimmunity 34(2): 123-32.

- Greco, T. M., R. Hodara, et al. (2006). "Identification of S-nitrosylation motifs by site-specific mapping of the S-nitrosocysteine proteome in human vascular smooth muscle cells." Proc Natl Acad Sci U S A 103(19): 7420-5.
- Grynkiewicz, G., M. Poenie, et al. (1985). "A new generation of Ca²⁺ indicators with greatly improved fluorescence properties." J Biol Chem 260(6): 3440-50.
- Guerineau, N. C., X. Bonnefont, et al. (1998). "Synchronized spontaneous Ca²⁺ transients in acute anterior pituitary slices." J Biol Chem 273(17): 10389-95.
- Guse, A. H. (1999). "Cyclic ADP-ribose: a novel Ca²⁺-mobilising second messenger." Cell Signal 11(5): 309-16.
- Hancock, J. T. (1997). "Superoxide, hydrogen peroxide and nitric oxide as signalling molecules: their production and role in disease." Br J Biomed Sci 54(1): 38-46.
- Hand, A. R. (1972). "Adrenergic and cholinergic nerve terminals in the rat parotid gland. Electron microscopic observations on permanganate-fixed glands." Anat Rec 173(2): 131-9.
- Harden, T. K., E. R. Lazarowski, et al. (1997). "Release, metabolism and interconversion of adenine and uridine nucleotides: implications for G protein-coupled P2 receptor agonist selectivity." Trends Pharmacol Sci 18(2): 43-6.
- Harmer, A. R., D. V. Gallacher, et al. (2001). "Role of Ins(1,4,5)P₃, cADP-ribose and nicotinic acid-adenine dinucleotide phosphate in Ca²⁺ signalling in mouse submandibular acinar cells." Biochem J 353(Pt 3): 555-60.
- Harmer, A. R., P. M. Smith, et al. (2001). "The role of InsP₃, cADPr and NAADP in Ca²⁺ signalling in mouse submandibular acinar cells." Biochem J 353: 555-560.
- Harmer, A. R., P. M. Smith, et al. (2005). "Local and global calcium signals and fluid and electrolyte secretion in mouse submandibular acinar cells." Am J Physiol Gastrointest Liver Physiol 288(1): G118-24.
- Harris, L. K., J. McCormick, et al. (2008). "S-nitrosylation of proteins at the leading edge of migrating trophoblasts by inducible nitric oxide synthase promotes trophoblast invasion." Exp Cell Res 314(8): 1765-76.
- Hawkins, R. D., H. Son, et al. (1998). "Nitric oxide as a retrograde messenger during long-term potentiation in hippocampus." Prog Brain Res 118: 155-72.
- Haynes, V., S. Elfering, et al. (2004). "Mitochondrial nitric-oxide synthase: enzyme expression, characterization, and regulation." J Bioenerg Biomembr 36(4): 341-6.
- Hazes, J. M. and A. J. Silman (1990). "Review of UK data on the rheumatic diseases--2. Rheumatoid arthritis." Br J Rheumatol 29(4): 310-2.
- Heft, M. W. and B. J. Baum (1984). "Unstimulated and stimulated parotid salivary flow rate in individuals of different ages." J Dent Res 63(10): 1182-5.
- Hellmich, M. R. and F. Strumwasser (1991). "Purification and characterization of a molluscan egg-specific NADase, a second-messenger enzyme." Cell Regul 2(3): 193-202.

Hernandez, Y. L. and T. E. Daniels (1989). "Oral candidiasis in Sjogren's syndrome: prevalence, clinical correlations, and treatment." Oral Surg Oral Med Oral Pathol 68(3): 324-9.

Hess, D. T., A. Matsumoto, et al. (2005). "Protein S-nitrosylation: purview and parameters." Nat Rev Mol Cell Biol 6(2): 150-66.

Hilarp, N. (1959). "The construction and functional organisation of the autonomic innervation apparatus." Acta physiol. scand 46 Supplement 157: 3 -38.

Hirose, K., S. Kadowaki, et al. (1999). "Spatiotemporal dynamics of inositol 1,4,5-trisphosphate that underlies complex Ca²⁺ mobilization patterns." Science 284(5419): 1527-30.

Hrabie, J. A. (1993). "New Nitric Oxide-Releasing Zwitterions Derived from Polyamines." J. Org. Chem 58: 1472-1476.

Hu, Y., Y. Nakagawa, et al. (1992). "Functional changes in salivary glands of autoimmune disease-prone NOD mice." Am J Physiol 263(4 Pt 1): E607-14.

Huang, X., U. von Rad, et al. (2002). "Nitric oxide induces transcriptional activation of the nitric oxide-tolerant alternative oxidase in Arabidopsis suspension cells." Planta 215(6): 914-23.

Humphreys-Beher, M. G., J. Brayer, et al. (1999). "An alternative perspective to the immune response in autoimmune exocrinopathy: induction of functional quiescence rather than destructive autoaggression." Scand J Immunol 49(1): 7-10.

Humphreys-Beher, M. G., Y. Hu, et al. (1994). "Utilization of the non-obese diabetic (NOD) mouse as an animal model for the study of secondary Sjogren's syndrome." Adv Exp Med Biol 350: 631-6.

Humphreys-Beher, M. G. and A. B. Peck (1999). "New concepts for the development of autoimmune exocrinopathy derived from studies with the NOD mouse model." Arch Oral Biol 44 Suppl 1: S21-5.

Ignarro, L. J., G. M. Buga, et al. (1987). "Endothelium-derived relaxing factor produced and released from artery and vein is nitric oxide." Proc Natl Acad Sci U S A 84(24): 9265-9.

Ignarro, L. J., G. Cirino, et al. (1999). "Nitric oxide as a signaling molecule in the vascular system: an overview." J Cardiovasc Pharmacol 34(6): 879-86.

Ignarro, L. J., K. S. Wood, et al. (1982). "Activation of purified soluble guanylate cyclase by protoporphyrin IX." Proc Natl Acad Sci U S A 79(9): 2870-3.

Illei, G. G., E. Tackey, et al. (2004). "Biomarkers in systemic lupus erythematosus: II. Markers of disease activity." Arthritis Rheum 50(7): 2048-65.

Irving, H. R. and J. H. Exton (1987). "Phosphatidylcholine breakdown in rat liver plasma membranes. Roles of guanine nucleotides and P2-purinergic agonists." J Biol Chem 262(8): 3440-3.

- Jaffrey, S. R., H. Erdjument-Bromage, et al. (2001). "Protein S-nitrosylation: a physiological signal for neuronal nitric oxide." Nat Cell Biol 3(2): 193-7.
- Jaffrey, S. R. and S. H. Snyder (2001). "The biotin switch method for the detection of S-nitrosylated proteins." Sci STKE 2001(86): PL1.
- Jeyakumar, L. H., J. A. Copello, et al. (1998). "Purification and characterization of ryanodine receptor 3 from mammalian tissue." J Biol Chem 273(26): 16011-20.
- Jonsson, R., H.-J. Haga, et al. (2000). Sjogrens syndrome. Arthritis and Allied Conditions - A Textbook of Rheumatology. W. Koopman. Philadelphia, Lippincott Williams & Wilkins: 1826-49.
- Jonsson, R., H. J. Haga, et al. (2000). "Current concepts on diagnosis, autoantibodies and therapy in Sjogren's syndrome." Scand J Rheumatol 29(6): 341-8.
- Jonsson, R., K. Moen, et al. (2002). "Current issues in Sjogren's syndrome." Oral Dis 8(3): 130-40.
- Kahlenberg, J. M. and G. R. Dubyak (2004). "Mechanisms of caspase-1 activation by P2X7 receptor-mediated K⁺ release." Am J Physiol Cell Physiol 286(5): C1100-8.
- Kassimos, D. G., P. J. Shirlaw, et al. (1997). "Chronic sialadenitis in patients with nodal osteoarthritis." Br J Rheumatol 36(12): 1312-7.
- Katan, M. (1998). "Families of phosphoinositide-specific phospholipase C: structure and function." Biochim Biophys Acta 1436(1-2): 5-17.
- Katz, A. M. (1992). "Physiology of the Heart " New York Press, Raven Press 2nd Edition.
- Khan, M. T., L. Wagner, 2nd, et al. (2006). "Akt kinase phosphorylation of inositol 1,4,5-trisphosphate receptors." J Biol Chem 281(6): 3731-7.
- King, B. F., A. Townsend-Nicholson, et al. (1998). "Metabotropic receptors for ATP and UTP: exploring the correspondence between native and recombinant nucleotide receptors." Trends Pharmacol Sci 19(12): 506-14.
- Kinoshita, H., M. Tsutsui, et al. (1997). "Tetrahydrobiopterin, nitric oxide and regulation of cerebral arterial tone." Prog Neurobiol 52(4): 295-302.
- Kishore, B. K., Z. Wang, et al. (1997). "Upregulation of P2Y2 purinoreceptors during ischemic reperfusion injury (IRI): possible relevance to diuresis of IRI." J Am Soc Nephrol 9: 581 (abstract).
- Kong, L., N. Ogawa, et al. (1997). "Fas and Fas ligand expression in the salivary glands of patients with primary Sjogren's syndrome." Arthritis Rheum 40(1): 87-97.
- Konttinen, Y. T., L. A. Platts, et al. (1997). "Role of nitric oxide in Sjogren's syndrome." Arthritis Rheum 40(5): 875-83.
- Koshiba, M., S. Apasov, et al. (1997). "Transient up-regulation of P2Y2 nucleotide receptor mRNA expression is an immediate early gene response in activated thymocytes." Proc Natl Acad Sci U S A 94(3): 831-6.

- Kostenis, E., F. Y. Zeng, et al. (1999). "Structure-function analysis of muscarinic receptors and their associated G proteins." Life Sci 64(6-7): 355-62.
- Kroneld, U., A. K. Halse, et al. (1997). "Differential immunological aberrations in patients with primary and secondary Sjogren's syndrome." Scand J Immunol 45(6): 698-705.
- Kunapuli, S. P. and J. L. Daniel (1998). "P2 receptor subtypes in the cardiovascular system." Biochem J 336 (Pt 3): 513-23.
- Kusakabe, T., A. Matsuda, et al. (1997). "Distribution of neuropeptide-containing nerve fibres in the human submandibular gland, with special reference to the difference between serous and mucous acini." Cell Tissue Res 288: 25-31.
- Kusakabe, T., H. Matsuda, et al. (1998). "Distribution of VIP receptors in the human submandibular gland: an immunohistochemical study." Histol Histopathol 13(2): 373-8.
- Lancaster, J. R., Jr., G. Werner-Felmayer, et al. (1994). "Coinduction of nitric oxide synthesis and intracellular nonheme iron-nitrosyl complexes in murine cytokine-treated fibroblasts." Free Radic Biol Med 16(6): 869-70.
- Larsson, O. and L. Olgart (1989). "The enhancement of carbachol-induced salivary secretion by VIP and CGRP in rat parotid gland is mimicked by forskolin." Acta Physiol Scand 137(2): 231-6.
- Lee, H. C. (1991). "Specific binding of cyclic ADP-ribose to calcium-storing microsomes from sea urchin eggs." J Biol Chem 266(4): 2276-81.
- Lee, H. C. and R. Aarhus (1991). "ADP-ribosyl cyclase: an enzyme that cyclizes NAD⁺ into a calcium-mobilizing metabolite." Cell Regul 2(3): 203-9.
- Lee, H. C., R. Aarhus, et al. (1993). "Calcium mobilization by dual receptors during fertilization of sea urchin eggs." Science 261(5119): 352-5.
- Lee, M. G., X. Xu, et al. (1997). "Polarized expression of Ca²⁺ channels in pancreatic and salivary gland cells. Correlation with initiation and propagation of [Ca²⁺]_i waves." J Biol Chem 272(25): 15765-70.
- Li, H., M. Dai, et al. (2004). "A T cell intrinsic role of Id3 in a mouse model for primary Sjogren's syndrome." Immunity 21(4): 551-60.
- Liu, X., B. B. Singh, et al. (1999). "ATP-dependent activation of K(Ca) and ROMK-type K(ATP) channels in human submandibular gland ductal cells." J Biol Chem 274(35): 25121-9.
- Loewi, O. (1921). "Über humorale Übertragbarkeit der Herznervenwirkung. I." Pflugers Archiv für die Gesamte Physiologie Menschen und der Tiere 189: 239-242.
- Lomniczi, A., A. M. Suburo, et al. (1998). "Role of nitric oxide in salivary secretion." Neuroimmunomodulation 5: 226-33.
- Looms, D., K. Tritsarlis, et al. (2002). "Nitric oxide signalling in salivary glands." J Oral Pathol Med 31(10): 569-84.

Looms, D. K., K. Tritsarlis, et al. (2001). "Nitric oxide and cGMP activate Ca^{2+} -release processes in rat parotid acinar cells." Biochem J 355(Pt 1): 87-95.

Ludviksdottir, D., C. Janson, et al. (1999). "Increased nitric oxide in expired air in patients with Sjogren's syndrome. BHR study group. Bronchial hyperresponsiveness." Eur Respir J 13(4): 739-43.

MacAllister, R. J., H. Parry, et al. (1996). "Regulation of nitric oxide synthesis by dimethylarginine dimethylaminohydrolase." Br J Pharmacol 119(8): 1533-40.

MacMicking, J., Q. W. Xie, et al. (1997). "Nitric oxide and macrophage function." Annu Rev Immunol 15: 323-50.

Maggio, R., P. Barbier, et al. (1995). "Sodium nitroprusside induces internalization of muscarinic receptors stably expressed in Chinese hamster ovary cell lines." J Neurochem 65(2): 943-6.

Mak, D. O., S. M. McBride, et al. (2003). "Spontaneous channel activity of the inositol 1,4,5-trisphosphate (InsP3) receptor (InsP3R). Application of allosteric modeling to calcium and InsP3 regulation of InsP3R single-channel gating." J Gen Physiol 122(5): 583-603.

Malinski, T., Z. Taha, et al. (1993). "Diffusion of nitric oxide in the aorta wall monitored in situ by porphyrinic microsensors." Biochem Biophys Res Commun 193(3): 1076-82.

Mannick, J. B., A. Hausladen, et al. (1999). "Fas-induced caspase denitrosylation." Science 284(5414): 651-4.

Mannick, J. B. and C. M. Schonhoff (2004). "NO means no and yes: regulation of cell signaling by protein nitrosylation." Free Radic Res 38(1): 1-7.

Maragos, C. M., J. M. Wang, et al. (1993). "Nitric oxide/nucleophile complexes inhibit the in vitro proliferation of A375 melanoma cells via nitric oxide release." Cancer Res 53(3): 564-8.

Marchant, J. S. and I. Parker (2000). "Functional interactions in Ca^{2+} signaling over different time and distance scales." J Gen Physiol 116(5): 691-6.

Marks, A. R., P. Tempst, et al. (1989). "Molecular cloning and characterization of the ryanodine receptor/junctional channel complex cDNA from skeletal muscle sarcoplasmic reticulum." Proc Natl Acad Sci U S A 86(22): 8683-7.

Marletta, M. A. (1994). "Nitric oxide synthase: aspects concerning structure and catalysis." Cell 78(6): 927-30.

Marletta, M. A., A. R. Hurshman, et al. (1998). "Catalysis by nitric oxide synthase." Curr Opin Chem Biol 2(5): 656-63.

Marshall, H. E. and J. S. Stamler (2001). "Inhibition of NF-kappa B by S-nitrosylation." Biochemistry 40(6): 1688-93.

Marziali, G., D. Rossi, et al. (1996). "cDNA cloning reveals a tissue specific expression of alternatively spliced transcripts of the ryanodine receptor type 3 (RyR3) calcium release channel." FEBS Lett 394(1): 76-82.

Masuda, W. and T. Noguchi (2000). "ADP-Ribosyl cyclase in rat salivary glands." Biochem Biophys Res Commun 270(2): 469-72.

McMillian, M. K., S. P. Soltoff, et al. (1987). "Extracellular ATP elevates intracellular free calcium in rat parotid acinar cells." Biochem Biophys Res Commun 149(2): 523-30.

McMillian, M. K., S. P. Soltoff, et al. (1988). "Extracellular ATP increases free cytosolic calcium in rat parotid acinar cells. Differences from phospholipase C-linked receptor agonists." Biochem J 255(1): 291-300.

Melvin, J. E., D. Yule, et al. (2005). "Regulation of fluid and electrolyte secretion in salivary gland acinar cells." Annu Rev Physiol 67: 445-69.

Michikawa, H., Y. Mitsui, et al. (1998). "cGMP production is coupled to Ca(2+)-dependent nitric oxide generation in rabbit parotid acinar cells." Cell Calcium 23(6): 405-12.

Mikulicz, J. H. (1892). "Über eine eigenartige symmetrische Erkrankung der Tranen- und Mundspeicheldrüsen." Billroth GT, ed. Beitr. Chir. Fortschr.: 610-630.

Mitsui, Y., N. Yasuda, et al. (1997). "Nitric oxide synthase activities in mammalian parotid and submandibular salivary glands." Arch Oral Biol 42(9): 621-4.

Miyakawa, T., A. Mizushima, et al. (2001). "Ca(2+)-sensor region of IP(3) receptor controls intracellular Ca(2+) signaling." EMBO J 20(7): 1674-80.

Mogami, H., K. Nakano, et al. (1997). "Ca²⁺ flow via tunnels in polarized cells: recharging of apical Ca²⁺ stores by focal Ca²⁺ entry through basal membrane patch." Cell 88(1): 49-55.

Moncada, S. (1997). "Adventures in pharmacology, aspirin, prostacyclin and nitric oxide." Methods Find Exp Clin Pharmacol 19 Suppl A: 3-5.

Moncada, S. and A. Higgs (1993). "The L-arginine-nitric oxide pathway." N Engl J Med 329(27): 2002-12.

Moncada, S., R. M. Palmer, et al. (1991). "Nitric oxide: physiology, pathophysiology, and pharmacology." Pharmacol Rev 43(2): 109-42.

Moncada, S., M. W. Radomski, et al. (1988). "Endothelium-derived relaxing factor. Identification as nitric oxide and role in the control of vascular tone and platelet function." Biochem Pharmacol 37(13): 2495-501.

Moncada, S., D. D. Rees, et al. (1991). "Development and mechanism of a specific supersensitivity to nitrovasodilators after inhibition of vascular nitric oxide synthesis in vivo." Proc Natl Acad Sci U S A 88(6): 2166-70.

Mooren, F. C. and R. K. Kinne (1998). "Cellular calcium in health and disease." Biochim Biophys Acta 1406(2): 127-51.

Morgan, W. S. and B. Castleman (1953). "A clinicopathologic study of Mikulicz's disease." Am J Pathol 29(3): 471-503.

Moro, M. A., R. J. Russel, et al. (1996). "cGMP mediates the vascular and platelet actions of nitric oxide: confirmation using an inhibitor of the soluble guanylyl cyclase." Proc Natl Acad Sci U S A 93(4): 1480-5.

Morris, A. J. and C. C. Malbon (1999). "Physiological regulation of G protein-linked signaling." Physiol Rev 79(4): 1373-430.

Moutsopoulos, H. M., T. M. Chused, et al. (1980). "Sjogren's syndrome (Sicca syndrome): current issues." Ann Intern Med 92(2 Pt 1): 212-26.

Moutsopoulos, H. M., D. L. Mann, et al. (1979). "Genetic differences between primary and secondary sicca syndrome." N Engl J Med 301(14): 761-3.

Murad, F. (1978). "Effect of nitro-compound smooth muscle relaxants and other materials on cyclic GMP metabolism." Advances in Pharmacology and therapeutics 3: 123-132.

Nadif Kasri, N., G. Bultynck, et al. (2002). "The role of calmodulin for inositol 1,4,5-trisphosphate receptor function." Biochim Biophys Acta 1600(1-2): 19-31.

Nagaraju, K., A. Cox, et al. (2001). "Novel fragments of the Sjogren's syndrome autoantigens alpha-fodrin and type 3 muscarinic acetylcholine receptor generated during cytotoxic lymphocyte granule-induced cell death." Arthritis Rheum 44(10): 2376-86.

Nagato, T. and B. Tandler (1986). "Gap junctions in rat sublingual gland." Anat Rec 214(1): 71-5.

Nakamura, H., T. Koji, et al. (1998). "Apoptosis in labial salivary glands from Sjogren's syndrome (SS) patients: comparison with human T lymphotropic virus-I (HTLV-I)- seronegative and -seropositive SS patients." Clin Exp Immunol 114(1): 106-12.

Nakamura, T., M. Matsui, et al. (2004). "M(3) muscarinic acetylcholine receptor plays a critical role in parasympathetic control of salivation in mice." J Physiol 558(Pt 2): 561-75.

Nathanson, M. H., M. B. Fallon, et al. (1994). "Localization of the type 3 inositol 1,4,5-trisphosphate receptor in the Ca²⁺ wave trigger zone of pancreatic acinar cells." J Biol Chem 269(7): 4693-6.

Ngezahayo, A. and H. A. Kolb (1993). "Gap junctional conductance tunes phase difference of cholecystokinin evoked calcium oscillations in pairs of pancreatic acinar cells." Pflugers Arch 422(4): 413-5.

North, R. A. (1996). "P2X receptors: a third major class of ligand-gated ion channels." Ciba Found Symp 198: 91-105; discussion 105-9.

North, R. A. (2002). "Molecular physiology of P2X receptors." Physiol Rev 82(4): 1013-67.

Ohlsson, M., K. Skarstein, et al. (2001). "Fas-induced apoptosis is a rare event in Sjogren's syndrome." Lab Invest 81(1): 95-105.

Okajima, F., Y. Tokumitsu, et al. (1987). "P2-purinergic receptors are coupled to two signal transduction systems leading to inhibition of cAMP generation and to production of inositol trisphosphate in rat hepatocytes." J Biol Chem 262(28): 13483-90.

Olesen, S. P., J. Drejer, et al. (1998). "Characterization of NS 2028 as a specific inhibitor of soluble guanylyl cyclase." Br J Pharmacol 123(2): 299-309.

Ostrom, R. S., C. Gregorian, et al. (2001). "Key role for constitutive cyclooxygenase-2 of MDCK cells in basal signaling and response to released ATP." Am J Physiol Cell Physiol 281(2): C524-31.

Palmer, R. K., D. I. Yule, et al. (1996). "Intra- and intercellular calcium signaling in human neuroepithelioma cells." J Lipid Mediat Cell Signal 14(1-3): 169-74.

Park, M. K., R. C. Garrad, et al. (1997). "Changes in P2Y1 nucleotide receptor activity during the development of rat salivary glands." Am J Physiol 272(4 Pt 1): C1388-93.

Pedersen, A. M., S. Dissing, et al. (2000). "Innervation pattern and Ca²⁺ signalling in labial salivary glands of healthy individuals and patients with primary Sjogren's syndrome (pSS)." J Oral Pathol Med 29(3): 97-109.

Pedersen, P. S. (1991). "Separate agonist-specific oscillatory mechanisms in cultured human sweat duct cells." J Physiol 433: 549-59.

Pedersen, S., S. F. Pedersen, et al. (1999). "Mechanical stress induces release of ATP from Ehrlich ascites tumor cells." Biochim Biophys Acta 1416(1-2): 271-84.

Perez Leiros, C., L. Sterin-Borda, et al. (1999). "Activation of nitric oxide signaling through muscarinic receptors in submandibular glands by primary Sjogren syndrome antibodies." Clin Immunol 90(2): 190-5.

Pertovaara, M., J. Anttonen, et al. (2007). "Endothelial nitric oxide synthase +894 polymorphism is associated with recurrent salivary gland swelling and early onset in patients with primary Sjogren's syndrome." Ann Rheum Dis 66(10): 1400-1.

Petersen, C. C. and O. H. Petersen (1991). "Receptor-activated cytoplasmic Ca²⁺ spikes in communicating clusters of pancreatic acinar cells." FEBS Lett 284(1): 113-6.

Petersen, O. H., M. Michalak, et al. (2005). "Calcium signalling: past, present and future." Cell Calcium 38(3-4): 161-9.

Petersen, O. H., A. Tepikin, et al. (2001). "The endoplasmic reticulum: one continuous or several separate Ca(2+) stores?" Trends Neurosci 24(5): 271-6.

Petersen, O. H. and A. V. Tepikin (2008). "Polarized calcium signaling in exocrine gland cells." Annu Rev Physiol 70: 273-99.

Pickles, R. J., D. J. Brayden, et al. (1991). "Synchronous transporting activity in epithelial cells in relation to intracellular calcium concentration." Proc Biol Sci 245(1312): 53-8.

Pillemer, S. R., E. L. Matteson, et al. (2001). "Incidence of physician-diagnosed primary Sjogren syndrome in residents of Olmsted County, Minnesota." Mayo Clin Proc 76(6): 593-9.

Pinkstaff, C. A. (1979). "The cytology of salivary glands." Int Rev Cytol 63: 141-261.

Pochet, S., A. Gomez-Munoz, et al. (2003). "Regulation of phospholipase D by P2X7 receptors in submandibular ductal cells." Cell Signal 15(10): 927-35.

Pralong, W. F., C. B. Wollheim, et al. (1988). "Measurement of cytosolic free Ca²⁺ in individual pancreatic acini." FEBS Lett 242(1): 79-84.

Putney, J. W., Jr. (1990). "Capacitative calcium entry revisited." Cell Calcium 11(10): 611-24.

Quissell, D. O., K. A. Barzen, et al. (1997). "Development and characterization of SV40 immortalized rat submandibular acinar cell lines." In Vitro Cell Dev Biol Anim 33(3): 164-73.

Quissell, D. O., K. A. Barzen, et al. (1998). "Development and characterization of SV40 immortalized rat parotid acinar cell lines." In Vitro Cell Dev Biol Anim 34(1): 58-67.

Ramos-Casals, M., J. M. Anaya, et al. (2004). "Cutaneous vasculitis in primary Sjogren syndrome: classification and clinical significance of 52 patients." Medicine (Baltimore) 83(2): 96-106.

Ramos-Casals, M. and J. Font (2005). "Primary Sjogren's syndrome: current and emergent aetiopathogenic concepts." Rheumatology (Oxford) 44(11): 1354-67.

Rebecchi, M. J. and S. N. Pentylala (2000). "Structure, function, and control of phosphoinositide-specific phospholipase C." Physiol Rev 80(4): 1291-335.

Reilly, W. M., V. L. Saville, et al. (1987). "An assessment of the antagonistic activity of reactive blue 2 at P1- and P2-purinoceptors: supporting evidence for purinergic innervation of the rabbit portal vein." Eur J Pharmacol 140(1): 47-53.

Rhee, S. G. and Y. S. Bae (1997). "Regulation of phosphoinositide-specific phospholipase C isozymes." J Biol Chem 272(24): 15045-8.

Rhodus, N. L. (1997). "Oral pilocarpine HCl stimulates labial (minor) salivary gland flow in patients with Sjogren's syndrome." Oral Dis 3(2): 93-8.

Richardson, P. J. and S. J. Brown (1987). "ATP release from affinity-purified rat cholinergic nerve terminals." J Neurochem 48(2): 622-30.

Ritter, M. and F. Lang (1991). "Effect of bradykinin, ATP and adrenaline on cell membrane resistances of Madin-Darby canine kidney cells." J Physiol 443: 45-54.

Robb-Gaspers, L. D. and A. P. Thomas (1995). "Coordination of Ca²⁺ signaling by intercellular propagation of Ca²⁺ waves in the intact liver." J Biol Chem 270(14): 8102-7.

Robinson, C. P., J. Brayer, et al. (1998). "Transfer of human serum IgG to nonobese diabetic Igμ null mice reveals a role for autoantibodies in the loss of secretory

function of exocrine tissues in Sjogren's syndrome." Proc Natl Acad Sci U S A 95(13): 7538-43.

Robinson, C. P., J. Cornelius, et al. (1998). "Characterization of the changing lymphocyte populations and cytokine expression in the exocrine tissues of autoimmune NOD mice." Autoimmunity 27(1): 29-44.

Rodbell, M. (1995). "Signal transduction: evolution of an idea." Environ Health Perspect 103(4): 338-45.

Ross, P. E., G. R. Ehrling, et al. (1997). "Dynamics of ATP-induced calcium signaling in single mouse thymocytes." J Cell Biol 138(5): 987-98.

Rottingen, J. and J. G. Iversen (2000). "Ruled by waves? Intracellular and intercellular calcium signalling." Acta Physiol Scand 169(3): 203-19.

Rottingen, J. A., E. Camerer, et al. (1997). "Synchronized Ca²⁺ oscillations induced in Madin Darby canine kidney cells by bradykinin and thrombin but not by ATP." Cell Calcium 21(3): 195-211.

Saez, J. C., J. A. Connor, et al. (1989). "Hepatocyte gap junctions are permeable to the second messenger, inositol 1,4,5-trisphosphate, and to calcium ions." Proc Natl Acad Sci U S A 86(8): 2708-12.

Sage, S. O., D. J. Adams, et al. (1989). "Synchronized oscillations in cytoplasmic free calcium concentration in confluent bradykinin-stimulated bovine pulmonary artery endothelial cell monolayers." J Biol Chem 264(1): 6-9.

Saito, A., M. Tnui, et al. (1989). "Mass measurement of the feet structures/ calcium release channel of sarcoplasmic reticulum by scanning transmission electron microscope (STEM)." Biophys. J 55: 206.

Saito, T., H. Fukuda, et al. (1997). "Salivary gland scintigraphy with 99mTc-pertechnetate in Sjogren's syndrome: relationship to clinicopathologic features of salivary and lacrimal glands." J Oral Pathol Med 26(1): 46-50.

Sandberg, K., H. Ji, et al. (1992). "Intercellular communication between follicular angiotensin receptors and *Xenopus laevis* oocytes: mediation by an inositol 1,4,5-trisphosphate-dependent mechanism." J Cell Biol 117(1): 157-67.

Sanderson, M. J. (1995). "Intercellular calcium waves mediated by inositol trisphosphate." Ciba Found Symp 188: 175-89; discussion 189-94.

Sarih, M., V. Souvannavong, et al. (1993). "Nitric oxide synthase induces macrophage death by apoptosis." Biochem Biophys Res Commun 191(2): 503-8.

Sato, A. and S. Miyoshi (1988). "Ultrastructure of the main excretory duct epithelia of the rat parotid and submandibular glands with a review of the literature." Anat Rec 220(3): 239-51.

Sato, A. and S. Miyoshi (1998). "Cells in the duct system of the rat submandibular gland." Eur J Morphol 36 Suppl: 61-6.

Schrader, A. M., J. M. Camden, et al. (2005). "P2Y₂ nucleotide receptor up-regulation in submandibular gland cells from the NOD.B10 mouse model of Sjogren's syndrome." Arch Oral Biol 50(6): 533-40.

Schrammel, A., S. Behrends, et al. (1996). "Characterization of 1H-[1,2,4]oxadiazolo[4,3-a]quinoxalin-1-one as a heme-site inhibitor of nitric oxide-sensitive guanylyl cyclase." Mol Pharmacol 50(1): 1-5.

Scully, C. (1986). "Sjogren's syndrome: clinical and laboratory features, immunopathogenesis, and management." Oral Surg Oral Med Oral Pathol 62(5): 510-23.

Segawa, A., H. Takemura, et al. (2002). "Calcium signalling in tissue: diversity and domain-specific integration of individual cell response in salivary glands." J Cell Sci 115(Pt 9): 1869-76.

Seye, C. I., A. P. Gadeau, et al. (1997). "Overexpression of P2Y2 purinoceptor in intimal lesions of the rat aorta." Arterioscler Thromb Vasc Biol 17(12): 3602-10.

Seye, C. I., Q. Kong, et al. (2002). "Functional P2Y2 nucleotide receptors mediate uridine 5'-triphosphate-induced intimal hyperplasia in collared rabbit carotid arteries." Circulation 106(21): 2720-6.

Shiozawa, S., Y. Tanaka, et al. (1998). "Single-blinded controlled trial of low-dose oral IFN-alpha for the treatment of xerostomia in patients with Sjogren's syndrome." J Interferon Cytokine Res 18(4): 255-62.

Ship, J. A. and B. J. Baum (1990). "Is reduced salivary flow normal in old people?" Lancet 336(8729): 1507.

Ship, J. A., P. C. Fox, et al. (1999). "Treatment of primary Sjogren's syndrome with low-dose natural human interferon-alpha administered by the oral mucosal route: a phase II clinical trial. IFN Protocol Study Group." J Interferon Cytokine Res 19(8): 943-51.

Sjögren, H. (1933). "Zur Kenntnis der Keratoconjunctivitis sicca." Acta Ophtalmolo 11(Suppl. II): 1-151.

Smart, M. L., B. Gu, et al. (2003). "P2X7 receptor cell surface expression and cytolytic pore formation are regulated by a distal C-terminal region." J Biol Chem 278(10): 8853-60.

Smith, P. M. (1996). Mechanisms of secretion in salivary glands. Saliva and Oral Health. W. M. Edgar and D. O'Mullane: 9-25.

Smith, P. M. and D. V. Gallacher (1992). "Acetylcholine- and caffeine-evoked repetitive transient Ca^{2+} -activated K^{+} and Cl^{-} currents in mouse submandibular cells." J Physiol (Lond) 449: 109-20.

Smith, P. M. and D. V. Gallacher (1994). "Thapsigargin-induced Ca^{2+} mobilization in acutely isolated mouse lacrimal acinar cells is dependent on a basal level of $\text{Ins}(1,4,5)\text{P}_3$ and is inhibited by heparin." Biochem J 299(Pt 1): 37-40.

Smith, P. M. and H. E. Reed (1996). "Amplification of the thapsigargin-evoked increase in the cytosolic free Ca^{2+} concentration by acetylcholine in acutely isolated mouse submandibular acinar cells." Biochem J 317(Pt 3): 779-83.

Soff, G. A., T. L. Cornwell, et al. (1997). "Smooth muscle cell expression of type I cyclic GMP-dependent protein kinase is suppressed by continuous exposure to

nitrovasodilators, theophylline, cyclic GMP, and cyclic AMP." J Clin Invest 100(10): 2580-7.

Soltoff, S. P., M. K. McMillian, et al. (1990). "Effects of extracellular ATP on ion transport systems and $[Ca^{2+}]_i$ in rat parotid acinar cells. Comparison with the muscarinic agonist carbachol." J Gen Physiol 95(2): 319-46.

Southam, E., S. L. Charles, et al. (1996). "The nitric oxide-cyclic GMP pathway and synaptic plasticity in the rat superior cervical ganglion." Br J Pharmacol 119(3): 527-32.

Sreebny, L. M. (1996). Xerostomia: diagnosis, management and clinical complications. Saliva and Oral Health. W. M. Edgar and D. O'Mullane: 43-66.

St Clair, E. W. (1992). "Sjogren's syndrome and autoimmunity." Concepts Immunopathol 8: 161-88.

Stamler, J. S., S. Lamas, et al. (2001). "Nitrosylation. the prototypic redox-based signaling mechanism." Cell 106(6): 675-83.

Stauffer, P. L., H. Zhao, et al. (1993). "Gap junction communication modulates $[Ca^{2+}]_i$ oscillations and enzyme secretion in pancreatic acini." J Biol Chem 268(26): 19769-75.

Stefano, G. B., Y. Liu, et al. (1996). "Cannabinoid receptors are coupled to nitric oxide release in invertebrate immunocytes, microglia, and human monocytes." J Biol Chem 271(32): 19238-42.

Stone (1981). "A multidisciplinary approach." Neuroscience 6: 523-555.

Sun, J., C. Xin, et al. (2001). "Cysteine-3635 is responsible for skeletal muscle ryanodine receptor modulation by NO." Proc Natl Acad Sci U S A 98(20): 11158-62.

Sun, J., L. Xu, et al. (2003). "Nitric oxide, NOC-12, and S-nitrosoglutathione modulate the skeletal muscle calcium release channel/ryanodine receptor by different mechanisms. An allosteric function for O₂ in S-nitrosylation of the channel." J Biol Chem 278(10): 8184-9.

Surprenant, A., F. Rassendren, et al. (1996). "The cytolytic P_{2Z} receptor for extracellular ATP identified as a P_{2X} receptor (P_{2X7})." Science 272(5262): 735-8.

Tabuchi, A., E. Oh, et al. (1996). "Rapid attenuation of AP-1 transcriptional factors associated with nitric oxide (NO)-mediated neuronal cell death." J Biol Chem 271(49): 31061-7.

Taha, Z., F. Kiechle, et al. (1992). "Oxidation of nitric oxide by oxygen in biological systems monitored by porphyrinic sensor." Biochem Biophys Res Commun 188(2): 734-9.

Takai, N., K. Uchihashi, et al. (1999). "Localization of neuronal-constitutive nitric oxide synthase and secretory regulation by nitric oxide in the rat submandibular and sublingual glands." Arch Oral Biol 44(9): 745-50.

Takemura, H., S. Yamashina, et al. (1999). "Millisecond analyses of Ca²⁺ initiation sites evoked by muscarinic receptor stimulation in exocrine acinar cells." Biochem Biophys Res Commun 259(3): 656-60.

Takuma, K., P. Phuaphong, et al. (2002). "The nitric oxide donor NOC12 protects cultured astrocytes against apoptosis via a cGMP-dependent mechanism." Jpn J Pharmacol 89(1): 64-71.

Tao, H. W. and M. Poo (2001). "Retrograde signaling at central synapses." Proc Natl Acad Sci U S A 98(20): 11009-15.

Thomas, E., E. M. Hay, et al. (1998). "Sjogren's syndrome: a community-based study of prevalence and impact [see comments]." Br J Rheumatol 37(10): 1069-76.

Thorn, P., O. Gerasimenko, et al. (1994). "Cyclic ADP-ribose regulation of ryanodine receptors involved in agonist evoked cytosolic Ca²⁺ oscillations in pancreatic acinar cells." Embo J 13(9): 2038-43.

Thorn, P., A. M. Lawrie, et al. (1993). "Local and global cytosolic Ca²⁺ oscillations in exocrine cells evoked by agonists and inositol trisphosphate." Cell 74(4): 661-8.

Tishler, M., I. Yaron, et al. (1999). "Hydroxychloroquine treatment for primary Sjogren's syndrome: its effect on salivary and serum inflammatory markers." Ann Rheum Dis 58(4): 253-6.

Tobin, G. (1995). "Muscarinic receptor subtypes in the submandibular gland and the urinary bladder of the rabbit: in vivo and in vitro functional comparisons of receptor antagonists." J Auton Pharmacol 15(6): 451-63.

Tobin, G. (2002). "Presynaptic muscarinic receptor mechanisms and submandibular responses to stimulation of the parasympathetic innervation in bursts in rats." Auton Neurosci 99(2): 111-8.

Tobin, G., D. Giglio, et al. (2002). "Studies of muscarinic receptor subtypes in salivary gland function in anaesthetized rats." Auton Neurosci 100(1-2): 1-9.

Tordjmann, T., B. Berthon, et al. (1997). "Coordinated intercellular calcium waves induced by noradrenaline in rat hepatocytes: dual control by gap junction permeability and agonist." EMBO J 16(17): 5398-407.

Toyofuku, T., M. Yabuki, et al. (1998). "Intercellular calcium signaling via gap junction in connexin-43-transfected cells." J Biol Chem 273(3): 1519-28.

Tritsaris, K., D. K. Looms, et al. (2000). "Nitric oxide synthesis causes inositol phosphate production and Ca²⁺ release in rat parotid acinar cells." Pflugers Arch 440(2): 223-8.

Tsianos, E. B., A. G. Tzioufas, et al. (1985). "Sialochemistry of patients with autoimmune rheumatic disease with and without histological manifestations of Sjogren's syndrome." Ann Rheum Dis 44(6): 412-4.

Tsien, R. Y. (1980). "New calcium indicators and buffers with high selectivity against magnesium and protons: design, synthesis, and properties of prototype structures." Biochemistry 19(11): 2396-404.

Tsukimoto, M., H. Harada, et al. (2005). "Involvement of chloride in apoptotic cell death induced by activation of ATP-sensitive P2X7 purinoceptor." J Biol Chem 280(4): 2653-8.

Turner, J. T., L. A. Landon, et al. (1999). "Salivary gland P2 nucleotide receptors." Crit Rev Oral Biol Med 10(2): 210-24.

Turner, J. T., G. A. Weisman, et al. (1997). "Upregulation of P2Y2 nucleotide receptors in rat salivary gland cells during short-term culture." Am J Physiol 273(3 Pt 1): C1100-7.

Valera, S., N. Hussy, et al. (1994). "A new class of ligand-gated ion channel defined by P2x receptor for extracellular ATP." Nature 371(6497): 516-9.

Virginio, C., A. MacKenzie, et al. (1999). "Kinetics of cell lysis, dye uptake and permeability changes in cells expressing the rat P2X7 receptor." J Physiol 519 Pt 2: 335-46.

Virta, E., J. Tornwall, et al. (1992). "Substance P and neurokinin A immunoreactive nerve fibres in the developing salivary glands of the rat." Histochemistry 98(5): 317-25.

Vitali, C., S. Bombardieri, et al. (2002). "Classification criteria for Sjogren's syndrome: a revised version of the European criteria proposed by the American-European Consensus Group." Ann Rheum Dis 61(6): 554-8.

Vitali, C., S. Bombardieri, et al. (1993). "Preliminary criteria for the classification of Sjogren's syndrome. Results of a prospective concerted action supported by the European Community." Arthritis Rheum 36(3): 340-7.

Vitali, C., S. Bombardieri, et al. (1996). "Assessment of the European classification criteria for Sjogren's syndrome in a series of clinically defined cases: results of a prospective multicentre study. The European Study Group on Diagnostic Criteria for Sjogren's Syndrome." Ann Rheum Dis 55(2): 116-21.

Vites, A. M. and A. J. Pappano (1994). "Distinct modes of inhibition by ruthenium red and ryanodine of calcium-induced calcium release in avian atrium." J Pharmacol Exp Ther 268(3): 1476-84.

Wanchu, A., M. Khullar, et al. (2000). "Elevated nitric oxide production in patients with primary Sjogren's syndrome." Clin Rheumatol 19(5): 360-4.

Wang, G., N. H. Moniri, et al. (2006). "Nitric oxide regulates endocytosis by S-nitrosylation of dynamin." Proc Natl Acad Sci U S A 103(5): 1295-300.

Wang, Y. G., C. E. Rechenmacher, et al. (1998). "Nitric oxide signaling mediates stimulation of L-type Ca²⁺ current elicited by withdrawal of acetylcholine in cat atrial myocytes." J Gen Physiol 111(1): 113-25.

Weisman, G. A., M. Wang, et al. (2005). "Molecular determinants of P2Y2 nucleotide receptor function: implications for proliferative and inflammatory pathways in astrocytes." Mol Neurobiol 31(1-3): 169-83.

Wess, J., N. Blin, et al. (1995). "Muscarinic acetylcholine receptors: structural basis of ligand binding and G protein coupling." Life Sci 56(11-12): 915-22.

- White, T. D. (1984). "Characteristics of neuronal release of ATP." Prog Neuropsychopharmacol Biol Psychiatry 8(4-6): 487-93.
- Wilden, P. A., Y. M. Agazie, et al. (1998). "ATP-stimulated smooth muscle cell proliferation requires independent ERK and PI3K signaling pathways." Am J Physiol 275(4 Pt 2): H1209-15.
- Wolin, M. S., K. S. Wood, et al. (1982). "Guanylate cyclase from bovine lung. A kinetic analysis of the regulation of the purified soluble enzyme by protoporphyrin IX, heme, and nitrosyl-heme." J Biol Chem 257(22): 13312-20.
- Wollheim, F. A. (1999). "A humble gentleman at 100. 1951 [classical article]." Clin Exp Rheumatol 17(6): 648-52.
- Worley, P. F., J. M. Baraban, et al. (1987). "Characterization of inositol trisphosphate receptor binding in brain. Regulation by pH and calcium." J Biol Chem 262(25): 12132-6.
- Yamaki, H., K. Morita, et al. (1998). "Cyclic ADP-ribose induces Ca²⁺ release from caffeine-insensitive Ca²⁺ pools in canine salivary gland cells." J Dent Res 77(10): 1807-16.
- Yamamoto-Hino, M., A. Miyawaki, et al. (1998). "Apical vesicles bearing inositol 1,4,5-trisphosphate receptors in the Ca²⁺ initiation site of ductal epithelium of submandibular gland." J Cell Biol 141(1): 135-42.
- Young and van Lennep (1978). "The morphology of salivary glands." London, New York, San Fransico: Academic Press.
- Yu, H. X. and J. T. Turner (1991). "Functional studies in the human submandibular duct cell line, HSG-PA, suggest a second salivary gland receptor subtype for nucleotides." J Pharmacol Exp Ther 259(3): 1344-50.
- Yule, D. I., E. Stuenkel, et al. (1996). "Intercellular calcium waves in rat pancreatic acini: mechanism of transmission." Am J Physiol 271(4 Pt 1): C1285-94.
- Zhang, X., J. Wen, et al. (1999). "Ryanodine and inositol trisphosphate receptors are differentially distributed and expressed in rat parotid gland." Biochem J 340(Pt 2): 519-27.
- Zhao, Y., P. E. Brandish, et al. (2000). "Inhibition of soluble guanylate cyclase by ODQ." Biochemistry 39(35): 10848-54.
- Zimmermann, B. and B. Walz (1997). "Serotonin-induced intercellular calcium waves in salivary glands of the blowfly *Calliphora erythrocephala*." J Physiol 500 (Pt 1): 17-28.
- Zoukhri, D., R. R. Hodges, et al. (1998). "Lacrimal gland innervation is not altered with the onset and progression of disease in a murine model of Sjogren's syndrome." Clin Immunol Immunopathol 89(2): 126-33.
- Zoukhri, D., R. R. Hodges, et al. (1998). "Ca²⁺ signaling by cholinergic and alpha1-adrenergic agonists is up-regulated in lacrimal and submandibular glands in a murine model of Sjogren's syndrome." Clin Immunol Immunopathol 89(2): 134-40.

Zucchi, R. and S. Ronca-Testoni (1997). "The sarcoplasmic reticulum Ca^{2+} channel/ryanodine receptor: modulation by endogenous effectors, drugs and disease states." Pharmacol Rev 49(1): 1-51.